

# Nanoscale and Microscale Approaches for Engineering the *in vitro* Cellular Microenvironment

by

**Ali Khademhosseini**

B.A.Sc. Chemical Engineering, University of Toronto, 1999

M.A.Sc. Chemical Engineering, University of Toronto, 2001

Submitted to the Division of Biological Engineering  
in Partial Fulfillment of the Requirements for the Degree of

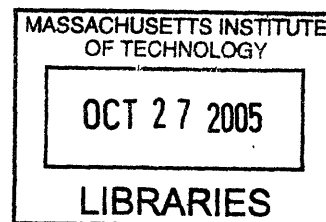
**Doctor of Philosophy in Bioengineering**

at the

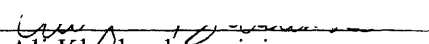
**Massachusetts Institute of Technology**

June 2005

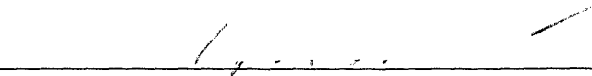
© Massachusetts Institute of Technology  
All rights reserved



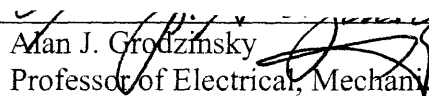
Signature of Author

  
Ali Khademhosseini  
Division of Biological Engineering

Certified by

  
Robert S. Langer  
Thesis Supervisor  
Massachusetts Institute of Technology Institute Professor  
Professor of Chemical and Biomedical Engineering

Accepted by

  
Alan J. Grodzinsky  
Professor of Electrical, Mechanical, & Biological Engineering  
Chair, BE Graduate Program Committee

**ARCHIVES**

This doctoral thesis has been examined by the following Thesis Committee:

**Robert S. Langer, Sc.D.** \_\_\_\_\_

Thesis Advisor

Massachusetts Institute of Technology Institute Professor

Professor of Chemical and Biomedical Engineering

Biological Engineering Division and Department of Chemical Engineering

Massachusetts Institute of Technology

**Douglas A. Lauffenburger, Ph.D.** \_\_\_\_\_

Whitaker Professor of Bioengineering

Biological Engineering Division

Massachusetts Institute of Technology

**James Sherley, M.D., Ph.D.** \_\_\_\_\_

Associate Professor of Biological Engineering

Biological Engineering Division

Massachusetts Institute of Technology

**Joseph P. Vacanti, M.D.** \_\_\_\_\_

John Homans Professor of Surgery

Department of Surgery

Massachusetts General Hospital

Harvard Medical School

*To my family, friends and mentors*

# **Nanoscale and Microscale Approaches for Engineering the *in vitro* Cellular Microenvironment**

by

Ali Khademhosseini

Micro- and nanofabrication approaches have dramatically changed our society through their use in microelectronics and telecommunication industries. These engineering tools are also useful for many biological applications ranging from drug delivery to DNA sequencing, since they can be used to fabricate small features at a low cost and in a reproducible manner. The goal of this thesis was to develop techniques based on the merger of novel materials and nano and microfabrication approaches to manipulate cell microenvironment in culture. To control cell migration and to restrict cell or colony size, cells and proteins were patterned by using molding or printing methods. Poly(ethylene glycol)-based molecules and polysaccharides were used to control cell-substrate interactions and to prevent cell adhesion on specific regions of a substrate. To control cell-cell contact, layer-by-layer deposition of ionic biopolymers (i.e. negatively charged hyaluronic acid and positively charged poly-L-lysine) was used to generate patterned co-cultures. In addition, to control cell-soluble factor interactions, microfluidic-based approaches were developed. To pattern cells and proteins within microchannels, a soft lithographic method was developed to pattern microchannel substrates using printing and molding approaches. To easily immobilize cells within channels, poly(ethylene glycol) microstructures were used to capture cells within low shear stress regions. These techniques also allowed for the fabrication of multiphenotype cell arrays. In addition, techniques were developed to control the interaction of cells within hydrogels by controlling the spatial properties of hydrogels.

Thesis Advisor: Robert S. Langer, Sc. D.

Massachusetts Institute of Technology Institute Professor



## **Acknowledgements**

I would like to thank my supervisor Prof. Robert Langer for providing me with the opportunity to join the fantastic research environment of his lab. Bob is a fantastic mentor and a constant source of inspiration. I also would like to thank Bob for giving me the freedom to explore my ideas and become a more complete and mature researcher. Throughout my life no one has made a bigger contribution to my career and academic success.

I also would like to thank Prof. Doug Lauffenburger for his guidance and teachings over the past few years. Doug's vision and leadership in the development of the 'Biological Engineering Division' has been instrumental in my development and becoming a member of the MIT community.

I am grateful to my thesis committee members Profs. Doug Lauffenburger, James Sherley and Jay Vacanti for their time and critical assessment of this work. Also, I would like to thank my former advisors Prof. Peter Zandstra and Prof. Michael Sefton for getting me 'excited about science'. I have been blessed with excellent teachers and wonderful mentors and the challenge of living up to their standards of excellence is a rewarding experience.

I have benefited greatly from my association with all past and present members of the Langer lab, in particular Kahpyang Suh, Omid Farokhzad, Sangyong Jon, Jason Burdick, Jeff Karp, Shulamit Levenberg, David LaVan, Jen Ming Yang, Chun Wang, Blaine Pfeiffer, Thanh-Nga T. Tran, Hyongshin Park, Milica Radisic and David Berry. A simple thank you is insufficient for George Eng and Judy Yeh (the other members of the JAG team) and other UROPs and students including Hirokazu Kaji, Alice Kiselyuk, Guan-Jong Chen, Aurelia Hermmann, without whom I would not have accomplished nearly as much.

My graduate work has also been a learning experience in teamwork and leadership through organizations such as TechLink, Graduate student council, Biological engineering student leadership board and diversity initiative. I would like to thank all staff and students whose interactions made me a more complete individual. In particular, I would like to acknowledge

Siddhartha Jain, Maxine Jonas, Lisa Joslin, Ale Wolf-Yadin, Thomas Gervais, Nate Tedford and the rest of the incoming Bioengineering classes of 2001-2005 for their support.

I also would like to acknowledge the funding sources for Prof. Langer as well as NSERC-PGSB and Poitras fellowship for providing the support for my Ph.D. studies. Finally, I would like to thank my family and friends for their unconditional support and love.

## TABLE OF CONTENTS

ABSTRACT.....	iv
ACKNOWLEDGEMENTS.....	v
TABLE OF CONTENTS.....	vii
LIST OF TABLES.....	vi
LIST OF FIGURES.....	x
ABBREVIATIONS.....	xii
THESIS SCOPE AND FORMAT.....	xv
<b>1 Introduction and background.....</b>	<b>1</b>
Motivation.....	1
Cell microenvironment.....	2
Patterning cells on a chip.....	4
Cells and microchannels.....	8
References.....	12
<b>2 Soft lithographic fabrication of poly(ethylene glycol) microstructures for protein and cell patterning using capillary force lithography.....</b>	<b>19</b>
Introduction.....	19
Materials and methods.....	21
Results and discussion.....	22
Conclusions.....	31
References.....	33
<b>3 Synthesis of a novel PEG-based polymer and its application for fabrication of protein and cell resistant micro/nanostructures.....</b>	<b>36</b>
Introduction.....	36
Materials and methods.....	38
Results and discussion.....	41
Conclusions.....	61
References.....	62

<b>4</b>	<b>Characterization of hyaluronic acid immobilized on solid substrates and its application for patterning</b>	<b>65</b>
	Introduction	65
	Materials and methods	66
	Results and discussion	70
	Conclusions	84
	References	85
<b>5</b>	<b>Layer-by-layer deposition of hyaluronic acid and poly-L-lysine for patterned cell cultures</b>	<b>89</b>
	Introduction	89
	Materials and methods	92
	Results	94
	Discussion	105
	Conclusions	106
	References	107
<b>6</b>	<b>Surface patterned microfluidic channels for improving the cell / microdevice interface</b>	<b>110</b>
	Introduction	110
	Materials and methods	111
	Results and discussion	115
	Conclusions	124
	References	125
<b>7</b>	<b>Molded poly(ethylene glycol) microstructures for capturing cells within microfluidic channels</b>	<b>128</b>
	Introduction	128
	Materials and methods	129
	Results and discussion	133

Conclusions.....	141
References.....	142
<b>8 Cell docking inside microwells within reversibly sealed microfluidic channels for fabricating multiphenotype cell arrays.....</b>	<b>145</b>
Introduction.....	145
Materials and methods.....	147
Results and discussion.....	149
Conclusions.....	158
References.....	159
<b>9 Fabrication of Gradient Hydrogels Using a Microfluidics / Photopolymerization Process.....</b>	<b>162</b>
Introduction.....	162
Materials and methods.....	162
Results and discussion.....	164
Conclusions.....	173
References.....	174
<b>10 Summary and Outlook.....</b>	<b>176</b>
Summary.....	176
Outlook.....	180
References.....	182

## LIST OF TABLES

Table 3.1 Elemental composition of the PMs on Si/SiO <sub>2</sub> wafer measured by XPS.....	42
Table 3.2 High resolution XPS C 1s composition at 0° and 55° take-off angles from surface normal.....	42
Table 4.1 Atomic mass percentage of carbon, nitrogen, oxygen and silicon elements for HA films formed under various conditions.....	74
Table 4.2 Atomic mass percentage of GAG surfaces and control surfaces.....	75

## LIST OF FIGURES

Figure 1.1 Various components of cellular microenvironment and BioMEMS approaches that aim to control these parameters in culture.....	2
Figure 1.2 Schematic of the soft lithography process for fabricating microfluidic channels and surface patterning.....	6
Figure 1.3 Schematic diagram of the process of photolithography, microcontact printing and capillary force lithography.....	8
Figure 1.4 Technologies and disciplines relating to “living cells on chips”.....	11
Figure 2.1 Schematic diagram of the PEG patterning experimental procedure.....	23
Figure 2.2 Schematic diagram of the effect of mold / polymer surface interactions on desired structures.....	24
Figure 2.3 AFM images of patterned PEG microstructures.....	26
Figure 2.4 FTIR spectra of a cured PEGDM film at different UV exposure times.....	27
Figure 2.5 Fluorescent images of protein adsorption of PEGDM patterns.....	29
Figure 2.6 Optical micrographs of NIH-3T3 cells deposited on patterned PEG substrates.....	31
Figure 3.1 Chemical structure of poly(TMSMA-r-PEGMA) and its monolayer structure.....	37
Figure 3.2 Effects of immersion times and copolymer concentrations on the thicknesses of PMs.....	42
Figure 3.3 Tapping mode AFM height images of PMs.....	43
Figure 3.4 The characterization of the PMs on Si/SiO <sub>2</sub> wafers by glancing angle XPS.....	45
Figure 3.5 Protein adsorption on control and PMs on Si/SiO <sub>2</sub> wafer.....	46
Figure 3.6 Ellipsometric measurement of nonspecific adsorption of proteins on PMs. ....	46
Figure 3.7 Characterization of the polymer-coated PDMS and glass by high resolution C(1s) XPS.....	47
Figure 3.8 Protein resistance of polymer-coated PDMS and glass by high resolution N(1s) XPS.....	47
Figure 3.9 Fluorescence images of microchannels after flowing aqueous solution of FITC-BSA through the channel.....	48
Figure 3.10 Microfluidic device with capillary tubing connected to channels.....	49
Figure 3.11 NIH-3T3 fibroblasts cultured on unmodified glass and the polymer-coated glass....	50
Figure 3.12 Schematic diagram of the patterning process.....	52
Figure 3.13 Light microscope images of patterns generated using various polymer concentrations and approaches.....	53
Figure 3.14 AFM images of patterned surfaces using 5, 50 and 100 mg mL <sup>-1</sup> poly(TMSMA-r-PEGMA) in methanol.....	54
Figure 3.15 BSA and FN adsorption onto patterned poly(TMSMA-r-PEGMA) surfaces.....	56
Figure 3.16 NIH-3T3 cells on patterns of PMs after 6 hours in culture.....	58
Figure 3.17 NIH-3T3 cells on PM patterns over time.....	59
Figure 4.1 High-resolution XPS spectra of HA modified surfaces .....	71
Figure 4.2 XPS spectra for the detection of a HA layer .....	72
Figure 4.3 AFM images of surface roughness and the fluorescent images for protein adsorption .....	73
Figure 4.4 FN adsorption onto GAG surfaces was measured by quantifying the fluorescence intensity.....	76
Figure 4.5 The stability of HA surfaces as a function of PBS exposure time.....	77

Figure 4.6	Typical soft lithographic techniques used to pattern HA on surfaces.....	78
Figure 4.7	Optical micrographs of molded HA films.....	79
Figure 4.8	Fluorescent micrographs for protein resistance and HA microstructures.....	82
Figure 4.9	Optical micrographs of cells on HA patterns.....	83
Figure 5.1	Schematic diagram of the HA-PLL layering approach to pattern co-cultures.....	91
Figure 5.2	Protein adsorption and cell adhesion to various surfaces.....	95
Figure 5.3	Cell and protein patterning of HA coated surfaces.....	96
Figure 5.4	PLL attachment on patterned HA surfaces and immobilized cells.....	98
Figure 5.5	Random Co-cultures of hepatocytes or ES cells with fibroblasts.....	100
Figure 5.6	Patterned co-cultures of ES cells with fibroblasts.....	101
Figure 6.1	Schematic diagram of the approach to pattern within microfluidic channels.....	112
Figure 6.2	Fluorescent images of the unprotected and protected sections patterned substrate exposed to oxygen plasma .....	117
Figure 6.3	Light micrograph and fluorescent images of patterned microfluidic channels.....	118
Figure 6.4	Fluorescent images of microfluidic channels in which laminar flow was used to immobilize two different proteins on the patterned substrate.....	120
Figure 6.5	NIH-3T3 fibroblast adhesion and patterning within microfluidic channels at $t = 0$ and after 6 hours.....	121
Figure 6.6	Light and fluorescent images of NIH-3T3 fibroblasts patterned on microfluidic channels that have been treated with ethidium homodimer and calcein AM.....	122
Figure 7.1	Schematic diagram for the fabrication of exposed and non-exposed microstructures inside microchannels.....	132
Figure 7.2	Scanning electron micrographs of molded PEG lanes or microwells.....	135
Figure 7.3	Light and fluorescent images of microstructures with non-exposed and exposed underlying substrates.....	136
Figure 7.4	NIH-3T3 cell adhesion of the non-exposed (a) and exposed (b) and PEG microwells.....	136
Figure 7.5	Cells flowing through microchannels could dock within microstructures of various sizes and shapes .....	138
Figure 7.6	NIH-3T3 cells were immobilized within microwells generated from PEG microstructures.....	139
Figure 7.7	NIH-3T3 cells were captured and adhered on channels with fibronectin coated substrates.....	140
Figure 8.1	Schematic diagram of reversible sealing of microfluidic arrays onto microwell patterned substrates to fabricate multiphenotype cell arrays.....	150
Figure 8.2	Leak-proof reversibly sealed microfluidic channels.....	152
Figure 8.3	Cell docking within microchannel arrays.....	154
Figure 8.4	Formation of multi-phenotype cell arrays on two-dimensional substrates or within microfluidic channels.....	156
Figure 8.5	Microfluidic arrays with upstream microfluidic mixers.....	157
Figure 9.1	The effects of flow rates on the mixing properties of tracer dye within each channel.....	165
Figure 9.2	Effects of flow rate on the gradients in the main channel.....	165
Figure 9.3	Schematic of the method used to model the microfluidic channel behavior.....	166
Figure 9.4	A microfluidic system was fabricated to generate stable concentration gradients of soluble molecules.....	167



Figure 9.5 Comparison between the experimental and the simulation results.....168  
Figure 9.6 Schematic of the channel used in the microfluidics/photopolymerization process...169  
Figure 9.7 Light micrographs of endothelial cells attached to the surface of hydrogels fabricated with various combinations of RGD peptide.....171  
Figure 9.8 SEM micrographs of cross-sections of dried hydrogels fabricated with varying polymer concentrations and cross-linking density.....172  
Figure 9.9 Fluorescent micrographs of rhodamine encapsulated in a gradient hydrogel of 10 wt% PEG4000DA to 50 wt% PEG1000DA immediately after polymerization .....173

## ABBREVIATIONS

Å	angstrom
Acr	acryloyl
Acr-PEG-RGDS	acryloyl-poly(ethylene glycol)-RGDS
AFM	atomic force microscopy
AIBN	2,2'-azobisisobutyronitrile
ANOVA	analysis of variance
ATCC	Advanced Type Culture Collection
BioMEMS	biological micro-electromechanical systems
BSA	bovine serum albumin
CO <sub>2</sub>	carbon dioxide
CFSE	carboxyfluorescein diacetate succinimidyl ester
CK	cytokeratin
CS A	chondroitin sulfate A
CS B	chondroitin sulfate B
D	daltons
DiH <sub>2</sub> O	deionized water
DMEM	Dulbecco's modified eagle medium
DMSO	dimethyl sulfoxide
DMPA	2,2-dimethoxy-2-phenylacetophenone
DS	dermatan sulfate
ECM	extracellular matrix
ES	embryonic stem
FACS	fluorescence activated cell sorting
FBS	fetal bovine serum
FITC	fluorescein
FITC-BSA	fluorescein Isothiocyanate-labelled bovine serum albumin
FTIR	Fourier transform infrared spectroscopy
FN	fibronectin
GPC	gel permeation chromatography
HA	hyaluronic acid
HBSS	Hank's balanced salt solution
HRP	horseradish peroxidase
HS	heparin sulfate
HUVECs	human umbilical vein endothelial cells
IgG	immunoglobulin G
MEM	minimum essential medium
MEMS	microelectro-mechanical systems
mL, ml	milliliter
MW	molecular weight
PBS	phosphate-buffered saline
PDMS	poly(dimethylsiloxane)
PE	phycoerythrin
PEG	poly(ethylene glycol)

PEG-4000DA	Poly(ethylene glycol)-4000 diacrylate
PEGDM	poly(ethylene glycol dimethacrylate)
PEGMA	poly(ethylene glycol) methyl ether methacrylate
PI	propidium iodide
PLL	poly-L-lysine
PM	polymeric monolayer
PSAM	polymeric self-assembled monolayer
ppm	parts per million
SAMs	self-assembled monolayers
SEM	scanning electron microscopy
THF	tetrahydrofuran
TPM	3-(trichlorosilyl)propyl methacrylate
TR-BSA	Texas red labeled bovine serum albumin
TMSMA	3-(trimethoxysilyl)propyl methacrylate
$\mu$ CP	microcontact printing
USA	United States of America
UV	ultraviolet

## THESIS SCOPE AND FORMAT

BioMEMS approaches were developed to control various aspects of the cell microenvironment including cell-cell, cell-ECM and cell-soluble signals. With the underlying premise that micro- and nanoscale engineering tools could be used to control cell behavior, **the objective of this thesis was to develop tools to control the various microenvironmental parameters with emphasis on making tools that can be easily used by biological labs.**

The thesis is divided into four sections (excluding introduction and outlook) comprised of ten chapters. Each chapter is written as a ‘complete story’ in order to allow the reader to quickly focus on a particular technology. Each of the four sections develops tools and approaches to control a specific aspect of the microenvironment of the cells. **Chapter 1** provides the background for the work and introduces the previous research regarding various aspects of the project. The next two chapters provide the contents for Section 1. ***Section 1*** introduces capillary force lithography (CFL) as a method of patterning substrates in order to localize cells within particular regions of a substrate. **Chapter 2** shows the use of photo-crosslinkable PEG molecules for patterning cells and proteins while **Chapter 3** demonstrates the synthesis and the use of a novel polymer that maximizes the power of CFL to fabricate features with various heights and shapes with simple modifications to the process. These approaches aim to control the location of cells of the same cell type relative to each other and to prevent cell adhesion. Another important aspect of the microenvironment is the cell-cell contact between different cell types. ***Section 2*** is comprised of the next two chapters. It discusses new approaches to localize cells relative to each other within patterned co-cultures. **Chapter 4** discusses surface modification and patterning approaches to immobilize various polysaccharides (including hyaluronic acid (HA)) on substrates by physical adsorption. **Chapter 5** provides a detailed account of the rationale and the method used to pattern cellular co-cultures based on the layer-by-layer deposition of ionic biopolymers. ***Section 3*** shows improved methods of interfacing cells within microdevices. **Chapter 6** provides the basis of simple soft lithographic approaches that can be used to pattern cells and proteins inside microchannels, while **Chapter 7** discusses the use of PEG microwells to capture and immobilize cells within specific regions of microfluidic channels. **Chapter 8** outlines the use of the techniques established in the previous chapters to fabricate arrays of cells containing multiple cell types. ***Section 4*** introduces new methods of controlling the interaction of cells with

hydrogels based on the merger of materials science and microengineering to fabricate gradients of molecules in hydrogels (as shown in **Chapter 9**). Finally, **Chapter 10** provides an outline of the conclusions and recommends directions for future work.

# 1. Introduction and Background

## MOTIVATION

Recently many scientific fields have changed significantly in the scale of information and experimental capability that is required. For example, each member of a chemical compound library, comprised of millions of members, must be tested to identify potential candidate drugs. In addition, the sequencing of the human genome and the need to minimize costly animal experiments and optimize drugs have greatly increased the need to test many different samples simultaneously. In addition to high-throughput experimentation, there is the emerging need to better engineer a cell's microenvironment in culture. In most culture systems, cells are removed from their natural environment and placed within an artificial environment which lacks the complexity and the architecture associated with tissues *in vivo*. In addition, cells in tissue culture are randomly organized, and therefore there is an inherent difference in the microenvironment of each cell.

One potential way to alleviate the need to perform high-throughput experimentation and to control cell microenvironment is through the use of micro- and nanoscale technologies. Micro- and nanoscale approaches miniaturize assays so that they can be performed in a high-throughput manner, with the potential of performing cost effective tests for many input and output parameters. In addition, such technology could be potentially used to control cell interaction with its environment at scales which are relevant for cell biology. The merger of such technologies and biological systems, including cells, has resulted in the formation of the field of biological microelectromechanical systems (BioMEMS). In this field, the tools that have been traditionally developed for microelectronics industry are applied to biological systems. BioMEMS is particularly important due to the inherent complexity of biological systems. For example, to understand cell behavior, the interaction of a cell with its microenvironment must be correlated to the expression and dynamics of the many proteins and genes that are expressed in the cell. Therefore, BioMEMS approaches could be used to tightly control a cell's environment and then analyze the cell's response with respect to dynamics and the level of expression of multiple genes.

This chapter will describe previously developed techniques that have been used to interface cells within microscale devices. The chapter will be divided into three sections. The first section discusses various elements of the cellular microenvironment and potential BioMEMS approaches used to control them. The second section describes techniques that have been developed to pattern substrates, while the third section focuses on previous work on interfacing cells within microchannels. It is important to note that since each chapter in this thesis contains detailed background information for specific applications, the aim of this chapter is to provide a broad overview of various technologies.

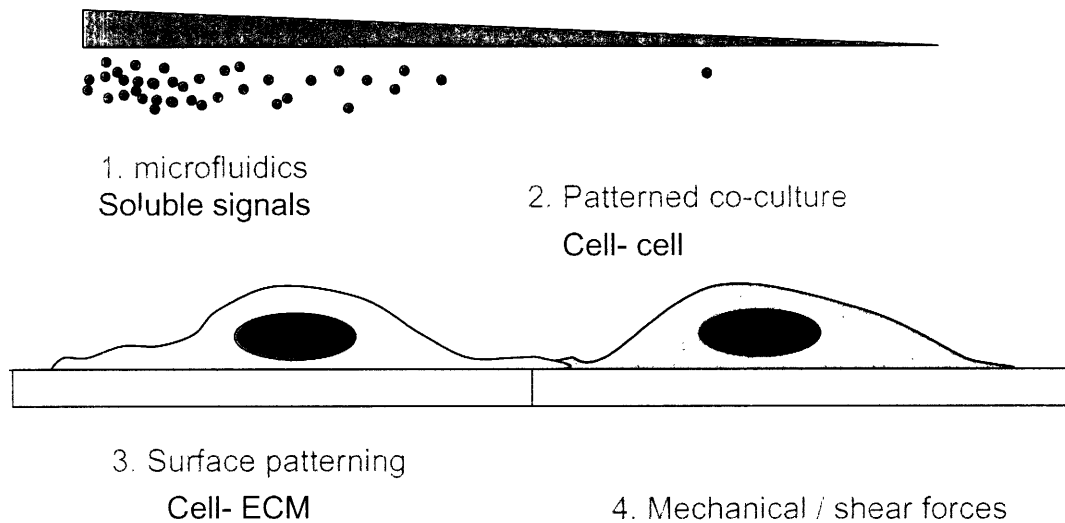


Figure 1.1. Various components of the cellular microenvironment and BioMEMS approaches that aim to control these parameters in culture.

## CELL MICROENVIRONMENT

*In vivo*, cells reside in a complex microenvironment characterized by their local geometry (structural and physicochemical), by specific types of surrounding tissue cells, and by soluble and ECM components<sup>1,2</sup>. The properties of this microenvironment are dynamic and depend on specific tissues and are affected by factors such as vascularization and loading. Importantly, our analysis and understanding of the role of the microenvironment on cell responses should be motivated by more than the desire to simply mimic the *in vivo* milieu. The *in vivo* microenvironment dynamically exposes cells to positive and negative regulators of specific cell responses – the selective application of these regulatory mechanisms during *in vitro* culture will

ultimately depend upon the type of cell response we want to elicit and our ability to control dominant (i.e., response-determining) culture parameters. One of the advantages of using BioMEMS approaches in regulating cell behavior is that the various aspects of a cell's microenvironment could be potentially engineered in a homogeneous and controlled manner. These microenvironmental factors include cell-extracellular matrix (ECM), cell-soluble factor and cell-cell interactions (**Figure 1.1**).

Cytokines and growth factors are important regulators of the tissue microenvironment. They are produced by cells and/or their neighboring cells in an autocrine or paracrine manner and often combine with other microenvironmental components to elicit non-linear responses (i.e. threshold-based<sup>3</sup> or synergistic responses). Another important factor is the interaction of a cell with its surrounding matrix. *In vivo*, cells are typically in direct contact with surrounding cells and ECM. ECM is a dynamic assembly of interacting molecules that recognizes and regulates cell function in response to endogenous and exogenous stimuli<sup>4</sup>. ECM is produced by cells and consists of collagens, proteoglycans, adhesive glycoproteins and glycoasaminoglycans and associated bound protein modulators of cell function. Along with providing a framework within which cells form tissues, ECM directly modulates cell attachment, shape, morphology, migration, orientation and proliferation. ECM also serves as a reservoir for various growth factors. It has been proposed that the existence of matrix is essential for the activity of many growth factors (such as HGF, TGF- $\beta$  and acidic and basic FGF)<sup>5</sup>. The complex combination of signals provided by the ECM provides the cell with information unique to the tissue of origin and is important for the regulation of various cell functions such as self-renewal, differentiation and homing. Further insight into understanding such signals will facilitate the design of culture technologies that mimic critical aspects of the *in vivo* microenvironment and facilitate better control over cell responses *in vitro*. Therefore, it is important to not only control the interaction of cells with ECM, but also to test various ECM combinations in order to control cell fate decisions in culture. BioMEMS approaches can be used to interface cells and expose them to many ECM combinations simultaneously<sup>6, 7</sup> or to control the presence of spatially oriented signals on cell behavior<sup>8, 9</sup>.



Cell-cell contact has also been shown to greatly influence cell behavior and function<sup>10-11</sup>. A comprehensive example of the importance of cell-cell interactions in the modulation of cell fate is in the hematopoietic stem cell (HSC) microenvironment. Although the presence of stromal cells and their interactions with HSCs has been known for a long time<sup>1,2,12-15</sup>, more recent studies have shown that direct contact between osteoblasts and HSCs is required for the maintenance of stem cell numbers *in vivo*<sup>16,17</sup>. Similar observations have been made regarding the role of cell-cell contact between fibroblasts and hepatocytes in maintaining hepatocyte function<sup>18-21</sup>. Therefore, methods in which the degree of homotypic and heterotypic cell-cell contact is controlled will be beneficial for a variety of cell based applications such as tissue engineering and drug discovery.

Another microenvironmental cue that influences the *in vivo* and *in vitro* responses of cells is mechanical stimuli. It has long been known that mechanical forces play an important role in the development and maintenance of vascular, muscle and bone tissues<sup>22-24</sup>. Mechanical stimuli may initiate mechanotransductive signaling pathways that are still largely unresolved<sup>25</sup>. For example, compressing marrow-derived stromal cells thought to contain mesenchymal stem cells (MSCs) encourages bone development, while stretching MSCs that have been immobilized in a matrix encourages tendon and cartilage formation<sup>26</sup>. Chapter 9 of this thesis provides a new approach that could be potentially useful in studying the mechanical forces on cells.

## **PATTERNING CELLS ON A CHIP**

Microfabrication techniques have been widely utilized for generating patterns of living cells on surfaces with potential applications in fundamental cell biology, tissue engineering, and cell-based bioelectronics. Cellular micropatterning enables the spatial control of cells in culture and the visualization of the effect of surface properties on cell functions. Many strategies have employed variations in surface charge, hydrophobicity, and topography to regulate cell functions such as attachment.

Typically top-down nano- and microfabrication methods have involved either photolithography or soft lithography to pattern substrates. Photolithography has been widely used for patterning cells and materials on hard materials<sup>20, 27-29</sup>. In one variation of this technique, materials of interest (e.g. poly-L-lysine (PLL), fibronectin (FN), or collagen) are patterned using a lift-off

technique. The material is applied on the photoresist pattern, and the photoresist is then removed from the substrate by sonication in acetone. Therefore, the desired pattern of the material to which cells are specifically bound is fabricated. The surface is then incubated with a solution of cells in suspension, and the desired cell pattern can be obtained. Alternatively, it is possible to place a mask directly above a thin film of a photo-crosslinkable material that is either cell-resistant or cell-adhesive. The pattern can then be generated by shining the UV light on particular regions of a substrate<sup>30-34</sup>. Although photolithography has been the main approach in making small features, it has disadvantages which include high costs associated with photolithographic equipment (aligners and spinners) and clean room usage, as well as the chemically harsh conditions that are not compatible with biomolecules.

Recently, a set of alternative techniques collectively called soft lithography has been developed which is widely applicable for biological applications<sup>32, 35</sup> (**Figure 1.2**). This technique which was pioneered by Whitesides and colleagues can be used to fabricate functional structures with dimensions in the range of tens of nanometers to hundreds of micrometers<sup>32, 35, 36</sup>. Soft lithographic approaches commonly utilized a microstructured surface made with an elastomeric material, poly(dimethylsiloxane) (PDMS) to generate patterns on surfaces. PDMS is optically transparent, permeable to gases, elastomeric, and durable which makes it also suitable for cell applications. PDMS structures are made by curing the prepolymer on previously fabricated masters. This master is typically a photoresist pattern, which is microfabricated by photolithography. However, after the initial step of photolithographic patterning, the subsequent fabrication steps can be performed in 'wet labs'. Therefore, soft lithographic approaches minimize the amount of clean room time and equipment that are required.

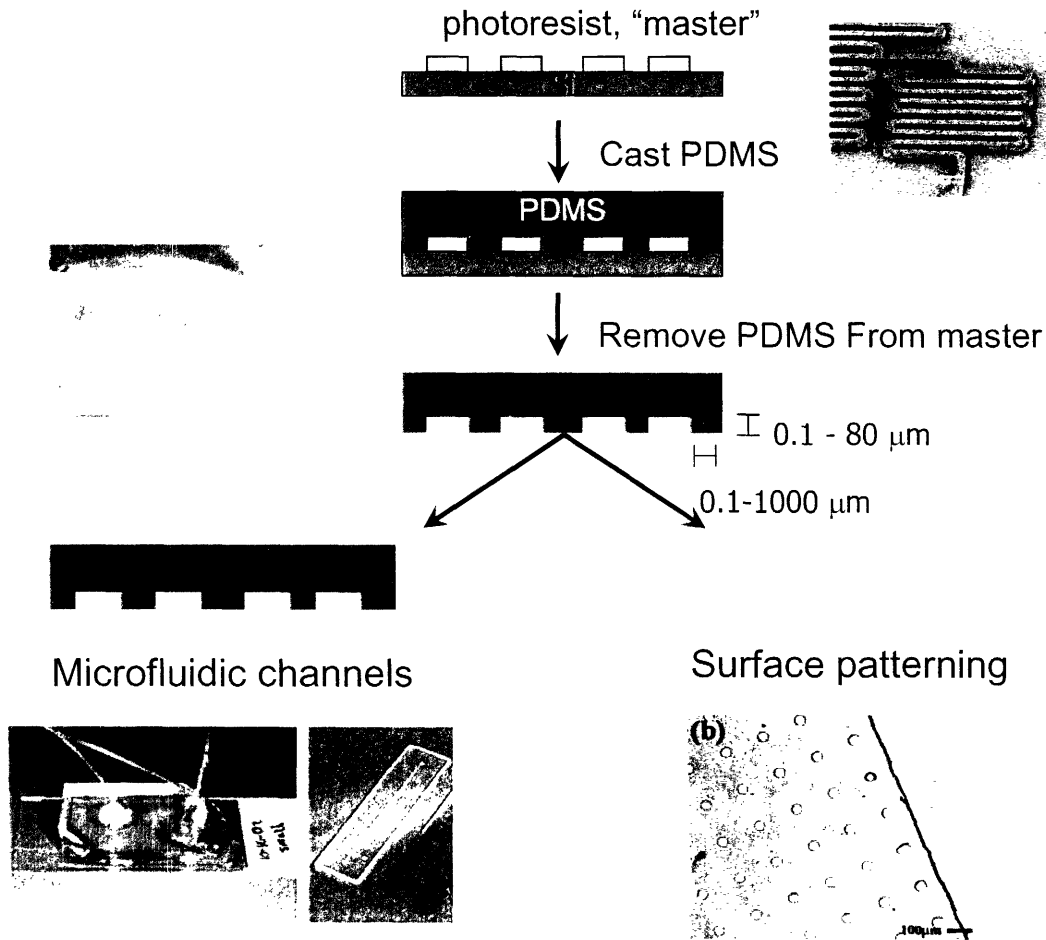


Figure 1.2. A schematic of the process of soft lithography for fabricating microfluidic channels and surface patterning.

The most commonly used soft lithographic method to modify surfaces for cell and protein patterning is microcontact printing ( $\mu$ CP). Microcontact printing is based on the pattern transfer of the material of interest from PDMS stamp onto the substrate surface<sup>37</sup> (**Figure 1.3**). Many protein and cell patterning studies using  $\mu$ CP have used self-assembled monolayers (SAMs) of alkanethiols on gold or silver<sup>37-41</sup>. The alkanethiol is transferred from the PDMS stamp onto the substrate surface. The bare areas of the substrate surface that the stamp has not contacted can then be exposed to other types of alkanethiol molecules (i.e. alkanethiols that are terminated with functional groups such as PEG). Patterned deposition of SAMs on surfaces can be used to control the adsorption of proteins and adhesion of cells. In addition, the direct transfer of cell-adhesive proteins (e.g. PLL and FN) from the PDMS stamp to non-metal surface such as glass and tissue culture dish can also be used to pattern substrates<sup>42-45</sup>. One potential limitation of

$\mu$ CP is the lack of control that is obtained in controlling surface topography. In most cases the resulting topographical features from microcontact printed surfaces are a few nanometers in size, which is much smaller than those generated using photolithographic patterning.

In addition to  $\mu$ CP, there are a number of other methods that have been developed. One such technique is microfluidic patterning in which a network of microchannels can selectively deliver the materials for cell adhesion or cell suspension to desired regions of a substrate<sup>36,46</sup>. By using this method, proteins can be immobilized only on the areas exposed to the protein solution, and cells can be selectively delivered to desired areas of a substrate<sup>47,48</sup>. Alternatively, a thin piece of material containing holes (stencil) can be used for patterning cells on surfaces. In this approach, a PDMS stencil is applied to the substrate before seeding cells<sup>49,50</sup>. The stencil is then used to selectively block cells from interacting with parts of the substrates that are covered by the PDMS stencil, while the other areas are left exposed. After cells are allowed to attach, the stencil is peeled off. Then, cellular islands that have the same shape as the stencil holes remain on the substrate. Both microfluidic and stencil patterning can be used to pattern cells, and the resulting patterns are stable. Electrochemistry is also an effective technique for patterning cells on surfaces, since it can be performed under mild cell culture conditions. Kaji *et al* have reported a cellular patterning technique using a microelectrode<sup>51</sup>. Since the cytophobic features of the substrate which are coated with a blocking agent (e.g., albumin) switch to cell-adhesive by exposure to an oxidizing agent, the micropatterns of living cells can be drawn by scanning the microelectrode closely on the substrate while electrogenerating the oxidizing agent. Mrksich and colleagues have developed a microcontact printing-based electrochemical method for *in situ* control of cell adhesion<sup>52, 53</sup>. The technique uses the electrochemical oxidation of a hydroquinone-terminated to a quinone-terminated SAM on a gold substrate. This step is followed by a Diels-Alder reaction to immobilize a cyclopentadiene-conjugated cell-adhesive peptide sequence to activated inert surface for the attachment of cells. Also, temperature-responsive polymers such as poly(*N*-isopropylacrylamide) (PIPAAm) are also useful for patterning cells<sup>34, 54,56</sup>. Yamato *et al* have reported the use of PIPAAm-patterned polystyrene substrate<sup>54</sup>. The PIPAAm-grafted surface exhibits dehydrated properties above this polymer's lower critical solution temperature (LCST, 32 °C), and hydrated properties below the LCST. Cells are allowed to adhere only to the PIPAAm-lacking polystyrene areas below the LCST.

After the culture temperature is increased over the LCST, the second cell type is allowed to attach to the PIPAAm-grafted areas. Although these technologies provide interesting methods of patterning cells on substrates, they are difficult to use since they require extensive expertise and materials typically inaccessible to most biologically-oriented laboratories.

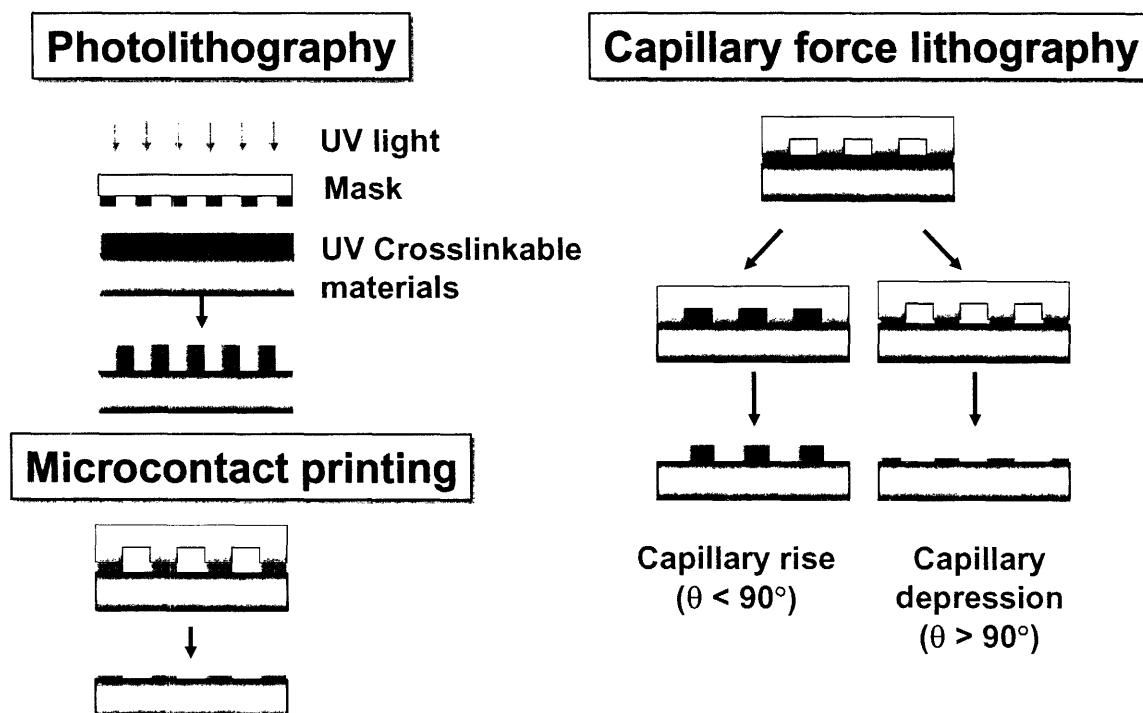


Figure 1.3. Schematic diagram of the process of photolithography, microcontact printing and capillary force lithography.

One of the aims of this thesis was to develop simple techniques to pattern cells on surfaces by using a combination of novel materials and unique patterning approaches. In order to do this, we focused on a technique called capillary force lithography. Details regarding this process will be described in chapters 2 and 3. This approach uses the surface and capillary force interactions between the patterning material and the PDMS stamp in order to control the shape of the desired patterns.

## CELLS AND MICROCHANNELS

In the last decade, there has been an increased interest in research on microfluidic systems, so-called Micro Total Analysis Systems ( $\mu$ TAS) or Lab-on-Chip, since they would provide a

powerful platform for a wide range of chemical and biological research fields. Initially, these approaches focused on miniaturization of analytical chemical methods for amino acids and DNA<sup>57-61</sup>. Then,  $\mu$ TAS have been used for protein analysis<sup>57,62</sup>. More recently, the new focus has been on using microfluidic systems for analysis of even more complex biological systems such as living cells. The use of microfluidic systems for biological assays and cell biology experimentation offer many advantages, including low requirements for solvents, reagents, and cells, short reaction times, portability, low cost and energy consumption, versatility in design, and potential for parallel operation and integration with other miniaturized devices.

Microfluidic systems take advantage of the laminar flow of fluids within narrow channels (<100  $\mu$ m) to allow for the formation of concentration gradients of soluble factors. For example, in a typical channel which is 50  $\mu$ m wide with a velocity of 0.6 cm/s, the Reynold's number (Re) is  $\sim$ 1. Typically, fluids with  $Re \ll 2000$  flow laminarily. Because of laminar flow, two fluid streams that flow into a common channel mix only by normal diffusion. Therefore, it is possible to have multiple streams entering a tube, each with distinct chemical properties<sup>32</sup>. This can be used to generate a gradient perpendicular to the direction of fluid flow<sup>63-67</sup>.

The ability to flow multiple laminarily flowing streams side-by-side provides a potential way of controlling cell microenvironment. Whitesides and others have used the laminar flow of fluids in microfluidics channels to create chemical gradients over individual cells<sup>47, 68, 69</sup>. This method can be used to study the subcellular processes by positioning the interface between two adjacent streams over a single adhered cell in the microchannel<sup>68</sup>. In addition, gradients can also be generated within microchannels. Gradients of molecules in solution having cell-attracting or repelling properties play an important role in a variety of biological processes. Gradients of complex shapes such as linear, parabolic and periodic shapes can be generated using microfluidic networks to control diffusive mixing of substances<sup>63, 64, 70</sup>. Jeon *et al* used a microfluidic gradient generator to investigate chemotaxis of neutrophils in response to various gradients of interleukin-8 (IL-8)<sup>70</sup>. In general, neutrophils migrate towards higher concentration of IL-8. However, in gradients where IL-8 concentration increased and decreased gradually (as opposed to increasingly gradually but decreasing suddenly), the cells would migrate towards and past the maximum concentration before finally returning to the area of maximum IL-8 concentration.

The gradient generator allowed studies of migratory cells under a variety of conditions not accessible by earlier techniques. Microfluidic systems have also been used for tissue engineering applications<sup>71-75</sup>. For example, Borenstein *et al* have used microfluidic systems to fabricate tissue engineering scaffolds. These scaffolds were successfully seeded with endothelial cells in the channels with dimensions as small as the capillaries.

Microfluidics may also reduce much of the possible transport limitations that are associated with static cultures. It is known that the oxygen and growth factor concentrations adjacent to cells may be considerably different from those of bulk fluid concentrations (particularly for metabolically active cells such as embryonic stem (ES) cells). The use of continuous streams allows for faster replenishment of the medium immediate to the cells. This will further allow for control of the cells' microenvironment.

To use microfluidics for miniaturizing assays or studying cell behavior, the spatial location of cells and proteins within microchannels must be controlled. The patterning of cells within microchannels requires the merger of the microfluidics and micropatterning techniques. Previous approaches to pattern microchannels have included laminar flow patterning<sup>47</sup> or photolithographic patterning. Each of these approaches has potential advantages and limitations. For example, although laminar flow patterning is simple, and it can be used to precisely localize the cells along the path of the fluid stream, the geometry of the patterns is limited to the geometry of the flowing streams. Also, even though photolithographic techniques have been used to pattern cells, proteins<sup>47</sup> or hydrogels<sup>76-78</sup>, direct the flow of liquids<sup>79, 80</sup>, as well as etch<sup>69</sup> or build microstructures<sup>69</sup> within microchannels, they have a number of disadvantages. These include potentially cytotoxicity of the photoinitiator<sup>81</sup>, the need for specialized equipment, and the difficulty in patterning the surface without modifying the surface topography<sup>76, 77</sup>. Therefore, the development of simple and direct techniques for fabricating microstructures within microchannels with precise control over the surface properties of the microstructures could be of benefit. This thesis describes techniques and tools that have been developed to solve some of these limitations. As can be seen in **Figure 1.4**, the merger of living cells on a chip is an interdisciplinary area. This approach has many potential applications which make the development of tools and technologies developed in this thesis valuable for many fields.

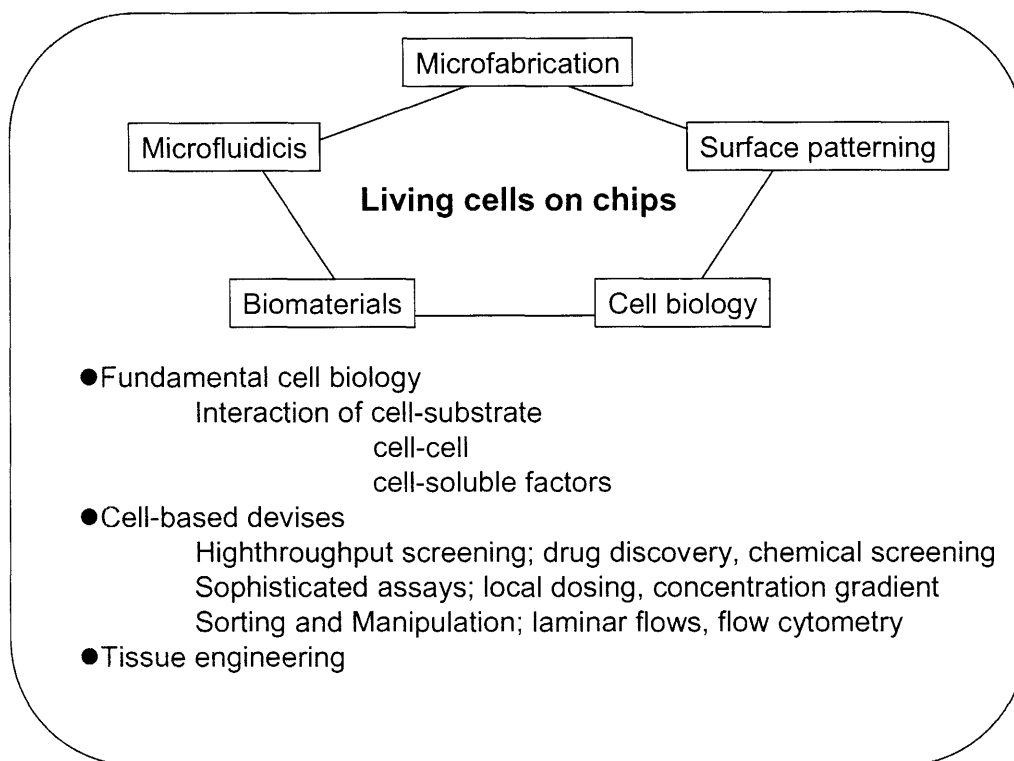


Figure 1.4 Technologies and disciplines relating to “living cells on chips”.



## REFERENCES

- (1) Koller, M. R.,Manchel, I.,Palsson, B. O. Importance of parenchymal:stromal cell ratio for the ex vivo reconstitution of human hematopoiesis. *Stem Cells*, **15**, 4, 1997.
- (2) Koller, M. R.,Bender, J. G.,Miller, W. M.,Papoutsakis, E. T. Expansion of primitive human hematopoietic progenitors in a perfusion bioreactor system with IL-3, IL-6, and stem cell factor. *Biotechnology (N Y)*, **11**, 3, 1993.
- (3) Zandstra, P. W.,Jervis, E.,Haynes, C. A.,Kilburn, D. G.,Eaves, C. J.,Piret, J. M. Concentration-dependent internalization of a cytokine/cytokine receptor complex in human hematopoietic cells. *Biotechnol Bioeng*, **63**, 4, 1999.
- (4) Slater, M. Dynamic interactions of the extracellular matrix. *Histol Histopathol*, **11**, 1, 1996.
- (5) Flaumenhaft, R.,Rifkin, D. B. Extracellular matrix regulation of growth factor and protease activity. *Curr Opin Cell Biol*, **3**, 5, 1991.
- (6) Flaim, C. J.,Chien, S.,Bhatia, S. N. An extracellular matrix microarray for probing cellular differentiation. *Nature Methods*, **2**, 2, 2005.
- (7) Anderson, D. G.,Levenberg, S.,Langer, R. Nanoliter-scale synthesis of arrayed biomaterials and application to human embryonic stem cells. *Nat Biotechnol*, **22**, 7, 2004.
- (8) Khademhosseini, A.,Suh, K. Y.,Jon, S.,Chen, G.,Eng, G.,Yeh, J.,Langer, R. A soft lithographic approach for fabricating patterned microfluidic channels. *Analytical Chemistry*, **76**, 13, 2004.
- (9) Burdick, J. A.,Khademhosseini, A.,Langer, R. Fabrication of gradient hydrogels using a microfluidics/photopolymerization process. *Langmuir*, **20**, 13, 2004.
- (10) Prosper, F.,Verfaillie, C. M. Regulation of hematopoiesis through adhesion receptors. *J Leukoc Biol*, **69**, 3, 2001.
- (11) Ploemacher, R. E.,Mayen, A. E.,De Koning, A. E.,Krenacs, T.,Rosendaal, M. Hematopoiesis: Gap Junction Intercellular Communication is Likely to be Involved in Regulation of Stroma-dependent Proliferation of Hemopoietic Stem Cells. *Hematol*, **5**, 2, 2000.
- (12) Gupta, P.,McCarthy, J. B.,Verfaillie, C. M. Stromal fibroblast heparan sulfate is required for cytokine-mediated ex vivo maintenance of human long-term culture-initiating cells. *Blood*, **87**, 8, 1996.

- (13) Gupta, P., Oegema, T. R., Jr., Brazil, J. J., Dudek, A. Z., Slungaard, A., Verfaillie, C. M. Structurally specific heparan sulfates support primitive human hematopoiesis by formation of a multimolecular stem cell niche. *Blood*, **92**, 12, 1998.
- (14) Verfaillie, C. M., Benis, A., Iida, J., McGlave, P. B., McCarthy, J. B. Adhesion of committed human hematopoietic progenitors to synthetic peptides from the C-terminal heparin-binding domain of fibronectin: cooperation between the integrin alpha 4 beta 1 and the CD44 adhesion receptor. *Blood*, **84**, 6, 1994.
- (15) Muller-Sieburg, C. E., Deryugina, E. The stromal cells' guide to the stem cell universe. *Stem Cells*, **13**, 5, 1995.
- (16) Zhang, J., Niu, C., Ye, L., Huang, H., He, X., Tong, W. G., Ross, J., Haug, J., Johnson, T., Feng, J. Q., Harris, S., Wiedemann, L. M., Mishina, Y., Li, L. Identification of the haematopoietic stem cell niche and control of the niche size. *Nature*, **425**, 6960, 2003.
- (17) Calvi, L. M., Adams, G. B., Weibrecht, K. W., Weber, J. M., Olson, D. P., Knight, M. C., Martin, R. P., Schipani, E., Divieti, P., Bringhurst, F. R., Milner, L. A., Kronenberg, H. M., Scadden, D. T. Osteoblastic cells regulate the haematopoietic stem cell niche. *Nature*, **425**, 6960, 2003.
- (18) Bhatia, S. N., Balis, U. J., Yarmush, M. L., Toner, M. Probing heterotypic cell interactions: hepatocyte function in microfabricated co-cultures. *J Biomater Sci Polym Ed*, **9**, 11, 1998.
- (19) Bhatia, S. N., Balis, U. J., Yarmush, M. L., Toner, M. Microfabrication of hepatocyte/fibroblast co-cultures: role of homotypic cell interactions. *Biotechnol Prog*, **14**, 3, 1998.
- (20) Bhatia, S. N., Balis, U. J., Yarmush, M. L., Toner, M. Effect of cell-cell interactions in preservation of cellular phenotype: cocultivation of hepatocytes and nonparenchymal cells. *Faseb J*, **13**, 14, 1999.
- (21) Bhatia, S. N. Customizing cellular microenvironments for hepatic tissue engineering. *Abstracts of Papers of the American Chemical Society*, **221**, 2001.
- (22) Li, C., Xu, Q. Mechanical stress-initiated signal transductions in vascular smooth muscle cells. *Cell Signal*, **12**, 7, 2000.
- (23) Burger, E. H., Klein-Nulén, J. Responses of bone cells to biomechanical forces in vitro. *Adv Dent Res*, **13**, 1999.

- (24) Fisher, A. B.,Chien, S.,Barakat, A. I.,Nerem, R. M. Endothelial cellular response to altered shear stress. *Am J Physiol Lung Cell Mol Physiol*, **281**, 3, 2001.
- (25) Ingber, D. E. Integrins, tensegrity, and mechanotransduction. *Gravit Space Biol Bull*, **10**, 2, 1997.
- (26) Pittenger, M. F.,Mackay, A. M.,Beck, S. C.,Jaiswal, R. K.,Douglas, R.,Mosca, J. D.,Moorman, M. A.,Simonetti, D. W.,Craig, S.,Marshak, D. R. Multilineage potential of adult human mesenchymal stem cells. *Science*, **284**, 5411, 1999.
- (27) Britland, S.,Clark, P.,Connolly, P.,Moores, G. Micropatterned substratum adhesiveness: a model for morphogenetic cues controlling cell behavior. *Exp Cell Res*, **198**, 1, 1992.
- (28) Kleinfeld, D.,Kahler, K. H.,Hockberger, P. E. Controlled outgrowth of dissociated neurons on patterned substrates. *J Neurosci*, **8**, 11, 1988.
- (29) Healy, K. E.,Thomas, C. H.,Rezania, A.,Kim, J. E.,McKeown, P. J.,Lom, B.,Hockberger, P. E. Kinetics of bone cell organization and mineralization on materials with patterned surface chemistry. *Biomaterials*, **17**, 2, 1996.
- (30) Revzin, A.,Russell, R. J.,Yadavalli, V. K.,Koh, W. G.,Deister, C.,Hile, D. D.,Mellott, M. B.,Pishko, M. V. Fabrication of poly(ethylene glycol) hydrogel microstructures using photolithography. *Langmuir*, **17**, 18, 2001.
- (31) Koh, W. G.,Revzin, A.,Simonian, A.,Reeves, T.,Pishko, M. Control of mammalian cell and bacteria adhesion on substrates micropatterned with poly(ethylene glycol) hydrogels. *Biomedical Microdevices*, **5**, 1, 2003.
- (32) Whitesides, G. M.,Ostuni, E.,Takayama, S.,Jiang, X.,Ingber, D. E. Soft lithography in biology and biochemistry. *Annu Rev Biomed Eng*, **3**, 2001.
- (33) Koh, W. G.,Revzin, A.,Pishko, M. V. Poly(ethylene glycol) hydrogel microstructures encapsulating living cells. *Langmuir*, **18**, 7, 2002.
- (34) Ito, Y.,Chen, G. P.,Guan, Y. Q.,Imanishi, Y. Patterned immobilization of thermoresponsive polymer. *Langmuir*, **13**, 10, 1997.
- (35) Xia, Y. N.,Whitesides, G. M. Soft lithography. *Angewandte Chemie-International Edition*, **37**, 5, 1998.
- (36) Kane, R. S.,Takayama, S.,Ostuni, E.,Ingber, D. E.,Whitesides, G. M. Patterning proteins and cells using soft lithography. *Biomaterials*, **20**, 23-24, 1999.

- (37) Kumar, A., Whitesides, G. M. Features of Gold Having Micrometer to Centimeter Dimensions Can Be Formed through a Combination of Stamping with an Elastomeric Stamp and an Alkanethiol Ink Followed by Chemical Etching. *Applied Physics Letters*, **63**, 14, 1993.
- (38) Mrksich, M., Dike, L. E., Tien, J., Ingber, D. E., Whitesides, G. M. Using microcontact printing to pattern the attachment of mammalian cells to self-assembled monolayers of alkanethiolates on transparent films of gold and silver. *Exp Cell Res*, **235**, 2, 1997.
- (39) Chen, C. S., Mrksich, M., Huang, S., Whitesides, G. M., Ingber, D. E. Geometric control of cell life and death. *Science*, **276**, 5317, 1997.
- (40) Singhvi, R., Kumar, A., Lopez, G. P., Stephanopoulos, G. N., Wang, D. I., Whitesides, G. M., Ingber, D. E. Engineering cell shape and function. *Science*, **264**, 5159, 1994.
- (41) Lopez, G. P., Albers, M. W., Schreiber, S. L., Carroll, R., Peralta, E., Whitesides, G. M. Convenient Methods for Patterning the Adhesion of Mammalian-Cells to Surfaces Using Self-Assembled Monolayers of Alkanethiolates on Gold. *Journal of the American Chemical Society*, **115**, 13, 1993.
- (42) Nishizawa, M., Takoh, K., Matsue, T. Micropatterning of HeLa cells on glass substrates and evaluation of respiratory activity using microelectrodes. *Langmuir*, **18**, 9, 2002.
- (43) Yeung, C. K., Lauer, L., Offenhausser, A., Knoll, W. Modulation of the growth and guidance of the rat brain stem neurons using patterned extracellular matrix proteins (vol 301, pg 147, 2001). *Neuroscience Letters*, **305**, 3, 2001.
- (44) Branch, D. W., Wheeler, B. C., Brewer, G. J., Leckband, D. E. Long-term maintenance of patterns of hippocampal pyramidal cells on substrates of polyethylene glycol and microstamped polylysine. *IEEE Trans Biomed Eng*, **47**, 3, 2000.
- (45) James, C. D., Davis, R., Meyer, M., Turner, A., Turner, S., Withers, G., Kam, L., Banker, G., Craighead, H., Isaacson, M., Turner, J., Shain, W. Aligned microcontact printing of micrometer-scale poly-L-lysine structures for controlled growth of cultured neurons on planar microelectrode arrays. *Ieee Transactions on Biomedical Engineering*, **47**, 1, 2000.
- (46) Folch, A., Toner, M. Cellular micropatterns on biocompatible materials. *Biotechnol Prog*, **14**, 3, 1998.

- (47) Takayama, S., McDonald, J. C., Ostuni, E., Liang, M. N., Kenis, P. J. A., Ismagilov, R. F., Whitesides, G. M. Patterning cells and their environments using multiple laminar fluid flows in capillary networks. *Proc Natl Acad Sci U S A*, **96**, 10, 1999.
- (48) Folch, A., Ayon, A., Hurtado, O., Schmidt, M. A., Toner, M. Molding of deep polydimethylsiloxane microstructures for microfluidics and biological applications. *J Biomech Eng*, **121**, 1, 1999.
- (49) Ostuni, E., Kane, R., Chen, C. S., Ingber, D. E., Whitesides, G. M. Patterning mammalian cells using elastomeric membranes. *Langmuir*, **16**, 20, 2000.
- (50) Folch, A., Jo, B. H., Hurtado, O., Beebe, D. J., Toner, M. Microfabricated elastomeric stencils for micropatterning cell cultures. *J Biomed Mater Res*, **52**, 2, 2000.
- (51) Kaji, H., Kanada, M., Oyamatsu, D., Matsue, T., Nishizawa, M. Microelectrochemical approach to induce local cell adhesion and growth on substrates. *Langmuir*, **20**, 1, 2004.
- (52) Yousaf, M. N., Houseman, B. T., Mrksich, M. Turning on cell migration with electroactive substrates. *Angewandte Chemie-International Edition*, **40**, 6, 2001.
- (53) Yeo, W. S., Yousaf, M. N., Mrksich, M. Dynamic interfaces between cells and surfaces: electroactive substrates that sequentially release and attach cells. *J Am Chem Soc*, **125**, 49, 2003.
- (54) Yamato, M., Konno, C., Utsumi, M., Kikuchi, A., Okano, T. Thermally responsive polymer-grafted surfaces facilitate patterned cell seeding and co-culture. *Biomaterials*, **23**, 2, 2002.
- (55) Chen, G., Imanishi, Y., Ito, Y. Effect of protein and cell behavior on pattern-grafted thermoresponsive polymer. *J Biomed Mater Res*, **42**, 1, 1998.
- (56) Hirose, M., Kwon, O. H., Yamato, M., Kikuchi, A., Okano, T. Creation of designed shape cell sheets that are noninvasively harvested and moved onto another surface. *Biomacromolecules*, **1**, 3, 2000.
- (57) Auroux, P. A., Iossifidis, D., Reyes, D. R., Manz, A. Micro total analysis systems. 2. Analytical standard operations and applications. *Anal Chem*, **74**, 12, 2002.
- (58) Reyes, D. R., Iossifidis, D., Auroux, P. A., Manz, A. Micro total analysis systems. 1. Introduction, theory, and technology. *Anal Chem*, **74**, 12, 2002.

- (59) Simpson, P. C., Roach, D., Woolley, A. T., Thorsen, T., Johnston, R., Sensabaugh, G. F., Mathies, R. A. High-throughput genetic analysis using microfabricated 96-sample capillary array electrophoresis microplates. *Proc Natl Acad Sci U S A*, **95**, 5, 1998.
- (60) Liu, S., Shi, Y., Ja, W. W., Mathies, R. A. Optimization of high-speed DNA sequencing on microfabricated capillary electrophoresis channels. *Anal Chem*, **71**, 3, 1999.
- (61) Harrison, D. J., Fluri, K., Seiler, K., Fan, Z. H., Effenhauser, C. S., Manz, A. Micromachining a Miniaturized Capillary Electrophoresis-Based Chemical-Analysis System on a Chip. *Science*, **261**, 5123, 1993.
- (62) Lion, N., Rohner, T. C., Dayon, L., Arnaud, I. L., Damoc, E., Youhnovski, N., Wu, Z. Y., Roussel, C., Jossierand, J., Jensen, H., Rossier, J. S., Przybylski, M., Girault, H. H. Microfluidic systems in proteomics. *Electrophoresis*, **24**, 21, 2003.
- (63) Jeon, N. L., Dertinger, S. K. W., Chiu, D. T., Choi, I. S., Stroock, A. D., Whitesides, G. M. Generation of solution and surface gradients using microfluidic systems. *Langmuir*, **16**, 22, 2000.
- (64) Dertinger, S. K. W., Chiu, D. T., Jeon, N. L., Whitesides, G. M. Generation of gradients having complex shapes using microfluidic networks. *Analytical Chemistry*, **73**, 6, 2001.
- (65) Kamholz, A. E., Weigl, B. H., Finlayson, B. A., Yager, P. Quantitative analysis of molecular interaction in a microfluidic channel: The T-sensor. *Analytical Chemistry*, **71**, 23, 1999.
- (66) Weigl, B. H., Yager, P. Microfluidics - Microfluidic diffusion-based separation and detection. *Science*, **283**, 5400, 1999.
- (67) Macounova, K., Cabrera, C. R., Holl, M. R., Yager, P. Generation of natural pH gradients in microfluidic channels for use in isoelectric focusing. *Analytical Chemistry*, **72**, 16, 2000.
- (68) Takayama, S., Ostuni, E., LeDuc, P., Naruse, K., Ingber, D. E., Whitesides, G. M. Subcellular positioning of small molecules. *Nature*, **411**, 6841, 2001.
- (69) Kenis, P. J. A., Ismagilov, R. F., Whitesides, G. M. Microfabrication inside capillaries using multiphase laminar flow patterning. *Science*, **285**, 5424, 1999.
- (70) Jeon, N. L., Baskaran, H., Dertinger, S. K. W., Whitesides, G. M., Van de Water, L., Toner, M. Neutrophil chemotaxis in linear and complex gradients of interleukin-8 formed in a microfabricated device. *Nature Biotechnology*, **20**, 8, 2002.

- (71) Andersson, H., van den Berg, A. Microfabrication and microfluidics for tissue engineering: state of the art and future opportunities. *Lab Chip*, **4**, 2, 2004.
- (72) Kaihara, S., Borenstein, J., Koka, R., Lalan, S., Ochoa, E. R., Ravens, M., Pien, H., Cunningham, B., Vacanti, J. P. Silicon micromachining to tissue engineer branched vascular channels for liver fabrication. *Tissue Engineering*, **6**, 2, 2000.
- (73) Borenstein, J. T., Terai, H., King, K. R., Weinberg, E. J., Kaazempur-Mofrad, M. R., Vacanti, J. P. Microfabrication technology for vascularized tissue engineering. *Biomedical Microdevices*, **4**, 3, 2002.
- (74) Powers, M. J., Domansky, K., Kaazempur-Mofrad, M. R., Kalezi, A., Capitano, A., Upadhyaya, A., Kurzawski, P., Wack, K. E., Stolz, D. B., Kamm, R., Griffith, L. G. A microfabricated array bioreactor for perfused 3D liver culture. *Biotechnol Bioeng*, **78**, 3, 2002.
- (75) Tilles, A. W., Berthiaume, F., Yarmush, M. L., Tompkins, R. G., Toner, M. Bioengineering of liver assist devices. *J Hepatobiliary Pancreat Surg*, **9**, 6, 2002.
- (76) Zhan, W., Seong, G. H., Crooks, R. M. Hydrogel-based microreactors as a functional component of microfluidic systems. *Analytical Chemistry*, **74**, 18, 2002.
- (77) Heo, J., Thomas, K. J., Seong, G. H., Crooks, R. M. A microfluidic bioreactor based on hydrogel-entrapped *E. coli*: Cell viability, lysis, and intracellular enzyme reactions. *Analytical Chemistry*, **75**, 1, 2003.
- (78) Beebe, D. J., Moore, J. S., Bauer, J. M., Yu, Q., Liu, R. H., Devadoss, C., Jo, B. H. Functional hydrogel structures for autonomous flow control inside microfluidic channels. *Nature*, **404**, 6778, 2000.
- (79) Zhao, B., Moore, J. S., Beebe, D. J. Surface-directed liquid flow inside microchannels. *Science*, **291**, 5506, 2001.
- (80) Zhao, B., Moore, J. S., Beebe, D. J. Principles of surface-directed liquid flow in microfluidic channels. *Analytical Chemistry*, **74**, 16, 2002.
- (81) Liu, V. A., Bhatia, S. N. Three-dimensional photopatterning of hydrogels containing living cells. *Biomedical Microdevices*, **4**, 4, 2002.

## **2. Soft lithographic fabrication of poly(ethylene glycol) microstructures for protein and cell patterning using capillary force lithography**

### **INTRODUCTION**

Conventional methods for creating microscopic structures and patterns using microfabrication technologies have been successfully applied to protein or cell patterning because they can provide the ability to spatially control protein or cell adhesion. Although photolithography is one of the most established techniques for microfabrication, its usage is restricted by the harsh conditions that must be carried out<sup>1</sup>. A more biocompatible method is the photolithographic patterning of poly(ethylene glycol) (PEG) hydrogels, which generally involves three steps: spin-coating of a PEG solution onto a substrate, exposing the gel precursor through a photomask, and then development using solvents such as water, toluene, or supercritical CO<sub>2</sub><sup>2-4</sup>. Using this process, PEG microstructures have been successfully used to fabricate enzyme electrodes<sup>2</sup>, pH sensitive microelectro-mechanical system (MEMS) devices<sup>3</sup>, and optical sensors<sup>4</sup>. However, photolithography is complicated and expensive and therefore alternative techniques that allow widespread use of such techniques is desirable.

Soft lithography is the collective name for a set of lithographic techniques that involve the use of an elastomer such as poly(dimethylsiloxane) (PDMS). To transfer biomolecules and modify surfaces to a negative relief of the pattern, a number of soft lithographic techniques have been used including microfluidic networking<sup>5-7</sup>, micromolding in capillaries<sup>5,8</sup> and microcontact printing ( $\mu$ CP)<sup>9-13</sup>. Of these, self-assembled monolayers (SAMs) terminated with PEG chains



have been extensively used in  $\mu$ CP to immobilize biological species such as proteins or cells. This technique involves selective modification of surfaces with a non-biofouling agent like PEG<sup>14, 15</sup>, allowing the creation of patterned surfaces.

A number of other methods have also been developed to generate patterns of proteins and cells on surfaces. These methods include membrane-based lift-off<sup>16</sup>, polymer template using  $\mu$ CP<sup>17-20</sup>, manipulation of surface charge<sup>21</sup>, hydrophilicity<sup>21</sup>, and topography<sup>22</sup>.

Although  $\mu$ CP is relatively simple and versatile for micropatterning, it cannot provide control over topographical surface. To obtain topographical patterns, microfluidic networking or micromolding in capillaries can be used. However, these techniques are limited in that the mold should have a network structure and feature sizes below 1  $\mu$ m are difficult to fabricate<sup>23</sup>.

In this chapter, a new technique in the form of capillary force lithography (CFL)<sup>24, 25</sup>, which is based on the capillarity and wettability of the polymer within the stamp is introduced. In comparison to  $\mu$ CP, the molded PEG structure acts as a physical and chemical barrier for the adhesion of proteins and cells. Such a barrier shows a unique regulation of surface patterning. Furthermore, capillary force lithography provides a general platform for patterning a broad range of materials since it can be applied to various substrates such as glass, silicon, silicon dioxide and polymer surfaces. As a result, it may be a valuable tool to fabricate protein chips and high-throughput cell screening devices, since the feature size can be easily controlled (~500 nm to ~500  $\mu$ m) on a large area with suitably prepared PDMS molds.

## **MATERIALS AND METHODS**

*PDMS stamp fabrication:* PDMS stamps were fabricated by casting PDMS (Sylgard 184 Silicon elastomer, Essex Chemical) against a complementary relief structure prepared by photolithographic method. To cure, a 1:10 ratio of the curing agent and the pre-polymer were mixed and incubated at 70 °C for 1 hour. The PDMS mold was then peeled off from the silicon wafer and cut prior to use. The stamps had protruding (positive) features with the lateral dimension ranging from 10 to 500  $\mu\text{m}$ .

*Patterning of PEG films:* Silicon and glass were used as the substrate. Prior to spin-coating, the substrates were cleaned by rinsing with acetone and ethanol several times to remove excess organic molecules and dried in nitrogen. Four different concentrations of PEGDM dissolved in methanol (20, 50, 80, and 100 wt% or pure polymer) were prepared. 1 wt % of the UV initiator (2,2-dimethoxy-2-phenylacetophenone (DMPA), Aldrich) with respect to the amount of polymer was added in the solutions. The solution of PEGDM was then spin-coated (Model CB 15, Headaway Research, Inc.) onto a substrate at 3000 rpm for 10 seconds. The film thickness ranged from 300 nm to 2  $\mu\text{m}$  as measured by ellipsometry. The patterned PDMS stamp was carefully placed onto the surface to make conformal contact<sup>25</sup> and the sample was placed under a 365 nm, 15 mW/cm<sup>2</sup> low-power Black-light inspection lamp (ELC-251, Electro-Lite Corp.) for crosslinking.

*Protein adsorption:* Fluorescein isothiocyanate-labelled bovine serum albumin (FITC-BSA) and fibronectin (FN) (Sigma) were dissolved in 10 mM phosphate buffer saline (PBS) (Sigma)

solution (pH = 7.4; 10 mM sodium phosphate buffer, 2.7 mM KCl, and 137 mM NaCl) at a concentration of 250  $\mu\text{g}/\text{mL}$  and 100  $\mu\text{g}/\text{mL}$ , respectively. A few drops of the protein solution was evenly distributed onto the patterned substrates and stored at room temperature for 30 min. The patterned substrates were rinsed with PBS solution and water, and blown dry in a stream of nitrogen and then directly analyzed under fluorescent microscope (Axiovert 200, Zeiss).

*Cell cultures:* NIH-3T3 murine embryonic fibroblasts (Advanced Type Culture Collection (ATCC)) were maintained in Dulbecco's modified eagle medium (DMEM) (Gibco Invitrogen Corp.) supplemented with 10 % fetal bovine serum (FBS) (Gibco Invitrogen Corp.) at 37 °C and 5% CO<sub>2</sub> environment. Once the cells were confluent, they were trypsinized (0.25% in EDTA, Sigma) and passaged at a 1:5 subculture ratio. To pattern fibronectin onto PEG patterned or control surfaces, glasses were treated with 100  $\mu\text{g}/\text{mL}$  of fibronectin in PBS for 20 minutes. The surfaces were then washed with PBS to remove excess solution from the surfaces. NIH-3T3 cells suspended in medium at a concentration of  $1 \times 10^6$  cells/mL were then plated on to the surfaces. To analyze, glass slides were rinsed with PBS to remove non-adhered cells from the non-adhered regions.

## RESULTS AND DISCUSSIONS

To fabricate a PEG film onto a substrate and to prevent the immobilized PEG from dissolving in water, we used a low molecular weight PEG dimethacrylate (PEGDM, Mw = 330) because it enables a high crosslinking density. A modified form of capillary force lithography was used (**Figure 2.1**) compared to the previously reported results<sup>24, 25</sup>. When a polymer film is mobile (i.e., above glass transition temperature) and is in conformal contact with a patterned PDMS

stamp, capillary forces move the polymer into the void space of the stamp, resulting in a negative

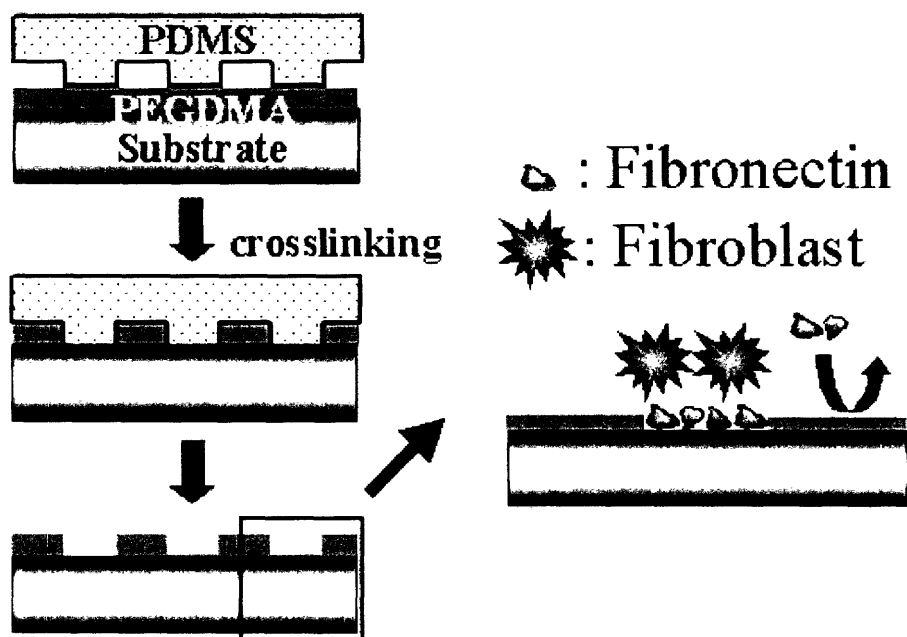


Figure 2.1. Schematic diagram of the PEG patterning experimental procedure. Initially, a uniform PEGDM film is prepared by spin-coating and then molded by capillary force lithography. This pattern is utilized for subsequent protein and cell patterning using PEGDM as the blocking layer.

replica of the stamp. When a hydrophobic polymer is used such as polystyrene or poly(styrene-butadiene-styrene) copolymer, the polymer partially wets the hydrophobic PDMS wall (acute contact angle), thus rising into the void space<sup>24</sup>. On the other hand, capillary rise will be depressed within a void space if the contact angle is larger than  $90^\circ$  (capillary depression) (**Figure 2.2**). In capillary force lithography, the polymer in contact with the stamp gets depleted during the capillary rise and finally the substrate surface becomes exposed as shown in **Figure 2.1**. As expected, this is only possible when the polymer is relatively thin with respect to the mold's step height. The resulting patterned substrates consist of two regions: first the molded PEGDM surface that acts as a resistant layer and second, the exposed substrate surface that promotes protein or cell adsorption. Contact angle measurements of PEGDM on a fresh PDMS

stamp ( $\sim 65^\circ$ ) show that PEGDM is slightly hydrophilic and mobile on the PDMS surface such that the substrate surface can be easily exposed in comparison to hydrophobic polystyrene<sup>24</sup>.

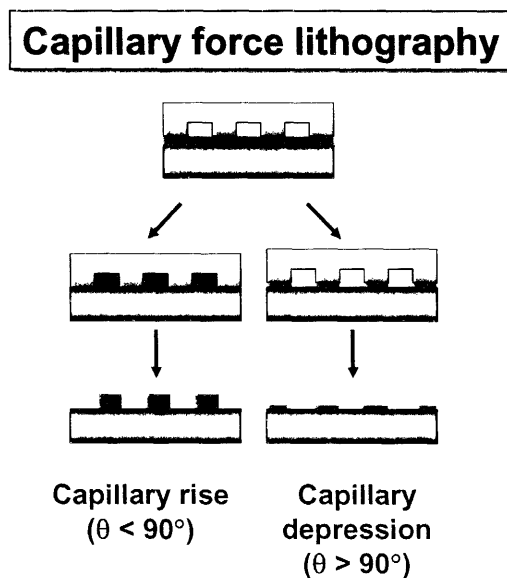


Figure 2.2. Schematic diagram of the effect of mold / polymer surface interactions on desired structures.

To pattern the substrates using capillary force lithography, a PDMS stamp was directly placed onto a wet polymer surface. This technique generally consists of three steps: placing a patterned PDMS stamp on the surface of a spin-coated polymer film, allowing the stamp to absorb solvent, and then letting the stamp and the substrate remain undisturbed for a period of time in order to facilitate drying or to crosslink the polymer. The microstructure thus formed shows high pattern fidelity without distortions or defects<sup>25</sup>.

To pattern the surfaces, a PDMS stamp was directly placed onto the polymer surface after spin coating for only 10 seconds to make a wet film (i.e., PEG + methanol), forming a conformal contact with the surface. As the solvent evaporates, PEGDM in contact with the protruding PDMS features spontaneously recedes and moves into the void space of the PDMS mold by

means of capillary action. According to a previous report<sup>25</sup>, this capillary action is completed within a few minutes. Because of the hydrophilic nature of PEGDM, it is expected that the substrate surface would be easily exposed on a hydrophobic substrate such as polymer or clean silicon wafer. In this case, the repelling forces at the PEGDM/substrate interface facilitate the mass transfer, squeezing the film under the contact region into the adjacent regions. However, it was observed that relatively hydrophilic substrate surfaces such as silicon dioxide and glass could also be exposed as confirmed by optical microscopy and atomic force microscopy (AFM), which indicates that solvent evaporation appears to play a crucial role in mass transfer. No dewetting takes place in spite of the large contact angle because the polymer is confined within the PDMS stamp and the mobility of the polymer is not sufficient to give rise to dewetting. Once the solvent is fully evaporated, the cured PEG layer acts as a barrier, or as a confined wall for adsorbed proteins or cells. The aspect ratio of barriers can be controlled using different film thicknesses for a given feature size of the PDMS stamp.

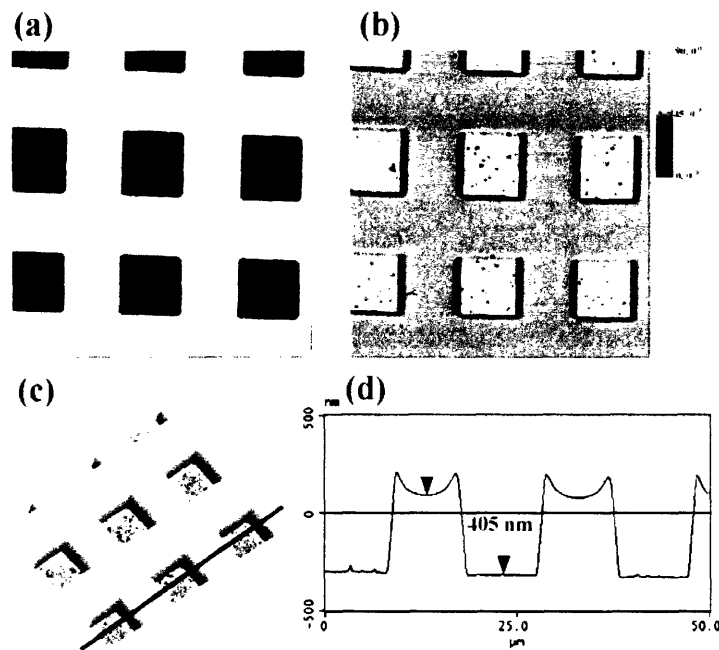
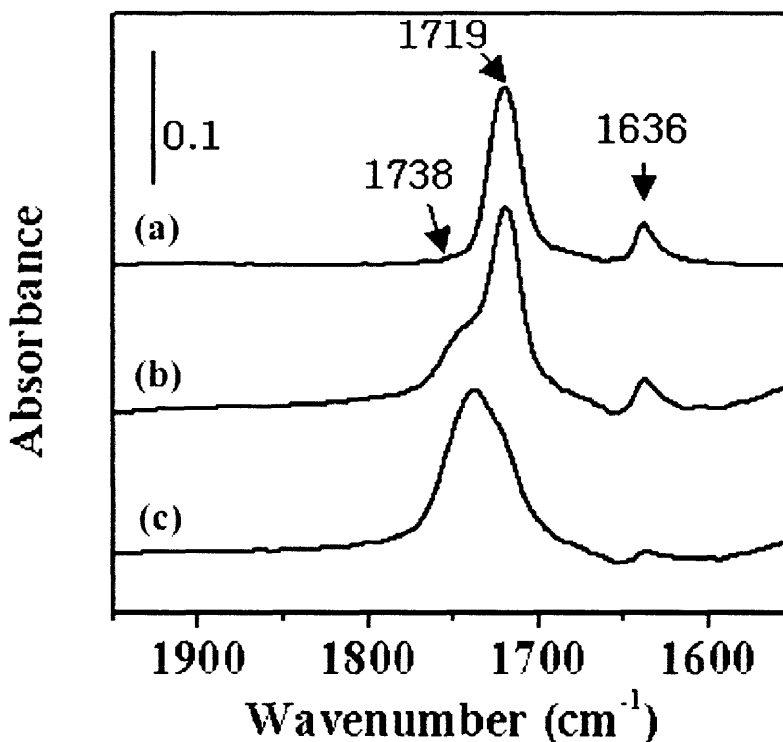


Figure 2.3 AFM images of patterned PEG microstructures. Two-dimensional height (a) and phase (b) images of a molded PEGDM film for 10  $\mu\text{m}$  box pattern. A sharp contrast in the phase image indicates that the substrate surface is completely exposed. (c) A three-dimensional presentation of (a) and (d) a cross-sectional view of the line in (c). The scan size is 50 $\times$ 50  $\mu\text{m}^2$ .

**Figure 2.3** shows typical AFM images of a polymer microstructure (10  $\mu\text{m}$  boxes) that was fabricated on a silicon wafer when a 50% solution was used for molding. As seen from the figure, the topographical features are well defined with high pattern fidelity (**Figures 2.3 (a), (c), and (d)**). A good contrast in the phase image in **Figure 2.3 (b)** represents two different kinds of interactions of the AFM tip with the surface, thus indicating that the substrate surface is completely exposed. The step height of the mold was 500 nm, which is nearly the same as the height from bottom to top of the cross-sectional image in **Figure 2.3 (d)**. If the concentration of the polymer solution decreases, the topographical height also decreases, ultimately leading to polymer islands rather than a flat film within the void region when the concentration is lower than a certain critical value (mass depletion). Although mass depletion is mainly responsible for

the morphology, the competition between capillarity and surface tension also play a role in determining the particular morphology, which makes the molding process complicated to quantitatively describe<sup>26</sup>. Furthermore, the topography is also dependent on other driving forces such as alterations to pressure, viscosity, and surface properties of the various components of the system. In **Figure 2.3 (d)**, a meniscus is observed within the void space of the stamp, which is attributed to the contact angle at the PEGDM/PDMS/air interface.



*Figure 2.4. FTIR spectra of a cured PEGDM ( $M_w = 300$ ) film at different UV exposure times: (a) before UV exposure, (b) after 2 hours, and (c) 5 hours. To monitor the curing of PEGDM films, we carried out Fourier transform infrared spectroscopy (FTIR) as a function of UV exposure time. **Figure 2.4** shows the transition of two peaks that are assigned to C=O and C=C stretch, respectively. The IR spectrum prior to UV exposure features sharp bands at 1719 cm<sup>-1</sup> and at 1636 cm<sup>-1</sup>, which are characteristic of conjugated ester and terminal C=C of methacrylates,*



respectively (**Figure 2.4 (a)**). After exposure for 2 hours (**Figure 2.4 (b)**), some of the methacrylates (i.e., conjugated esters) reacted and a peak at  $1738\text{ cm}^{-1}$ , which corresponds to the C=O stretch of a saturated aliphatic ester, started to appear. In addition, the peaks of conjugated ester ( $1719\text{ cm}^{-1}$  and  $1636\text{ cm}^{-1}$ ) decreased compared to their initial intensities, which indicate the presence of crosslinked methacrylate chains. The degree of C=C conversion after 2 hours of illumination is about 63% by taking into account the ratio of two peaks around  $1636\text{ cm}^{-1}$  in **Figures 2.4 (a)** and **2.4 (b)**. A careful examination of surface morphology at this conversion shows that the film absorbs a small amount of water and swells in PBS such that bubbles are observed after immersion for 24 hours. However, this bubbled surface also turned out to be effective for selective protein and cell adsorption. If the crosslinking density is too low (when exposure time is less than 1 hour), however, the film dissolves or delaminates from the substrate due to the swelling stress at the PEGDM/substrate interface. After 5 hours of exposure, the peak of C=O stretching completely shifted to  $1738\text{ cm}^{-1}$  and that of C=C ( $1636\text{ cm}^{-1}$ ) is substantially reduced, which means that the film was completely crosslinked.

To examine the effectiveness of the PEG patterns and surfaces to reduce protein adsorption, we prepared FITC-BSA and fibronectin solutions dissolved in PBS. As PEG surfaces are well known for resisting protein adsorption<sup>27</sup>, BSA and fibronectin are expected to adsorb only on the exposed glass surface. As shown in **Figure 2.5**, we observed a spatially well-defined fluorescent image from FITC-BSA for  $10\text{ }\mu\text{m}$  lines (**Figure 2.5 (a)**) and from fibronectin for  $10\text{ }\mu\text{m}$  boxes (**Figure 2.5 (b)**). This indicates that the cured PEGDM film also shows protein resistance as with PEG terminated SAM molecule<sup>27</sup>, which can be readily understood in that the molecular backbone is maintained regardless of crosslinking and its density.

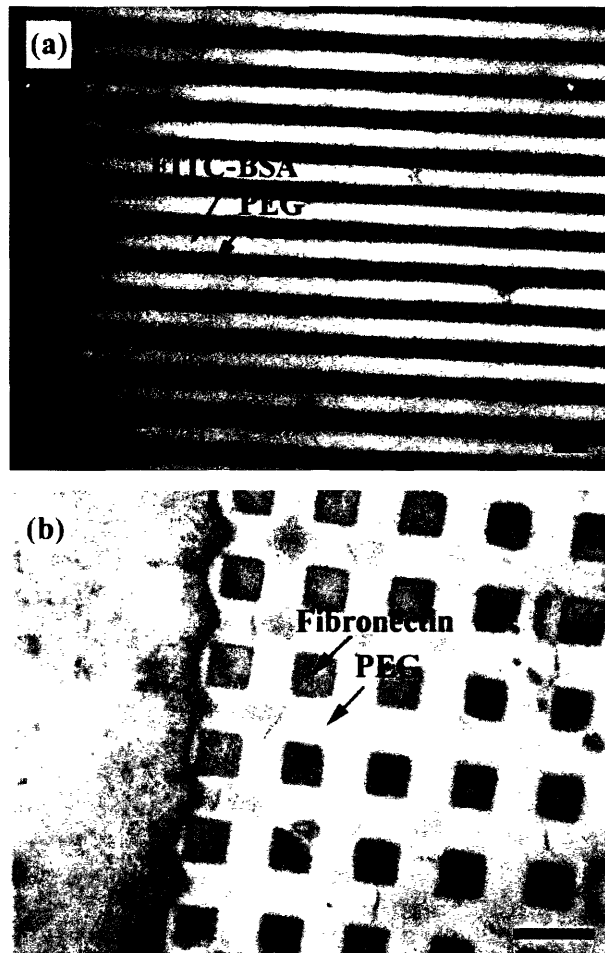


Figure 2.5. Fluorescent images of protein adsorption of PEGDM patterns. (a) A fluorescent micrograph of FITC-BSA that is selectively adsorbed on the 10  $\mu\text{m}$  lines of PEGDM surface. Sharp contrasts are observed. (b) A fluorescent micrograph of fibronectin selectively adsorbed on the 10  $\mu\text{m}$  boxes of PEGDM surface. The scale bars indicate 20  $\mu\text{m}$ .

Since fibronectin is known to mediate cell adhesion<sup>16,27</sup>, patterned cell arrays were prepared with the aid of adsorbed fibronectin islands. Prior to patterning, PEG patterns were prepared on glasses and silicon wafers and treated with fibronectin for 20 minutes. NIH-3T3 cells suspended in medium (at a concentration of  $1 \times 10^6$ ) were then plated onto the surfaces and the cell cultures were analyzed at various times. **Figure 2.6** shows typical cell images that can be obtained with patterned PEGDM surfaces when incubated for 4 hours. As expected, cells appear

to deposit only on the exposed glass or silicon wafer, not on PEG surfaces. Also the number of cells on the surface can be controlled by varying the size of the patterns. The initial cell size of NIH-3T3 is estimated to be about 10  $\mu\text{m}$ . Once the cell is immobilized on the surface, it spreads and grows in size. One to three cells can be deposited within the barriers for  $15 \times 75 \mu\text{m}^2$  ovals (**Figures 2.6 (a) and 2.6 (b)**) and a single cell for 25  $\mu\text{m}$  diameter circles (**Figures 2.6 (c) and 2.6 (d)**). Also, the feature size and cell seeding density can control the number of adsorbed cells on each island. In addition, PEG microstructures form a physical barrier, which further prevents cell spreading in comparison to techniques in which only the substrate surface is modified. Although a PDMS membrane has been used for physical confinement<sup>16</sup>, its application is limited in that the pattern size is typically on the order of a hundred  $\mu\text{m}$  and PDMS is not inert for the adhesion of cells.

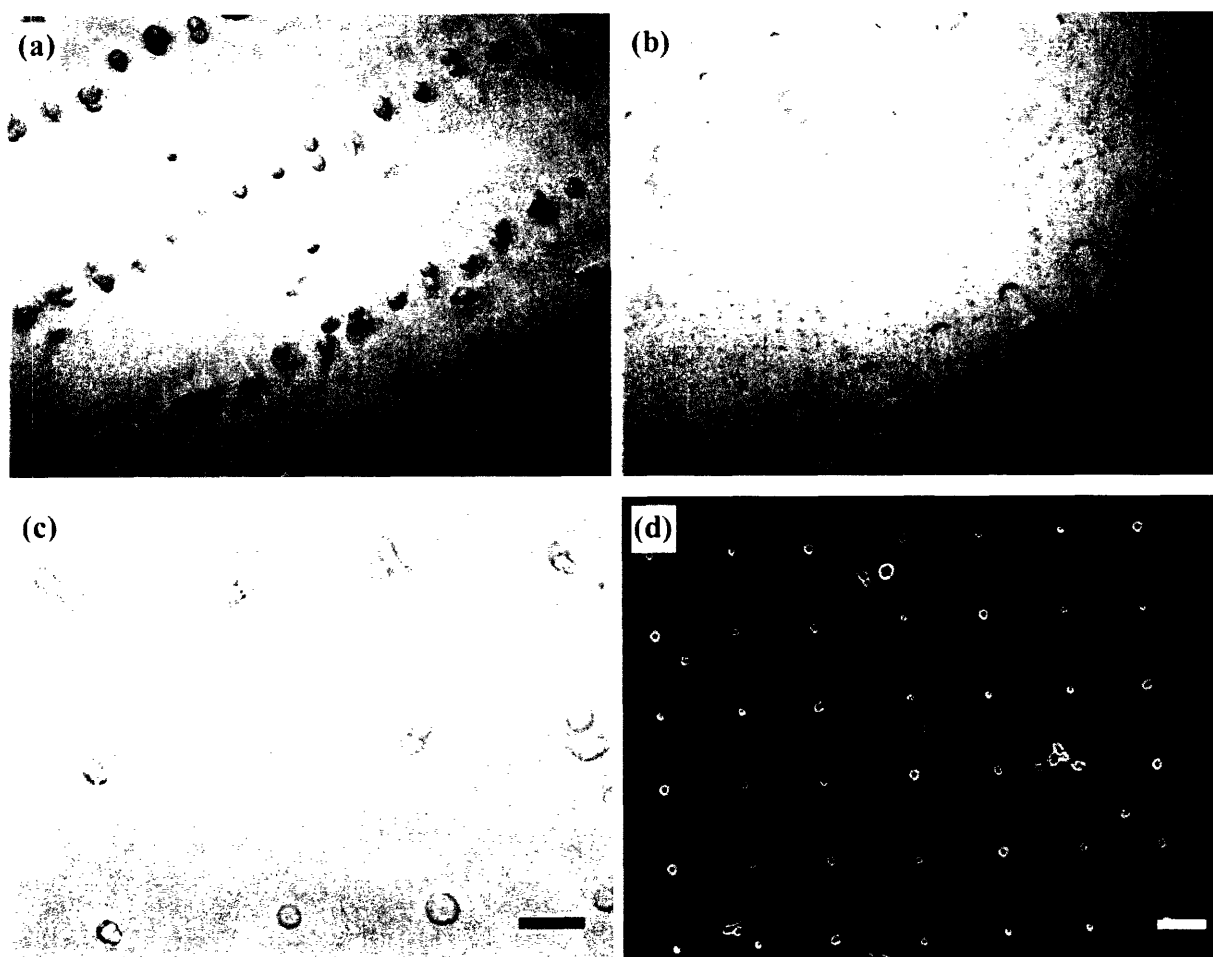


Figure 2.6. Optical micrographs of NIH-3T3 cells deposited on (a)  $15 \times 75 \mu\text{m}^2$  ovals on silicon wafer, (b) the same as (a) (magnified), (c)  $25 \mu\text{m}$  circles on silicon wafer, and (d)  $25 \mu\text{m}$  circles on glass. As shown in the figure, cells are confined in PEGDM barriers with numbers strictly controlled by the feature sizes. The scale bar indicates  $50 \mu\text{m}$ .

## CONCLUSIONS

We have developed capillary force lithography as a tool for general-purpose lithography for protein and cell patterning. By introducing PEGDM as the patterned polymer, spatially well-defined images of selective protein and cell adsorption are observed on a large area, which could open new pathways for fabricating protein chips and high-throughput cell screening devices. The

number of cells in a given barrier can be controlled depending on the feature size. As the demand for strict control of cell position and function is increasing for applications ranging from cellular to tissue engineering and biosensors<sup>28</sup>, the technique presented here could be increasingly useful for such purposes.

## REFERENCES

- (1) Xia, Y. N., Whitesides, G. M. Soft lithography. *Angewandte Chemie-International Edition*, **37**, 5, 1998.
- (2) Lesho, M. J., Sheppard, N. F. Adhesion of polymer films to oxidized silicon and its effect on performance of a conductometric pH sensor. *Sensors and Actuators B-Chemical*, **37**, 1-2, 1996.
- (3) Beebe, D. J., Moore, J. S., Bauer, J. M., Yu, Q., Liu, R. H., Devadoss, C., Jo, B. H. Functional hydrogel structures for autonomous flow control inside microfluidic channels. *Nature*, **404**, 6778, 2000.
- (4) Revzin, A., Russell, R. J., Yadavalli, V. K., Koh, W. G., Deister, C., Hile, D. D., Mellott, M. B., Pishko, M. V. Fabrication of poly(ethylene glycol) hydrogel microstructures using photolithography. *Langmuir*, **17**, 18, 2001.
- (5) Papra, A., Bernard, A., Juncker, D., Larsen, N. B., Michel, B., Delamarche, E. Microfluidic networks made of poly(dimethylsiloxane), Si, and Au coated with polyethylene glycol for patterning proteins onto surfaces. *Langmuir*, **17**, 13, 2001.
- (6) Takayama, S., Ostuni, E., Qian, X. P., McDonald, J. C., Jiang, X. Y., LeDuc, P., Wu, M. H., Ingber, D. E., Whitesides, G. M. Topographical micropatterning of poly(dimethylsiloxane) using laminar flows of liquids in capillaries. *Advanced Materials*, **13**, 8, 2001.
- (7) Patel, N., Padera, R., Sanders, G. H. W., Cannizzaro, S. M., Davies, M. C., Langer, R., Roberts, C. J., Tendler, S. J. B., Williams, P. M., Shakesheff, K. M. Spatially controlled cell engineering on biodegradable polymer surfaces. *Faseb Journal*, **12**, 14, 1998.
- (8) Chiu, D. T., Jeon, N. L., Huang, S., Kane, R. S., Wargo, C. J., Choi, I. S., Ingber, D.

- E., Whitesides, G. M. Patterned deposition of cells and proteins onto surfaces by using three-dimensional microfluidic systems. *Proceedings of the National Academy of Sciences of the United States of America*, **97**, 6, 2000.
- (9) Tan, J. L., Tien, J., Chen, C. S. Microcontact printing of proteins on mixed self-assembled monolayers. *Langmuir*, **18**, 2, 2002.
- (10) Kane, R. S., Takayama, S., Ostuni, E., Ingber, D. E., Whitesides, G. M. Patterning proteins and cells using soft lithography. *Biomaterials*, **20**, 23-24, 1999.
- (11) Craighead, H. G., James, C. D., Turner, A. M. P. Chemical and topographical patterning for directed cell attachment. *Current Opinion in Solid State & Materials Science*, **5**, 2-3, 2001.
- (12) Lahann, J., Balcells, M., Rodon, T., Lee, J., Choi, I. S., Jensen, K. F., Langer, R. Reactive polymer coatings: A platform for patterning proteins and mammalian cells onto a broad range of materials. *Langmuir*, **18**, 9, 2002.
- (13) Lahann, J., Choi, I. S., Lee, J., Jensen, K. F., Langer, R. A new method toward microengineered surfaces based on reactive coating. *Angewandte Chemie-International Edition*, **40**, 17, 2001.
- (14) Harris, J. M., Zalipsky, S. *Poly(ethylene glycol): Chemistry and Biological Applications*; Am. Chem. Soc.: Washington, DC, 1997.
- (15) Wang, Y. C., Ferrari, M. Surface modification of micromachined silicon filters. *Journal of Materials Science*, **35**, 19, 2000.
- (16) Ostuni, E., Kane, R., Chen, C. S., Ingber, D. E., Whitesides, G. M. Patterning mammalian cells using elastomeric membranes. *Langmuir*, **16**, 20, 2000.
- (17) Ghosh, P., Amirpour, M. L., Lackowski, W. M., Pishko, M. V., Crooks, R. M. A simple lithographic approach for preparing patterned, micron-scale corrals for controlling cell

- growth. *Angewandte Chemie-International Edition*, **38**, 11, 1999.
- (18) Rowan, B., Wheeler, M. A., Crooks, R. M. Patterning bacteria within hyperbranched polymer film templates. *Langmuir*, **18**, 25, 2002.
  - (19) Hyun, J., Ma, H., Zhang, Z., Beebe, T. P., Chilkoti, A. Universal route to cell micropatterning using an amphiphilic comb polymer. *Advanced Materials*, **15**, 2003.
  - (20) Yamato, M., Konno, C., Utsumi, M., Kikuchi, A., Okano, T. Thermally responsive polymer-grafted surfaces facilitate patterned cell seeding and co-culture. *Biomaterials*, **23**, 2, 2002.
  - (21) Ito, Y. Surface micropatterning to regulate cell functions. *Biomaterials*, **20**, 23-24, 1999.
  - (22) Chen, C. S., Mrksich, M., Huang, S., Whitesides, G. M., Ingber, D. E. Geometric control of cell life and death. *Science*, **276**, 5317, 1997.
  - (23) Kim, E., Xia, Y. N., Whitesides, G. M. Polymer Microstructures Formed by Molding in Capillaries. *Nature*, **376**, 6541, 1995.
  - (24) Suh, K. Y., Kim, Y. S., Lee, H. H. Capillary force lithography. *Advanced Materials*, **13**, 18, 2001.
  - (25) Kim, Y. S., Suh, K. Y., Lee, H. H. Fabrication of three-dimensional microstructures by soft molding. *Applied Physics Letters*, **79**, 14, 2001.
  - (26) Suh, K. Y., Park, J., Lee, H. H. Controlled polymer dewetting by physical confinement. *Journal of Chemical Physics*, **116**, 17, 2002.
  - (27) Whitesides, G. M., Ostuni, E., Takayama, S., Jiang, X. Y., Ingber, D. E. Soft lithography in biology and biochemistry. *Annual Review of Biomedical Engineering*, **3**, 2001.
  - (28) Chovan, T., Guttman, A. Microfabricated devices in biotechnology and biochemical processing. *Trends in Biotechnology*, **20**, 3, 2002.



### **3. Synthesis of a novel PEG-based polymer and its application for fabrication of protein and cell resistant micro/nanostructures**

#### **INTRODUCTION**

The construction of protein- or cell-resistant surfaces is a crucial requirement for medical or analytical devices in contact with biological fluids. Such devices include biosensors, chip-based diagnostic assays, affinity chromatography columns, and biomaterials used for implants<sup>1, 2</sup> and tissue engineering<sup>3, 4</sup>. One strategy to reduce biofouling adsorption is surface modification by poly(ethylene glycol) (PEG) which has protein- and cell-repellent properties. Previous attempts at grafting PEG onto oxide surfaces have involved covalent bond formation such as chemical coupling reactions<sup>5</sup>. However, such approaches require pre-generation of functional groups on the substrate surfaces by multi-step heterogeneous reactions. An alternative is direct PEG modifications onto bare oxide surfaces using various PEG-graft copolymers either by physical adsorption<sup>6</sup> or by electrostatic interaction<sup>5, 7-9</sup>. On the other hand, nonbiofouling surfaces can be prepared either using self-assembled monolayers (SAMs) of oligo(ethylene glycol)<sup>10</sup> or using self-assembly of surface-reactive polymers<sup>11</sup> on gold. On oxide surfaces, however, few studies have been reported using such SAMs<sup>12</sup>.

Techniques that control topographical features and spatial presentation of surface molecules are important for the development of cell and protein arrays for drug discovery, diagnostic assays and biosensors<sup>13</sup>. Cells and proteins have been previously patterned on various substrates using self-assembled monolayers (SAMs)<sup>10, 14-19</sup>, metal templates<sup>20</sup>, stamped proteins and peptides<sup>21</sup>, bio<sup>22-25</sup> and comb polymers<sup>26</sup>, microfluidic channels<sup>27</sup> and membranes<sup>28, 29</sup>. Although these techniques may result in changes in surface topography based on deposition of a patterned molecule<sup>26-29</sup>, various properties of these features such as height are typically uncontrolled. To obtain features with controlled topographical features, techniques such as micromachining<sup>13</sup>, photolithography<sup>30</sup> or molding<sup>31, 32</sup> have been used. Therefore, the development of simple approaches that provide control over both surface topography and spatial presentation of surface molecules for large-area substrates over a variety of feature sizes and heights is beneficial.

In this chapter, first the synthesis and characterization of a PEG-based polymer is presented that is capable of forming nonbiofouling ultrathin polymeric monolayers (PMs) on bare oxide substrates. Then, the use of this material for surface patterning at various length scales with control over the features of the structures is presented. Polymeric self-assembly of surface-reactive block copolymers has been used for the construction of nano- and micropatterned polymer brushes on silicon dioxide<sup>14</sup>. A random copolymer composed of ‘anchor part’ (trialkoxysilane) and ‘function part’ (PEG) was synthesized. The chemical structure of the copolymer and its proposed self-assembled structure onto Si/SiO<sub>2</sub> surface are shown in **Figure 3.1**. Incorporation of the surface-reactive trimethoxysilyl group in the monomer can allow the copolymer to form multiple covalent bonds onto oxide surfaces along with multiple PEG immobilizations. Consequently, nonspecific protein adsorption and cell adhesion can be significantly reduced.

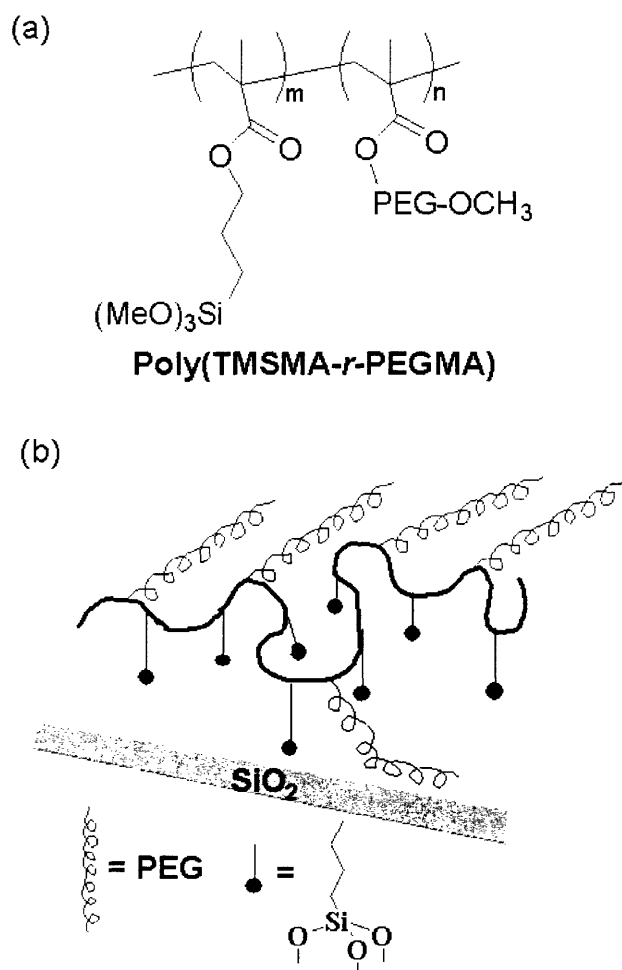


*Figure 3.1. Chemical structure of poly(TMSMA-*r*-PEGMA) and its monolayer structure. (a) A chemical structure of (trimethoxysilyl)propyl methacrylate and PEG methacrylate random copolymer, poly(TMSMA-*r*-PEGMA). (b) A schematic diagram of monolayers of the copolymer on SiO<sub>2</sub> surface.*

In addition to the polymer a simple process is described that can be used to pattern oxide-based substrates with biofouling-resistant polymers with precise control over surface topography. The technique uses a molding process to pattern a polyethylene glycol (PEG)-based random copolymer, (poly(TMSMA-*r*-PEGMA)), in the form of polymeric monolayers (PMs) or microstructures with simple modifications to the fabrication procedure. The use of this technique to generate features varying in height is demonstrated and it is shown that it can be applied for patterning proteins and cells.

PEG-based surface modification is widely used for creating surfaces that resist cells and proteins. For example, PEG-derived alkanethiol SAMs<sup>14-16, 18</sup> have been used to pattern proteins and cells on gold substrates. While surface patterning through SAMs on gold is well characterized, stable patterning on other substrates is still under development. Recently, polyionic PEG-grafted polymers have been patterned on oxide surfaces using electrostatic interaction between cationic polymer backbone and anionic oxide surfaces<sup>33</sup>. However, the non-covalent interactions in this system may hinder its stability for long-term application. Furthermore, PEG-based alkanethiol SAMs cannot be used to create microstructures. To create PEG microstructures, photolithographic methods have been used<sup>30, 34</sup>, however, the cost and complexities associated with photolithography provides a barrier to its widespread application for cell and protein patterning. In another approach, polymeric deposition of PEG based comb polymer was used to generate topographical changes, but no direct control over feature height was demonstrated<sup>26</sup>. To address the issues associated with stability, cost, topography, and ease of use, and control over feature height, we synthesized a poly(TMSMA-*r*-PEGMA) copolymer that can be easily synthesized using commercially available monomers<sup>35</sup>. This copolymer provides the functionality of PEG (i.e. hydrophilic and non-biofouling), yet it can bind covalently with oxide surfaces to form monolayers or crosslink to form 3D structures. Thus, by utilizing the combination of this polymer and capillary force lithography, we have developed a universal approach to create features of varying sizes and shapes that could be applicable for patterning proteins and cells.

## **MATERIALS AND METHODS:**

*Materials:* 3-(Trimethoxysilyl)propyl methacrylate, poly(ethylene glycol) methyl ether methacrylate (average  $M_n = ca. 475$ ), and 2,2'-azobisisobutyronitrile (AIBN) were purchased from Aldrich Chemical Co. NIH 3T3 fibroblasts, Dulbecco's modified Eagle's medium, fetal bovine serum, and other cell culture supplies were purchased from ATCC. All organic solvents were used

as received. All substrates used herein such as Si/SiO<sub>2</sub> wafer, poly(dimethylsiloxane) (PDMS), and glass slide were first cleaned using detergent, followed by washing with deionized water and methanol several times. Prior to form the polymeric films, all the substrates were treated with O<sub>2</sub> plasma for 1 minute to generate -OH groups as well as to clean the surfaces unless specially noted like 'no plasma treatment'.

*Synthesis of the copolymer comprising 3-(trimethoxysilyl)propyl methacrylate (TMSMA) and poly(ethylene glycol) methyl ether methacrylate (PEGMA): poly(TMSMA-r-PEGMA):* Prior to polymerization, neat PEGMA was flowed through the inhibitor removal column (Aldrich Chemical Co.). PEGMA (4.75 g, 10 mmol, 1 equiv), TMSMA (2.5 g, 10 mmol, 1 equiv), and AIBN (16.5 mg, 0.1 mmol, 0.01 equiv) were placed in a vial and dissolved in tetrahydrofuran (anhydrous, inhibitor free, 99.9 %, 10 mL). The mixture was degassed for 20 minutes using Ar gas stream, after which the vial was sealed with a Teflon-lined screw-cap. The polymerization reaction was carried out at 70 °C for 24 hours. After evaporation of solvent under vacuum, the polymer was obtained as a viscous liquid.

*Cell culture:* The copolymer-coated glass slides (ca. 1 cm x 1.5 cm dimensions) were prepared by immersing the slides in the copolymer solution (10 mg/mL in methanol) for 2 hours followed by washing with methanol and then by curing in 120 °C oven for 15 minutes. The coated glass slides were sterilized by UV radiation for 20 minutes. Subsequently each glass slide was placed in a 24-well plate, soaked in growth medium for 30 minutes and replaced with fresh medium. Each well was seeded with 100,000 NIH-3T3 fibroblasts and grown at 37 °C, 5% CO<sub>2</sub> in Dulbecco's modified Eagle's medium, 90%; FBS, 10%; penicillin, 100 units/mL; streptomycin, 100 µg/mL. For cell patterning experiments, the cells were trypsinized and washed and directly seeded on the patterned surfaces in serum containing medium at a cell density of  $\sim 10^4$  cells cm<sup>-2</sup>. Cell attachment to the patterned substrates was subsequently examined under a phase-contrast microscope at various times. To analyze, glass slides were rinsed with PBS to remove non-adhered cells from the non-adhered regions.

*PDMS mold fabrication:* PDMS molds were fabricated by curing prepolymer (Sylgard 184, Essex Chemical) on silicon masters that had been patterned with SU-8 photoresist. The patterns on the masters have protruding holes in the shape of cylinders (ranging in size from 20 µm to 160 µm), which result in PDMS replicas with receding cylinders. To cure the PDMS prepolymer, a mixture of 10:1 prepolymer and the curing agent was poured on the master and placed at 70 °C for 2 hours.

The PDMS mold was then peeled from the silicon wafer and plasma cleaned for 5 minutes prior to use.

*Patterning technique:* To pattern the polymer onto substrate, a solution of co-polymer dissolved in methanol (ranging from 5 to 100 mg mL<sup>-1</sup>) was spin-coated at 1000 rpm for 10 seconds on a plasma cleaned glass substrate. A plasma cleaned PDMS mold was then immediately brought in conformal contact with the copolymer surface and stored at room temperature for 1 hour. Molds were then detached from the glass substrate. To obtain PMs, the patterned surfaces were washed with methanol for 1 hour and subsequently cured at 110 °C for 15 minutes. To obtain the polymeric microstructures, the patterns left from the PDMS mold were directly cured at 110 °C for 15 minutes.

*Protein adsorption:* FITC-labeled BSA, FITC-labeled IgG and fibronectin (Sigma) were dissolved in phosphate buffered saline (PBS) (Sigma) at 50 µg mL<sup>-1</sup>, 50 µg mL<sup>-1</sup> and 20 µg mL<sup>-1</sup> respectively. To test for BSA and IgG protein adhesion, a few drops of the protein solution was evenly distributed onto the patterned substrates and stored at room temperature for 30 minutes. The patterned substrates were then washed and directly analyzed under fluorescent microscope (Axiovert 200, Zeiss). To coat with fibronectin, surfaces were dipped into fibronectin solution for 15 minutes. To measure fibronectin adhesion, the surfaces were stained with anti-fibronectin antibody (Sigma) for an additional 45 minutes, followed by 1 hour incubation with the FITC-labeled anti-rabbit secondary antibody. The surfaces were then washed with water and analyzed. Fluorescent images were quantified using Scion Image software. Pixel intensities were averaged for various regions for at least 2 independent experiments. Unstained glass slides that were analyzed at same exposure were used as negative controls.

*Atomic force microscopy:* Scanning force micrographs (1.0 x 1.0 µm<sup>2</sup> and 90 × 90 µm<sup>2</sup>) were performed in tapping mode on a NanoScope III Dimension instrument (Digital Instruments) in air, using NSC15 tips (MikroMasch) at a scan rate of 0.25 Hz and 256 lines were scanned per sample.. Some of the images shown were flattened but not further manipulated. Data were processed using Nanoscope III 4.31r6 software (Veeco Instruments Inc.).

*Ellipsometry:* Thickness measurements were carried out on an Gaertner L116A ellipsometer (Gaertner Scientific Corp.). Optical constants were measured prior to deposition and used to calculate thickness of the PEG layer after deposition. A refractive index of 1.46 was used for all films, and a three-phase model was used to calculate thicknesses. The maximum variation in the measured thickness between 3-4 spots on any sample was  $\pm 8\text{\AA}$ . Reported thicknesses are the average of at least 2 independent experiments where each sample was characterized by ellipsometry for at least three different locations on its surface.

*Contact angle measurement:* A Ramé-Hart goniometer (Mountain Lakes, NJ) equipped with video camera and monitor was used to measure contact angles in both the advancing and receding modes ( $\sim 1\ \mu\text{L/s}$ ) on drops of  $\sim 3\ \mu\text{L}$  in volume. Reported values represent averages of at least three independent measurements.

*NMR and GPC measurements:*  $^1\text{H}$  NMR (400 MHz) and  $^{13}\text{C}$  NMR (100 MHz) spectra were recorded on a Bruker instrument (Avance DPX 400). Organic phase gel permeation chromatography (GPC) was performed using a Hewlett-Packard 1100 series isocratic pump, a Rheodyne model 7125 injector with a  $100\ \mu\text{L}$  injection loop, and two PL-Gel mixed-D columns in series ( $5\ \mu\text{m}$ ,  $300 \times 7.5\ \text{mm}$ , Polymer Laboratories).  $\text{CHCl}_3$  was used as the eluent at a flow rate of  $1.0\ \text{mL/min}$ .

*XPS measurements:* XPS spectra were obtained using a Kratos AXIS Ultra Imaging X-ray Photoelectron Spectrometer with a monochromatized Al K X-ray source and a  $160\ \text{mm}$  concentric hemispherical energy analyzer for acquisition of spectra and scanned images, lateral resolution down to  $20\ \mu\text{m}$ . The spot size was  $300\ \mu\text{m}$  by  $700\ \mu\text{m}$ .

## RESULTS AND DISCUSSION

### Polymer synthesis

The random copolymer, poly(TMSMA-*r*-PEGMA) was synthesized by the radical polymerization reaction of commercially available 3-(trimethoxysilyl)propyl methacrylate (1.0 equiv) and PEG methyl ether methacrylate (1.0 equiv) in THF at  $70\ ^\circ\text{C}$  for 24 hours (0.01 equiv of AIBN as an initiator). The molecular weight of poly(TMSMA-*r*-PEGMA) was  $M_n = 26,000$  with  $M_w/M_n = 1.88$  as measured by gel permeation chromatography (GPC) relative to monodisperse polystyrene standards. A feed ratio of two monomers was initially 1 to 1. By comparing the integration value of the peak at  $\delta = 4.13$  ( $\text{CO}_2\text{-CH}_2$  at PEGMA) with that of the peak at  $\delta = 3.92$  ( $\text{CO}_2\text{-CH}_2$  at TMSMA)

in  $^1\text{H}$  NMR spectrum, the molar ratio of two monomer units in the copolymer was calculated to be the same as the corresponding feed ratio.

### Polymer coating synthesis and characterization

Polymeric monolayers (PMs) of the copolymer onto  $\text{SiO}_2$ -based substrates were prepared by immersing the substrates in methanol solution of the copolymer (5-10 mg/mL) at ambient temperature followed by washing with methanol. No ultrasonic washing procedure was required. The PMs were then cured at  $120\text{ }^\circ\text{C}$  for 15 min. When Si/SiO<sub>2</sub> wafers as model oxide surfaces were immersed in the copolymer solution (5 mg/mL in methanol) for 1 hour, ultrathin films of the polymer were generated with average ellipsometric thickness of *ca.* 11 Å. Thickness of the film remained unchanged after immersion times up to 48 hours (**Figure 3.2a**), whereas it is known that monomeric trialkoxysilyl groups give different coating thickness with different immersion times<sup>17</sup>. In addition, the formation of the PMs was not dependent on concentrations of the polymer up to 50 mg/mL (**Figure 3.2b**). This indicates that the adsorbed polymer layers can limit further diffusion of other polymer chains to the surface. Furthermore, we did not observe any thickness change of the PMs after baking at  $120\text{ }^\circ\text{C}$  for 2 hours, autoclaving for 1 hour, and incubation in PBS (pH 7.4) at  $37\text{ }^\circ\text{C}$  for 2 weeks.

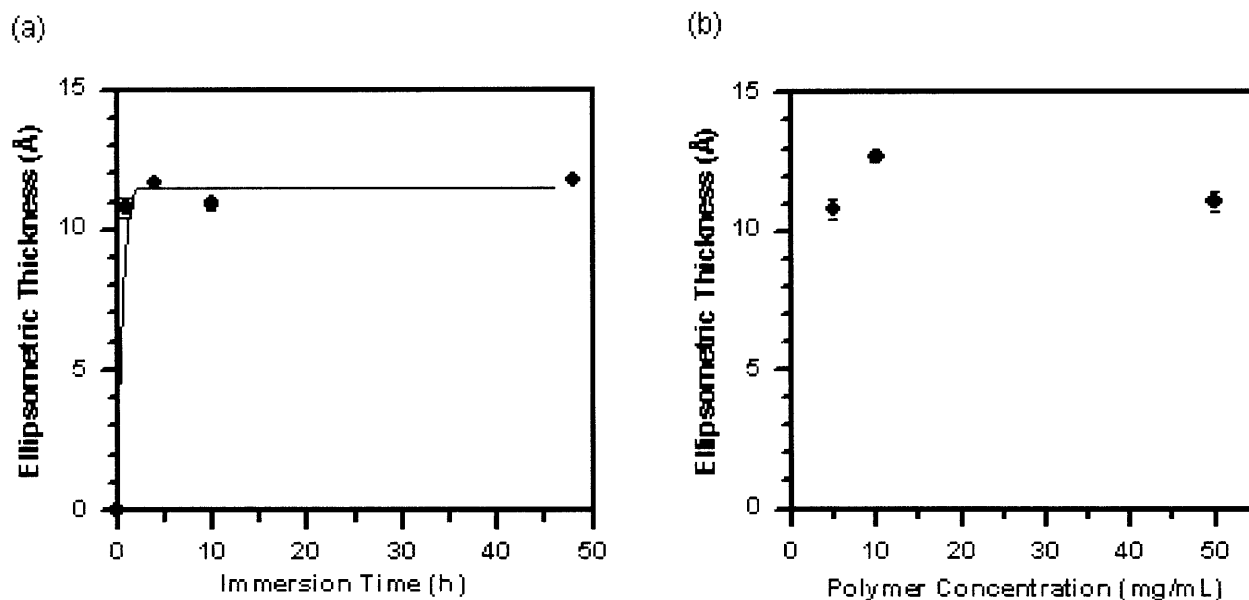
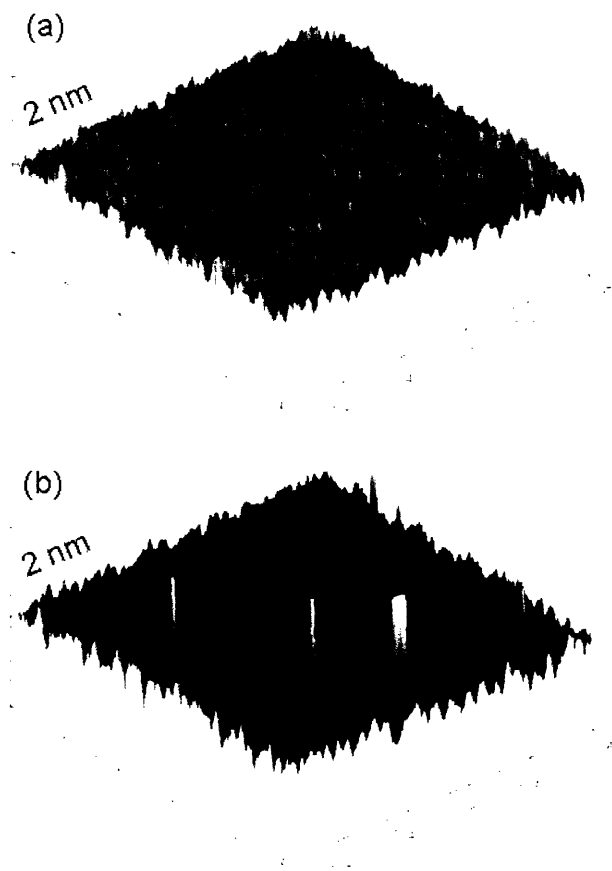


Figure 3.2. Effects of immersion times and copolymer concentrations on the thicknesses of the PMs.  $\text{O}_2$  plasma treated-Si/SiO<sub>2</sub> wafers were immersed in copolymer dissolved in methanol. The thicknesses of the PMs on Si/SiO<sub>2</sub> wafers were measured (a) with times, and (b) with concentrations.

The surface topography of the PMs of the polymer on Si/SiO<sub>2</sub> wafers was examined by tapping mode atomic force microscopy (AFM). Three different positions per substrate were taken. **Figure**

**3.3a** shows the surface of the PMs on  $O_2$  plasma treated-Si/SiO<sub>2</sub> wafers was smooth with average roughness of 1.3 Å (root mean square) and had uniform topographical pattern with vertical distance of 3-5 Å from the base polymeric layer on crosssectional analysis. Based on ellipsometry data which revealed average thickness of *ca.* 11 Å for the PMs, the thickness of the base polymer layer could be derived to be less than 6 Å. In addition, copolymer aggregates were not detected for the  $O_2$  plasma treated-substrate (**Figure 3.3a**), whereas randomly distributed polymer aggregates (about 30 nm wide and 5 nm high) could be detected for the untreated-substrate (no plasma treatment) (**Figure 3.3b**). Such aggregation may be attributed to the cross-linking between unreacted trimethoxysilyl groups in the copolymer chains. It is anticipated that  $O_2$  plasma treatment generates more Si-OH groups on the surface of the substrate and thus results in a lower fraction of trimethoxysilyl groups that remained unreacted with the surface after the formation of the PMs in comparison to the untreated substrate (no plasma treatment). Therefore, this result suggests that plasma treatment enhances the uniformity of the PMs on Si/SiO<sub>2</sub> substrates.



*Figure 3.3. Tapping mode AFM height images of poly(TMSMA-*r*-PEGMA) monolayers. (a) on  $O_2$  plasma treated-Si/SiO<sub>2</sub> wafer and (b) on untreated-Si/SiO<sub>2</sub> wafer (no plasma treatment).*

Since poly(TMSMA-*r*-PEGMA) is a random copolymer, it is difficult to predict the structure of its monolayers on oxide surfaces. According to the thickness data, however, it appeared that the PEG



side chains stretch over the surface rather than align vertically, as the expected film thickness for the latter structure would be at least 20 Å. The polymer-coated films were also characterized by glancing angle X-ray photoelectron spectroscopy (XPS). **Table 3.1** summarizes elemental compositions of the unmodified and the polymer-coated Si/SiO<sub>2</sub> surfaces. After the Si/SiO<sub>2</sub> was modified with the polymer, the carbon content was increased by 25% and the silicon content was decreased by 23%. High resolution C(1s) XPS composition shown in **Table 3.2** further confirms the formation of the PMs on Si/SiO<sub>2</sub> wafers. (See **(Figure 3.4)** for high resolution C(1s) X-ray photoelectron spectra and peak analysis). Three carbon species (hydrocarbon, ether carbon in the PEG chain, and carbonyl carbon) were observed. If the PEG chains align vertically on the surface, it is expected that the ratio of C-O in PEG moieties to O-C=O in polymer backbone would increase with increasing take-off angle. However, as take-off angle was changed from 0° to 55° (from surface normal), the ratio decreased by 8 %, suggesting that PEG chains seem to lie horizontally over the surface as suggested from the thickness data.

Substrate	Elemental Composition (%)		
	O	C	Si
Unmodified Si/SiO <sub>2</sub>	38 ± <1	7 ± <1	55 ± <1
PMs on Si/SiO <sub>2</sub>	34 ± <1	34 ± 3	32 ± 2

<sup>a</sup> 55° take-off angle from surface normal was taken.

*Table 3.1. Elemental composition of the PMs on Si/SiO<sub>2</sub> wafer measured by XPS<sup>a</sup>*

Take-Off Angle	Composition (%)		
	CH <sub>2</sub>	C-O	C(=O)O
0°	30 ± 3	61 ± 3	9 ± <1
55°	35 ± 2	56 ± 2	9 ± <1

*Table 3.2. High resolution XPS C1s composition at 0° and 55° take-off angles from surface normal.*

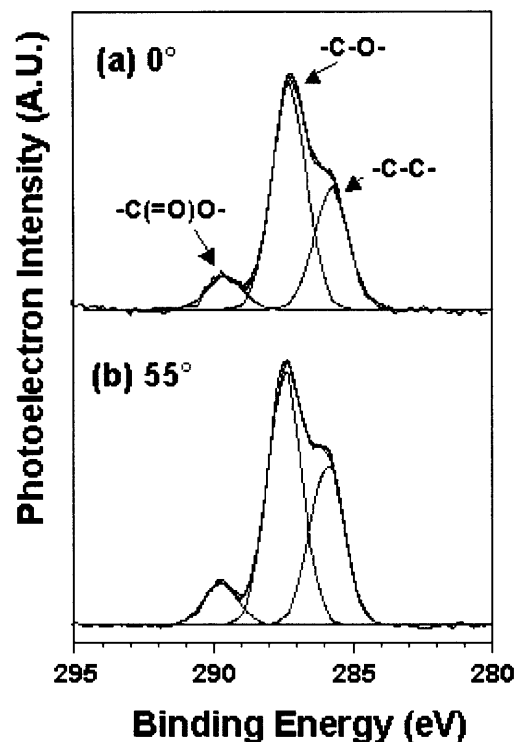


Figure 3.4 The characterization of the PMs on Si/SiO<sub>2</sub> wafers by glancing angle XPS. The high resolution C(1s) X-ray photoelectron spectra of the PMs on Si/SiO<sub>2</sub> wafers as take-off angle was changed from (a) 0°, to (b) 55° from surface normal.

To evaluate protein-resistances of the PMs, the polymer-coated Si/SiO<sub>2</sub> wafers were immersed in several proteins solutions (0.25 mg/mL in PBS, pH 7.4) for 2 hours. The degree of nonspecific proteins adsorption onto the PMs were obtained from the high resolution N(1s) XPS spectrum (**Figure 3.5**). For all three proteins studied, the PMs showed significantly lower (up to 98 %) protein adsorption in comparison to the unmodified Si/SiO<sub>2</sub> wafer. In both cases of a positive-charged protein (Lysozyme, pI = 11.1) and a partially negative-charged protein (Insulin, pI = 5.4), the polymer-coated substrates were highly resistant to protein adsorption by 95% and 97%, respectively. In addition, we observed about 98 % resistance to fibrinogen (pI = 5.5) adsorption, which is abundant in blood plasma and serum and is a well-known protein for its stickiness. Thickness changes of the substrates before and after incubation in each protein solution were also obtained by ellipsometry (**Figure 3.6**). Similar protein-resistance trends were also observed with the polymer-coated glass and PDMS substrates. The polymer films on glass and PDMS substrates were prepared by immersing the substrates in methanol solution of the copolymer (10 mg/mL) for 2 hours and then curing at 120 °C for 15 minutes. The polymer films were characterized by XPS at 55° angle (**Figure 3.7**) and the degree of nonspecific proteins adsorption were also obtained from the high resolution N(1s) XPS spectrum at 55°. The polymer films on PDMS and on glass seemed

to have relatively lower protein resistances (i.e., 81 % and 94 % for insulin, respectively) compared to that of Si/SiO<sub>2</sub> wafers (95 %). The result is attributed to large differences in the extents of nonspecific protein adsorption of each unmodified substrate. According to the absolute peak intensity, however, the amount of each protein adsorption is similar each other for all three substrates (**Figure 3.8**).

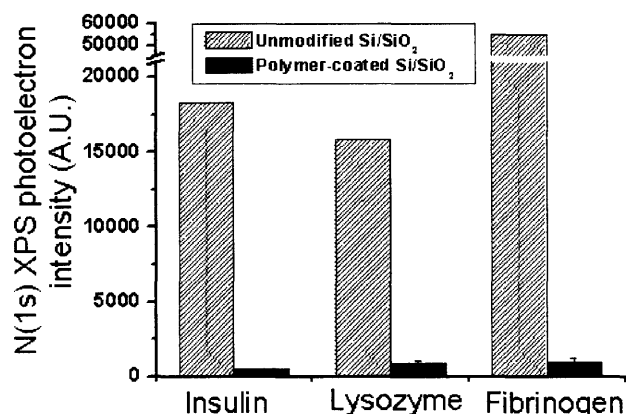


Figure 3.5. Protein adsorption on control (unmodified) and polymer treated Si/SiO<sub>2</sub> surfaces. The relative amount of each protein on the surface is denoted as a N(1s) XPS photoelectron intensity.

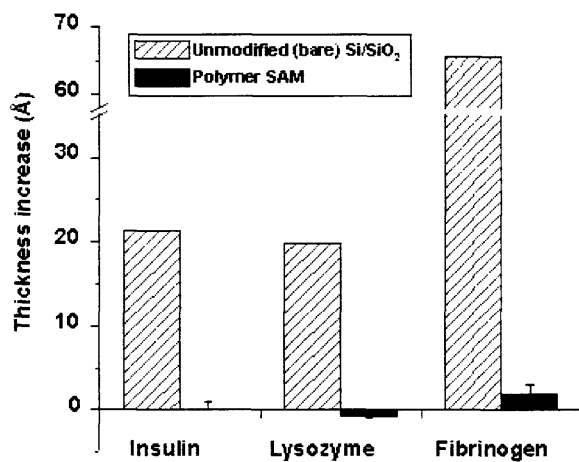


Figure 3.6. Ellipsometric measurement of nonspecific adsorption of proteins on PMs. Ellipsometric thickness changes in the substrates before and after immersion into each protein solution (0.25 mg/mL in PBS, pH 7.4) at ambient temperature.

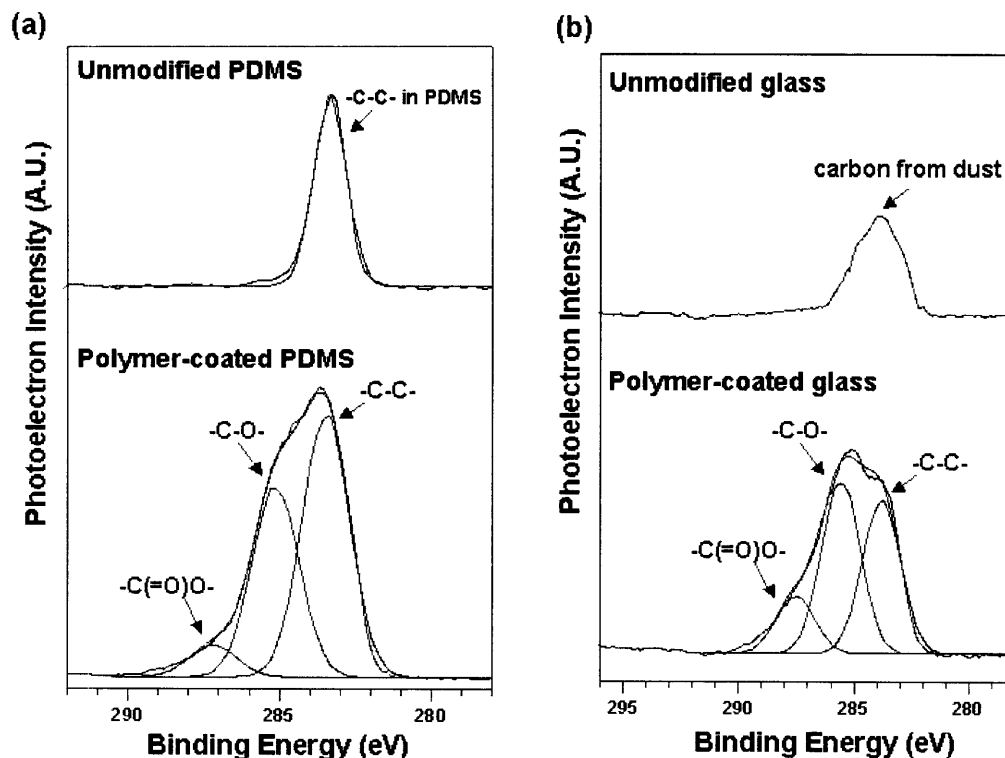


Figure 3.7. Characterization of the polymer-coated PDMS and glass by high resolution C(1s) XPS. High resolution C(1s) XPS spectra of (a) the unmodified and the polymer-coated PDMS and (b) the unmodified and the polymer-coated glass. Take-off angle was 55°.

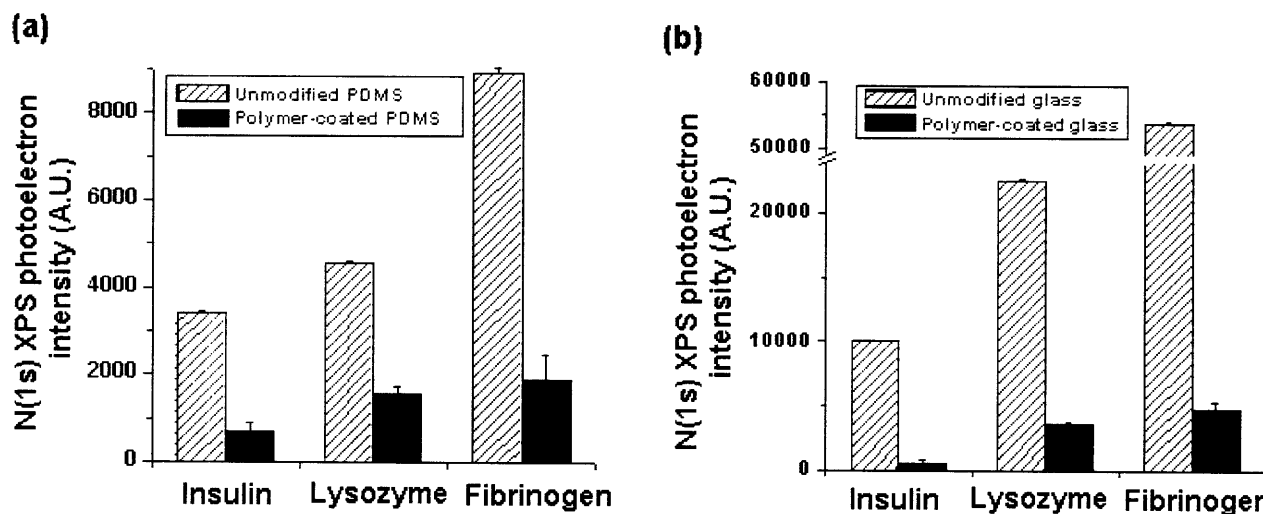
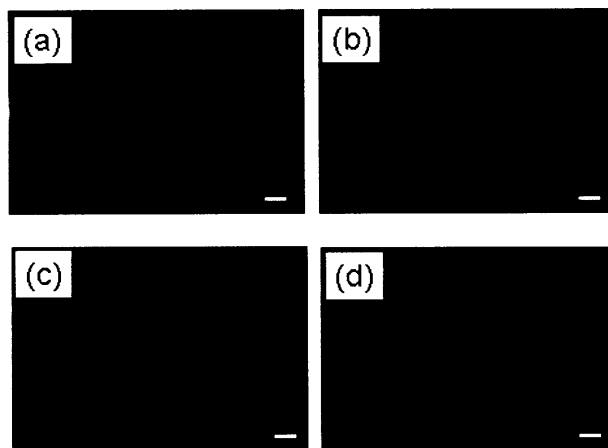
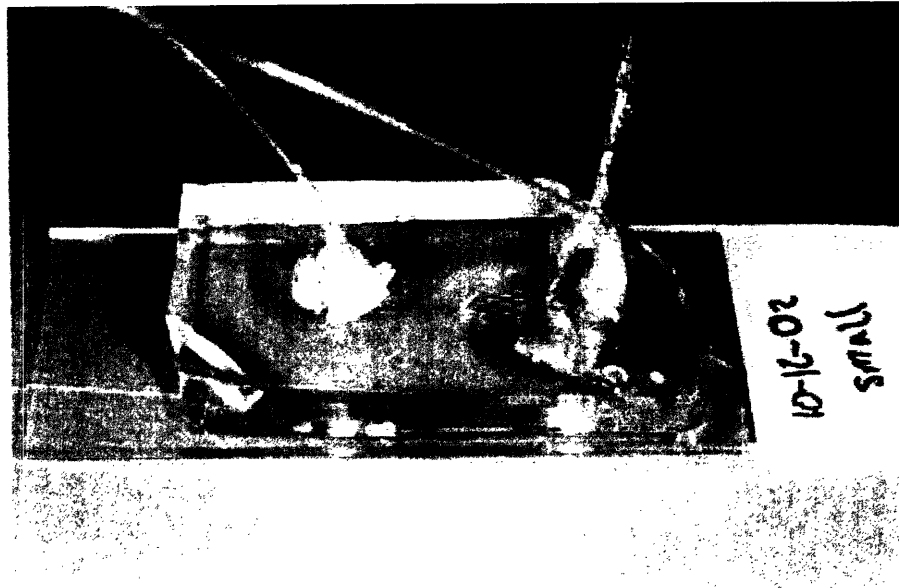


Figure 3.8. Protein resistance of polymer-coated PDMS and glass by high resolution N(1s) XPS. Protein resistances of (a) the unmodified and the polymer-coated PDMS and (b) the unmodified and the polymer-coated glass evaluated by the increases in N(1s) XPS photoelectron intensities upon protein adsorption.

**Figure 3.9** shows one potential application of the present strategy to the preparation of nonbiofouling capillary channels that are needed in electrophoresis, microfluidics or bio-MEMS devices<sup>21</sup>. The microfluidic channels (80  $\mu\text{m}$  height, 500  $\mu\text{m}$  width) that were fabricated using standard soft lithography approaches from PDMS were placed on glass slide and then adhesion between PDMS and glass was made using  $\text{O}_2$  plasma (**Figure 3.10**). First, the microfluidic channel walls were coated by flowing the copolymer solution (10 mg/mL in methanol) through the channels for 2 hours at a rate of 2  $\mu\text{L}/\text{min}$ . During this procedure swelling of PDMS was minimized by using methanol as a solvent. Then FITC-labeled bovine serum albumin (FITC-BSA) (0.1 mg/mL in PBS, pH 7.4) was flown through the channel at a rate of 5  $\mu\text{L}/\text{min}$  for 30 min. The channel was subsequently washed with PBS solution for 15 minutes. PDMS and glass parts are separated and fluorescence images were taken for each channel area. As shown in fluorescence images, little protein adsorption was observed on the polymer-coated channel walls in both glass (**Figure 3.9b**) and PDMS (**Figure 3.9d**) compared to those of unmodified glass and PDMS (**Figure 3.9a and 3.9c**, respectively).



*Figure 3.9. Fluorescence images of microchannels after flowing aqueous solution of FITC-BSA through the channel: unmodified glass (a) and PDMS (c); polymer-coated glass (b) and PDMS (d). The scale bar indicates 100  $\mu\text{m}$ .*



*Figure 3.10. Image of the microfluidic device with capillary tubes connected to the channel. The tubes are connected to a syringe pump where the flow can be controlled in the range of 0.001 mL/min to 20 mL/min.*

### **Cell resistant properties of polymer coated surfaces**

To investigate the cell-resistant properties of the PMs, we carried out cell culture experiment. Adherent NIH-3T3 fibroblasts, were seeded on unmodified glass and the polymer-coated glass. After 24 hours, each glass substrate was gently washed with the same culture medium and optical microscopic images were taken. Fibroblasts grew on unmodified glass slide to form confluent monolayers with density of  $\sim 1.4 \times 10^5$  cells/cm<sup>2</sup> (**Figure 3.11a**), however, the polymer-coated glass slide was resistant to cell adhesion as well as to cell spreading (**Figure 3.11b**) with density of  $\sim 4.3 \times 10^3$  cells/cm<sup>2</sup>. This result may be attributed to high resistance of the copolymer layers to serum proteins in the cell culture medium.

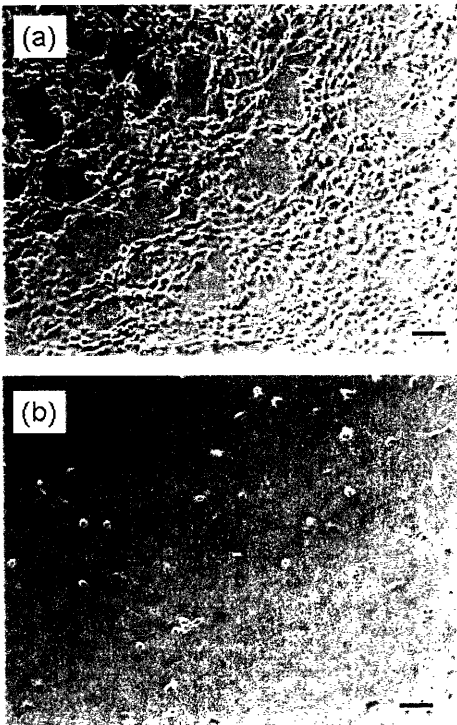


Figure 3.11. NIH-3T3 fibroblasts cultured on unmodified glass (a) and the polymer-coated glass (b) for 24 h with initial seeding density of  $5.3 \times 10^4$  cells/cm<sup>2</sup>. The scale bar indicates 100  $\mu$ m.

Therefore, nonbiofouling surfaces were prepared on bare Si/SiO<sub>2</sub> substrates by forming polymeric layers of the surface-reactive PEG-grafted copolymer. The PMs on Si/SiO<sub>2</sub> wafers were reproducibly generated at the ambient environments without special care for anhydrous conditions. The resulting ultrathin films showed great reduction in nonspecific protein adsorption (up to 98%) and cell adhesion. The present approach may be potentially applied to other substrates such as metal oxides (*e.g.*, Al<sub>2</sub>O<sub>3</sub>, TiO<sub>2</sub>) and polymer surfaces. Since functional units other than PEG (*e.g.*, biotin, fluorocarbons) can be also incorporated into the copolymer as monomer units, the combined copolymer system of the ‘anchor part’ (trialkoxysilane) and the ‘function part’ may have warrant applications in the preparation of functional surfaces of medical and analytical devices.

### **Patterning of poly(TMSMA-*r*-PEGMA)**

In capillary force lithography, direct contact of a patterned polydimethylsiloxane (PDMS) stamp on a mobilized polymer film provides the basis for pattern formation<sup>31, 32</sup>. When a PDMS stamp is placed on a wet polymer film, the polymer spontaneously moves into the void space as a result of capillary action, thus forming a negative replica of the stamp. When the film thickness is relatively thin with respect to the stamp’s step height and the feature size is relatively large, instead of rising into the void space, the polymer migrates to the edge of the stamp and is localized there as a result of meniscus breakdown<sup>36</sup>. From a thermodynamic standpoint, this process can be interpreted to

minimize the contact with the stamp and the substrate, which has been observed for other polymer systems<sup>36, 37</sup>. As the stamp has the feature size that is typically on the order of 10 - 100  $\mu\text{m}$  for patterning biological species, the dewetting would occur throughout the molding process.

To pattern, thin films of the poly(TMSMA-*r*-PEGMA) were spin coated onto silicon oxide surfaces (typically wafers or glass slides). Immediately after coating, a PDMS mold was placed on the substrate to form a reversible seal (**Figure 3.12**). For these experiments we used PDMS molds with evenly spaced receding cylinders (ranging from 15 to 150  $\mu\text{m}$  in diameter and 80  $\mu\text{m}$  in height). As reported previously<sup>32</sup>, this capillary action is completed within a few minutes, which prevents the formation of a PM at the dewetted regions. In the course of the capillary action and solvent evaporation, the polymer within the void space spontaneously migrated to the PDMS wall, with the substrate surface completely exposed, forming an additional physical barrier into the replicated pattern<sup>36, 37</sup>. At the same time, the polymer that is in contact with the substrate reacts with the exposed silicon oxide, resulting in a robust, stable interface. The topographical features of the physical barrier are determined by the initial film thickness and PDMS feature width<sup>36</sup>. For example, the height of the barrier increases with increasing film thickness and decreasing feature width. The PDMS molds were kept on glass slides for 1 hour since it was observed that complete coverage of the surface is reached within that time<sup>35</sup>. Upon removal of the PDMS mold, the pattern is visible by the naked eye. This pattern can then be further processed to obtain either microstructures or PMs.

To prepare polymeric microstructures with controlled topographical features, PDMS stamps were removed and the patterns were cured at 110 °C and then rinsed with methanol and water (**Figure 3.12a**). During the curing step, polymer chains are cross-linked with each other through partially hydrolyzed trimethoxysilyl groups and form stable microstructures. Alternatively, patterned surfaces were first washed in methanol to remove unreacted polymer, leaving behind a thin polymer coating and then cured to obtain patterned PMs (**Figure 3.12b**).



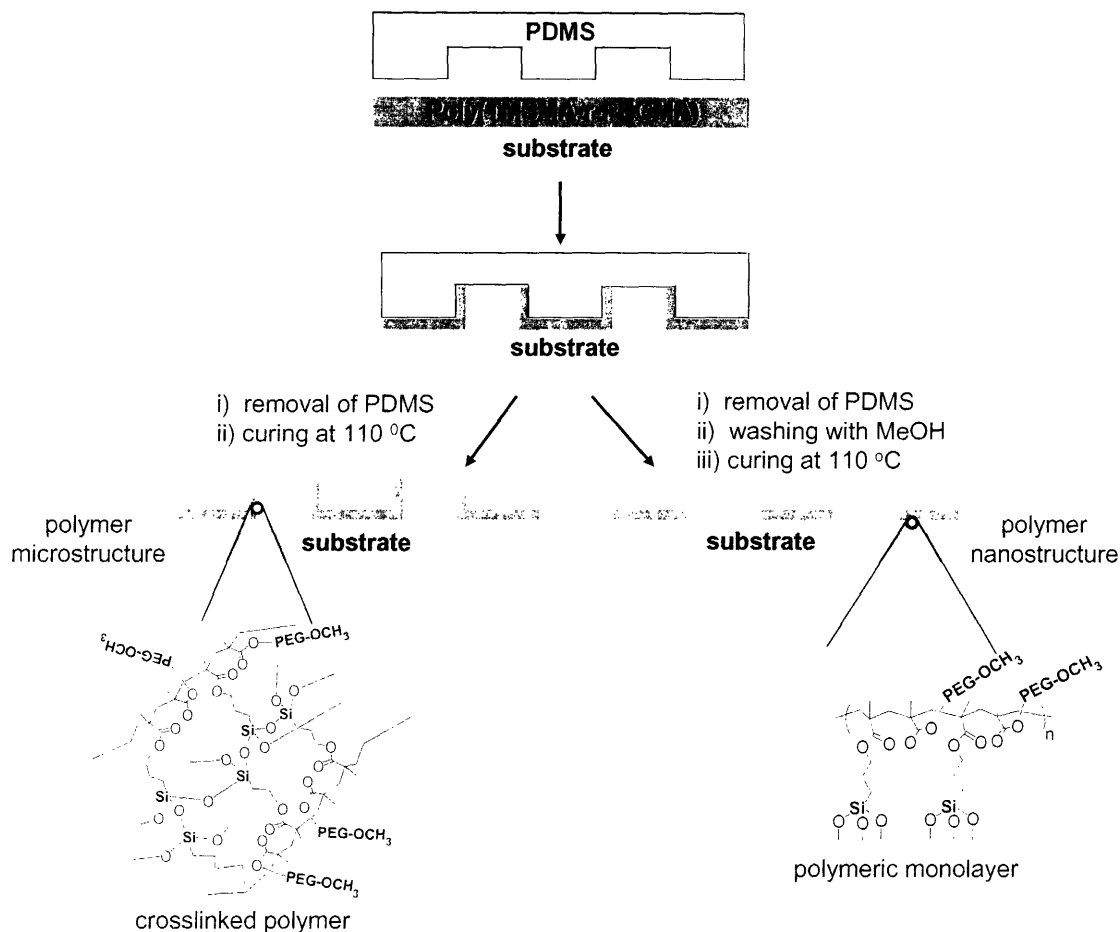
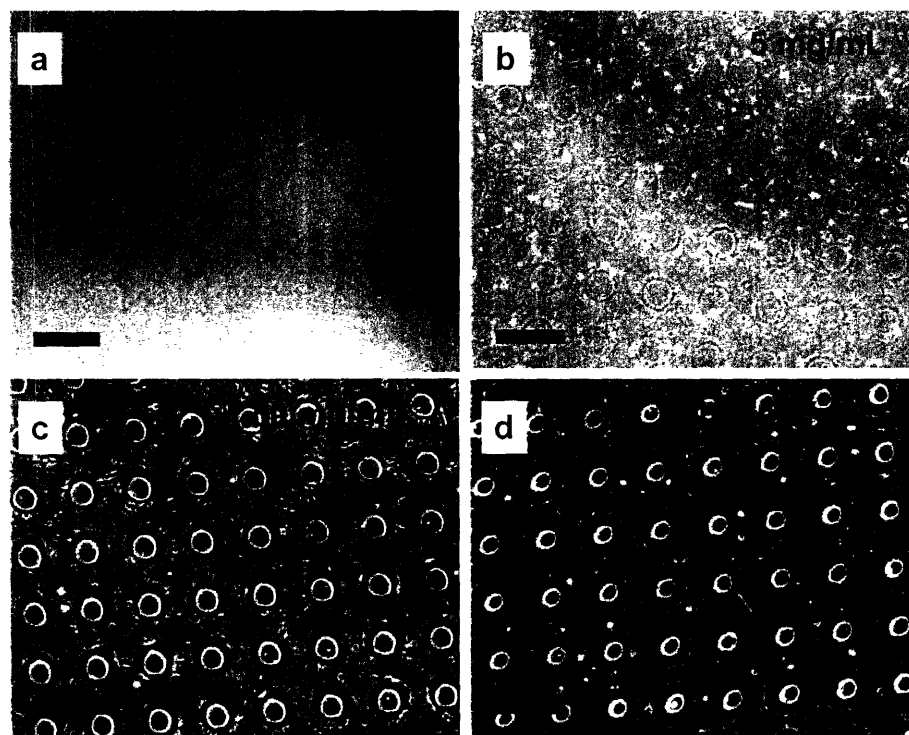


Figure 3.12. Schematic diagram of the patterning process. Thin films of Poly(TMSMA-*r*-PEGMA) were spin coated on silicon oxide substrates and molded using capillary force lithography. After 1 hour, PDMS molds were detached from the substrate. To form microstructures, patterned substrates were immediately cured, which crosslinked the polymer and formed stable microstructures (left panel). To obtain PMs, patterned substrates were washed with methanol and then cured. A thin patterned layer of PEG-based polymer remained on the substrate due to covalent bonding to the substrate (right panel).

To demonstrate the feasibility of this approach to form both monolayers and microstructures, oxide substrates were patterned with a solution of poly(TMSMA-*r*-PEGMA) in methanol (5 mg mL<sup>-1</sup>). Samples that were initially washed and then cured did not form visible patterns under light microscopy, whereas samples that were cured immediately after removal of the PDMS stamp, formed visible patterns (**Figure 3.13**). In these samples, a sharp boundary separated the exposed substrate from the polymer-coated regions. To further examine these differences, atomic force microscopy (AFM) measurements were performed (**Figure 3.14**). AFM images indicate that the thickness of PMs was ~1 nm (**Figures 3.14a and b**), which was confirmed independently using ellipsometry (12 ± 4 Å). In contrast, samples that had not been previously washed formed a much rougher and thicker film of ~6 nm (60 ± 7 Å). This film surrounded a 40-70 nm high structure, which formed a boundary between the exposed substrate and the polymer film. This ring shaped

structure, was formed by the spontaneous dewetting of the polymer solution within the receding PDMS cylinders. After the PDMS stamp was removed, the polymer remained, forming the walls observed in **Figure 3.14**. PMs were formed as a polymer monolayer on the surface stabilized by covalent bonds with the oxide surface. The methanol wash prior to crosslinking removed any non-surface reacted polymer, thus leaving a thin polymer film behind. Without thermal cross-linking, the thickness of this polymer film was not a function of time (up to 48 hours)<sup>35</sup>, thus thermal curing was required for the formation of thicker polymer films. In addition, this suggests that polymer crosslinking did not contribute greatly to the formation of the PM and that PM is stabilized by direct interaction with the surface.



*Figure 3.13. Light microscope images of patterns generated using various polymer concentrations and approaches.*

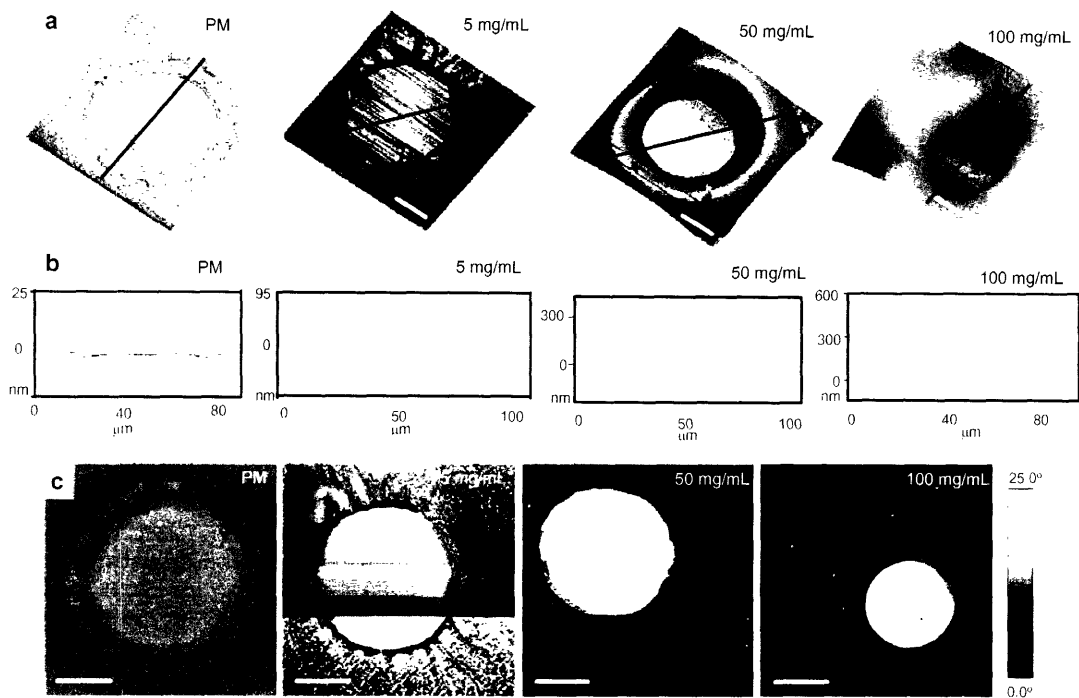


Figure 3.14. AFM images of patterned surfaces using 5, 50 and 100 mg mL<sup>-1</sup> poly(TMSMA-*r*-PEGMA) in methanol. PMs were prepared by washing the 5 mg mL<sup>-1</sup> structures prior to curing. Figure (a) represents 3D rendering of the height image obtained for various samples. Figure (b) illustrates representative cross-sectional height images for various structures. The height and the shape of the structures formed were directly related to polymer concentration and fabrication technique. Figure (c) is the phase images obtained from same samples as part (a). White bars indicate 20 μm.

To prepare features with higher topographical dimensions, we used 50 and 100 mg mL<sup>-1</sup> polymer solutions. Higher poly(TMSMA-*r*-PEGMA) concentrations gave rise to morphologically distinct structures. At 50 mg mL<sup>-1</sup>, the height of the polymeric structures surrounding each exposed region increased to 100-250 nm (Figures 3.14a and 3.14b). As the polymer concentration was further increased to 100 mg mL<sup>-1</sup>, the height of the structures increased to > 450 nm. Thus, the height and shape of the wells were directly correlated to the polymer concentration, which is readily understood in terms of mass conservation. The ring microstructure became larger as the polymer content in the solution increased. It is expected that the height of the features presented here would increase in aqueous solution due to PEG swelling in water, thus the values presented here provide lower limits of the topographical heights.

In addition, the inner diameter of the microwells formed in this approach was a function of the amount of deposited polymer, ranging from 50-60 μm for polymer concentrations up to 50 mg mL<sup>-1</sup> to 30 μm for 100 mg mL<sup>-1</sup> concentration (Figure 3.14). It is expected that this approach can be utilized to control the feature size at a given length scale.

We also used AFM to determine the spatial distribution of surface molecules. Phase contrast in an AFM image indicates differences in the molecular interactions of the AFM tip with the surface, thus providing a measure of surface exposure. As illustrated in **Figure 3.14c**, a sharp phase contrast was observed using all conditions tested. Furthermore, the contrast intensity increased as the thickness of the polymer film increased indicating a sharper difference in the surface properties of the exposed region and coated regions. This suggests that the regions within the ring-like structures were exposed to substrate and had not been coated by a thin polymeric layer.

### **Protein patterning**

To test the ability of the patterned surfaces to resist protein adsorption, patterned polymer microstructures or PMs were immersed in the solutions of FITC-labeled bovine serum albumin (BSA) and fibronectin (FN). Fluorescent images and quantitative analysis of the patterned surfaces demonstrate that BSA adhered to the co-polymer coated regions at ~4% of the exposed substrate (**Figures 3.15a, 3.15b and 3.15e**). Fibronectin was also selectively adhered to the exposed substrate for both PMs (**Figure 3.15c**) and microstructures (**Figure 3.15d**) at 2-3% of the surrounding regions. Interestingly, higher polymer concentrations did not significantly influence the protein resistant properties of the surface. This may suggest that the surface coverage of the monolayers is comparable to the thicker films. Protein adsorption was similar for a variety of pattern sizes as small as 15  $\mu\text{m}$  in diameter over substrates up to  $\sim 2 \times 3 \text{ cm}^2$ , thus demonstrating that this technique is simple and efficient for patterning proteins.

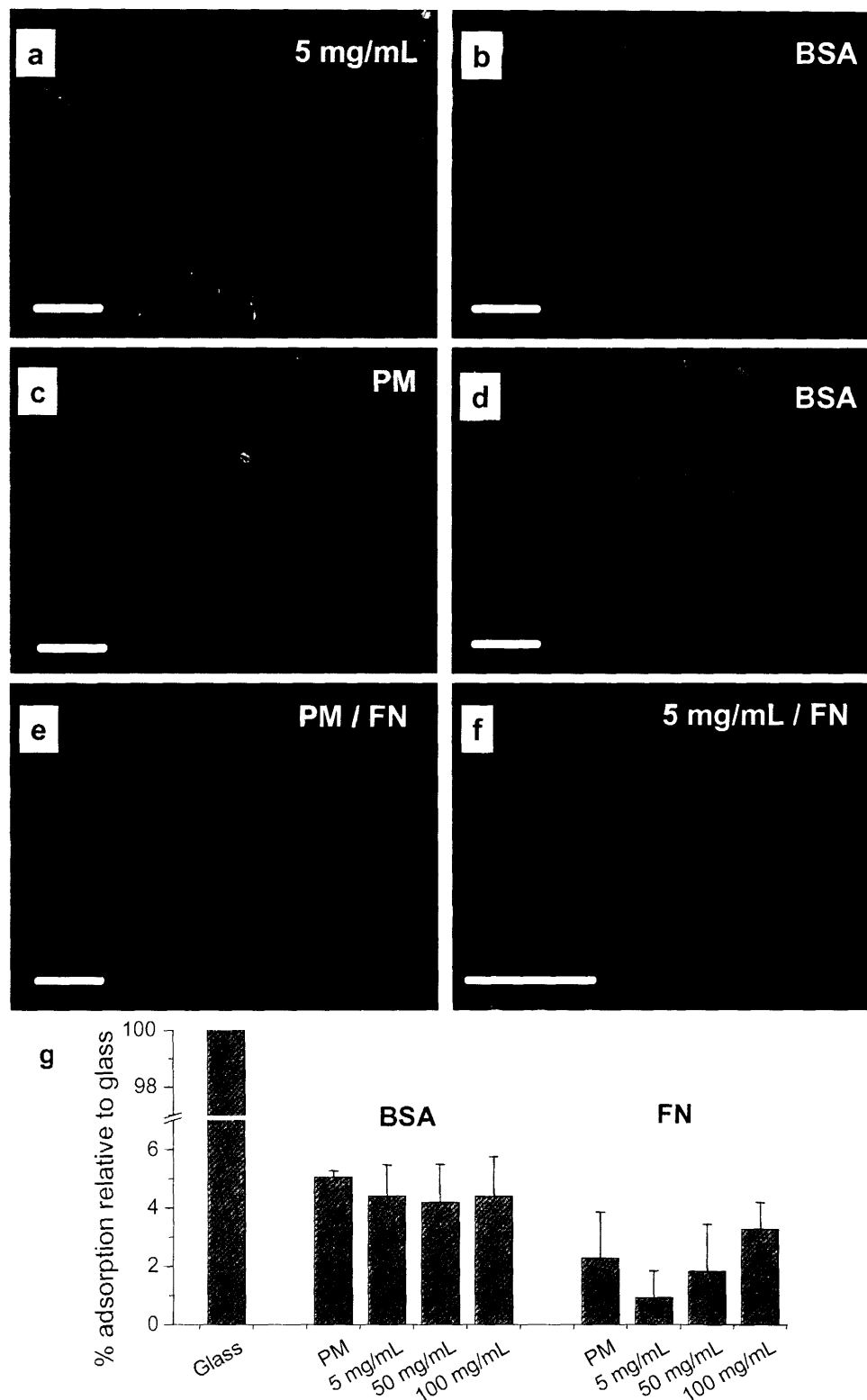


Figure 3.15. BSA and FN adsorption onto patterned poly(TMSMA-r-PEGMA) surfaces. (a-b) represent BSA staining of patterned microstructures (a) and PMs (b) for same sections. (c-d) are the FN staining micrographs for patterned PM (c) and microstructure (d). (e) is the quantitative values for the adsorption of FN and BSA on PEG coated regions in comparison to the exposed substrate. Protein and BSA adhered selectively to the exposed substrate in comparison to the polymer coated regions. In addition, increasing polymer concentration did not enhance the protein resistant properties of the patterns. Bar indicates 200  $\mu$ m.

## Cell patterning

To evaluate the feasibility of the patterned surfaces for selective cell attachment, NIH-3T3 fibroblasts were seeded on the patterned PMs and microstructures that had been pre-incubated with fibronectin. As expected, NIH-3T3 cells selectively adhered to fibronectin coated substrate within 6 hour after seeding for both PMs and microstructures (**Figure 3.16**). Cells were patterned over large areas in a reproducible manner for all samples for various pattern sizes (ranging from 15 to 150  $\mu\text{m}$  in diameter). The area of the exposed surface as well as cell seeding density determined the number of cells initially seeded per fibronectin patch. Distinct differences were observed depending on whether cells seeded were on PMs or in wells formed from microstructures. The most striking difference was the visible space between the cells and the walls of the microstructure. Thus, cells that were seeded within these wells remained confined to the bottom surface of the microwells and did not adhere to the polymeric walls.

Cells patterned on PMs were morphologically similar to previously obtained results by other groups<sup>16, 18, 19, 38</sup>. For PM patterns, selective cell adhesion was driven by adhesion to fibronectin and repulsion from PEG molecules, whereas for cells in microwells, the topographical features may have also contributed to cell patterning. As we demonstrated, the microstructures generated by this technique could range in size from 5 to  $>500$  nm, thus providing both an additional barrier to cell spreading and a favorable region for cells to deposit.

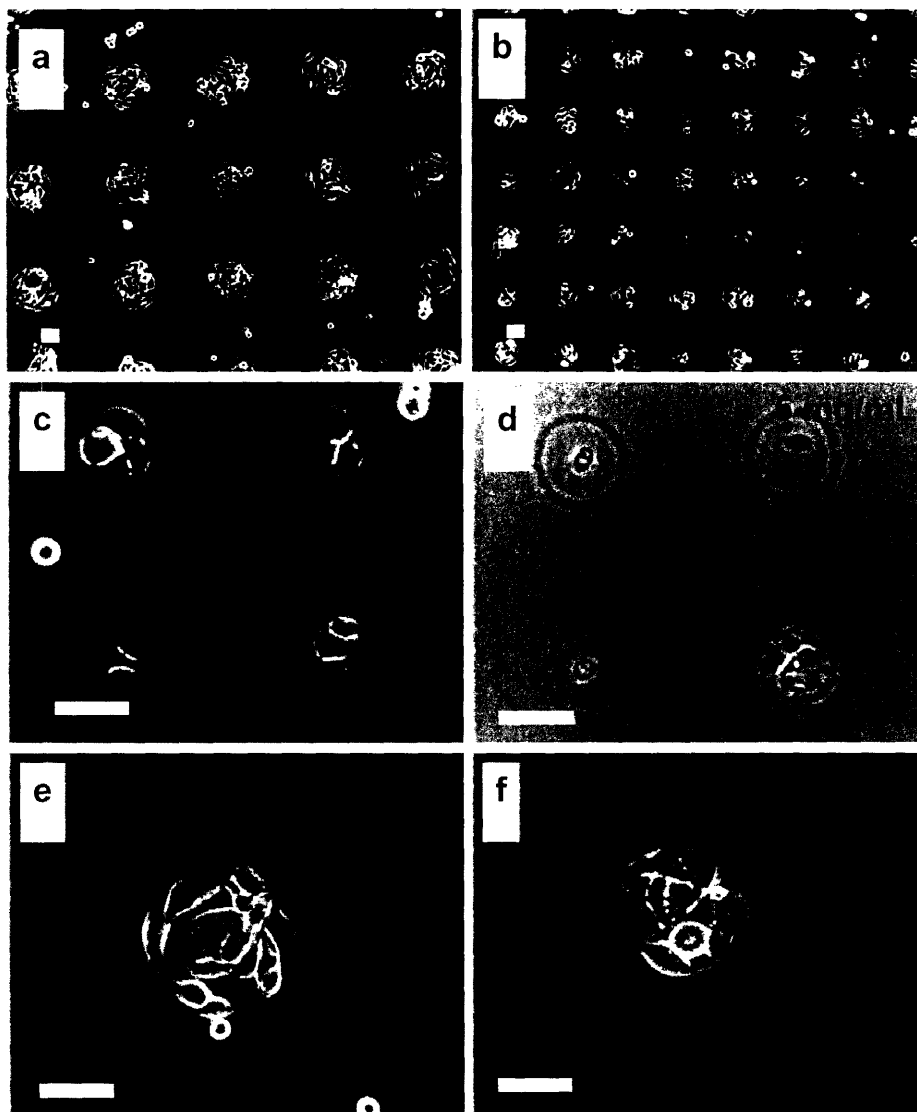


Figure 3.16. NIH-3T3 cells on patterns of PM (right panel),  $5 \text{ mg mL}^{-1}$  (left panel) after 6 hours in culture. Bar indicates  $50 \text{ }\mu\text{m}$ .

To determine the stability of these patterns, patterned cell arrays were tracked using phase contrast microscopy on PMs as well as on microstructures. Cell patterns on microstructures remained stable for at least 4 days (>95%) without many interconnections between adjacent cell islands (**Figures 3.17b, 3.17c and 3.17d**). However, cell patterns on PMs were less stable (>75%) and started forming interconnections within 4 days (**Figure 3.17a**). This behavior may be attributed to the effects of cell confinement within the microwells or PEG degradation of the monolayer, rather than incomplete initial coverage of the polymer.

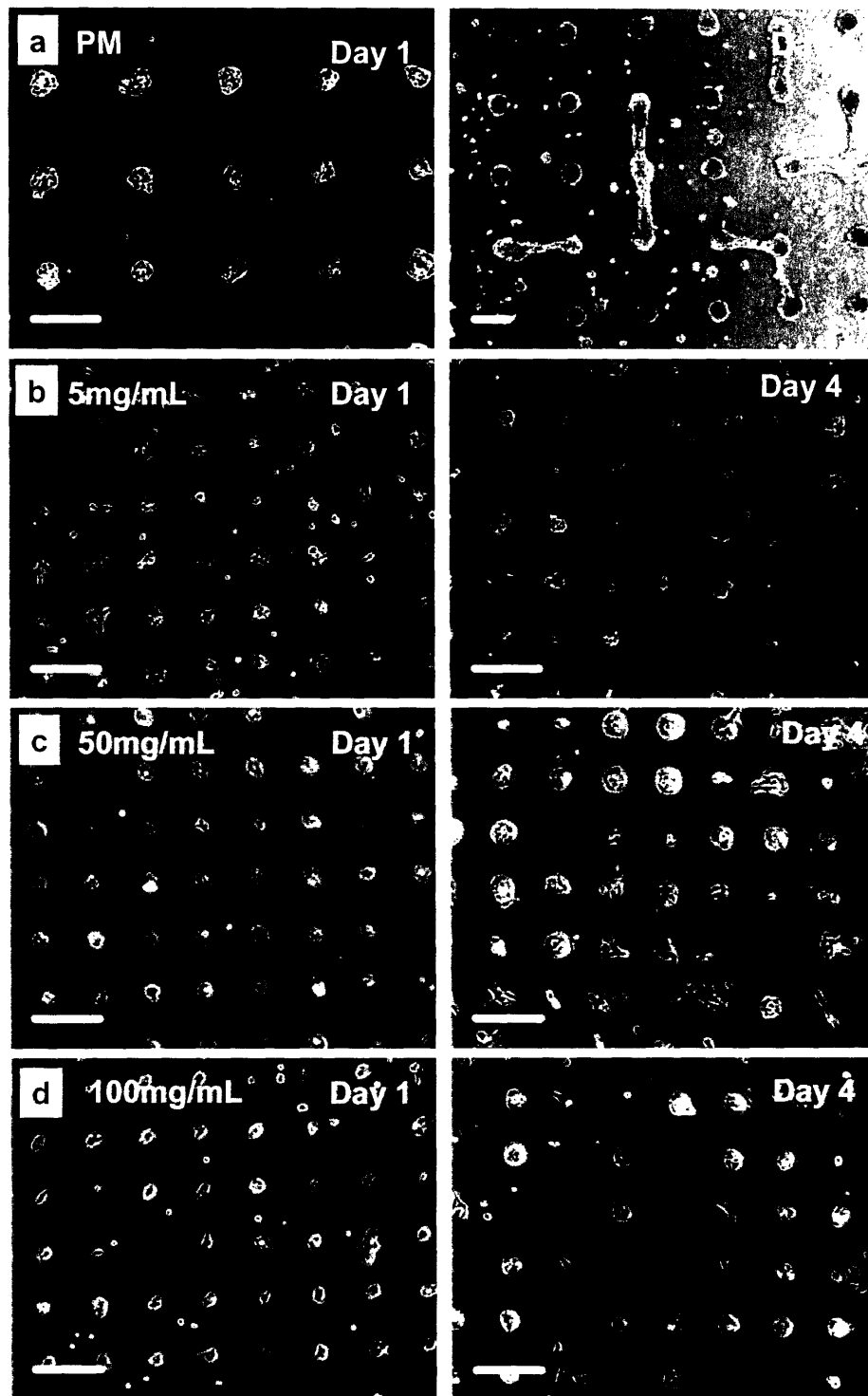


Figure 3.17. NIH-3T3 cells on patterns of PM (a),  $5 \text{ mg mL}^{-1}$  (b),  $50 \text{ mg mL}^{-1}$  (c) and  $100 \text{ mg mL}^{-1}$  (d) polymer concentrations over time. The time at which the image was taken is shown in the figure. Bar indicates  $200 \mu\text{m}$ .



A notable property of the current technique is the stability of the poly(TMSMA-*r*-PEGMA). Both the microwells and the PMs remained stable in water for at least two weeks. In addition, the microstructures were mechanically robust and could not be easily scratched from the substrate. Thus, the cross-linking of the methoxysilyl groups in the polymer units can generate patterns that are mechanically and chemically stable under the tested conditions.

Although we have used a ‘negative’ stamp in this paper, enhanced pattern fidelity can be ensured by using ‘positive’ stamps. We have observed that positive stamps can be used to create patterns through minor alterations to the protocol. To ensure dewetting of contact regions between the PDMS and glass, surfaces were not plasma cleaned. In addition, water was used as the polymer solvent, which further repels PDMS and allows for pattern formation through dewetting. Patterns formed with positive stamps resemble the negative structures of the PDMS stamps with only slight deformations due to the presence of meniscus.

In this chapter, we have patterned SiO<sub>2</sub> based substrates by taking advantage of the covalent bonding of a multivalent polymer. Moreover, the technique presented here can potentially be easily expanded to a variety of other substrates that can be modified to present surface reactive hydroxyl groups. The approach could also be expanded to a variety of tissue culture materials such as polystyrene and poly(methyl methacrylate) that have been treated with oxygen plasma. There are a number of possible advantages associated with this technique in comparison to the previously described methods of generating patterned surfaces. These include greater control over surface topography, ease in the synthesis of the polymer, and stability of the patterned features. This technique could be useful for applications that require control over both the topography as well as the molecular control of the surface. For example, this approach may be used to fabricate arrays of microwells with non-reactive walls for biological assays that desire molecules to react, hybridize or adsorb only to the bottom surface.

## CONCLUSIONS

The synthesis of a PEG-grafted surface-reactive random copolymer and its self-assembled structure on Si/SiO<sub>2</sub> substrates for construction of nonbiofouling surfaces are reported. The copolymer, poly(TMSMA-r-PEGMA), which is comprised of ‘anchor part’ (trimethoxysilane) and ‘function part’ (PEG), was synthesized by radical polymerization reaction. The copolymer spontaneously formed monolayers on Si/SiO<sub>2</sub> wafers with average thickness of 11 Å. The tapping mode AFM revealed that the surface of the polymer monolayers was smooth with an average roughness of 1.3 Å (root mean square). Protein-resistances of the polymer monolayers on Si/SiO<sub>2</sub> wafers were evaluated with insulin, lysozyme, and fibrinogen. For all tested proteins, the polymer monolayers showed significant reduction (up to 98 %) in nonspecific protein adsorption compared to the unmodified Si/SiO<sub>2</sub> wafers. In addition, cell adhesion was significantly reduced on the polymer-coated glass substrates in comparison to unmodified glass substrates.

The combination of the polymer (since it can be used to both form monolayers or crosslink to form structures) and capillary force lithography were used to design a unique method of fabricating a variety of structures using the same patterning stamp. The patterns could be used for cell and protein patterns that remained stable with time. In conclusion, we present a novel method of patterning cells and proteins with a copolymer comprising poly-anchoring group. The technique allows for control over surface topography and surface molecules.

## REFERENCES

- (1) Langer, R. Biomaterials in drug delivery and tissue engineering: one laboratory's experience. *Acc Chem Res*, **33**, 2, 2000.
- (2) Sefton, M. V., Sawyer, A., Gorbet, M., Black, J. P., Cheng, E., Gemmell, C., Pottinger-Cooper, E. Does surface chemistry affect thrombogenicity of surface modified polymers? *J Biomed Mater Res*, **55**, 4, 2001.
- (3) Langer, R. S., Vacanti, J. P. Tissue engineering: the challenges ahead. *Sci Am*, **280**, 4, 1999.
- (4) Langer, R., Vacanti, J. P. Tissue engineering. *Science*, **260**, 5110, 1993.
- (5) Malmsten, M., Emoto, K., Van Alstine, J. M. Effect of chain density on inhibition of protein adsorption by poly(ethylene glycol) based coatings. *Journal of Colloid and Interface Science*, **202**, 2, 1998.
- (6) Irvine, D. J., Mayes, A. M., Griffith, L. G. Nanoscale clustering of RGD peptides at surfaces using comb polymers. 1. Synthesis and characterization of comb thin films. *Biomacromolecules*, **2**, 1, 2001.
- (7) Huang, N. P., Michel, R., Voros, J., Textor, M., Hofer, R., Rossi, A., Elbert, D. L., Hubbell, J. A., Spencer, N. D. Poly(L-lysine)-g-poly(ethylene glycol) layers on metal oxide surfaces: Surface-analytical characterization and resistance to serum and fibrinogen adsorption. *Langmuir*, **17**, 2, 2001.
- (8) Kenausis, G. L., Voros, J., Elbert, D. L., Huang, N. P., Hofer, R., Ruiz-Taylor, L., Textor, M., Hubbell, J. A., Spencer, N. D. Poly(L-lysine)-g-poly(ethylene glycol) layers on metal oxide surfaces: Attachment mechanism and effects of polymer architecture on resistance to protein adsorption. *Journal of Physical Chemistry B*, **104**, 14, 2000.
- (9) Spencer, N. D., Kenausis, G. L., Elbert, D. L., Huang, N. P., Hofer, R., Ruiz-Taylor, L., Voros, J., Textor, M., Hubbell, J. A. Poly((L)-lysine)-G-poly(ethylene glycol) layers on metal-oxide surfaces. *Abstracts of Papers of the American Chemical Society*, **219**, 2000.
- (10) Prime, K. L., Whitesides, G. M. Self-assembled organic monolayers: model systems for studying adsorption of proteins at surfaces. *Science*, **252**, 5010, 1991.
- (11) Bearinger, J. P., Terrettaz, S., Michel, R., Tirelli, N., Vogel, H., Textor, M., Hubbell, J. A. Chemisorbed poly(propylene sulphide)-based copolymers resist biomolecular interactions. *Nature Materials*, **2**, 4, 2003.
- (12) Lee, S. W., Laibinis, P. E. Protein-resistant coatings for glass and metal oxide surfaces derived from oligo(ethylene glycol)-terminated alkyltrichlorosilanes. *Biomaterials*, **19**, 18, 1998.

- (13) Chovan, T.,Guttman, A. Microfabricated devices in biotechnology and biochemical processing. *Trends in Biotechnology*, **20**, 3, 2002.
- (14) Singhvi, R.,Kumar, A.,Lopez, G. P.,Stephanopoulos, G. N.,Wang, D. I.,Whitesides, G. M.,Ingber, D. E. Engineering cell shape and function. *Science*, **264**, 5159, 1994.
- (15) Mrksich, M.,Whitesides, G. M. Using self-assembled monolayers to understand the interactions of man-made surfaces with proteins and cells. *Annu Rev Biophys Biomol Struct*, **25**, 1996.
- (16) Mrksich, M.,Dike, L. E.,Tien, J.,Ingber, D. E.,Whitesides, G. M. Using microcontact printing to pattern the attachment of mammalian cells to self-assembled monolayers of alkanethiolates on transparent films of gold and silver. *Exp Cell Res*, **235**, 2, 1997.
- (17) Whitesides, G. M.,Ostuni, E.,Takayama, S.,Jiang, X.,Ingber, D. E. Soft lithography in biology and biochemistry. *Annu Rev Biomed Eng*, **3**, 2001.
- (18) Mrksich, M.,Chen, C. S.,Xia, Y.,Dike, L. E.,Ingber, D. E.,Whitesides, G. M. Controlling cell attachment on contoured surfaces with self-assembled monolayers of alkanethiolates on gold. *Proc Natl Acad Sci U S A*, **93**, 20, 1996.
- (19) Chen, C. S.,Mrksich, M.,Huang, S.,Whitesides, G. M.,Ingber, D. E. Geometric control of cell life and death. *Science*, **276**, 5317, 1997.
- (20) O'Neill, C.,Jordan, P.,Riddle, P.,Ireland, G. Narrow linear strips of adhesive substratum are powerful inducers of both growth and total focal contact area. *J Cell Sci*, **95 ( Pt 4)**, 1990.
- (21) Hyun, J.,Zhu, Y. J.,Liebmann-Vinson, A.,Beebe, T. P.,Chilkoti, A. Microstamping on an activated polymer surface: Patterning biotin and streptavidin onto common polymeric biomaterials. *Langmuir*, **17**, 20, 2001.
- (22) Bhatia, S. N.,Balis, U. J.,Yarmush, M. L.,Toner, M. Microfabrication of hepatocyte/fibroblast co-cultures: role of homotypic cell interactions. *Biotechnol Prog*, **14**, 3, 1998.
- (23) Bhatia, S. N.,Balis, U. J.,Yarmush, M. L.,Toner, M. Probing heterotypic cell interactions: hepatocyte function in microfabricated co-cultures. *J Biomater Sci Polym Ed*, **9**, 11, 1998.
- (24) Bhatia, S. N.,Yarmush, M. L.,Toner, M. Controlling cell interactions by micropatterning in co-cultures: hepatocytes and 3T3 fibroblasts. *J Biomed Mater Res*, **34**, 2, 1997.
- (25) Bhatia, S. N.,Balis, U. J.,Yarmush, M. L.,Toner, M. Effect of cell-cell interactions in preservation of cellular phenotype: cocultivation of hepatocytes and nonparenchymal cells. *Faseb J*, **13**, 14, 1999.
- (26) Hyun, J.,Ma, H.,Zhang, Z.,Beebe, T. P.,Chilkoti, A. Universal route to cell micropatterning using an amphiphilic comb polymer. *Adv Mat*, **15**, 7-8, 2003.

- (27) Takayama, S., McDonald, J. C., Ostuni, E., Liang, M. N., Kenis, P. J. A., Ismagilov, R. F., Whitesides, G. M. Patterning cells and their environments using multiple laminar fluid flows in capillary networks. *Proc Natl Acad Sci U S A*, **96**, 10, 1999.
- (28) Ostuni, E., Kane, R., Chen, C. S., Ingber, D. E., Whitesides, G. M. Patterning mammalian cells using elastomeric membranes. *Langmuir*, **16**, 20, 2000.
- (29) Folch, A., Jo, B. H., Hurtado, O., Beebe, D. J., Toner, M. Microfabricated elastomeric stencils for micropatterning cell cultures. *J Biomed Mater Res*, **52**, 2, 2000.
- (30) Revzin, A., Russell, R. J., Yadavalli, V. K., Koh, W. G., Deister, C., Hile, D. D., Mellott, M. B., Pishko, M. V. Fabrication of poly(ethylene glycol) hydrogel microstructures using photolithography. *Langmuir*, **17**, 18, 2001.
- (31) Suh, K. Y., Kim, Y. S., Lee, H. H. Capillary force lithography. *Adv Mater*, **13**, 18, 2001.
- (32) Kim, Y. S., Suh, K. Y., Lee, H. H. Fabrication of three-dimensional microstructures by soft molding. *Appl Phys Lett*, **79**, 14, 2001.
- (33) Ruiz-Taylor, L. A., Martin, T. L., Zaugg, F. G., Witte, K., Indermuhle, P., Nock, S., Wagner, P. Monolayers of derivatized poly(L-lysine)-grafted poly(ethylene glycol) on metal oxides as a class of biomolecular interfaces. *Proc Natl Acad Sci U S A*, **98**, 3, 2001.
- (34) Chan-Park, M. B., Yan, Y., Neo, W. K., Zhou, W., Zhang, J., Yue, C. Y. Fabrication of high aspect ratio poly(ethylene glycol)containing microstructures by UV embossing. *Langmuir*, **19**, 2003.
- (35) Jon, S. Y., Seong, J. H., Khademhosseini, A., Tran, T. N. T., Laibinis, P. E., Langer, R. Construction of nonbiofouling surfaces by polymeric self-assembled monolayers. *Langmuir*, **19**, 24, 2003.
- (36) Suh, K. Y., Yoo, P. J., Lee, H. H. Meniscus formation and breakdown of thin polymer films in microchannels. *Macromolecules*, **35**, 11, 2002.
- (37) Suh, K. Y., Park, J., Lee, H. H. Controlled polymer dewetting by physical confinement. *Journal of Chemical Physics*, **116**, 17, 2002.
- (38) Chiu, D. T., Jeon, N. L., Huang, S., Kane, R. S., Wargo, C. J., Choi, I. S., Ingber, D. E., Whitesides, G. M. Patterned deposition of cells and proteins onto surfaces by using three-dimensional microfluidic systems. *Proc Natl Acad Sci U S A*, **97**, 6, 2000.

## **4. Characterization of hyaluronic acid immobilized on solid substrates and its application for patterning**

### **INTRODUCTION**

Polysaccharide coatings have attracted much attention in biomaterials research due to their ability to reduce fouling of surfaces by biological species<sup>1-11</sup>. Although the mechanism of protein or cell resistance is not completely understood, conformation and dehydration of polysaccharides through interactions with water, as well as charge interactions are believed to be important<sup>1</sup>. A variety of polysaccharides have been explored for use as potential low-fouling surface modifiers. These include dextrans<sup>2-5</sup>, carboxymethylated dextrans<sup>6-8</sup>, and other carboxylated polysaccharides such as alginic acid and hyaluronic acid (HA)<sup>9-11</sup>. Of these polysaccharides, HA has received much attention due to its unique properties. HA is a linear polysaccharide composed of repeating disaccharide units of N-acetyl-D-glucosamine linked to D-glucuronic acid, and unlike all other glycosaminoglycans (GAGs), HA is not sulfated. As a component of the extracellular matrix, HA plays an important role in lubrication, water-sorption, water-retention, and a number of cellular functions such as attachment, migration, and proliferation<sup>12, 13</sup>. HA is therefore an attractive building block for new biocompatible and biodegradable polymers that have applications in drug delivery, tissue engineering, and viscosupplementation<sup>14-17</sup>.

The formation of a stable HA coating has potential biomedical applications ranging from bioactive surfaces to the formation of multilayer polyelectrolyte films<sup>18-20</sup>. To generate HA coated surfaces various immobilization techniques have been employed ranging from covalent attachment with emphasis on a well-pinned, dense polymer layers<sup>9, 21-23</sup>, layer-by-layer deposition<sup>24,25</sup>, and binding with natural ligands such as p32<sup>26</sup>. These strategies, however, involve potentially complicated synthetic approaches that require the use of chemicals, UV light or cumbersome procedures to prepare additional binding layers, potentially limiting their application as a general route to HA surface immobilization. Furthermore, such attachment methods are not easily applicable to simple patterning techniques such as soft lithography.

In this chapter, the formation of a stable, chemisorbed HA layer on hydrophilic surfaces, such as glass and silicon oxides, is demonstrated and characterized using X-ray photoelectron microscopy (XPS), ellipsometry, and atomic force microscopy (AFM). In addition, the underlying mechanism for this process is probed by studying the HA layer formation at various pH conditions and with washing procedures. Evidence suggests that the HA is stabilized on the surface through hydrogen bonding between the hydrophilic moieties in HA, such as carboxylic acid (-COOH) or hydroxyl (-OH) groups with silanol (-SiOH), carboxylic acid or hydroxyl groups on the hydrophilic substrates. The chemisorbed HA layer remains stable in phosphate buffered saline (PBS) for at least 7 days without losing its resistant properties. HA is therefore an important biological molecule that can be directly immobilized on substrates with high efficiency and stability. In addition, we tested the ability of HA to form surface patterns. Although a number of biomaterials have been tested in soft lithography, there essentially have been no previous reports dealing with soft lithographic uses of polysaccharides in part due to the fact that polysaccharides are highly hydrophilic (i.e., not compatible with a stamp prior to oxygen plasma treatment) and soluble in water (i.e., coatings would be washed away in the following steps). Also in this chapter, we report that HA is compatible with  $\mu$ CP provided that the stamp is hydrophilic as obtained by oxygen plasma treatment and also with soft molding without additional treatment. This is mainly possible by the fact that a HA film forms a stable, chemisorbed layer even after extensive washing on hydrophilic surfaces such as glass and silicon oxides as measured by X-ray photoelectron microscopy (XPS), ellipsometry, and atomic force microscopy (AFM). The HA patterns thus obtained were used to create a variety of protein or cell patterns.

## **MATERIALS AND METHODS**

*Materials:* HA (lot # 904572,  $M_n = 2.1$  MDa. by light scattering) was kindly supplied by Genzyme Inc.. Silicon dioxide wafers (1  $\mu$ m of SiO<sub>2</sub> on Si) were purchased from International Wafer Service and used without further treatment. Heparin and heparin sulfate (HS) were from Celsus Laboratories. Chondroitin sulfate A (CS A), chondroitin sulfate C (CS C), dermatan sulfate (DS), fluorescein isothiocyanate-labeled bovine serum albumin (FITC-BSA), goat anti-rabbit immunoglobulin G (FITC-IgG), fibronectin (FN), and anti-FN antibody were purchased

from Sigma. Glass slides were treated with O<sub>2</sub> plasma for 1 min to generate -OH groups as well as to clean the surfaces unless otherwise indicated.

*Surface characterization:* Fluorescent optical images were obtained using an inverted microscope (Axiovert 200, Zeiss). XPS spectra were recorded using a Kratos AXIS Ultra spectrometer. Spectra were obtained with a monochromatic Al K<sub>α</sub> X-ray source (1486.6 eV). Pass energy was 160 eV for survey spectra and 10 eV for high-resolution spectra. All spectra were calibrated with reference to the unfunctionalized aliphatic carbon at a binding energy of 285.0 eV. Spectra were recorded with similar setting (number of sweeps, integration times, etc.) from sample to sample to enable comparisons to be made. The analysis of the XPS spectra was performed on the basis of 90° unless otherwise indicated. Atomic force micrographs were obtained with tapping mode on a NanoScope III Dimension (Veeco Instruments) in air. The scan rate was 0.5 Hz and 256 lines were scanned per sample. Tapping mode tips, NSC15 - 300 kHz, were obtained from MikroMasch. Data were processed using Nanoscope III 4.31r6 software (Veeco Instruments Inc.). The thickness of the chemisorbed HA layer was measured with a Gaertner L116A ellipsometer (Gaertner Scientific Corp.) with a 632.8 nm He-Ne laser. A refractive index of 1.46 was used for all HA films, and a three-phase model was used to calculate thicknesses.

*Construction and stability of a chemisorbed layer and testing protein adsorption:* A few drops of HA solution (5 mg/mL in distilled water) were placed on the surface and spin coated (Model CB 15, Headaway Research, Inc.) at 1000 rpm for 10 seconds. The samples were stored overnight at room temperature to allow the solvent to evaporate. To examine the effect of washing, some samples were washed several times within 30 minutes of spin coating and then dried with a mild nitrogen stream. To examine the effect of pH, the silicon oxide surfaces were exposed for several hours to the solutions of pH 2, 7, and 11, respectively, leading to different oxidization states. HA films were prepared on those surfaces using the same procedure described above. In addition to HA, thin films of the other polysaccharides were prepared in the same manner.



To measure the immobilization of HA, heparin, HS, CS A, CS C, and DS films, was performed fluorescent staining for adhesion of various proteins on the coated surfaces. FITC-labeled BSA (50  $\mu\text{g}/\text{mL}$ ), IgG (50  $\mu\text{g}/\text{mL}$ ) and FN (20  $\mu\text{g}/\text{mL}$ ) were dissolved in PBS solution (pH = 7.4; 10 mM sodium phosphate buffer, 2.7 mM KCl, and 137 mM NaCl). To measure FN adsorption, the surfaces were stained with anti-FN antibody for 45 min, followed by a 1 hour incubation with the FITC-labeled anti-rabbit secondary antibody. A few drops of the protein solution were evenly distributed onto the HA surfaces. After storing at room temperature for 30 minutes, the surfaces were rinsed with PBS solution and water and then blown dry in a stream of nitrogen. To analyze stability, HA surfaces were placed in a PBS bath at various times and stored at room temperature for up to 7 days. The PBS solution was changed daily to prevent readsorption of dissociated HA onto the surface. The stability was subsequently analyzed by testing for FN adsorption as described. The slides were then examined under a fluorescent microscope under a UV light exposure of 2 seconds. Blank glass slides with or without FN staining were used as positive and negative controls respectively. The fluorescent images were analyzed quantitatively using Scion Image and the statistical analysis was performed using one-sided ANOVA tests with  $p < 0.05$  to distinguish between statistical significance.

For patterned substrates, patterns were analyzed by evenly distributing a few drops of the protein solution onto the patterned HA surfaces, storing at room temperature for 30 minutes, rinsing subsequently with PBS solution and water and then blowing dry in a stream of nitrogen. The surface was then imaged using an inverted microscope (Axiovert 200, Zeiss).

To analyze pattern stability, HA patterned glass substrates were placed in a PBS bath at various times and stored at room temperature for up to 7 days. The PBS solution was changed daily to prevent readsorption of dissociated HA onto the surface. The stability of the pattern was subsequently analyzed by testing for fibronectin adsorption as previously stated. The slides were then examined under a fluorescent microscope under a UV light exposure of 2 seconds. Blank glass slides with or without fibronectin staining were used as positive and negative controls respectively. The fluorescent images were analyzed quantitatively using Scion Image.

*Fabrication of PDMS stamps:* PDMS stamps were fabricated by casting PDMS (Sylgard 184 elastomer, Essex Chemical) against silicon masters prepared by photolithography (1:10 ratio of the curing agent). Then the pre-polymer was well mixed and incubated at 70 °C for 1 hour. After curing, PDMS stamps were detached from the master and cut.

*Microcontact printing:* PDMS stamps were plasma cleaned for 5 minutes (model PDC-001, Harrick Scientific Inc.) to ensure proper cleaning and to increase its wettability. After cleaning, a 5 mg/mL solution of HA (Genzyme Inc.) in deionized water was applied to the surface using a cotton swap. HA was coated three times to ensure complete coverage with HA and subsequently placed onto glass slides that were plasma cleaned for 1 minute. The stamp was left for 20 minutes and then peeled off. The printed slides were allowed to sit for 12 hours before further usage.

*Soft molding:* A few drops of the solution were placed on a glass slide and a thin film of HA was coated by spin coating (Model CB 15, Headway Research, Inc.) at 1000 rpm for 10 seconds. To make conformal contact, PDMS stamps were carefully placed onto the surface and the samples were stored overnight at room temperature to allow for evaporation of the solvent. The film thickness after solvent evaporation is about 606 nm as determined by ellipsometry and AFM.

*Cell cultures and adhesion:* NIH-3T3 murine embryonic fibroblasts (ATTC) were maintained in Dulbecco's modified eagle medium (DMEM) (Gibco Invitrogen Corp.) supplemented with 10 % fetal bovine serum (FBS) (Gibco Invitrogen Corp.) at 37 °C and 5% CO<sub>2</sub> environment. For cell attachment experiments, the patterned surfaces of HA were treated with 500 µg/mL of fibronectin in PBS for 15 minutes and then the cells were trypsinized and washed and directly seeded on the patterned surfaces at a cell density of  $\sim 10^4$  cells/cm<sup>2</sup>. The cell patterns were examined under phase-contrast microscope after removing non-adhered cells by rinsing with PBS. To determine patterned cell stability, the cells were tracked for 5 days under phase contrast microscope.

## RESULTS AND DISCUSSION

### Detection of a chemisorbed HA layer

The presence of a chemisorbed HA layer on silicon dioxide substrates or glass was verified by analyzing the elemental composition (carbon, oxygen, nitrogen, and silicon) of the surfaces using XPS. In particular, the detection of nitrogen in the XPS spectra was strong evidence to support the presence of a residual HA layer (**Figure 4.1**) since nitrogen is found in HA but not the substrate. As expected, no nitrogen was detected on the bare silicon oxide. The intensity at 400.1 eV (N 1s) decreased to about 25% of its original intensity after washing with PBS, though the peak remained, indicating a residual layer of HA (**Figure 4.1(a)**). A new XPS peak was also detected at 402.3 eV (15.5%) after washing, suggesting a modified oxidation state of nitrogen, denoted N<sup>\*</sup>C. It was hypothesized that the new peak originates from the partial protonation or hydrogen bonding of nitrogen to silanol groups (-SiOH) on the surface. The persistence of the nitrogen peak and the emergence of a new oxidized state (N<sup>\*</sup>C) generated after washing are consistent with a residual layer on the surface formed by chemical interactions between the layer and the substrate.

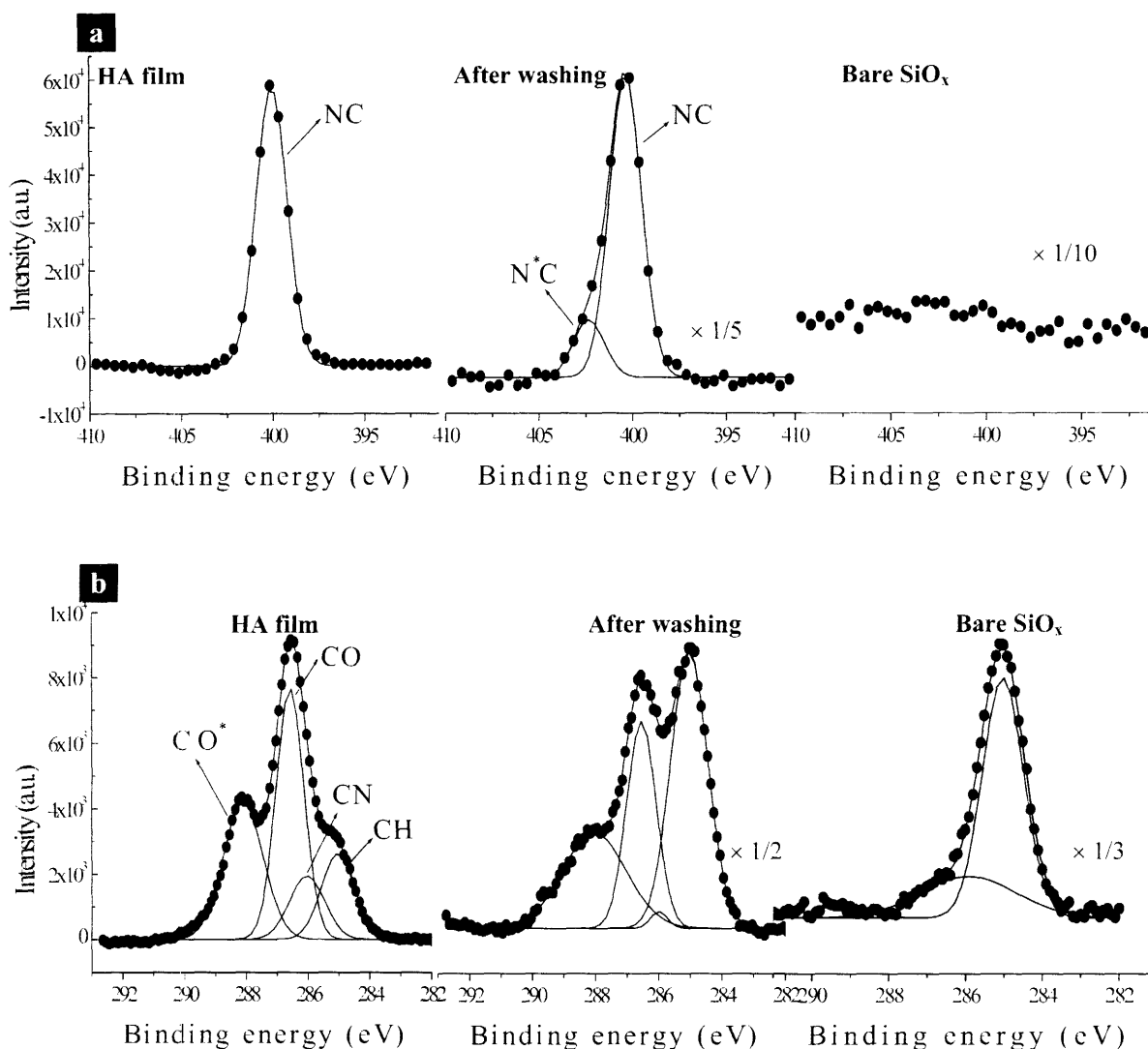
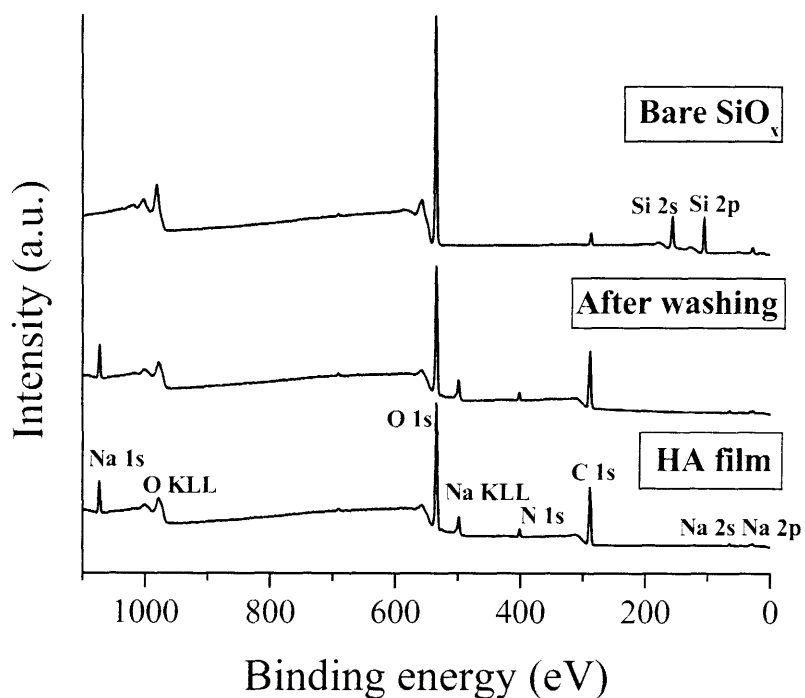


Figure 4.1. High-resolution XPS spectra of HA modified surfaces. These spectra are for (a) nitrogen (N 1s) and (b) carbon (C 1s) peaks in HA recorded for an as-spun, a washed, and a bare silicon oxide substrate, respectively. Note that the nitrogen peak did not disappear and a new oxidized state (N<sup>\*</sup>C) was generated after washing, suggesting that there is a residual layer on the surface and the layer chemically interacts with the substrate surface. For carbon peaks of an as-spun and a washed film, the spectra were deconvoluted with four Gaussian peaks that are assigned at each oxidized state. For convenience, the peak for the strongly oxidized carbon (CO<sup>\*</sup>) was not deconvoluted in detail. All films were prepared and characterized on the silicon oxide substrate to take advantage of the flat surface.

The carbon peak (C 1s) of an as-spun film contains four peaks that are located at 285.0 (16.1%), 286.1 (12.7%), 286.6 (40.0%), and 288.1 (31.2%), consistent with previous reports (**Figure**

**4.1(b))**<sup>27</sup>. The amount of unfunctionalized hydrocarbon (285 eV) was higher than expected (7.1%)<sup>27</sup>, which may be attributed to carbon adsorption from the air. In order of increasing binding energies these peaks represent the hydrocarbon environment (HC), carbon singly bound to nitrogen (CN), carbon singly bound to oxygen (CO), strongly oxidized carbons (CO\*) including carbon doubly bound to oxygen and a combined peak representing both amide and carboxylate ion carbon atoms (CON and COO)<sup>27</sup>. In contrast to the as-spun coatings, the relative intensities were substantially changed after washing with the peak locations slightly shifted. Two factors potential reasons are the increased portion of unfunctionalized hydrocarbon from the substrate, and the surface interactions between HA and the substrate. Based on the modified oxidation state of nitrogen in the XPS spectra and hydrophilic moieties in HA some strong interactions, such as hydrogen bonding, may play an important role in the formation of the chemisorbed layer. In a separate experiment, the HA film was completely washed away on hydrophobic substrates such as untreated polystyrene, which indicates that other hydrophobic interactions could be ruled out in examining the origin of the HA layer.



*Figure 4.2. XPS spectra for the detection of a HA layer. The wide scans reveal that silicon peaks were not seen for an as-spun, thick HA film and a washed film whereas the peaks were observed for a bare silicon oxide when the electron take-off angle from the surface was 30°. This indicates that the substrate surface is fully covered with the chemisorbed layer.*

To analyze the thickness of the HA film, ellipsometry, AFM and XPS measurements at two different angles were utilized. At a 90° take-off angle (long penetration depth), silicon peaks were not seen for an as-spun sample (i.e. thick HA film on a glass), as opposed to bare silicon oxide and washed film controls. On the other hand, silicon peaks were nearly absent on the washed film when 30° was used (short penetration depth) (Figure 4.2). This indicates that the residual film was extremely thin, less than 5–10 nm depending on the element and electron selected, the thickness ranging within the penetration depth and the substrate surface is nearly fully covered with the chemisorbed layer. The presence of the chemisorbed layer was further confirmed by ellipsometry and AFM measurements. The ellipsometry results indicated the initial thickness of the HA film was about 330 nm, which decreased drastically to about 3 nm after washing and then remained at the same value. Furthermore, the roughness of a residual layer (2.1 nm) is between that of the substrate (1.8 nm) and the as-spun film (2.3 nm), which also supports the presence of a residual layer (Figure 4.3).

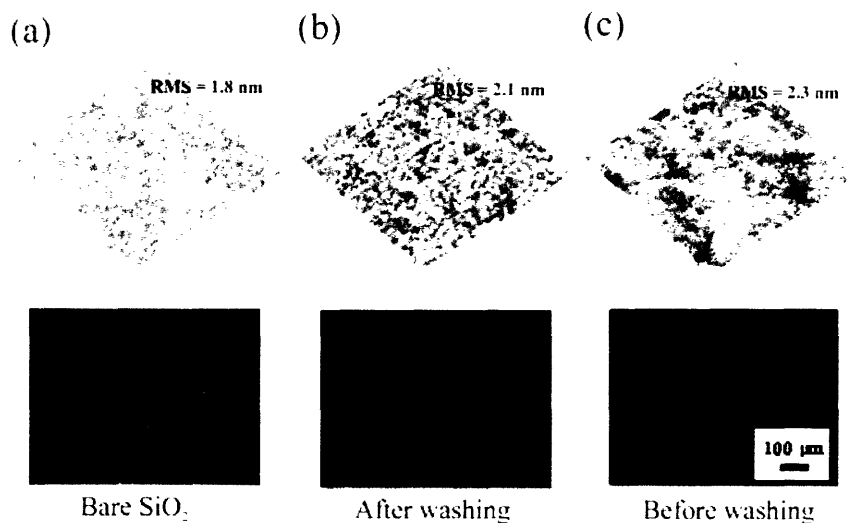


Figure 4.3. AFM images of surface roughness and the corresponding fluorescent images for FN adsorption for (a) a bare silicon oxide substrate, (b) a HA surface after thorough washing, and (c) an as-coated HA film. Note that the roughness of the film after washing locates between those of the other two surfaces, supporting the presence of a chemisorbed layer. The height scale is 5 nm and the scan size is  $1 \times 1 \mu\text{m}^2$ . The fluorescent images reveal that the surface is fully covered with HA even after extensive washing.

To further explore the potential mechanism of adhesion, we exposed silicon oxide surfaces to three different pH values of 2, 7, and 11 to test the effects of surface charge and hydrophobicity

on the formation of a HA coating (see the experimental protocol). At acidic conditions (pH = 2), the hydroxyl groups present on the surface are protonated ( $\text{OH}_2^+$ ) such that the adsorption of HA should be enhanced due to negative charge of HA. In contrast, since the surface is negatively charged ( $\text{O}^-$ ), the adsorption would be reduced at basic conditions (pH = 11). At pH 11, the atomic mass percentage of nitrogen on the surface was 0.33 % whereas it increased to 3.61 % when exposed to pH 2 (**Table 4.1**). These results indicate that HA is more likely to adsorb to positively charged surfaces than negatively charged surfaces. Interestingly, neutral surfaces (pH = 7) were also effective in HA (3.34 %), which also supports the presence of hydrogen bonding between HA and the hydroxyl groups.

Sample	Atomic conc. %			
	C	N	O	Si
Exposure to pH 2	57.6	3.6	34.0	4.8
Exposure to pH 7	52.2	3.3	38.3	6.2
Exposure to pH 11	14.6	0.3	58.0	27.1
No washing + drying	49.2	2.7	38.8	9.3
Washing after 30 min + drying	11.7	0.7	64.6	23.0
Bare silicon dioxide	4.2	0	65.4	30.4

*Table 4.1. Atomic mass percentage of carbon, nitrogen, oxygen and silicon elements for HA films formed under various conditions. Errors are within 5 %.*

The ability of the current approach in immobilizing other polymers having hydrophilic moieties on hydrophilic substrates was also studied. A previous study reported that carboxyl ( $-\text{COOH}$ ) groups were confined onto hydrophilic surfaces with additional thermal polymerization<sup>28</sup>. Poly(ethylene glycol)s, however, detach from the substrates upon hydration despite having hydrophilic moieties ( $-\text{OH}$ ). We hypothesize that two factors are responsible for the formation of a chemisorbed HA layer. First, hydrogen bonding should be strong enough to endure the polymer swelling stress at the interface upon exposure to water. Second, the chemisorbed layer should have a dense molecular structure such as entanglement to prevent penetration of water molecules.

Thus, sufficiently strong hydrogen bonding is required to prevent the adsorbed layer from peeling off from the surface. In this regard, the HA film should have enough contact time with the surface to build a robust interface. As indicated by XPS, the amount of nitrogen adsorbed onto the surface was lower when the sample was washed within 30 minutes after spin coating (0.69 %) (**Table 4.1**) and significantly increased to 2.74 % when the sample was dried overnight prior to washing. This indicates that the duration of exposure and sample drying may be important in the adsorption of the HA onto the surfaces.

Sample	N	O	C	O : C
Untreated	0.00	92.4	7.6	12.2
HA	3.8	37.5	58.7	0.6
Heparin	0.2	89.4	10.4	8.6
HS	0.1	91.1	8.8	10.4
CS A	0.5	88.8	10.7	8.3
CS C	0.1	90.5	9.4	9.6
DS	0.4	89.0	10.6	8.4

*Table 4.2. Atomic mass percentage of GAG surfaces and control surfaces. XPS was performed on GAG surfaces formed on silicon dioxide after washing. Untreated surfaces are silicon dioxide only. Numbers for nitrogen, oxygen, and carbon refer to atomic mass percentage. Oxygen:Carbon is the atomic mass percentage of oxygen divided that by carbon. Errors are within 5 %.*

With respect to the density of the molecular structure, HA is a highly hydrated polyanion, which forms network between domains in solutions.<sup>29, 30</sup> In addition, the polymer shows intrinsic stiffness due to hydrogen bonds between adjacent saccharides. HA immobilized on silicon and other dioxide surfaces in much higher quantities than other polysaccharides including dextran sulfate, heparin, HS, chondroitin sulfate, DS, and alginic acid (**Table 4.2**) based on the highest nitrogen composition (3.75 %) and the lowest oxygen to carbon ratio (0.64 %). This behavior could be attributed to either intrinsic differences between the molecular structures of various polysaccharides or their lower molecular weights compared to HA.



### Protein resistance, degradability, and stability of a chemisorbed HA layer

To test the effectiveness of the HA surfaces for protein resistance, HA modified surfaces were exposed to FITC-BSA, FITC-IgG and FN. The adhesion of BSA (0.46%), IgG (7.81%), and FN (6.22%) was significantly reduced ( $p < 0.001$ ) on HA coated surfaces compared to glass controls (100%) as measured by fluorescence intensity. A typical example of the fluorescent images for a bare silicon oxide, a HA surface after thorough washing, and an as-coated HA film is shown in **Figure 4.3** when FN is applied to the surface with subsequent antibody staining (see the experimental protocol). As seen from the figure, HA is uniformly attached to the surface even after extensive washing. We also tested protein resistance of various other polysaccharide surfaces on glass using FN (**Figure 4.4**). Surfaces formed with other polysaccharides resisted the adsorption of FN significantly higher than glass controls ( $p < 0.05$ ). Despite this, most other polysaccharide surfaces were still significantly less resistant to FN absorption than HA coatings ( $p < 0.05$ ).

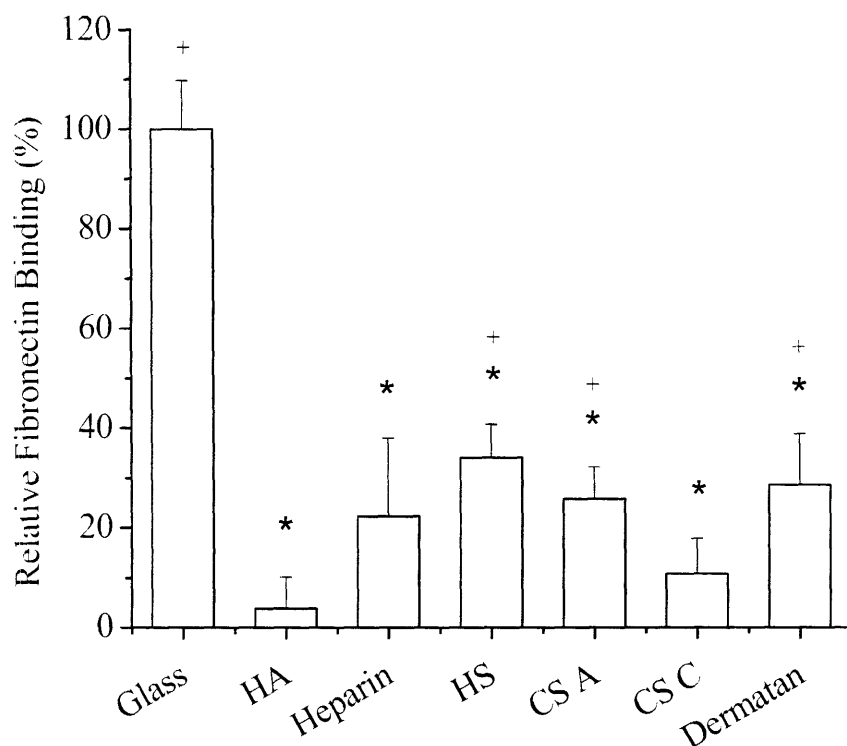


Figure 4.4. FN adsorption onto GAG surfaces was measured by quantifying the fluorescence intensity. The results are normalized to glass (defined as 100) as the positive control and no protein (defined as 0). Data is presented as a percentage of the difference between untreated and glass. \* denotes  $p < 0.05$  compared to glass, and + denotes  $p < 0.05$  compared to HA.

Although HA is biodegradable in nature, the possibility of degradation can presumably be ruled out herein since oxidants such as  $\text{HO}^\bullet$  and  $\text{HOCl}/\text{ClO}^-$  are believed to be important in the degradation of HA. The generation of reactive oxygen species is mediated by metal-ion catalysis ( $\text{HO}^\bullet$ ) *in vitro*<sup>31,32</sup> or myeloperoxidase catalyzed reaction of  $\text{H}_2\text{O}_2$  with  $\text{Cl}^-$  ( $\text{HOCl}/\text{ClO}^-$ ) *in vivo*. To investigate long-term stability, XPS was performed on the aged samples, which revealed persistent nitrogen peaks even after a week in PBS solution. However, the uniform distribution of HA is difficult to measure by means of XPS. We therefore used fluorescent staining of the samples as a function of time to obtain a global assessment of HA adsorption. The chemisorbed HA layer was also stable for at least 7 days as determined by the analysis of fluorescent images (**Figure 4.5**). The presence of the HA surface greatly reduced the adsorption of FN (>92%), even after the surface was exposed to PBS for 7 days prior to exposure FN adsorption and staining. These results indicate that at least in the case of silicon dioxide the formation of a chemisorbed layer of HA is stable for at least one week.

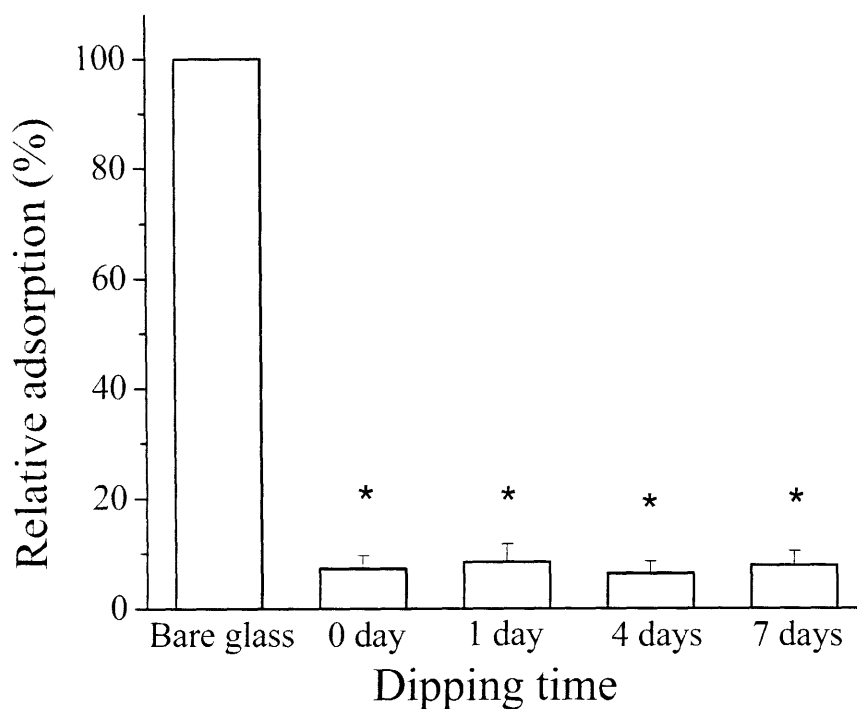


Figure 4.5. The stability of the HA surface was examined by the quantitative analysis of protein adsorption as a function of exposure times to PBS prior to exposure and subsequent staining to FN. Note that the surface is stable and greatly reduces protein adsorption more than 92% even after exposure to PBS for up to 7 days. No contrast enhancement was made throughout the analysis. \* denotes  $p < 0.05$ .

The formation of the stable HA layer has potential biomedical applications since the direct binding of bioactive molecules (e.g., enzymes, extracellular matrix components, antibodies, and peptides) to solid substrates provides excellent biocompatibility and specific responses. For example, glycosaminoglycans (GAGs) can be used to detect or recognize proteoglycan core proteins through specific oligosaccharide structures<sup>18-20</sup>. Furthermore, direct application of HA on surfaces without chemical treatment is useful since it might open a new pathway to construct a completely biocompatible, biodegradable platform as an alternative to PEG surfaces. Moreover, once immobilized, HA surfaces can be used to interact with CD44, allowing for a number of cell recognition processes<sup>20</sup>.

### **Patterning HA using micromolding and microcontact printing**

To demonstrate the applicability of HA for patterning proteins or cells utilizing the presence of the chemisorbed HA layer,  $\mu$ CP and soft molding techniques were used (**Figure 4.6**). For  $\mu$ CP, PDMS stamps were treated with oxygen plasma to improve adhesion of HA to the stamp because HA is highly hydrophilic. The transfer of HA layer to the substrate surface was successful only when the stamp was wet (i.e., prior to complete evaporation of solvent). When the stamp was dry, the fractional coverage appeared to be less than 1, leading to non-uniform protein adsorption or cell adhesion as confirmed by fluorescent images. Thus effective anti-adhesive surfaces can be obtained only if a high density of surface-linked polysaccharide chains is ensured<sup>2, 4, 33</sup>. For soft molding, the wetting environment is much different from previous studies since HA is a highly hydrophilic polymer. When a hydrophobic polymer is involved such as polystyrene or poly(styrene-butadiene-styrene) copolymer, the polymer partially wets the hydrophobic PDMS wall (acute contact angle), thus rising into the void space<sup>34, 35</sup>. On the other hand, capillary rise will be depressed within a void space due to an obtuse contact angle as water is completely incompatible with PDMS (contact angle is  $\sim 105^\circ$ )<sup>36</sup>. In this case, the HA polymer under a void region of stamp gets depleted until the substrate surface becomes exposed and accumulated in reservoirs near the edge to conserve mass. The HA pattern formed using this approach can be seen visually after peeling off the stamp and a typical example is shown in **Figure 4.7**. The exposure of the substrate surface can be measured in optical micrographs with the aid of sharp contrast, using delaminated regions as a guide (**Figures 4.7a and 4.7b**). Moreover, it was observed that sporadic HA reservoirs containing a relatively large amount of HA (**Figures 4.7c**

and 4.7d) for negative PDMS stamps (features sticking in), indicating capillary depression under the void space of the stamp. However, no reservoirs were observed in case of positive stamps (Figure 4.7b, features sticking out), suggesting that positive stamps are recommended in molding of hydrophilic polymers to ensure pattern fidelity over large areas.

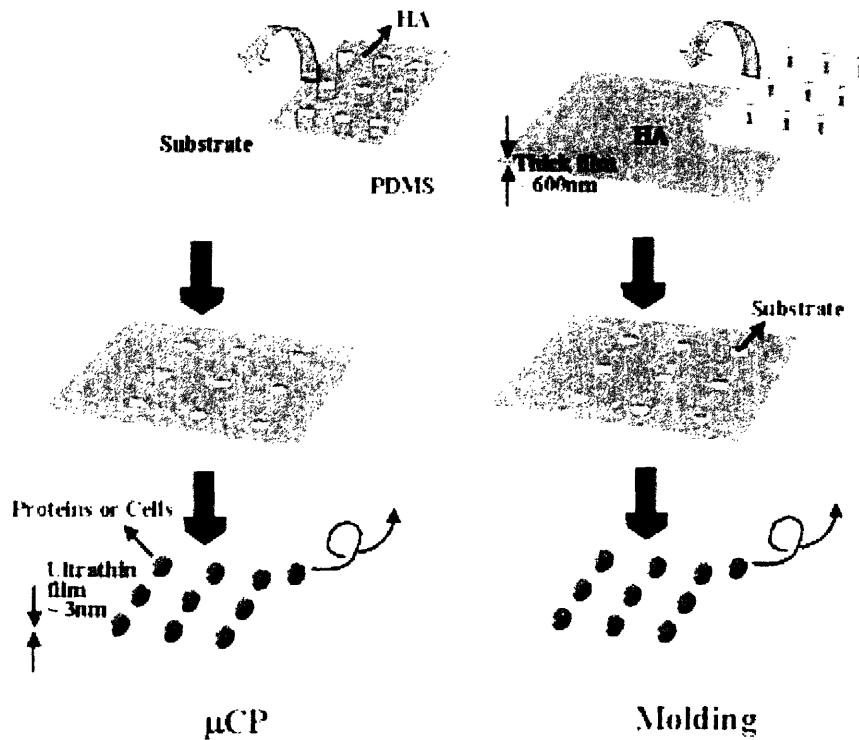


Figure 4.6. Typical soft lithographic techniques used to pattern HA on surfaces. The schematic illustration depicts two soft lithographic methods used in the experiments.  $\mu$ CP utilizes direct transfer from a stamp to a substrate whereas soft molding deals with pattern formation from a uniform polymer film into features of the stamp. HA film is compatible with these techniques.

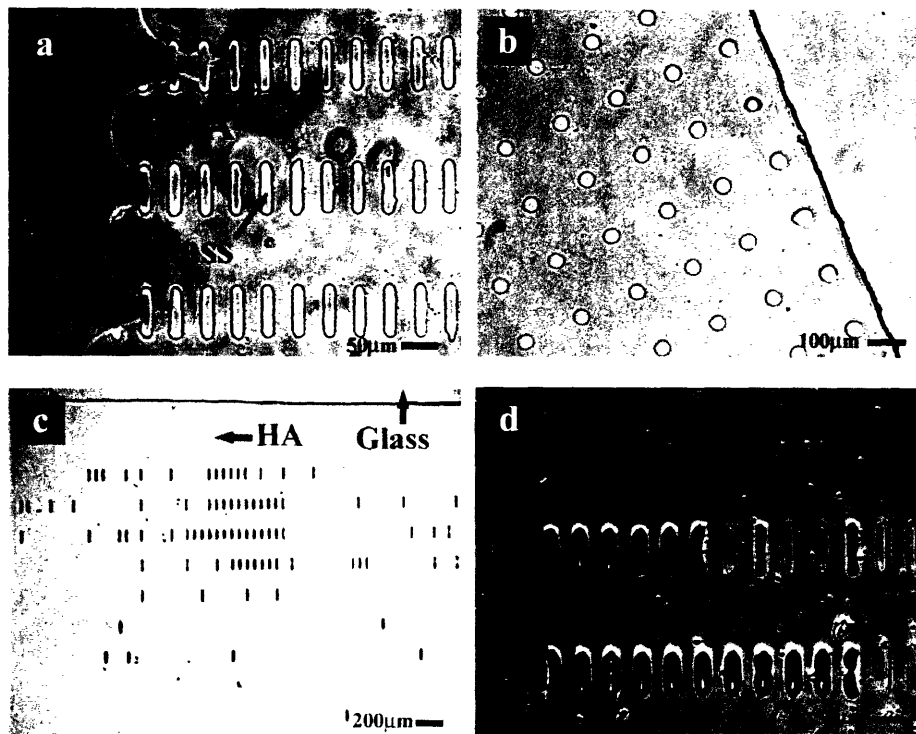


Figure 4.7. Optical micrographs of molded HA films. The patterns formed by soft molding can be easily seen after stamp removal regardless of the geometry of the stamp; (a)  $75 \times 15 \mu\text{m}^2$  ovals formed with a negative stamp. (b)  $50 \mu\text{m}$  holes with a positive stamp. (c, d) Sporadic formation of mass reservoirs near the edge for (c) a large-area view and (d) a magnified view. This indicates capillary depression during the soft molding as a result of the obtuse contact angle at the HA/PDMS/air interface. Thus, positive stamps are recommended to obtain pattern fidelity over large areas.

To test the effectiveness of the HA patterned surfaces for protein patterning, HA treated surfaces were treated with FITC-BSA and goat anti-rabbit FITC-IgG and fibronectin. **Figure 4.8** shows various protein patterns when HA was used as a resistant layer. The images reveal sharp contrast between binding and non-binding areas for a number of “sticky” proteins such as BSA **Figure 4.8 (a, b)**, IgG **(c)**, and fibronectin **(d)**, which demonstrate the excellent resisting properties of the surfaces toward protein adsorption. In addition, both soft molding (BSA) and  $\mu\text{CP}$  (IgG and fibronectin) methods were successfully applied for regulating protein adsorption, thus HA provides flexibility for use in various soft lithographic methods. Furthermore, a wide range of feature sizes (ranging from  $500 \text{ nm}$  to  $500 \mu\text{m}$ ) is easily patterned without cumbersome modifications. One example of fine patterns is shown in **Figures 4.8 (e) and (f)** using the molding process in which a  $5 \mu\text{m}$  box pattern was used. As seen from the figure, well-defined

fluorescent images can be seen over a large area with high pattern fidelity. The corresponding HA microstructure is shown in **Figure 4.8(g)**. In the course of the molding process, a considerable amount of the film is squeezed outside the stamp due to lower affinity of HA to PDMS stamp. For example, the average thickness was reduced to 65 nm in **Figure 4.8(g)** as calculated from the cross-sectional profile of the AFM image compared with the initial thickness of 606 nm. Although aspect ratio of original HA structures could be controlled using different concentrations and coating speeds, washing with water ultimately leads to a chemisorbed layer regardless of the initial structure.

Cells were also patterned on HA coated surfaces. Prior to patterning, HA patterned surfaces were treated with fibronectin for 15 minutes. The fibronectin adhered specifically to the exposed substrate thus creating a region for cell attachment. **Figure 4.9** is a typical image of a HA patterned surfaces that was seeded with NIH-3T3 murine embryonic fibroblasts and incubated for 6 hours. As expected, cells deposit only on the exposed glass, ranging from aggregated cell patterns (150  $\mu\text{m}$  holes in **Figures 4.9 (a)** and **(b)**) to single cell patterns (20  $\mu\text{m}$  holes in **Figures 4.9(c)** and **4.9(d)**) depending on the pattern size. In addition to fibroblasts, murine hepatocyte cells and embryonic stem cells were also successfully patterned on HA coated surfaces, which indicate the feasibility of this approach for various cell types (See Chapter 5).

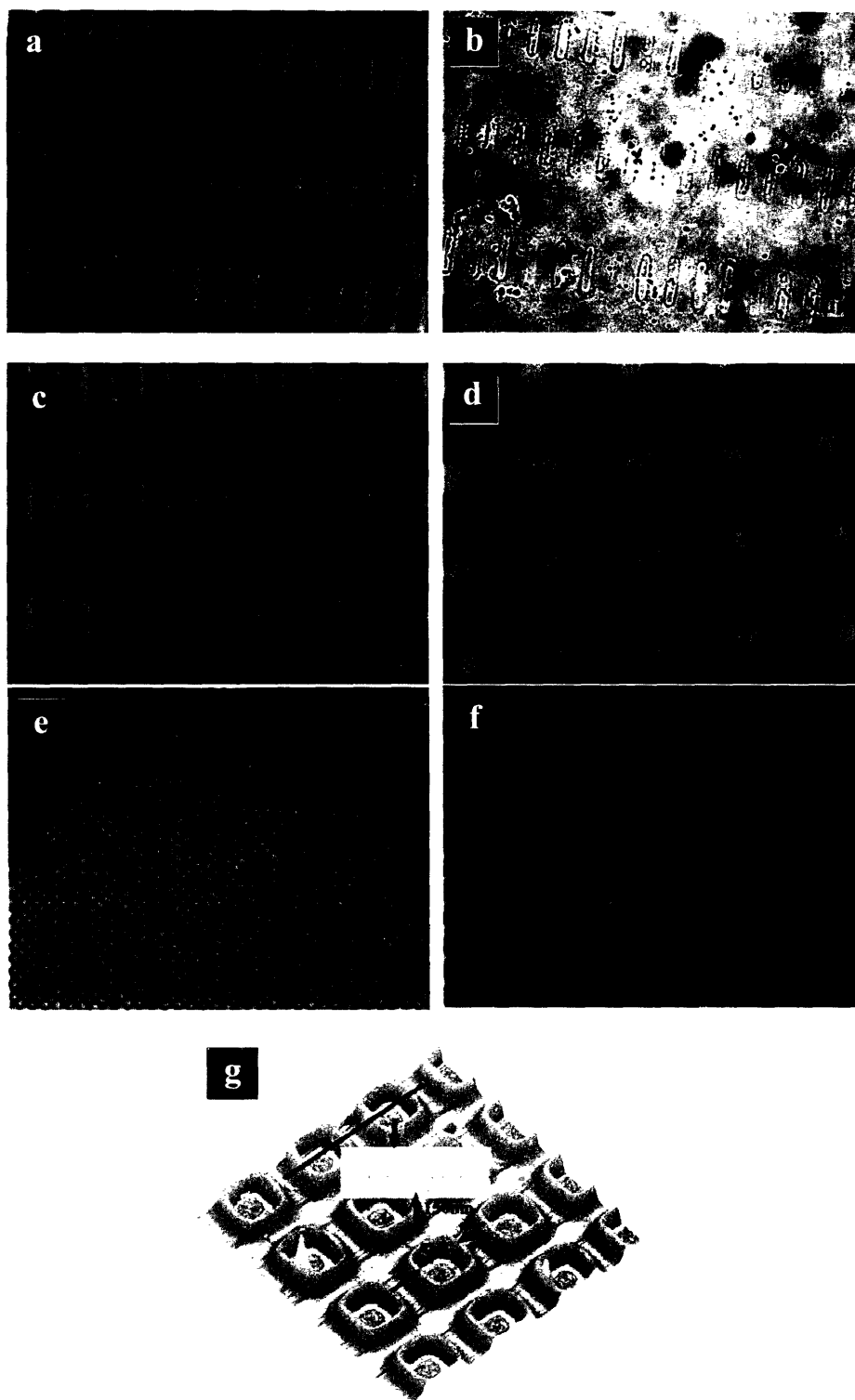
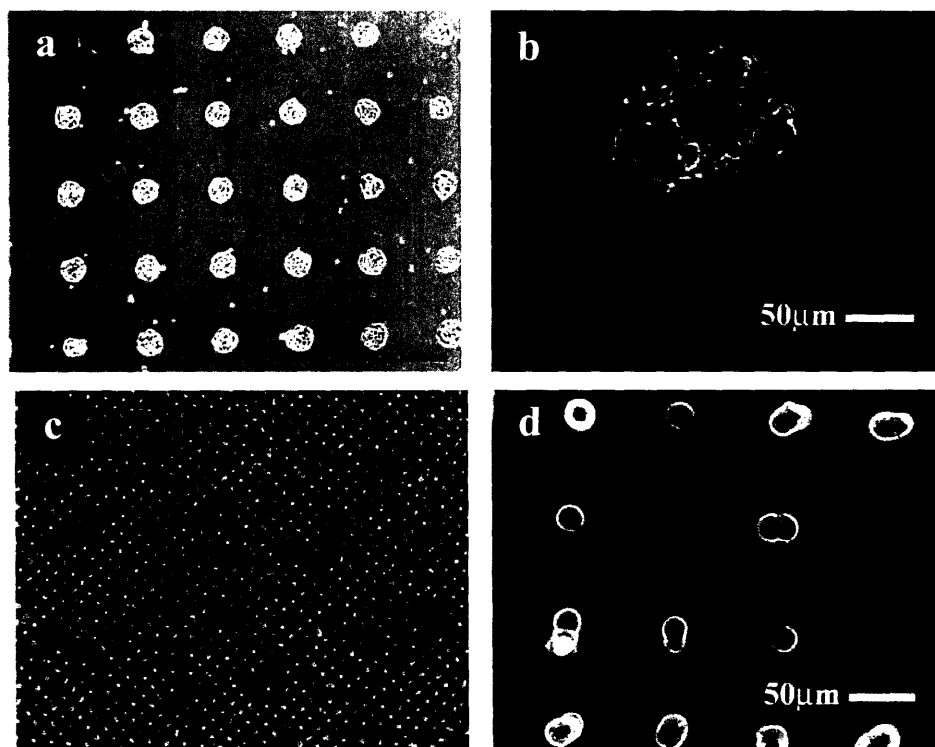


Figure 4.8. Fluorescent micrographs for protein resistance and HA microstructures. Various proteins were examined including (a, b) BSA, (c) IgG, and (d) FN. The patterns were constructed using either soft molding for (a, b) or  $\mu$ CP (c, d). Figure 4b shows the surface image after washing with PBS (the same location with (a)). Fine structures (less than  $10\ \mu\text{m}$ ) were also fabricated with the soft molding technique and one example is shown in (e, f) using a  $5\ \mu\text{m}$  box stamp. The corresponding microstructure is presented in Figure 4(g).



*Figure 4.9. Optical micrographs of cells on HA patterns. Using FN as an adhesion layer, NIH-3T3 cells were seeded on (a, b) 150  $\mu\text{m}$  and (c, d) 20  $\mu\text{m}$  islands. Depending on the pattern size, the number of cells was restricted such that aggregated or isolated cells were observed.*



## CONCLUSIONS

Despite the water solubility and hydrophilic nature of HA, it was demonstrated that HA can be directly immobilized onto glass and silicon oxide substrates because of hydrogen bonding and high molecular weight. An ultrathin HA layer of about 3 nm is left behind even after extensive washing with PBS or water. The presence of this layer was verified with XPS, ellipsometry, and AFM measurements. Fluorescent staining and XPS showed that the resulting surfaces remain stable for at least 7 days. The immobilization of HA does not involve any extensive chemistry or photochemistry, which would open a new way to attach other bioactive molecules having hydrophilic moieties to solid substrates. In addition, we have used chemisorbed HA layers to pattern proteins and cells using both  $\mu$ CP and molding methods, demonstrating the applicability of HA as a platform for cell and protein patterning. Oxygen plasma treatment was performed in the case of  $\mu$ CP to improve the adhesion of HA to PDMS stamps whereas no treatment was applied for soft molding. Thus, our approach could be a general route to the immobilization of HA and open a new way to attach other bioactive molecules having hydrophilic moieties to solid substrates. With its excellent resistant properties along with the formation of the stable, chemisorbed layer onto hydrophilic substrates, HA is an attractive alternative to PEG with unique applications in biodiagnostic and bioanalytical devices.

## REFERENCES

- (1) Morra, M. On the molecular basis of fouling resistance. *J Biomater Sci Polym Ed*, **11**, 6, 2000.
- (2) Piehler, J.,Brecht, A.,Hehl, K.,Gauglitz, G. Protein interactions in covalently attached dextran layers. *Colloids and Surfaces B-Biointerfaces*, **13**, 6, 1999.
- (3) Osterberg, E.,Bergstrom, K.,Holmberg, K.,Riggs, J. A.,Vanalstine, J. M.,Schuman, T. P.,Burns, N. L.,Harris, J. M. Comparison of Polysaccharide and Poly(Ethylene Glycol) Coatings for Reduction of Protein Adsorption on Polystyrene Surfaces. *Colloids and Surfaces a-Physicochemical and Engineering Aspects*, **77**, 2, 1993.
- (4) Osterberg, E.,Bergstrom, K.,Holmberg, K.,Schuman, T. P.,Riggs, J. A.,Burns, N. L.,Van Alstine, J. M.,Harris, J. M. Protein-rejecting ability of surface-bound dextran in end-on and side-on configurations: comparison to PEG. *J Biomed Mater Res*, **29**, 6, 1995.
- (5) Wang, D.,Liu, S.,Trummer, B. J.,Deng, C.,Wang, A. Carbohydrate microarrays for the recognition of cross-reactive molecular markers of microbes and host cells. *Nat Biotechnol*, **20**, 3, 2002.
- (6) Lofas, S.,Johnsson, B. A Novel Hydrogel Matrix on Gold Surfaces in Surface-Plasmon Resonance Sensors for Fast and Efficient Covalent Immobilization of Ligands. *Journal of the Chemical Society-Chemical Communications*, 21, 1990.
- (7) Dai, L.,Zientek, P.,St Johns, H.,Pasic, P.,Chatelier, R.,Griesser, H. J. In *Surface modification of polymeric biomaterials*; Ratner, B., Castner, D., Eds.; Plenum Press: New York, 1996, pp p 147.
- (8) Hartley, P. G.,McArthur, S. L.,McLean, K. M.,Griesser, H. J. Physicochemical properties of polysaccharide coatings based on grafted multilayer assemblies. *Langmuir*, **18**, 7, 2002.
- (9) Morra, M.,Cassinelli, C. Non-fouling properties of polysaccharide-coated surfaces. *J Biomater Sci Polym Ed*, **10**, 10, 1999.
- (10) Morra, M.,Cassinelli, C.,Pavesio, A.,Renier, D. Atomic force microscopy evaluation of aqueous interfaces of immobilized hyaluronan. *Journal of Colloid and Interface Science*, **259**, 2, 2003.
- (11) Yoshioka, T.,Tsuru, K.,Hayakawa, S.,Osaka, A. Preparation of alginic acid layers on stainless-steel substrates for biomedical applications. *Biomaterials*, **24**, 17, 2003.

- (12) Bulpitt, P., Aeschlimann, D. New strategy for chemical modification of hyaluronic acid: preparation of functionalized derivatives and their use in the formation of novel biocompatible hydrogels. *J Biomed Mater Res*, **47**, 2, 1999.
- (13) Oerther, S., Le Gall, H., Payan, E., Lapique, F., Presle, N., Hubert, P., Dexheimer, J., Netter, P. Hyaluronate-alginate gel as a novel biomaterial: mechanical properties and formation mechanism. *Biotechnol Bioeng*, **63**, 2, 1999.
- (14) Abantangelo, G., Weigel, P. *New frontiers in medical science: redefining hyaluronan*; Elsevier: Amsterdam, 2000.
- (15) Balazs, E. A., Denlinger, J. L. In *Clinical uses of hyaluronan: the biology of hyaluronan*; Evered, D., Welan, J., Eds.; Wiley: New York, 1989, pp p 265-280.
- (16) Piacquadio, D., Jarcho, M., Goltz, R. Evaluation of hylan b gel as a soft-tissue augmentation implant material. *J Am Acad Dermatol*, **36**, 4, 1997.
- (17) Pei, M., Solchaga, L. A., Seidel, J., Zeng, L., Vunjak-Novakovic, G., Caplan, A. I., Freed, L. E. Bioreactors mediate the effectiveness of tissue engineering scaffolds. *Faseb J*, **16**, 12, 2002.
- (18) Bernard, B. A., Newton, S. A., Olden, K. Effect of size and location of the oligosaccharide chain on protease degradation of bovine pancreatic ribonuclease. *J Biol Chem*, **258**, 20, 1983.
- (19) Lohmander, L. S., De Luca, S., Nilsson, B., Hascall, V. C., Caputo, C. B., Kimura, J. H., Heinegard, D. Oligosaccharides on proteoglycans from the swarm rat chondrosarcoma. *J Biol Chem*, **255**, 13, 1980.
- (20) Miyake, K., Underhill, C. B., Lesley, J., Kincade, P. W. Hyaluronate can function as a cell adhesion molecule and CD44 participates in hyaluronate recognition. *J Exp Med*, **172**, 1, 1990.
- (21) Mason, M., Vercruyse, K. P., Kirker, K. R., Frisch, R., Marecak, D. M., Prestwich, G. D., Pitt, W. G. Attachment of hyaluronic acid to polypropylene, polystyrene, and polytetrafluoroethylene. *Biomaterials*, **21**, 1, 2000.
- (22) Stile, R. A., Barber, T. A., Castner, D. G., Healy, K. E. Sequential robust design methodology and X-ray photoelectron spectroscopy to analyze the grafting of hyaluronic acid to glass substrates. *J Biomed Mater Res*, **61**, 3, 2002.

- (23) Chen, G., Ito, Y., Imanishi, Y., Magnani, A., Lamponi, S., Barbucci, R. Photoimmobilization of sulfated hyaluronic acid for antithrombogenicity. *Bioconj Chem*, **8**, 5, 1997.
- (24) Thierry, B., Winnik, F. M., Merhi, Y., Tabrizian, M. Nanocoatings onto arteries via layer-by-layer deposition: toward the in vivo repair of damaged blood vessels. *J Am Chem Soc*, **125**, 25, 2003.
- (25) Picart, C., Lavalle, P., Hubert, P., Cuisinier, F. J. G., Decher, G., Schaaf, P., Voegel, J. C. Buildup mechanism for poly(L-lysine)/hyaluronic acid films onto a solid surface. *Langmuir*, **17**, 23, 2001.
- (26) Sengupta, K., Schilling, J., Marx, S., Markus, F., Sackmann, E. Supported membrane coupled ultra-thin layer of hyaluronic acid: viscoelastic properties of a tissue-surface mimetic system. *Biophysical Journal*, **84**, 2, 2003.
- (27) Shard, A. G., Davies, M. C., Tendler, S. J. B., Bennedetti, L., Purbrick, M. D., Paul, A. J., Beamson, G. X-ray photoelectron spectroscopy and time-of-flight SIMS investigations of hyaluronic acid derivatives. *Langmuir*, **13**, 10, 1997.
- (28) Shibasaki, Y., Seki, A., Takeishi, N. Thermoanalytical Study on Anchoring Effects of Long-Chain Diynoic Acids in Thermal Polymerization. *Thermochimica Acta*, **253**, 1995.
- (29) Gribbon, P., Heng, B. C., Hardingham, T. E. The molecular basis of the solution properties of hyaluronan investigated by confocal fluorescence recovery after photobleaching. *Biophysical Journal*, **77**, 4, 1999.
- (30) Kobayashi, Y., Okamoto, A., Nishinari, K. Viscoelasticity of Hyaluronic-Acid with Different Molecular-Weights. *Biorheology*, **31**, 3, 1994.
- (31) Hawkins, C. L., Davies, M. J. Degradation of hyaluronic acid, poly- and monosaccharides and model compounds by hypochlorite: Evidence for radical intermediates and fragmentation. *Free Radical Biology and Medicine*, **24**, 9, 1998.
- (32) Miller, R. A., Britigan, B. E. The formation and biologic significance of phagocyte-derived oxidants. *Journal of Investigative Medicine*, **43**, 1, 1995.
- (33) Morra, M., Cassinelli, C. Simple model for the XPS analysis of polysaccharide-coated surfaces. *Surface and Interface Analysis*, **26**, 10, 1998.
- (34) Suh, K. Y., Kim, Y. S., Lee, H. H. Capillary force lithography. *Adv Mater*, **13**, 18, 2001.

- (35) Kim, Y. S., Suh, K. Y., Lee, H. H. Fabrication of three-dimensional microstructures by soft molding. *Appl Phys Lett*, **79**, 14, 2001.
- (36) Kim, E., Xia, Y. N., Whitesides, G. M. Polymer Microstructures Formed by Molding in Capillaries. *Nature*, **376**, 6541, 1995.

## 5. Layer-by-layer deposition of hyaluronic acid and poly-L-lysine for patterned cell co-cultures

### INTRODUCTION

Controlling cell-microenvironment interactions such as cell-cell contact and the presentation of extracellular matrix and soluble ligands is important for the development of tissue engineering constructs and *in vitro* cultures that mimic the organization and complexity of normal tissue architecture<sup>1</sup>. Despite this need, most commonly used cell culture systems lack the complexity and the organization that parallels the *in vivo* cellular microenvironment. Although co-cultures of two (or more) cell types have been used to better mimic *in vivo* systems, cell-cell interactions such as spatial signaling and the degree of homotypic and heterotypic interactions within these cultures are not easily controlled<sup>2</sup>.

Patterned co-cultures aim to enhance microenvironmental control through spatial localization of multiple cell types relative to each other. Approaches to generate patterned co-cultures could be categorized into one of three categories. In one approach, photolithographic techniques are used to pattern surfaces with materials that facilitate the selective adhesion of multiple cell types to specific regions. For example, co-cultures of hepatocytes and fibroblasts have been made by the selective adhesion of hepatocytes to micropatterned collagen islands to optimize cell-cell interactions for the functional maintenance of primary hepatocytes<sup>2-6</sup>. In the second approach, cells are delivered to particular regions of a substrate. For example, microfluidic channels were used to pattern multiple cell types to specific regions of a surface<sup>7,8</sup>. Similarly, elastomeric membranes were used to prevent cell attachment to regions of the substrate. Once the membrane was peeled off, the remaining surface could yield to the attachment of the second cell type<sup>7, 9-11</sup>. Both of these approaches have certain potential limitations. For example, photolithographic approaches require selective adhesion of one cell type to the patterned substrate which may limit its application to various cell systems. Also, microfluidic approaches are limited to specific geometries specified by the laminar fluid flow<sup>8</sup> or an intrinsic limit on the minimum space between two cell types as determined by the distance between channels or membrane holes<sup>12</sup>. An approach that aims to overcome much of these limitations is through the use of surfaces that can be turned from being cell and protein

repulsive to adhesive based on specific stimuli<sup>13-15</sup>. These approaches include the use of electroactive substrates that can be switched from a hydrophilic to a hydrophobic state to promote cell adhesion<sup>13</sup>, as well as thermally responsive polymer grafted surfaces<sup>14, 15</sup>. Although many elegant switchable surfaces have been developed<sup>16</sup>, the fabrication of these surfaces still requires specialized materials and extensive expertise that may limit their widespread use. Thus, the development of biocompatible, easily applicable and versatile surface engineering approaches that facilitate fabrication of patterned co-cultures is needed.

One potential method to switch surface properties that could potentially be useful for such applications is the use of layer-by-layer assembly of polyelectrolytes<sup>17</sup>. Typically such approaches have been used to construct thin polymer films with specific properties<sup>18</sup>. More recently, the layer-by-layer deposition of HA and chitosan has been proposed as a method of repair for damaged blood vessels<sup>19</sup>. Despite these advances, the potential of this approach as a tool for patterning co-cultures has not been investigated.

In continuation with the theme of HA patterning of previous chapters, here HA and poly-L-lysine (PLL) were used to switch surface properties. HA<sup>20-23</sup> and other polysaccharides<sup>24, 25</sup> have been shown to resist the adhesion of many proteins and cells, although not all proteins are repelled by HA<sup>26</sup>. Furthermore HA is negatively charged and can complex with cationic polymers such as PLL, providing for intriguing opportunities to generate surfaces that can be turned from one property to another. Therefore, this chapter describes a method to pattern two cell types on a surface by using the cell resistant properties of HA. It was hypothesized that the application of a multi-step fabrication would result in initial patterning of a desired cell and / or protein on the exposed adhering substrate. The remaining HA surface could then be converted to cell and protein adhesive through the application of PLL to the surface, which could subsequently facilitate the patterning of the second cell type (**Figure 5.1**). HA was patterned on glass using capillary force lithography, followed by adsorption of fibronectin (FN) onto the bare glass substrate. Primary cells were subsequently seeded, which specifically attached onto the fibronectin coated surfaces. Once the cells adhered, HA patterns were complexed with PLL which switched the patterns from non-biofouling to cell adherent. Secondary cells were subsequently seeded and adhered to the exposed PLL patterns (**Figure 5.1**).

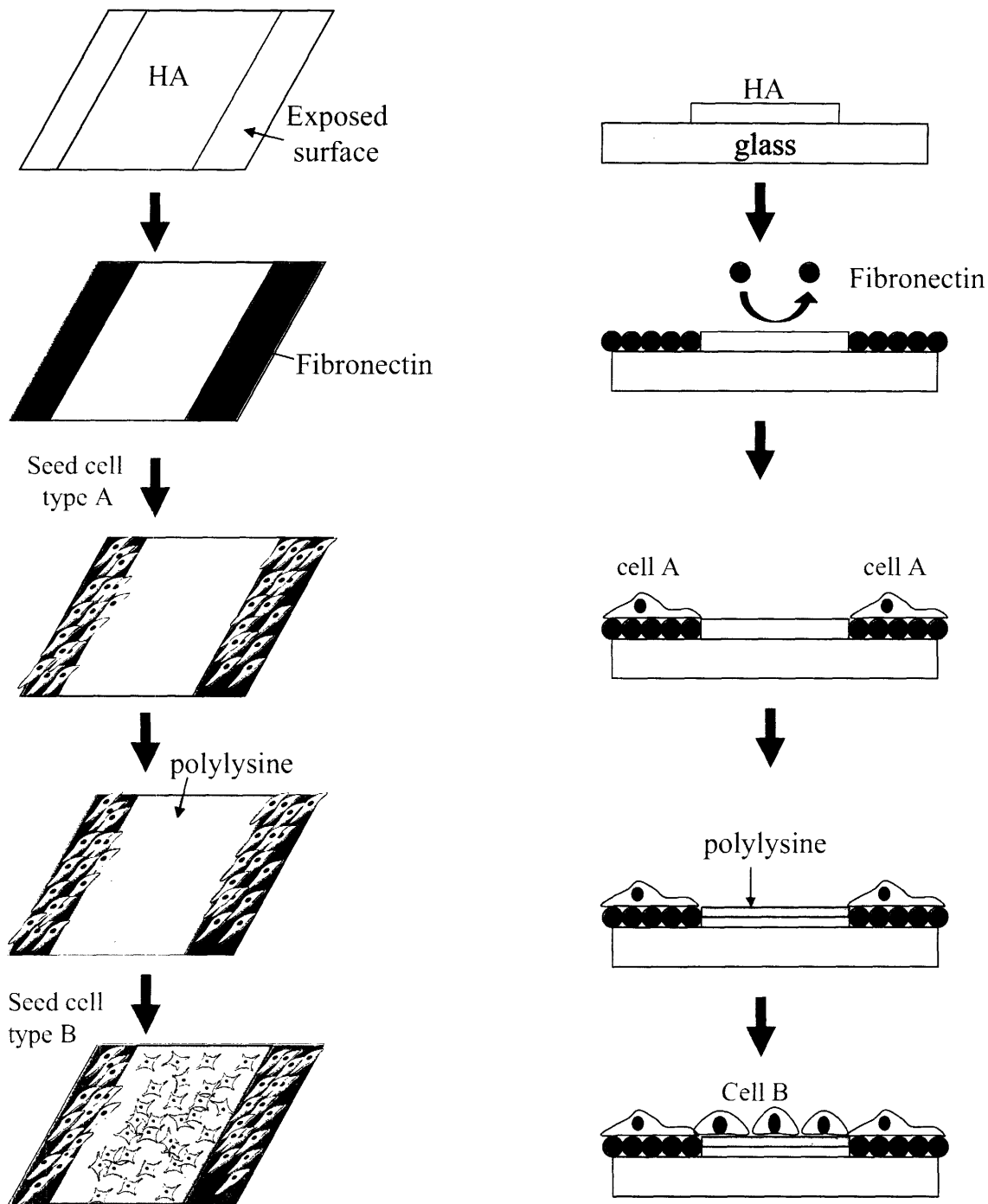


Figure 5.1. Schematic diagram of the HA-PLL layering approach to pattern co-cultures. To generate patterned co-cultures, a glass substrate is patterned with HA and subsequently stained with FN which adheres to the exposed substrate. The first cell type is then seeded and allowed to adhere to the FN coated regions. The non-biofouling properties of the HA patterns are subsequently switched by PLL deposition. Secondary cells can then be seeded, resulting in the formation of patterned co-cultures.



## **MATERIALS AND METHODS:**

All tissue culture media and serum were purchased from Gibco Invitrogen Corporation, cell lines were purchased from ATTC and all chemical were purchased from Sigma, unless otherwise indicated.

*Cell culture:* All cells were manipulated under sterile tissue culture hoods and maintained in a 5% CO<sub>2</sub> humidified incubator at 37 °C. NIH-3T3 cells were maintained in 10% fetal bovine serum (FBS) in Dulbecco's modified eagle medium (DMEM). AML12 murine hepatocytes were maintained in a medium comprised 90% of 1:1 (v/v) mixture of DMEM and Ham's F12 medium with 0.005 mg/mL insulin, 0.005 mg/mL transferrin, 5 ng/mL selenium, and 40 ng/mL dexamethasone, and 10% FBS. Confluent dishes of AML12 and NIH-3T3 cells were passaged and fed every 3-4 days. Murine embryonic stem (ES) cells (R1 strain) were maintained on gelatin treated dishes on a medium comprised of 15% ES-qualified FBS in DMEM knockout medium. ES cells were fed daily and passaged every 3 days at a subculture ratio of 1:4. Primary cell patterns were performed with serum supplemented medium specific to the seeded cell type. Depending on the cells, co-cultures were either maintained with medium used for ES cells or AML12 cells.

*PDMS mold fabrication:* PDMS molds were fabricated by curing prepolymer (Sylgard 184, Essex Chemical) on silicon masters patterned with SU-8 photoresist. The patterns on the masters had protruding cylindrical holes (ranging in diameter from 15 µm to 150 µm), which resulted in PDMS replicas with receding cylinders. To cure the PDMS prepolymer, a mixture of 10:1 silicon elastomer and the curing agent was poured on the master and placed at 70°C for 2 hours. The PDMS mold was then peeled from the silicon wafer and cleaned with ethanol and acetone prior to use.

*HA coating of surfaces:* HA films (Genzyme Inc.) were cast by spin-coating (Model CB 15, Headaway Research, Inc.) a solution containing 5 mg HA/mL in distilled water onto silicon dioxide substrates (glass slides or wafers) at 1500 rpm for 10 seconds. After drying for 12 hours at room temperature, the thickness of the resulting film was about 606 nm as measured by ellipsometry (Gaertner Scientific Corp.) and AFM (Digital Instrument).

*Patterning technique:* To pattern surfaces, capillary force lithography was used. PDMS molds were washed using soap and water, sterilized in ethanol, and dried and then plasma cleaned for 4 minutes and to increase its wettability (PDC-001, Harrick Scientific Co.). A few drops of HA was then spun coated onto a plasma cleaned slide at 1500 rpm for 10 seconds. The PDMS mold was then placed on the thin layer of HA until it visibly wetted the surface. The mold was left undisturbed for at least 12 hours, at which time a visible pattern could be seen.

*Cell Patterning:* Fibronectin was added to the HA patterned glass slides at a concentration of 100 µg/mL in phosphate buffered saline (PBS) and washed for 20 minutes. Primary cells at a concentration of  $1 \times 10^6$  cells/mL were added to the glass slides and allowed to grow overnight. To immobilize PLL, the culture medium was aspirated and replaced by PLL at a concentration of 40 µg/mL for 20 minutes. The slides were then gently washed to remove cells and then incubated overnight with secondary cells suspended in medium at a concentration of  $1 \times 10^6$  cells/mL. Cell cultures were analyzed at various times and imaged using an Axiovert 200 inverted microscope (Zeiss). Prior to analysis, glass slides were rinsed with PBS to remove non-adherent cells.

*Cell Staining:* To stain with PKH26 dye, cells were trypsinized and washed with DMEM medium without serum, and resuspended in a  $2 \times 10^6$  M PKH26 solution of diluent C at a concentration of  $1 \times 10^7$  cells/mL and incubated for 4 minutes at room temperature. To stain with carboxyfluorescein diacetate succinimidyl ester (CFSE) dye, cells suspended in 10 µg/mL CFSE in PBS solution at a concentration of  $1 \times 10^7$  cells/mL and incubated for 10 minutes at room temperature. Both staining reactions were quenched with addition of an equal volume of DMEM supplemented with 10% FBS and washed.

*Protein adsorption:* FITC-labeled BSA, FITC-labeled IgG and fibronectin were dissolved in PBS at 50 µg/mL, 50 µg/mL and 20 µg/mL respectively. To test for BSA and IgG protein adhesion, a few drops of the protein solution were evenly distributed onto the patterned substrates and incubated at room temperature for 45 minutes. To coat with fibronectin, surfaces were dipped into a fibronectin solution for 15 min and subsequently rinsed to remove

unbound fibronectin. To measure fibronectin adhesion, surfaces were stained with anti-fibronectin antibody for an additional 45 minutes, followed by 1 hour incubation with the phycoerythrin (PE)-labeled anti-rabbit secondary antibody. The patterned substrates were then washed with PBS and analyzed under a fluorescent microscope.

*Flow cytometry:* AML12, NIH-3T3 and ES cells were stained with propidium iodide (PI) (2 mg/mL) and subsequently analyzed under a FACScan flow cytometer (BD Biosciences). Data was collected and analyzed using the Cell Quest software.

## RESULTS

### *Protein and cell patterning of HA coated surfaces*

HA films were prepared on silicon dioxide or glass substrates by spin coating. In the previous chapter it was shown that water solubility, a thin layer of HA remained on the patterned surfaces even after extensive washing with PBS. The ability of HA coated surfaces to resist the adsorption of three different proteins was analyzed by quantifying the fluorescent expression of treated glass surfaces. Experiments demonstrated that the adhesion of BSA, IgG, and fibronectin was significantly reduced on HA coated surfaces in comparison to glass controls ( $p < 0.001$ ) (**Figure 5.2A**). This result is supported by previous reports which have indicated that surfaces containing immobilized HA resist protein adsorption<sup>21</sup>. In addition, less than 1% of the cells that were seeded onto HA coated surfaces adhered, significantly lower than fibronectin treated controls or glass substrates (**Figure 5.2B**). Interestingly, the addition of fibronectin on HA coated surfaces did not increase the cell adhesion properties of HA, due to low fibronectin adsorption on HA. These results confirm that the non-biofouling properties of HA coatings could be used to repel protein adsorption and cell adhesion.

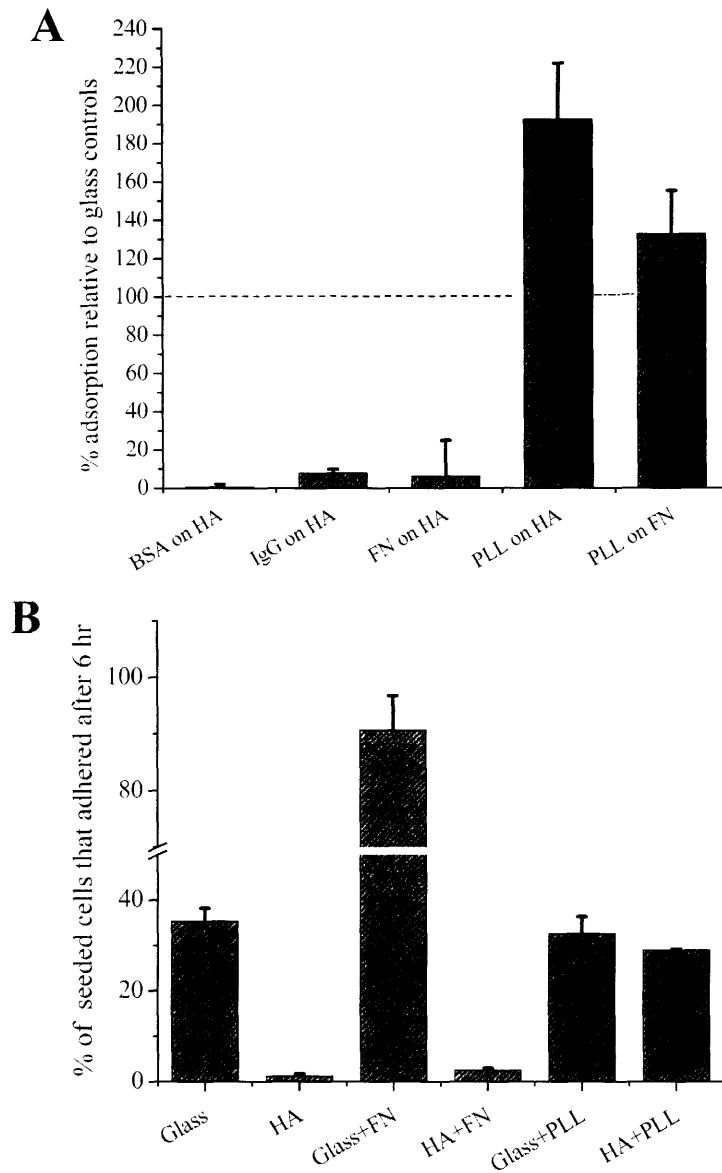
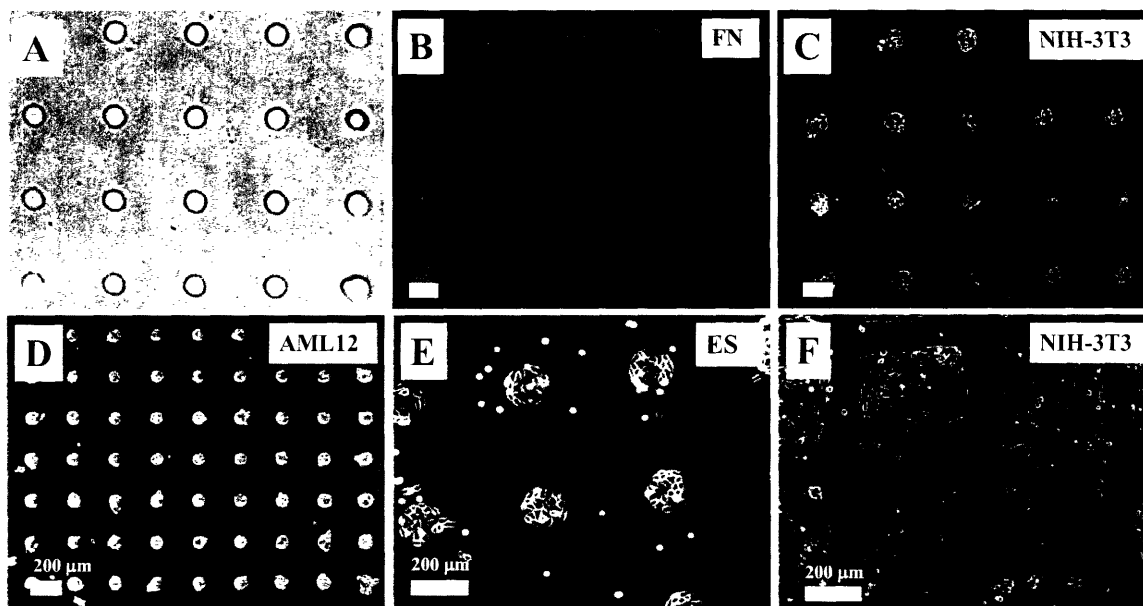


Figure 5.2. Protein adsorption and cell adhesion to various surfaces. Figure (A) is the protein adsorption of HA and FN coated surfaces relative to glass controls. BSA, IgG and FN adsorption to HA coated surfaces at significantly lower levels than glass controls ( $p < 0.001$ ). Interestingly, it was found that PLL adsorption to glass and FN coated surfaces were significantly higher than glass controls ( $p < 0.05$ ). Figure (B) is the NIH-3T3 cell adhesion to various surfaces. As it can be seen, cells did not adhere to HA or HA coated surfaces that were FN treated. In contrast, cells adhered to PLL treated HA surfaces at similar levels as PLL treated glass surfaces, indicating that PLL can be used to switch the surface properties of HA.

To test the ability of HA to complex with PLL, HA coated surfaces were treated with FITC-PLL. As illustrated in **Figure 5.2**, FITC-PLL adhered to the HA coated surfaces at significantly higher values than coated glass surfaces ( $p < 0.05$ ). In addition, cells adhered to PLL treated HA coatings at significantly higher values than HA coated controls ( $p < 0.05$ ) (**Figure 5.2B**), further indicating that PLL treatment could reverse the cell and protein resistant properties of HA coated surfaces. In addition, no significant difference was observed between the degree of NIH-3T3 adhesion to glass or PLL treated glass on HA substrates (**Figure 5.2B**), indicating that these cells have the same affinity to attach to PLL or glass surfaces.



*Figure 5.3. Cell and protein patterning of HA coated surfaces. Figure (A) is the optical image of an HA pattern on a glass substrate prior to washing, (B) is a fluorescent image of fibronectin adsorption on the surface of (A), and figure (C) illustrates fibroblast adhesion on the surface of (B). Figures (D-F) demonstrate the applicability of the technique for patterning various cell type including AML12 (D), ES (E), and NIH-3T3 cells (C, F) at various length scales.*

To pattern cells and proteins soft lithographic approaches were used (For details see previous chapter). Briefly, a thin film of HA was spun coated onto the substrate and PDMS mold was subsequently placed on top of the film. The dewetting of the polymer film and the capillary force action due to the features of the stamp results in the formation of patterned HA. The PDMS stamps were left for 12 hours to ensure stabilization of the patterns. HA patterns were visible under light microscopy prior to washing (**Figure 5.3A**) but could not be seen after the

surfaces were washed. Thus patterned HA deposited onto the surface could be easily washed away, leaving behind an adsorbed layer that maintained the biofouling resistant properties of HA. The generated HA patterns were capable of fabricating arrays of patterned protein such as fibronectin (**Figure 5.3B**). To examine the feasibility of the approach to pattern a wide array of cells murine embryonic fibroblasts (NIH-3T3), liver (AML12) and embryonic stem (ES) cells were immobilized onto the patterned surfaces that were treated with HA. All three cell lines were patterned on HA surfaces with high consistency and cell pattern fidelity (**Figure 5.3C-F**). In addition, the feature size of the cell patterns could be controlled to produce islands with individual cells (15  $\mu\text{m}$ ) to those with large multi-cellular aggregates ( $>200 \mu\text{m}$ ).

#### ***PLL adsorption on patterned protein and cells***

To examine the ability of PLL to adsorb to HA patterns, patterned surfaces that were treated with fibronectin, were incubated with a solution containing FITC-PLL. As illustrated in **Figure 5.4A**, labeled fibronectin patterns were clearly visible in the shape of grids through adsorption to the exposed substrate. In addition, PLL selectively adhered on HA patterns (square shaped), although lower levels of background adsorption could be observed on fibronectin coated regions (**Figure 5.4A**). These results correlate with the surface binding affinities of **Figure 5.2**, which indicates that both HA and fibronectin coated surfaces adsorb PLL at significantly higher levels than glass controls ( $1.9\pm 0.3$  and  $1.45\pm 0.3$  times respectively ( $p < 0.05$ )).

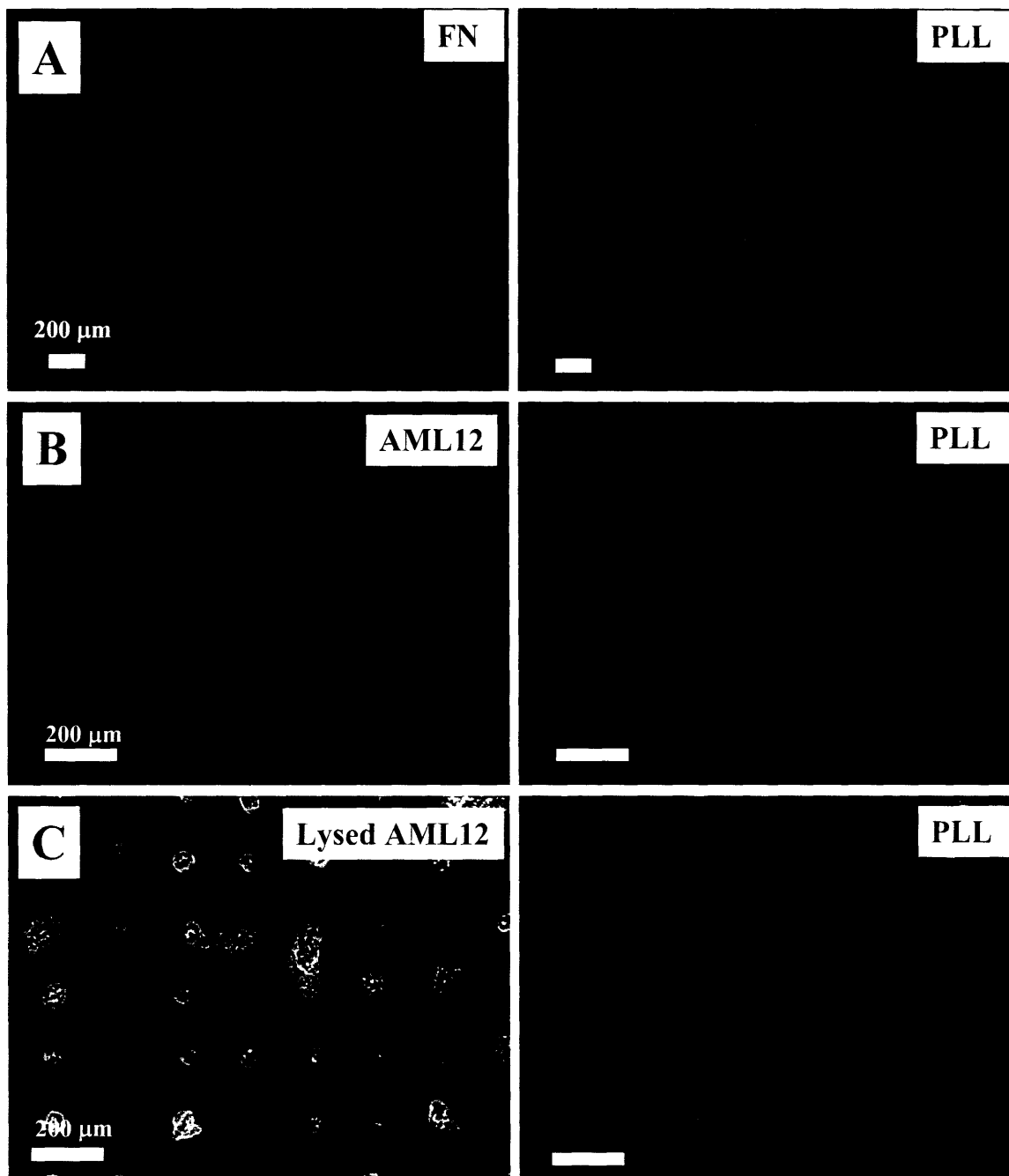


Figure 5.4. PLL attachment on patterned HA surfaces and immobilized cells. Figure (A) represents fluorescent images of HA patterned glass slides that were stained with FN (left) and subsequently treated with PLL (right). FN attached on the exposed grids, while PLL selectively adhered to the HA squares. As expected, background staining to the FN coated regions is detectable. PLL selectively adsorbed on HA coated regions in comparison to patterned AML12 hepatocytes (B). Interestingly, if the cells were lysed with 0.4% Triton-X prior to PLL treatment, PLL adhered to the cytoplasmic components of lysed cells (C) indicating that under normal PLL treatment many cells remained viable (NIH-3T3 and ES cells yielded similar images).

Despite the ability of PLL to adsorb onto fibronectin coated substrates, the feasibility of using PLL is dependant on its low adsorption onto cells, since cells cover fibronectin treated regions prior to PLL treatment. To further investigate this phenomenon, the competitive binding of PLL to patterned cells relative to HA surfaces was evaluated. Although flow cytometric staining of FITC-PLL treated cells, stained similarly as the co-cultures, indicate that PLL adsorbed to a large fraction of viable cells (71% for ES cells, 74% for AML12 cells and 79% for NIH-3T3 cells respectively), fluorescent images indicated that PLL adhered to the HA coated regions at detectably higher ratios than cells (**Figure 5.4B**) (other cell types yielded similar images, not shown). This may be attributed to the higher binding affinity of PLL to HA in comparison to membrane bound proteoglycans, glycosaminoglycans and other negatively charged constituents of cell membrane.

Since high concentrations of PLL have been shown to induce cell toxicity<sup>27</sup>, the viability of cells that were treated with PLL was also evaluated. PI staining of NIH-3T3, AML12 and ES cells indicated that >95% of adhered cells that were treated with PLL (at 40 µg for 20 min) were negative for PI, and therefore alive. Furthermore, PLL selectively adsorbed to cells that were lysed with Triton-X, possibly due to the adsorption of PLL to cytoplasmic components of the cell (**Figure 5.4C**). Therefore, the low number of stained cells after PLL treatment shown in **Figure 5.4B** is further evidence that cells remained alive after PLL treatment.

#### ***Patterned co-cultures of ES cells with fibroblasts***

To demonstrate the applicability of the patterned co-culture technique, two systems were tested. The first was the co-cultures of fibroblasts with hepatocytes which has been shown to better maintain the differentiated properties of primary hepatocytes in culture<sup>2,28</sup>. The other system was co-cultures of ES cells and embryonic fibroblasts that have been used to prevent the differentiation of ES cells<sup>29</sup>. Random co-cultures of hepatocytes or ES cells with fibroblasts have heterogeneous interactions that lack the control and spatial orientation that is present within the liver or the developing embryo (**Figure 5.5**). Thus, patterned co-cultures could potentially provide interesting opportunities to improve these systems.



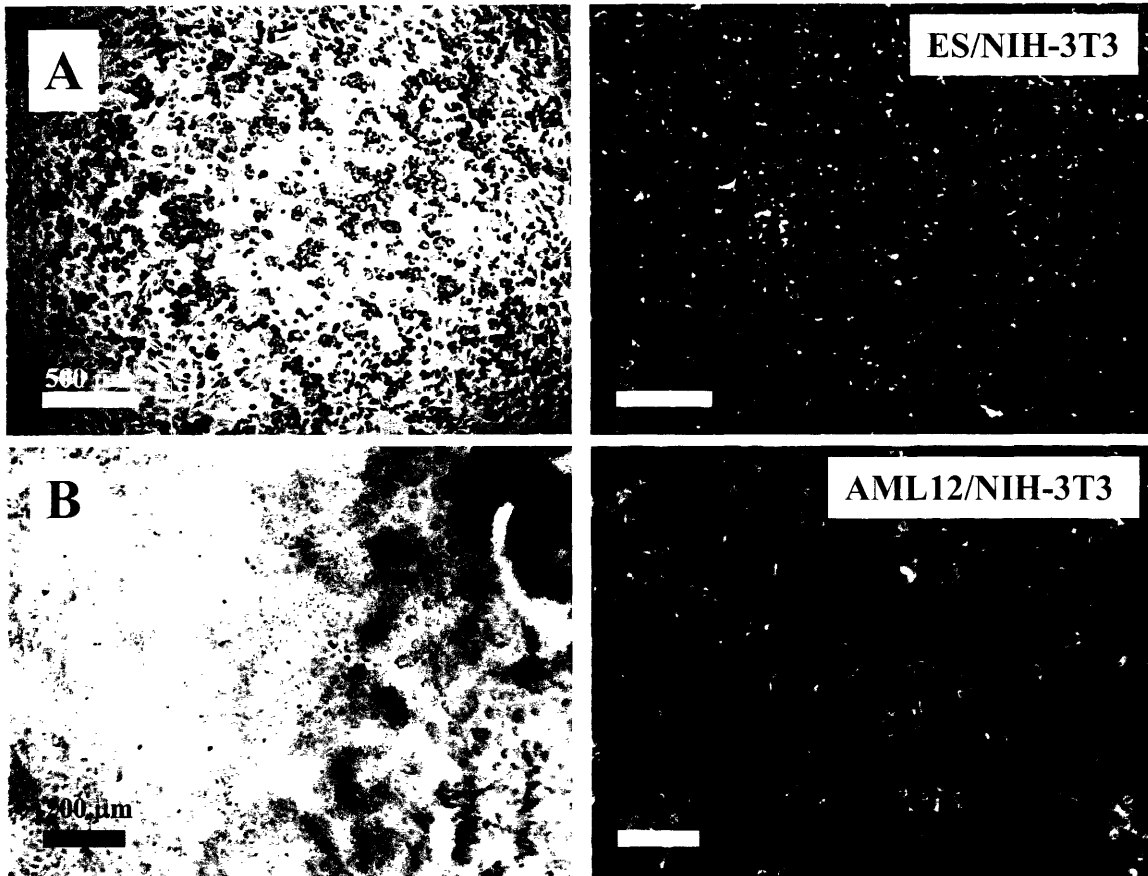


Figure 5.5. Random Co-cultures of hepatocytes or ES cells with fibroblasts. Light and fluorescent images of un-patterned co-cultures of ES cells (green) with (A-B) or AML12 hepatocytes with NIH-3T3 fibroblasts (red) (C-D) after 1 day.

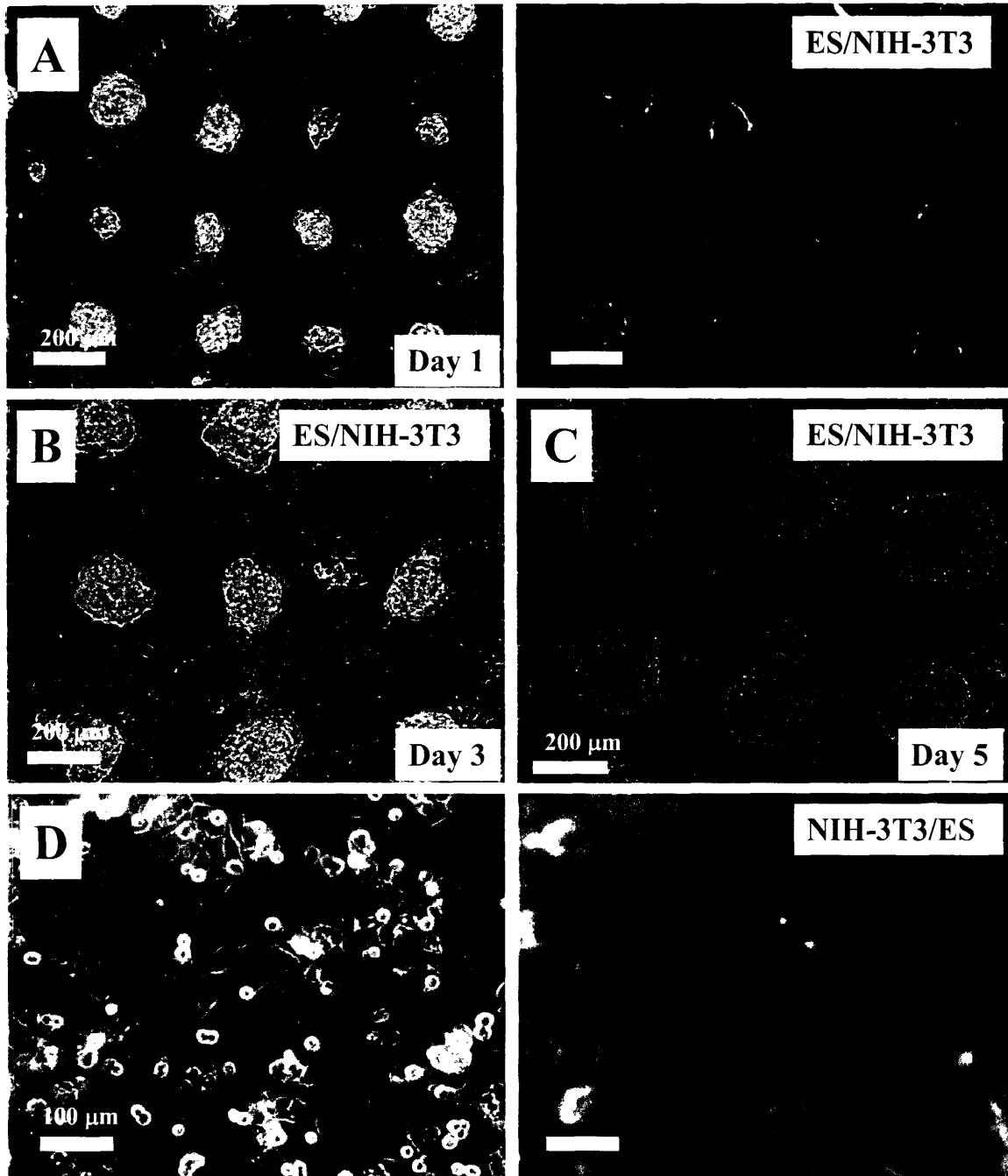


Figure 5.6 Patterned co-cultures of ES cells with fibroblasts. Figure (A) represents light (left) and fluorescent (right) images of patterned co-cultures of ES cells (red) with NIH-3T3 fibroblasts (green) after 1 day. Figures (B) and (C) illustrate that co-cultures remained stable for 3 and 5 days respectively. Figure (D) represents the reversal in the order of cell seeding in which NIH-3T3 fibroblasts (red) were initially seeded followed by ES cells as the secondary cells. Therefore the technique is independent from the type of cell initially seeded.

To generate patterned co-cultures, HA patterned substrates were treated with fibronectin in PBS and seeded with the first cell type and incubated for 24 hours. Once primary seeded cells were adhered, patterned substrates were treated with PLL, washed and seeded with the secondary cells. To visualize the co-cultures, each cell type was fluorescently labeled with either a membrane labeling dye (PKH26 – red) or cytoplasmic tracer (CFSE - green). At various times after initiation of the co-culture, cells were analyzed under light and fluorescent microscopy.

**Figure 5.6A** is an image of co-cultures of ES cells with NIH-3T3 fibroblast in patterned co-cultures of circular FN islands. Both light and fluorescent images indicate that ES cells were clearly patterned in dense spheroid aggregates against a background monolayer of NIH-3T3 cells. The aggregation of ES cells is due to strong self interactions that are associated with numerous cell adhesion molecules such as E-cadherin<sup>30</sup>. Fluorescent images confirmed that NIH-3T3 cells were restricted to the HA coated regions and were not seeded on top of ES cells as indicated by the lack of yellow regions on the aggregates (indicating the presence of both ES and NIH-3T3 cells). ES cell co-cultures remained stable for at least 5 days (**Figure 5.6 A-C**). At day 3 (**Figure 5.6B**), ES cell aggregates were ~150  $\mu\text{m}$  in diameter and increased to >200  $\mu\text{m}$  by day 5 (**Figure 5.6C**). In addition, the aggregates remained lodged in place and were not washed away by mechanical agitation and medium replacement. Fluorescent images of the cultures after 5 days confirmed that ES cells had not differentiated into cells with fibroblastic phenotype and were constrained within the spheroid geometry of the aggregate.

In addition, the versatility of the technique to form patterns upon reversing the order of cell seeding was validated. It was found that co-cultures could be established with fibroblasts being immobilized to the circular islands and the ES cells adhering to the remaining regions. These results were confirmed by morphological differences as well as fluorescent staining of the two cell types (**Figure 5.6D**).

### *Patterned co-cultures of hepatocytes with fibroblasts*

Patterned co-cultures of hepatocytes with fibroblasts were also established. In contrast to the sharp morphological difference that was observed between ES cell and NIH-3T3 co-cultures, hepatocyte co-cultures were morphologically more difficult to distinguish under light microscope (**Figure 5.7A**). Fluorescent images of stained co-cultures validated the formation of patterns. As it can be seen in **Figure 5.7A**, hepatocytes (red) were seeded on 100  $\mu\text{m}$  circular islands, while the fibroblasts (green) were seeded in the surrounding regions. The pattern fidelity of hepatocyte co-cultures was not as sharp as ES cell co-cultures, possibly due to stronger interactions between ES cells which prevented ES cells from migrating into the surrounding regions. In addition, after 24 hours a small fraction of NIH-3T3 cells could be seen attached on top of hepatocyte colonies, which could be attributed to higher binding affinity of hepatocytes to PLL in comparison to ES cells. Despite this, patterned co-cultures remained stable for at least 5 days after co-culture initiation (**Figure 5.7B**), although a larger fraction of cells had migrated out of their originally seeded regions in comparison to ES cell co-cultures. It is important to note that since fluorescence intensity of the tracer dye is halved upon each cell division stained cells in **Figure 5.7B** were less fluorescent in comparison to the original patterns.

To demonstrate that the patterning is independent of the cell type, patterned co-cultures comprised of only hepatocytes (**Figure 5.7C**) were generated. It was found that same cells could be used for patterned co-cultures, thus the approach is independent of the differences between primary and secondary seeded cells.

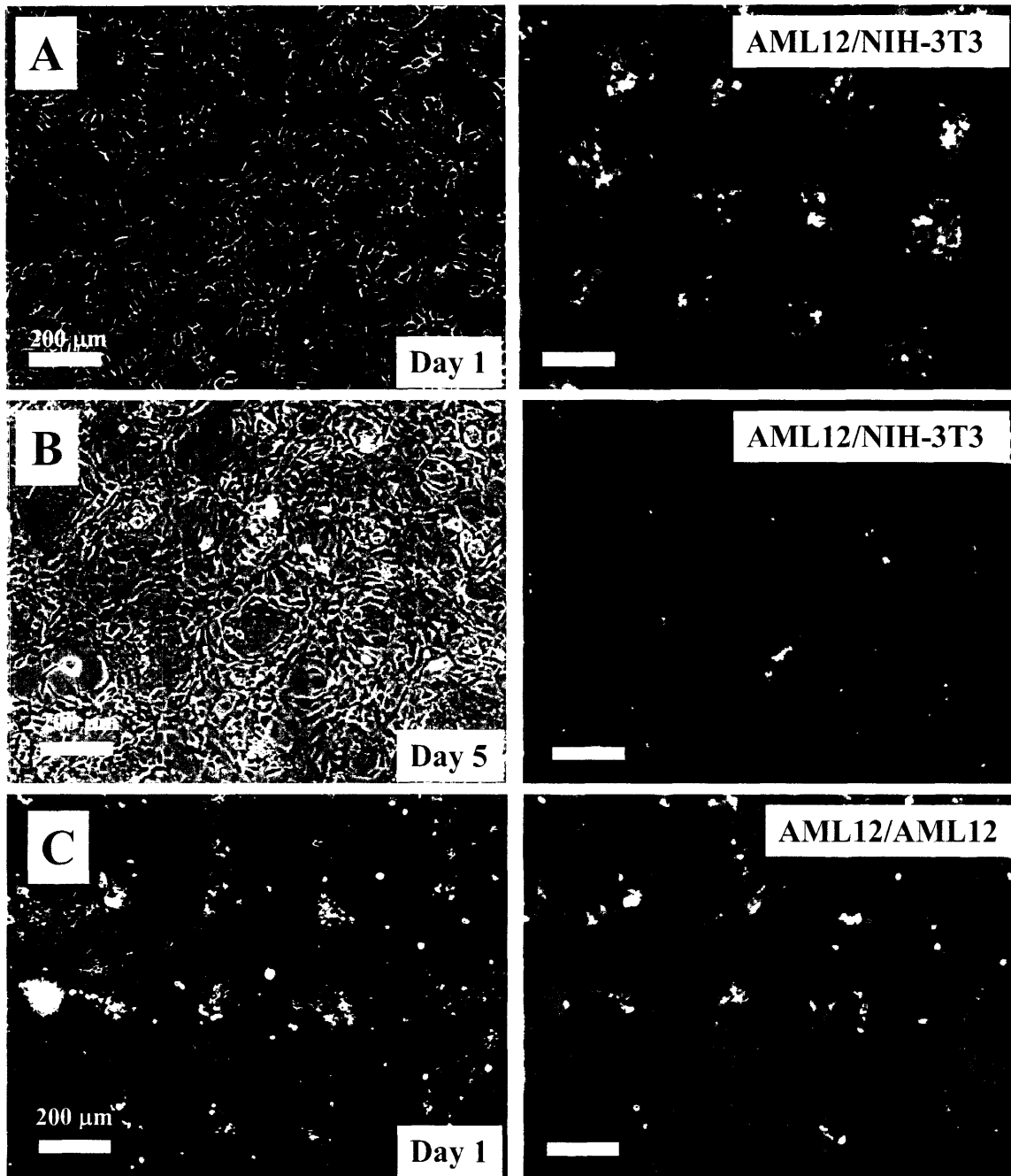


Figure 5.7 Patterned co-cultures of hepatocytes with fibroblasts. Figure (A) represents the light and fluorescent images of AML12 (red) in co-culture with NIH-3T3 fibroblasts (green) after 1 day in culture. In addition, the cultures remained stable for at least 5 days (B). Figure (C) demonstrates a co-culture of AML12 (red) cells with other AML12 cells (green), thereby same cell type could be patterned in co-cultures.

## DISCUSSION

The application of layer-by-layer deposition of polyionic molecules for cell and protein patterning was demonstrated. There are a number of advantages associated with this technique over previously developed co-culture approaches. For example, unlike approaches that are based on selective adhesion of two different cell types or exclusion of serum for cell seeding, the approach developed here is not dependant on selective cell adhesion or the absence of serum. In addition, this method provides all the advantages associated with soft lithography, while preventing the use of organic solvents that is used in photolithographic based co-cultures. Furthermore, the approach utilizes the advantages associated with switchable surfaces, yet it does not require changes in temperature or the need for electroactive surfaces that may be difficult to fabricate. Another important advantage with the approach is the availability of the materials used in the co-cultures. Both HA and PLL are commercially available and widely used. Furthermore, the immobilization of HA or PLL does not require any chemistry or complex techniques. The simplicity of this approach and off-the-shelf availability of PLL, HA and fibronectin, should make this technique easily applicable in biologically oriented labs which may lack the resources required for other patterned co-culture techniques.

Although we have focused on fibronectin and PLL, it is anticipated that the proposed approach would have a wide application in patterning of a multiple proteins on a surface. This is because proteins could be used to directly attach to PLL (Fig. 1A), or attached to biotinylated PLL. The applicability of PLL patterns for subsequent attachment of other polyionic molecules and proteins is currently under investigation.

One of the challenges with the described technique is the use of PLL which has been shown to be cytotoxic at high concentrations. In our protocol we chosen a PLL concentration in order to modify HA surfaces and minimize cell toxicity. At higher concentration cells would die while at lower concentration or shorter exposure time cells would not adhere to the coated regions. The use of other non-toxic adhesion molecules that can adsorb to HA could be potentially beneficial for overcoming this limitation. Another limitation with the current technique is the use of ionic molecules for the switching of surface properties. It is anticipated that this limits

the approach to a range of pH values that maintains that electrostatic interactions between the molecules, although for cell culture conditions this should not be a major concern.

Future studies could be directed at characterizing the biochemical behavior of the cells in these cultures. Although previous studies have found that the degree of and type of cell-cell interaction can have profound effect on the behavior of the hepatocytes and fibroblast co-cultures<sup>5,6</sup>, the role of such interactions in ES cell cultures has not been explored. In addition, since the patterned co-cultures are more homogenous in comparison to random co-cultures, it is expected that they will provide a more uniform cellular behavior. An intriguing possibility with the co-cultures is the use of co-cultures to study ES cell differentiation in co-culture with other cell types.

## **CONCLUSIONS**

In conclusion, an approach based on the layer-by-layer deposition of polyionic molecules for patterning of two cell types was introduced. The feasibility of the approach to immobilize PLL and FN on glass substrates was demonstrated. Furthermore, patterned co-cultures of two different cell types was generated for ES cell and hepatocytes in co-culture with fibroblasts. The generation of co-cultures was independent of the selective adhesion of the cell types as well as seeding order. In addition, the co-cultures remained stable for at least 5 days. It is anticipated that with the ever increasing use of soft lithography in biology, this simple approach to pattern co-cultures could potentially provide a valuable tool to study cell-cell interaction, maintain cells in culture and engineer organs for tissue engineering.

## REFERENCES

- (1) Langer, R., Vacanti, J. P. Tissue engineering. *Science*, **260**, 5110, 1993.
- (2) Bhatia, S. N., Balis, U. J., Yarmush, M. L., Toner, M. Effect of cell-cell interactions in preservation of cellular phenotype: cocultivation of hepatocytes and nonparenchymal cells. *Faseb J*, **13**, 14, 1999.
- (3) Bhatia, S. N., Toner, M., Tompkins, R. G., Yarmush, M. L. Selective adhesion of hepatocytes on patterned surfaces. *Ann N Y Acad Sci*, **745**, 1994.
- (4) Bhatia, S. N., Yarmush, M. L., Toner, M. Controlling cell interactions by micropatterning in co-cultures: hepatocytes and 3T3 fibroblasts. *J Biomed Mater Res*, **34**, 2, 1997.
- (5) Bhatia, S. N., Balis, U. J., Yarmush, M. L., Toner, M. Probing heterotypic cell interactions: hepatocyte function in microfabricated co-cultures. *J Biomater Sci Polym Ed*, **9**, 11, 1998.
- (6) Bhatia, S. N., Balis, U. J., Yarmush, M. L., Toner, M. Microfabrication of hepatocyte/fibroblast co-cultures: role of homotypic cell interactions. *Biotechnol Prog*, **14**, 3, 1998.
- (7) Ostuni, E., Kane, R., Chen, C. S., Ingber, D. E., Whitesides, G. M. Patterning mammalian cells using elastomeric membranes. *Langmuir*, **16**, 20, 2000.
- (8) Takayama, S., McDonald, J. C., Ostuni, E., Liang, M. N., Kenis, P. J. A., Ismagilov, R. F., Whitesides, G. M. Patterning cells and their environments using multiple laminar fluid flows in capillary networks. *Proc Natl Acad Sci U S A*, **96**, 10, 1999.
- (9) Folch, A., Toner, M. Cellular micropatterns on biocompatible materials. *Biotechnol Prog*, **14**, 3, 1998.
- (10) Folch, A., Jo, B. H., Hurtado, O., Beebe, D. J., Toner, M. Microfabricated elastomeric stencils for micropatterning cell cultures. *J Biomed Mater Res*, **52**, 2, 2000.
- (11) Folch, A., Toner, M. Microengineering of cellular interactions. *Annu Rev Biomed Eng*, **2**, 2000.
- (12) Chiu, D. T., Jeon, N. L., Huang, S., Kane, R. S., Wargo, C. J., Choi, I. S., Ingber, D. E., Whitesides, G. M. Patterned deposition of cells and proteins onto surfaces by using three-dimensional microfluidic systems. *Proc Natl Acad Sci U S A*, **97**, 6, 2000.



- (13) Yousaf, M. N.,Houseman, B. T.,Mrksich, M. Using electroactive substrates to pattern the attachment of two different cell populations. *Proc Natl Acad Sci U S A*, **98**, 11, 2001.
- (14) Yamato, M.,Konno, C.,Utsumi, M.,Kikuchi, A.,Okano, T. Thermally responsive polymer-grafted surfaces facilitate patterned cell seeding and co-culture. *Biomaterials*, **23**, 2, 2002.
- (15) Hirose, M.,Yamato, M.,Kwon, O. H.,Harimoto, M.,Kushida, A.,Shimizu, T.,Kikuchi, A.,Okano, T. Temperature-Responsive surface for novel co-culture systems of hepatocytes with endothelial cells: 2-D patterned and double layered co-cultures. *Yonsei Med J*, **41**, 6, 2000.
- (16) Lahann, J.,Mitragotri, S.,Tran, T. N.,Kaido, H.,Sundaram, J.,Choi, I. S.,Hoffer, S.,Somorjai, G. A.,Langer, R. A reversibly switching surface. *Science*, **299**, 5605, 2003.
- (17) Decher, G. Fuzzy nanoassemblies: Toward layered polymeric multicomposites. *Science*, **277**, 5330, 1997.
- (18) Vazquez, E.,Dewitt, D. M.,Hammond, P. T.,Lynn, D. M. Construction of hydrolytically-degradable thin films via layer-by-layer deposition of degradable polyelectrolytes. *Journal of the American Chemical Society*, **124**, 47, 2002.
- (19) Thierry, B.,Winnik, F. M.,Merhi, Y.,Tabrizian, M. Nanocoatings onto arteries via layer-by-layer deposition: Toward the in vivo repair of damaged blood vessels. *Journal of the American Chemical Society*, **125**, 25, 2003.
- (20) Pavesio, A.,Renier, D.,Cassinelli, C.,Morra, M. Anti-adhesive surfaces through hyaluronan coatings. *Med Device Technol*, **8**, 7, 1997.
- (21) Chen, G.,Ito, Y.,Imanishi, Y.,Magnani, A.,Lamponi, S.,Barbucci, R. Photoimmobilization of sulfated hyaluronic acid for antithrombogenicity. *Bioconjug Chem*, **8**, 5, 1997.
- (22) Barbucci, R.,Magnani, A.,Rappuoli, R.,Lamponi, S.,Consumi, M. Immobilisation of sulphated hyaluronan for improved biocompatibility. *J Inorg Biochem*, **79**, 1-4, 2000.
- (23) Magnani, A.,Albanese, A.,Lamponi, S.,Barbucci, R. Blood-interaction performance of differently sulphated hyaluronic acids. *Thromb Res*, **81**, 3, 1996.
- (24) Frazie, R. A.,Matthijs, G.,Davies, M. C.,Roberts, C. J.,Schacht, E.,Tendler, S. J. Characterization of protein-resistant dextran monolayers. *Biomaterials*, **21**, 9, 2000.

- (25) Osterberg, E., Bergstrom, K., Holmberg, K., Schuman, T. P., Riggs, J. A., Burns, N. L., Van Alstine, J. M., Harris, J. M. Protein-rejecting ability of surface-bound dextran in end-on and side-on configurations: comparison to PEG. *J Biomed Mater Res*, **29**, 6, 1995.
- (26) Miyake, K., Underhill, C. B., Lesley, J., Kincade, P. W. Hyaluronate can function as a cell adhesion molecule and CD44 participates in hyaluronate recognition. *J Exp Med*, **172**, 1, 1990.
- (27) Fischer, D., Li, Y., Ahlemeyer, B., Krieglstein, J., Kissel, T. In vitro cytotoxicity testing of polycations: influence of polymer structure on cell viability and hemolysis. *Biomaterials*, **24**, 7, 2003.
- (28) Talbot, N. C., Pursel, V. G., Rexroad, C. E., Jr., Caperna, T. J., Powell, A. M., Stone, R. T. Colony isolation and secondary culture of fetal porcine hepatocytes on STO feeder cells. *In Vitro Cell Dev Biol Anim*, **30A**, 12, 1994.
- (29) Richards, M., Fong, C. Y., Chan, W. K., Wong, P. C., Bongso, A. Human feeders support prolonged undifferentiated growth of human inner cell masses and embryonic stem cells. *Nat Biotechnol*, **20**, 9, 2002.
- (30) Dang, S. M., Kyba, M., Perlingeiro, R., Daley, G. Q., Zandstra, P. W. Efficiency of embryoid body formation and hematopoietic development from embryonic stem cells in different culture systems. *Biotechnol Bioeng*, **78**, 4, 2002.

## **6. Surface patterned microfluidic channels for improving the cell / microdevice interface**

### **INTRODUCTION**

Microdevices comprised of microfluidic components hold great promise in the development of improved bioanalytical and diagnostic devices<sup>1</sup>. Microfluidics allows for miniaturization of sample volumes while increasing the throughput and efficiency of analysis. Engineering the surface chemistry<sup>2-5</sup> and the location of surface molecules within microfluidic channels is important for many potential applications. For example, spatial patterning has been shown to induce fluid mixing<sup>6</sup>, direct fluid flow<sup>7</sup> and provide means of generating functional microfluidic components such as valves<sup>8</sup>. In addition, controlling the location of proteins and cells within a microfluidic channel is important for the development of high throughput analytical devices<sup>9</sup> and multi-step bioreactors<sup>10, 11</sup>.

Currently, the most commonly used approaches to pattern within microchannels are laminar flow patterning<sup>12</sup> and photolithography. These techniques have been used to pattern cells, proteins<sup>12</sup> or hydrogels<sup>8, 10, 11</sup>, direct the flow of liquids<sup>7, 13</sup>, as well as etch<sup>14</sup> or build microstructures<sup>14</sup> within microchannels. Despite the success of these approaches to control the surface properties of microchannels, there are potential limitations. For example, laminar flow patterning, a simple approach to pattern within microfluidic channels, is limited to generating geometrical patterns in the shape of the laminarly flowing streams. In addition, photolithography, a useful tool for many emerging applications<sup>15, 16</sup>, has limitations due to the potential cytotoxicity of the photoinitiator<sup>17</sup>, the need for specialized equipment, and the difficulty in patterning the surface without modifying the surface topography<sup>10, 11</sup>. Therefore, the development of simple and direct techniques for patterning the surface of microfluidic channels could be of benefit.

Soft lithographic approaches such as microcontact printing<sup>18</sup>, microfluidic patterning<sup>12, 19, 20</sup>, micromolding<sup>21-23</sup> and capillary force lithography<sup>24</sup> have served as inexpensive, convenient and scalable tools for patterning surfaces. Despite these attractive traits, the merger of soft lithographic patterning approaches and microfluidics has not been realized. To pattern

microfluidic channels using soft lithography, the surface patterning must occur prior to the attachment of the PDMS mold to the substrate. However, the formation of an irreversible seal between the PDMS mold with the substrate requires oxygen plasma treatment, which can destroy the patterns. To overcome exposure to oxygen plasma, patterned membranes have been sandwiched between two plasma treated PDMS surfaces<sup>9</sup>, however, this approach is time consuming and requires multiple steps. Furthermore, the presence of a non-adherent polycarbonate membrane may affect the robustness of the channels.

In this chapter, we introduce a novel technique that can be used with multiple soft lithographic patterning processes to directly pattern the substrate of microfluidic channels. In this approach (**Figure 6.1**), the patterned substrate was protected from oxygen plasma by controlling the dimensions of the PDMS stamp in order to pattern the desired regions of a substrate and by leaving the stamp intact during the plasma treatment process. The technique allowed for selective adsorption of fibronectin and BSA onto the patterned microfluidic channels and the deposition of various proteins within multiple or individual patterns using laminar flows. In addition, cells were patterned to generate cell-based biosensors and bioreactors that are capable of enzymatic reactions.

## **MATERIALS AND METHODS**

*Chemicals and Materials:* Poly(dimethylsiloxane) (PDMS) elastomer composed of prepolymer and curing agent was purchased from Essex Chemical Sylgard 184. Fluorescein isothiocyanate (FITC)-labeled bovine serum albumin (FITC-BSA), anti-fibronectin antibody, 3-(trimethoxysilyl)propyl methacrylate (TMSMA), poly(ethylene glycol) methyl ether methacrylate (PEGMA) (average  $M_n$  =ca. 475), FITC-labeled anti-rabbit secondary antibody, 2,2'-azobisisobutyronitrile (AIBN), propidium iodide (PI) and phosphate buffered saline (PBS) were purchased from Sigma-Aldrich Chemical Company. HA was obtained from Genzyme Inc. All cells were obtained from ATTC. For cell culture, Dulbecco's modified Eagle's medium (DMEM), fetal bovine serum (FBS), fibronectin (FN), Trypsin, and other cell culture reagents

were purchased from Gibco Invitrogen Corporation. Calcein AM, ethidium homodimer and Texas-red labeled BSA (TR-BSA) were purchased from Molecular Probes.

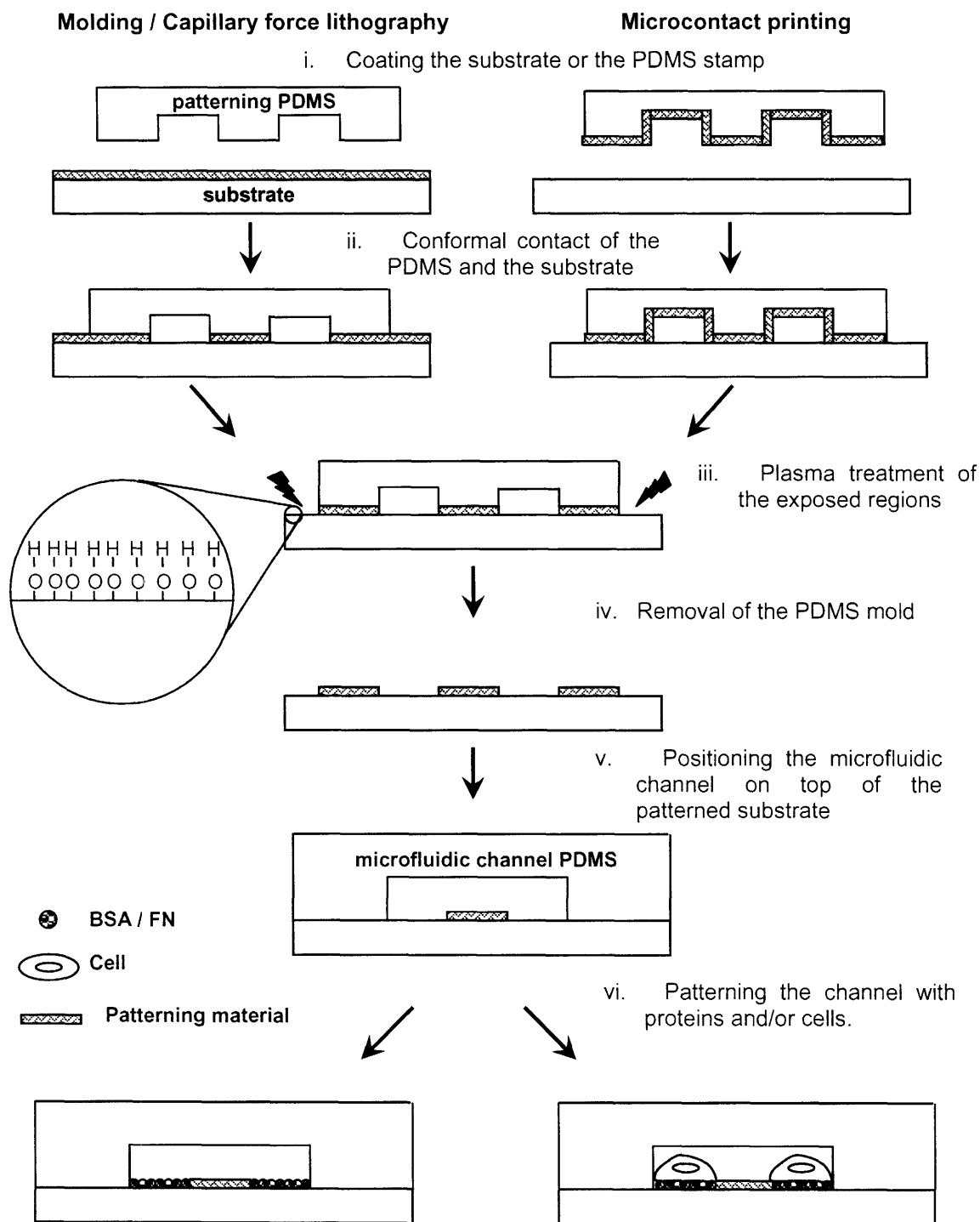


Figure 6.1. Schematic diagram of the approach to pattern within microfluidic channels.

*PDMS mold fabrication for surface patterning and microfluidics:* PDMS molds were fabricated by curing the prepolymer on silicon masters patterned with SU-8 photoresist. The masters used for patterning had protruding cylindrical features (ranging in diameter from 15  $\mu\text{m}$  to 150  $\mu\text{m}$ ), which resulted in PDMS replicas with the opposite sense (referred to as PDMS stamps). The masters used for microfluidics had protruding features with the impression of microfluidic channels (ranging from 50  $\mu\text{m}$  to 600  $\mu\text{m}$  in width and  $\sim 80$   $\mu\text{m}$  in height) (referred to as PDMS molds). To cure the PDMS prepolymer, a mixture of 10:1 silicon elastomer and the curing agent was poured on the master and placed at 70°C for 2 hours. The PDMS replica was then peeled from the silicon wafer and cut into narrow strips ( $\sim 0.3$  cm x 3 cm). These strips were sufficiently large to allow for the formation of patterns, while being small enough to allow for the major portion of the glass slide to be plasma cleaned.

*Fabrication of patterned microfluidic channels:* We generated patterned surfaces using microcontact printing and molding to demonstrate the versatility of the approach to pattern microchannels with various soft lithographic techniques. HA films were prepared by spin-coating (Model CB 15, Headway Research Inc.) a solution containing 5 mg HA/mL of distilled water onto silicon dioxide substrates (glass slides or wafers) at 1500 rpm for 15 seconds. Immediately after coating, a plasma cleaned PDMS stamp with negative features was brought into conformal contact with the substrate and left to be dried for 12 hours at room temperature. The patterned surfaces were then washed with PBS to remove the non-chemisorbed HA from the surface.

The procedure in Chapter 3 was used to synthesize poly(TMSMA-*r*-PEGMA). Briefly, PEGMA and TMSMA and AIBN were dissolved in THF at a molar ratio of 1.0 : 1.0 : 0.01 and degassed for 20 minutes and were reacted using free radical polymerization at 70 °C for 24 hours. The solvent was then evaporated leaving behind a viscous liquid. The synthesized poly(TMSMA-*r*-PEGMA) was used to pattern surfaces using both micromolding and microcontact printing. To pattern using micromolding, glass slides were plasma cleaned for 3 minutes and the poly(TMSMA-*r*-PEGMA) solution (10 mg/mL in methanol) was spin-coated onto each glass slide (1000 rpm for 10 seconds). A PDMS stamp was then immediately placed in conformal

contact with the spin coated surface and left undisturbed for 1 hour. To pattern the PEG-based copolymer using microcontact printing, the PDMS stamp was plasma cleaned for 3 minutes and subsequently a few drops of a solution of 10 mg/mL of polymer in methanol was placed on the stamp. To generate a uniform polymer coating, the PDMS stamps was either spin coated at 1000 rpm for 10 seconds or air dried until a thin film remained. The pattern on the PDMS stamp was then transferred onto the substrate by firmly pressing the stamp and the substrate together. All patterns were cured at 110 °C for 15 minutes.

To complete the device fabrication, a second PDMS mold with the features of the microfluidic channel and a patterned glass slide were plasma cleaned for 15-300 seconds (60 W, PDC-32G, Harrick Scientific, Ossining, NY), without disturbing the PDMS stamp used for patterning (i.e. in conformal contact with the substrate) (**Figure 6.1**). After plasma treatment, the first PDMS stamp was peeled from the substrate and the microfluidic channel PDMS mold was brought in conformal contact with the substrate and firmly pressed to form an irreversible seal. The microfluidic molds were aligned on the patterns either manually or after the addition of a drop of anhydrous ethanol (to assist in the alignment by delaying the irreversible binding) under the microscope. Fluids were driven through the channels using a SP200i syringe pump (World Precision Instruments, Sarasota, FL) that was connected to the device using polyethylene tubing (BD, Franklin Lakes, NJ).

*Protein adsorption within channels:* FITC-BSA, TR-BSA and fibronectin were dissolved in PBS (pH = 7.4) at a concentration of 50 µg/mL, 50 µg/mL and 20 µg/mL, respectively. To test for adhesion of protein within the patterned microfluidic channels, the primary protein was pumped through the microchannels for 30 minutes at a flow rate of 5 µL/min. For fibronectin staining, a solution of anti-fibronectin antibody was run through the channel for an additional 45 minutes, followed by 1 hour of FITC-labeled anti-rabbit secondary antibody. Protein patterns on patterned glass slides were generated by evenly distributing a few drops of the protein solution on the surfaces and storing the samples at room temperature for 30 minutes and then rinsing the patterns with PBS. All patterned surfaces were analyzed using an inverted fluorescent microscope (Axiovert 200, Zeiss). All protein staining experiments were done in triplicate to

ensure that multiple pictures were captured. Fluorescent images of various samples were then taken and quantified using NIH-Scion Image viewer. Blank glass slides analyzed under the same light exposure were used as background controls.

*Cell seeding and analysis within channels:* NIH-3T3 murine embryonic fibroblasts were maintained in DMEM supplemented with 10 % FBS at 37 °C and 5% CO<sub>2</sub> environment. For cell attachment experiments, a solution of 20 µg/mL of fibronectin in PBS was flowed through the channel for 15 minutes followed by a suspension of cells (~1-5 x 10<sup>7</sup> cells/mL) in medium containing serum at a flow rate of 5 µL/min. Once the cells were inside the channel, the fluid flow was redirected by closing the outlet of the channel and redirecting the fluid through a Y connector. Cells were maintained in the channels for at least 3 hours. Periodically, the cells were perfused with the medium at low flow rates (~0.1 mL/min) to ensure a constant supply of oxygen and nutrients. Once the cells adhered, the medium flow rate was increased to 1-3 µL/min and maintained throughout the experiment. The experiments involving cells and microfluidics were performed on an Axiovert 200 microscope (Zeiss, Germany) with an environmental chamber designed to maintain the temperatures at 37 °C and 5% CO<sub>2</sub>. The resulting cell patterns were directly examined under a phase-contrast microscope after removing the non-adhered cells by flowing PBS through the channel.

*Cell reactions and lyses within channels:* Calcein-AM and ethidium homodimer were dissolved at a concentration of 1 µg/mL in PBS. Once the cells adhered and excess cells were washed, the calcein-AM and ethidium homodimer were flowed through the channel for 30 minutes at a flow rate of 3 µL/min. For experiments in which the cells were lysed, a solution of 0.1% Triton-X in PBS was flown through the channel for 5 minutes at 3 µL/min. The cells were then stained with calcein-AM and ethidium homodimer as described above and analyzed under a fluorescent microscope.

## **RESULTS AND DISCUSSION**



### ***PDMS stamps protect micropatterns from plasma treatment***

Although the direct placement of a microfluidic mold on a glass slide, without any chemical modification, could be used to make channels with patterned substrates, the resulting channels can only be operated under low pressures, which would limit the range of fluid flows and the minimum size of the channels. To generate robust microchannels, the surfaces must be treated with oxygen plasma, which generates surface hydroxyl groups that can form covalent bonds between two plasma treated surfaces<sup>25</sup>. However, the oxidation reaction associated with plasma treatment can potentially destroy the micropatterns. It was hypothesized that surface patterns could be protected against plasma treatment by preventing their exposure to oxygen plasma. In this approach, the patterns were protected from oxidation by leaving the PDMS stamp intact during the plasma treatment. To ensure that only a small region of the substrate was protected while the remainder of the substrate was treated, the size of the PDMS stamp was limited to dimensions slightly greater than that of the channel. Thus, a small section of the substrate was patterned and remained protected while the rest of the substrate facilitated irreversible binding to the microfluidic mold.

Micropatterns were fabricated using both microcontact printing and molding techniques (For details see Chapter 5). The microcontact printed patterns were formed by transferring the polymer from the PDMS stamp to the substrate by direct contact. A thin layer of the PEG-based polymer was deposited on the PDMS stamp and the pattern was subsequently transferred to the substrate by firmly pressing the stamp onto the substrate. The molded patterns were generated by capillary force lithography<sup>24</sup>. A thin film was spin coated onto the substrate, and a PDMS stamp was subsequently brought into conformal contact with the surface and left until dried. The molding occurred as a result of capillary depression within the void spaces (i.e. repulsion of the hydrophilic polymer solution from the PDMS stamp) as well as the hydrodynamic forces at the contact regions<sup>26</sup>. Therefore, a thin film remained at the contact regions, while the void regions dewetted from the surface to expose the substrate.

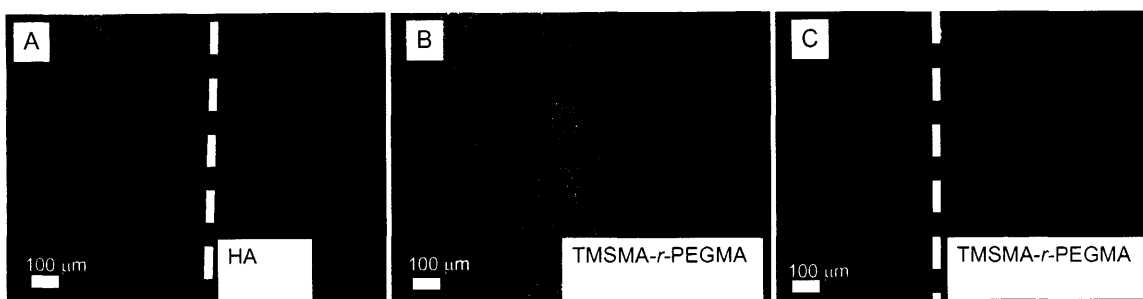


Figure 6.2. Fluorescent images of the unprotected (left) vs. protected (right) sections of a (A) molded HA and (B) poly(TMSMA-*r*-PEGMA) and (C) microcontact printed poly(TMSMA-*r*-PEGMA) substrates that were exposed to oxygen plasma for 45 seconds. The dashed lines indicate the boundary where the PDMS mold was maintained on the surface.

To directly analyze the stability of the plasma treated patterns as well as the protective effects of PDMS, stamps that were used to pattern the surface were gently cut into two pieces while maintaining the conformal contact with the patterns. One of the two pieces was then peeled from the surface while the other was left on the glass slide. The glass slide with PDMS stamp was then plasma cleaned for various durations and subsequently stained with FITC-BSA. For HA patterns, after 15 seconds of exposure to oxygen plasma the patterns became distorted as small sections of the patterns detached from the surface and by 45 seconds of exposure, the patterns had deteriorated further with many regions peeling from the surface (**Figure 6.2A (left)**). Similarly, poly(TMSMA-*r*-PEGMA) patterns that were made using both molding and microcontact printing deteriorated after 15 seconds and were completely destroyed after 45 seconds (**Figure 6.2 B-C (left)**). Interestingly, we did not observe a significant difference between the deterioration rate of the microcontact printed and molded PEG-copolymer patterns. As illustrated, protected patterns that were exposed to 45 seconds of plasma treatment did not lose their pattern fidelity (**Figure 6.2 (right)**). Furthermore, both HA and PEG-based patterns remained unaffected even after being plasma treated for 6 minutes. The patterns did not degrade when placed at low pressures similar to the conditions used for plasma treatment (200 millibars for up to 6 minutes) suggesting that the patterns were destroyed due to plasma treatment and not because of the vacuum associated with the plasma cleaning process. In these experiments molds with negative features were used (i.e. features sticking in), and the patterns were generated through the formation of thin polymeric monolayers between the contact regions of the PDMS and the substrate. Therefore, these results suggest that polymeric films formed between the contacted regions remain protected, indicating that the approach could be used for more commonly used techniques such as PEG-self assembled monolayers<sup>1</sup> and other forms of

microcontact printing. Furthermore, we anticipate that molded structures within the void regions of a PDMS stamp would also be protected from the oxygen plasma (as long as it sealed from the surrounding and not exposed to the oxygen plasma), suggesting that the approach may be used in conjunction with other molding and photocrosslinking techniques.

### *Patterned substrates within microfluidic channels*

We utilized the oxygen plasma protective features of the PDMS stamp to design an approach to fabricate stable microchannels with patterned substrates (**Figure 6.1**). In this approach, the polymers were patterned on oxide-based substrates. Unless noted otherwise, we patterned the channels using microcontact printed PEG-based copolymers or molded HA. After patterning, the substrate was plasma cleaned while maintaining the conformal contact between the PDMS stamp (used for patterning) and the glass slide. The PDMS stamp was then removed and a microfluidic channel was then aligned on the patterns and irreversibly attached to the substrate.

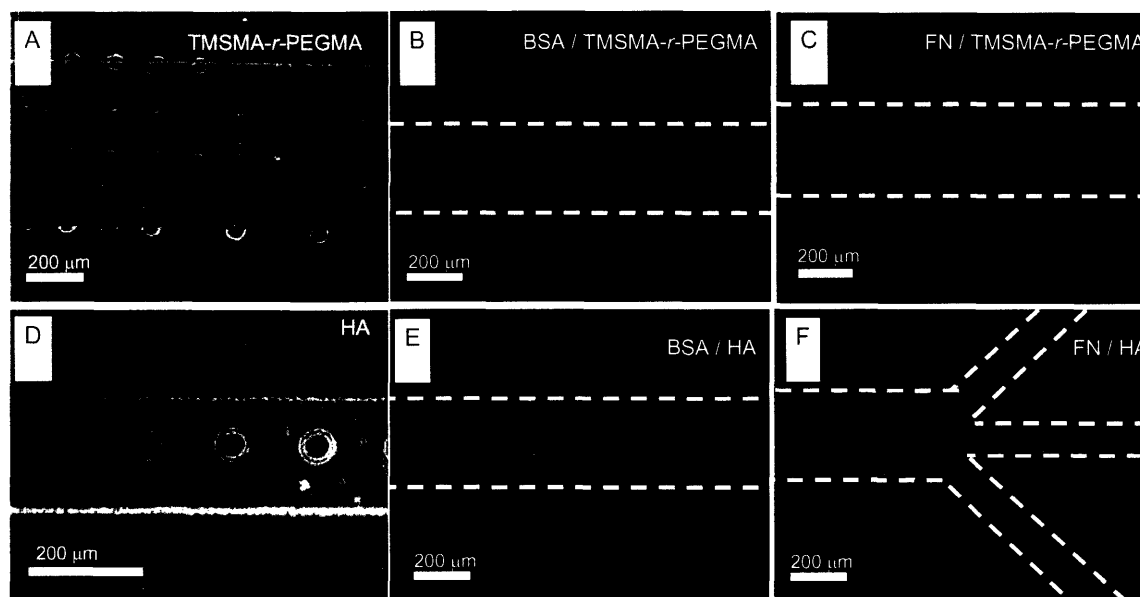


*Figure 6.3. Light micrograph (A, D) and fluorescent images (B, C, E, F) of patterned microfluidic channels. (A-C) represent microfluidic devices that were patterned with the PEG based copolymer, poly(TMSMA-r-PEGMA) while (D-F) represent microfluidic devices that were patterned with HA. The substrates were stained either with TR-BSA (B), FITC-BSA (E), or FN (C, F). The dashed lines indicate the boundary of the microfluidic channels.*

As shown in the light microscope images in **Figure 6.3**, channels were fabricated with PEG-based copolymer (**Figure 6.3A**) or HA (**Figure 6.3C-D**) patterns. The pattern edges in these images were clearly visible, which provided an easy way to detect pattern fidelity and to align the channel. To characterize the non-biofouling properties of these patterned microfluidic channels, protein adsorption experiments were performed by flowing FITC-BSA or TR-BSA or fibronectin through the channels. Fluorescent images in **Figure 6.3** are representative protein patterning images for various tested conditions. The fluorescence was limited to the exposed regions indicating that proteins attached directly to the patterns. Both PEG-based polymer as well as HA showed excellent protein resistance for BSA ( $95\pm 2\%$  and  $97\pm 3\%$  respectively) and fibronectin ( $96\pm 3\%$  and  $95\pm 3\%$  relative to bare glass) within the channels. These values were not significantly different from the protein adhesion results obtained immediately after patterning, indicating that the additional steps involved in fabrication and the shear stress associated with the flowing fluid did not alter the intrinsic non-biofouling properties of the patterned films.

In addition, to control the adsorption of multiple proteins to various regions of an exposed substrate, we used laminar flow patterning. It was demonstrated that laminar flow of multiple proteins could be used to generate patterned arrays of proteins within channels. As can be seen from **Figure 6.4A**, TR-BSA and FITC-BSA were adsorbed onto the various patterns within the channel. The adsorption of multiple proteins within single channels could be potentially useful for fabricating arrays of immunoassays for biosensors. Furthermore, individual patterns can be coated with two (or more) different proteins as illustrated in **Figure 6.4B**. In this case, TR-BSA and FITC-BSA were flowed side by side in a microfluidic channel directly above an exposed patterns being aligned at the region in between the two streams. The spatial patterning of multiple proteins within individual islands could be potentially useful in studying the effects of spatial organization of multiple extracellular matrix components on cell behavior such as asymmetric cell division<sup>27</sup>.

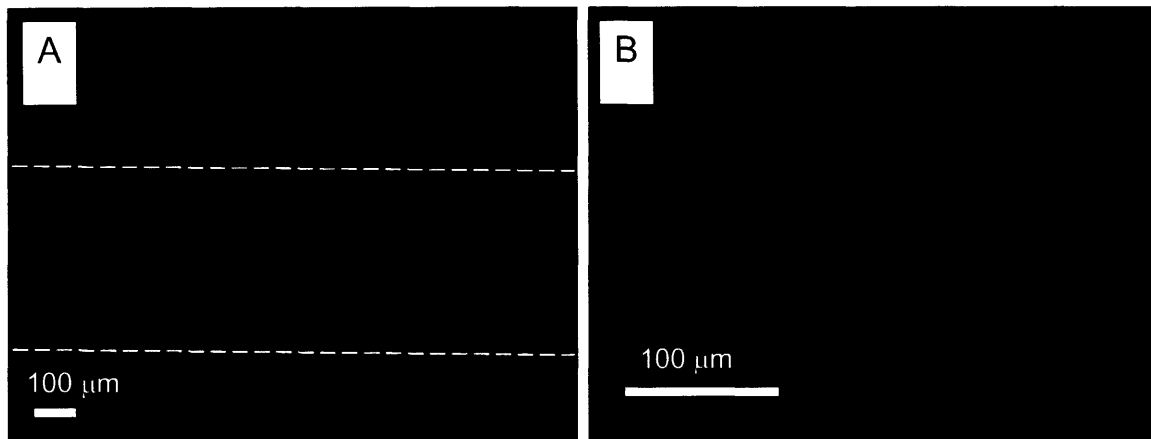


Figure 6.4. Fluorescent images of microfluidic channels in which laminar flow was used to immobilize two different proteins on the patterned substrate. (A) TR-BSA (red) and FITC-BSA (green) were flown through a channel resulting in the formation of red or green patches on various sides of the channel. (B) individual patterns were coated with TR-BSA and FITC-BSA.

### ***Patterning of cells within microfluidic channels***

To examine the potential of the patterned microfluidic channels for generating cellular arrays within microfluidic channels, patterned microfluidic channels were fabricated using both HA and PEG-based copolymer. Prior to cell seeding, a solution of fibronectin was flowed through the channels for 15 minutes. As previously shown, the fibronectin selectively adsorbs to the exposed regions forming strong anchoring sites for cells. A cell suspension of NIH-3T3 was then flowed in the channels. Once the cells were inside the channel, the outlet of the channel was closed and the fluid flow was redirected through a Y-connector that joined the polyethylene tubing from the syringe pump to the tubing from the microfluidic device. We found the use of this Y-connector was critical in maintaining the pressure within the channel since at lower pressures bubbles spontaneously formed and peeled the cells from the surface. A cell suspension of  $5 \times 10^7$  cells/mL was found to be optimum to form cellular monolayers or arrays. Concentrations of  $<1 \times 10^7$  cells/mL did not form confluent cell layers while concentrations  $>1 \times 10^8$  cells/mL clogged the channels.

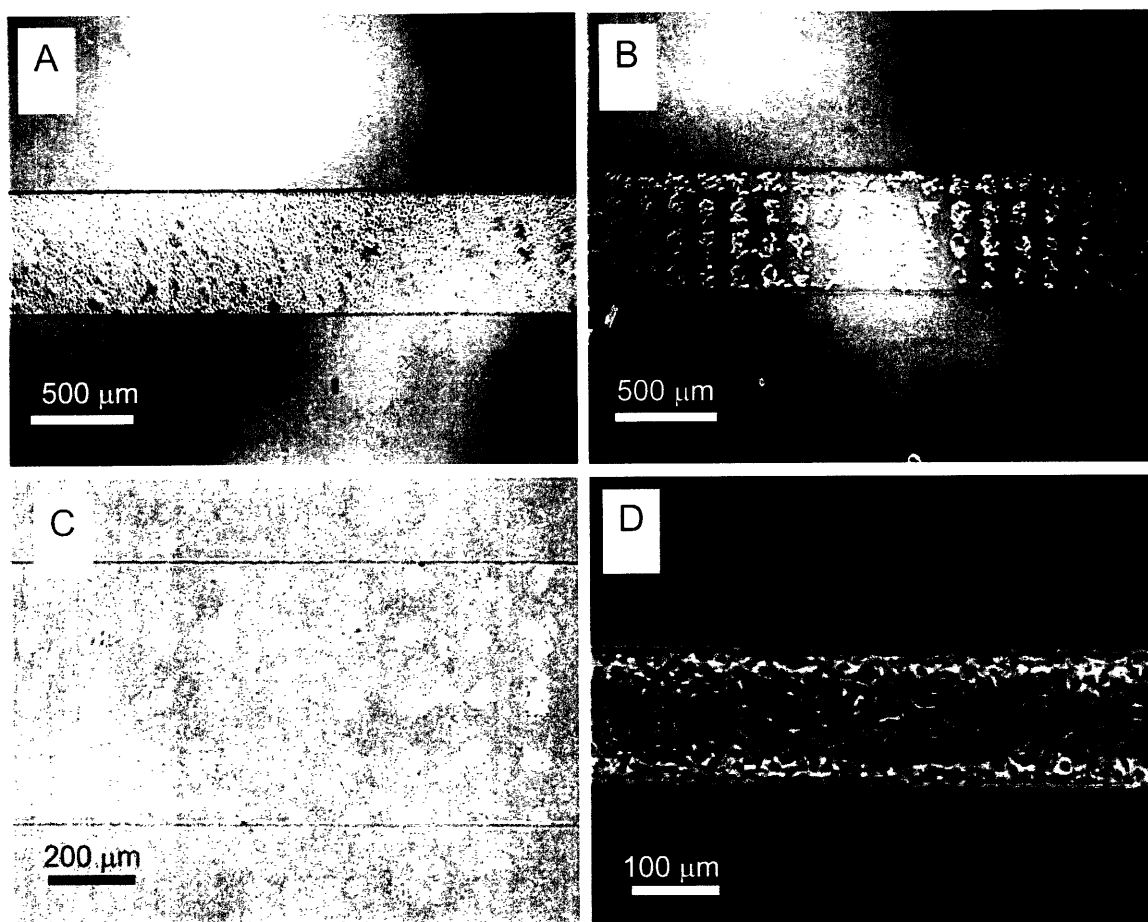


Figure 6.5. NIH-3T3 fibroblast adhesion and patterning within microfluidic channels at  $t = 0$  hours (A) and after 6 hours (B-D). (A) shows the initial cell density within the microfluidic channels while (B) and (C) represent the cell patterned channels on poly(TMSMA-r-PEGMA) and HA respectively. (D) represents fibroblast adhesion to non-patterned microchannels.

The morphology of the cells within the microchannels resembled that of the cells plated under normal tissue culture conditions. The cells entered the channels as spherical cell suspensions (**Figure 6.5A**) and started to spread on the surface within 2 hours. At this time, the non-adherent cells were removed by a gentle fluid flow, leaving behind partially adhered cells that fully adhered by 6 hours. Cells adhered to the fibronectin coated regions on patterns generated from HA or PEG-based copolymer (**Figure 6.5B-C**); while inside non-patterned channels, cells formed a confluent monolayer (**Figure 6.5D**). Once adhered in the channels, the cells did not stain for PI or Trypan blue dyes indicating that they remained viable. These results indicate that the cells could be patterned within microfluidic channels at high confluency and with high precision. Cells have been maintained within these microfluidic channels for at least 24 hours indicating that they can be maintained for durations that are relevant for bioanalytical and

biosensing applications. Furthermore, the use of HA as a patterning material may potentially lead to the generation of patterned co-cultures within microchannels using HA and poly-L-lysine<sup>28</sup>, which could enhance the functionality of the cells by controlling their cell-cell interactions.

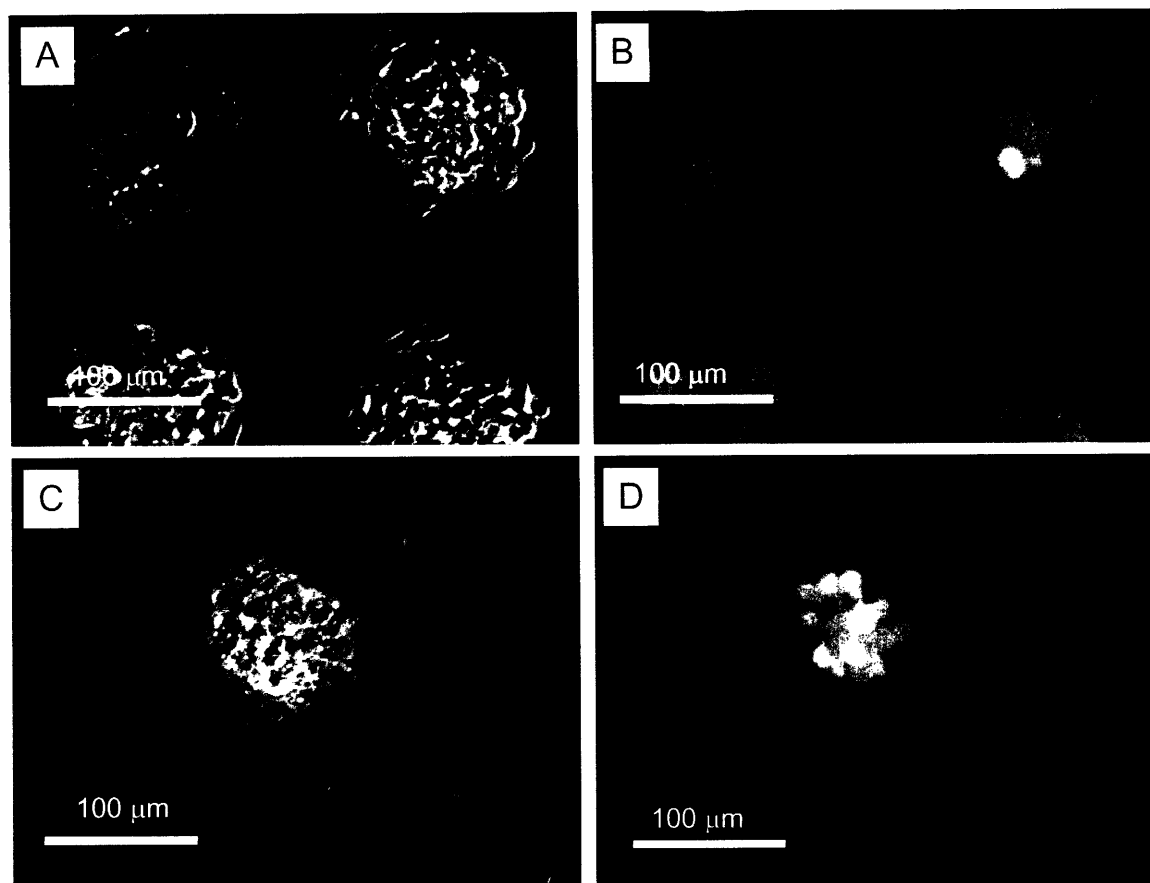


Figure 6.6. (A) light and (B) fluorescent images of NIH-3T3 fibroblasts patterned on microfluidic channels that have been treated with ethidium homodimer and calcein AM. (C-D) NIH-3T3 cells that were lysed by a pulse of Triton-X and subsequently treated with ethidium homodimer and calcein AM.

### ***Cellular reactions and lyses within microfluidic channel***

Recently, the ability to perform cellular reactions within microfluidic channels has been proposed as a method of fabricating biosensors<sup>10</sup>, improved systems to study cellular behavior<sup>5, 29</sup> and microreactors for biochemical synthesis<sup>11</sup>. This is particularly important as mammalian cells, capable of detecting toxins, pathogens, or capable of performing chemical reactions with fast response times are engineered<sup>30</sup>.

To analyze the potential of this patterning approach for various analytical applications, we tested the ability of the immobilized cells to carry out enzymatic reactions using ethidium homodimer and calcein-AM molecules. The membrane permeable calcein-AM enters all cells, and is enzymatically converted to green-fluorescent calcein in the cytoplasm. Cells with an intact plasma membrane (viable cells) retain calcein, and thus fluoresce green. Only cells with a compromised plasma membrane (dead cells) take up ethidium homodimer (seen as a red dye). Thus, we were able to analyze the viability and functionality of these cells within the channels. As illustrated in **Figure 6.6A**, NIH-3T3 cells remained viable and were also capable of performing enzymatic reactions (>98% of the cells stained only as green). To examine the potential of releasing the contents of the cells, a solution of Triton-X, a commonly used surfactant used to permeabilize cell membranes in culture, was flowed through the channel. This was followed by solution of calcein AM/ethidium homodimer after which the cells were analyzed under a fluorescent microscope. As shown in **Figure 6.6D**,  $58\pm 8\%$  of the cells that were treated with Triton-X were lysed as indicated by the permeation of ethidium homodimer across the membrane (red color). Interestingly, cells that were closer to the center of cellular aggregates remained viable suggesting that the mass transfer limitations associated with the diffusion of Triton-X to the center of these aggregates may have protected these cells.

A question arises here about the potential limitations of this approach with respect to the minimum size and the geometrical shape of the fabricated channel. The main limitation with the technique is the inability to precisely place the PDMS mold on the patterned substrate. However, the application of the process to smaller channels is technically feasible by aligning small channels (i.e.  $<10\ \mu\text{m}$ ) under the microscope through the use of a micromanipulator. In addition, appropriately designed PDMS stamps, could allow the fabrication of complex microchannel arrays at smaller length scales ( $< 10\ \mu\text{m}$ ). These PDMS stamps could have fabricated void regions between the stamp and the substrate that are exposed to the surroundings, allowing for plasma oxidation of the desired regions without the need to cut the stamps into smaller pieces.



## CONCLUSIONS

In conclusion, a technique was developed to fabricate stable microfluidic channels with precise control over the spatial patterning of the substrate. In this technique, the patterned regions were protected from oxygen plasma by controlling the dimensions of the PDMS stamp as well as the sequence of fabrication steps. Proteins were immobilized with precision on the substrate of the microfluidic channels. In addition, laminar flows were used to control the adsorption of multiple proteins within particular regions of multiple or individual patterns within the channels. Fibroblasts were patterned within the channels through adhesion to fibronectin coated regions. The cells remained viable and performed enzymatic reactions and could be lysed to potentially release intracellular components (i.e. proteins). The approach presented here can be potentially used with various soft lithographic patterning techniques to design and fabricate more sophisticated microfluidic devices for analytical applications and microreactors.

## REFERENCES

- (1) Whitesides, G. M., Ostuni, E., Takayama, S., Jiang, X., Ingber, D. E. Soft lithography in biology and biochemistry. *Annu Rev Biomed Eng*, **3**, 2001.
- (2) Lahann, J., Balcells, M., Rodon, T., Lee, J., Choi, I. S., Jensen, K. F., Langer, R. Reactive polymer coatings: A platform for patterning proteins and mammalian cells onto a broad range of materials. *Langmuir*, **18**, 9, 2002.
- (3) Yang, T. L., Jung, S. Y., Mao, H. B., Cremer, P. S. Fabrication of phospholipid bilayer-coated microchannels for on-chip immunoassays. *Analytical Chemistry*, **73**, 2, 2001.
- (4) Jon, S., Seong, J., Khademhosseini, A., Tran, T. T., Laibinis, P. E., Langer, R. Construction of Non-Biofouling Surfaces by Polymeric Self-Assembled Monolayers (PSAMs). *Langmuir*, **In Press**, 2003.
- (5) Dertinger, S. K. W., Jiang, X. Y., Li, Z. Y., Murthy, V. N., Whitesides, G. M. Gradients of substrate-bound laminin orient axonal specification of neurons. *Proceedings of the National Academy of Sciences of the United States of America*, **99**, 20, 2002.
- (6) Stroock, A. D., Dertinger, S. K. W., Ajdari, A., Mezic, I., Stone, H. A., Whitesides, G. M. Chaotic mixer for microchannels. *Science*, **295**, 5555, 2002.
- (7) Zhao, B., Moore, J. S., Beebe, D. J. Surface-directed liquid flow inside microchannels. *Science*, **291**, 5506, 2001.
- (8) Beebe, D. J., Moore, J. S., Bauer, J. M., Yu, Q., Liu, R. H., Devadoss, C., Jo, B. H. Functional hydrogel structures for autonomous flow control inside microfluidic channels. *Nature*, **404**, 6778, 2000.
- (9) Jiang, X. Y., Ng, J. M. K., Stroock, A. D., Dertinger, S. K. W., Whitesides, G. M. A miniaturized, parallel, serially diluted immunoassay for analyzing multiple antigens. *Journal of the American Chemical Society*, **125**, 18, 2003.
- (10) Zhan, W., Seong, G. H., Crooks, R. M. Hydrogel-based microreactors as a functional component of microfluidic systems. *Analytical Chemistry*, **74**, 18, 2002.
- (11) Heo, J., Thomas, K. J., Seong, G. H., Crooks, R. M. A microfluidic bioreactor based on hydrogel-entrapped *E. coli*: Cell viability, lysis, and intracellular enzyme reactions. *Analytical Chemistry*, **75**, 1, 2003.

- (12) Takayama, S., McDonald, J. C., Ostuni, E., Liang, M. N., Kenis, P. J. A., Ismagilov, R. F., Whitesides, G. M. Patterning cells and their environments using multiple laminar fluid flows in capillary networks. *Proc Natl Acad Sci U S A*, **96**, 10, 1999.
- (13) Zhao, B., Moore, J. S., Beebe, D. J. Principles of surface-directed liquid flow in microfluidic channels. *Analytical Chemistry*, **74**, 16, 2002.
- (14) Kenis, P. J. A., Ismagilov, R. F., Whitesides, G. M. Microfabrication inside capillaries using multiphase laminar flow patterning. *Science*, **285**, 5424, 1999.
- (15) Koh, W. G., Itle, L. J., Pishko, M. V. Molding of hydrogel multiphenotype cell microstructures to create microarrays. *Analytical Chemistry*, **75**, 21, 2003.
- (16) Koh, W. G., Revzin, A., Pishko, M. V. Poly(ethylene glycol) hydrogel microstructures encapsulating living cells. *Langmuir*, **18**, 7, 2002.
- (17) Liu, V. A., Bhatia, S. N. Three-dimensional photopatterning of hydrogels containing living cells. *Biomedical Microdevices*, **4**, 4, 2002.
- (18) Mrksich, M., Dike, L. E., Tien, J., Ingber, D. E., Whitesides, G. M. Using microcontact printing to pattern the attachment of mammalian cells to self-assembled monolayers of alkanethiolates on transparent films of gold and silver. *Exp Cell Res*, **235**, 2, 1997.
- (19) Delamarche, E., Bernard, A., Schmid, H., Bietsch, A., Michel, B., Biebuyck, H. Microfluidic networks for chemical patterning of substrate: Design and application to bioassays. *Journal of the American Chemical Society*, **120**, 3, 1998.
- (20) Takayama, S., Ostuni, E., LeDuc, P., Naruse, K., Ingber, D. E., Whitesides, G. M. Subcellular positioning of small molecules. *Nature*, **411**, 6841, 2001.
- (21) Folch, A., Ayon, A., Hurtado, O., Schmidt, M. A., Toner, M. Molding of deep polydimethylsiloxane microstructures for microfluidics and biological applications. *J Biomech Eng*, **121**, 1, 1999.
- (22) Kim, Y. S., Suh, K. Y., Lee, H. H. Fabrication of three-dimensional microstructures by soft molding. *Appl Phys Lett*, **79**, 14, 2001.
- (23) Zhao, X. M., Xia, Y. N., Whitesides, G. M. Fabrication of three-dimensional microstructures: Microtransfer molding. *Advanced Materials*, **8**, 10, 1996.
- (24) Suh, K. Y., Kim, Y. S., Lee, H. H. Capillary force lithography. *Adv Mater*, **13**, 18, 2001.
- (25) Xia, Y. N., McClelland, J. J., Gupta, R., Qin, D., Zhao, X. M., Sohn, L. L., Celotta, R. J., Whitesides, G. M. Replica molding using polymeric materials: A practical step toward nanomanufacturing. *Advanced Materials*, **9**, 2, 1997.

- (26) Khademhosseini, A., Jon, S., Suh, K. Y., Tran, T. N. T., Eng, G., Yeh, J., Seong, J., Langer, R. Direct Patterning of protein- and cell-resistant polymeric monolayers and microstructures. *Advanced Materials*, **15**, 23, 2003.
- (27) Yamashita, Y. M., Jones, D. L., Fuller, M. T. Orientation of asymmetric stem cell division by the APC tumor suppressor and centrosome. *Science*, **301**, 5639, 2003.
- (28) Khademhosseini, A., Suh, K. Y., Yang, J. M., Eng, G., Yeh, J., Levenberg, S., Langer, R. Layer-by-layer deposition of hyaluronic acid and poly-l-lysine for patterned cell co-cultures. *Biomaterials*, **25**, 17, 2004.
- (29) Jeon, N. L., Baskaran, H., Dertinger, S. K. W., Whitesides, G. M., Van de Water, L., Toner, M. Neutrophil chemotaxis in linear and complex gradients of interleukin-8 formed in a microfabricated device. *Nature Biotechnology*, **20**, 8, 2002.
- (30) Rider, T. H., Petrovick, M. S., Nargi, F. E., Harper, J. D., Schwoebel, E. D., Mathews, R. H., Blanchard, D. J., Bortolin, L. T., Young, A. M., Chen, J. Z., Hollis, M. A. A B cell-based sensor for rapid identification of pathogens. *Science*, **301**, 5630, 2003.

## **7. Molded poly(ethylene glycol) microstructures for capturing cells within microfluidic channels**

### **INTRODUCTION**

In the previous chapters novel methods of patterning cells and proteins were developed. These microdevices are advantageous in that they use very small volumes of reagents and can be potentially scaled up for high-throughput analysis<sup>1</sup>. Although great progress has been made in the fabrication of cell-based biosensors and high-throughput screening approaches, more research in interfacing cells with such microdevices is of benefit.

Cells are typically interfaced within microfluidic channels using one of two schemes. In one scenario, cells are flowed through the channel, either hydrodynamically or through electroosmotic pumping to separate and transport cells<sup>2,3</sup>. As the cells flow through the channel, they are potentially lysed, and the intracellular components of the cells are analyzed<sup>4,5</sup>. This approach is, however, potentially limited to non-adherent cells and transient analysis since unanchored cells exit the system and elude follow-up characterization. An alternative approach to analyze adherent cells is to immobilize cells within channels<sup>6</sup>. For example, anchorage dependent cells have been attached to microfluidic channels by a number of groups<sup>7,8</sup>. To immobilize cells within particular regions of a microfluidic channel, laminar flow<sup>9</sup>, pre-patterning with adhesive ligands<sup>10</sup>, and immobilization inside hydrogels<sup>11</sup> have been used. Despite the success of these approaches, there are potential limitations. For example, the geometrical shapes of the patterned regions using laminar flow patterning is restricted to the flow of the laminar streams, while the UV induced immobilization of cells inside hydrogels requires the exposure of cells to potentially toxic photoinitiators and radiation<sup>12</sup>. Also, the direct immobilization of cells on the substrate of the channels could lead to shear induced modifications in cell behavior<sup>13</sup>.

An alternative approach to immobilize cells within microfluidic channels is to capture and localize cells within particular regions of a channel using physical structures. For example, a dam structure between two parallel channels can be used to constrict cells within microfluidic

channels<sup>14</sup>. However, lack of control of the surface properties has hindered the widespread use of topographical heights in micro-scale analytical tools. Therefore, the development of simple and direct techniques for fabricating microstructures within microchannels with precise control over the surface properties of the microstructures could be of benefit.

Photolithography has been a useful tool to fabricate microstructures outside<sup>12, 15, 16</sup> or within microfluidic channels<sup>17, 18</sup>. One potential disadvantage of photolithography is that it requires multiple steps to fabricate microstructures with multiple heights. Molding of polymer under PDMS stamps is an alternative method of creating microstructures<sup>19-21</sup>. A previous study on molding of polystyrene has shown that the microstructures correlate with the initial thickness of the polymer film. It was hypothesized that the merger of the previously developed method of patterning inside microchannels (Chapter 6)<sup>10</sup> with polymer molding under a PDMS stamp could generate a unique approach in fabricating microstructures as integral components of microfluidic channels, with improved control over the surface properties of the channel.

In this chapter, a novel method of fabricating PEG microstructures within microchannels using a two step process is demonstrated. In the first step microstructures are generated by molding photocrosslinkable PEG onto a small predefined region of a substrate. To allow for irreversible bonding of the microfluidic mold, the size of the PDMS stamp is restricted to a small region of the substrate. The stamp is left undisturbed on the molded regions to protect the patterns from the plasma cleaning of the substrate. The stamp is then peeled from the substrate and the microfluidic mold is aligned on the substrate to allow for the formation of microstructures capable of capturing cells. Additional control of these features could be achieved by obtaining exposed (i.e. regions containing bare substrate) or non-exposed substrates (i.e. substrate is completely covered by PEG), thus facilitating the patterned deposition of proteins and cells.

## **MATERIALS AND METHODS**

*Materials:* Poly(ethylene glycol) dimethacrylate (PEGDM, MW=330, 575, 1000), bovine serum albumin (BSA), carbon tetrachloride, 2-hydroxy-2-methyl propiophenone, and *n*-heptane were purchased from Sigma-Aldrich Chemical Company. 3-(trichlorosilyl)propyl methacrylate (TPM) was obtained from Fluka Chemicals. PDMS elastomer composed of pre-polymer and

curing agent was purchased from Essex Chemical Sylgard 184. For cell culture, Dulbecco's modified Eagle's medium (DMEM), phosphate buffered saline (PBS), fetal bovine serum (FBS), fibronectin (FN), trypsin, and other cell culture reagents were purchased from Gibco Invitrogen Corporation. MC-480, the antibody against SSEA-1 was purchased from Developmental Hybridoma Bank. Phycoerythrin conjugated goat anti-mouse IgM antibody was purchased from Jackson ImmunoResearch. All cells were obtained from ATTC. Calcein AM, ethidium homodimer and Texas-red labeled BSA (TR-BSA) were purchased from Molecular Probes. 1 ml syringes and polyethylene tubing was purchased from Becton Dickinson. Metal tubing and Y connectors were purchased from Small Parts Inc.

*Cell culture:* Cell culture was performed under sterile tissue culture hoods, and cells were maintained in a 95% air/5% CO<sub>2</sub> humidified incubator at 37 °C. NIH-3T3 fibroblasts were maintained in DMEM supplemented with 10 % FBS. Mouse embryonic stem (ES) cells (R1 strain) were maintained on gelatin treated dishes in a medium comprised of 15% ES-qualified FBS in DMEM knockout medium. ES cells were fed daily and passaged every 3 days at a subculture ratio of 1:4. During the experiments the medium specific to the cell type was used.

*PDMS mold fabrication and substrate preparation:* PDMS molds were fabricated by curing the pre-polymer on silicon masters patterned with SU-8 photoresist. The masters used for patterning had receding cylindrical features (ranging from 15 to 150 μm in diameter), 100 μm lanes or larger grids which resulted in PDMS replicas with the opposite sense. The masters used for microfluidics had protruding features with the impression of microfluidic channels (ranging from 50 to 800 μm in width and ~80 μm in height). To cure the PDMS prepolymer, a mixture of 10:1 silicon elastomer and the curing agent was poured on the master and placed at 70°C for 2 hours. The PDMS stamps (i.e. used for patterning) and the microfluidic molds were then peeled from the masters and cut. The PDMS stamps were cut into narrow strips (~0.3 cm x 2 cm) that were sufficiently large to pattern the entire width of the channels, while allowing the rest of the substrate to be plasma cleaned<sup>10</sup>.

Prior to patterning, glass slides were plasma treated for 2 minutes, immersed in a solution of 30% H<sub>2</sub>O<sub>2</sub> and H<sub>2</sub>SO<sub>4</sub> (3:1 ratio) for 5 minutes and washed in DiH<sub>2</sub>O. The slides were then immersed in a 1 mM solution of 3-(trichlorosilyl)propyl methacrylate (TPM) for 5 minutes to enhance the adhesion of PEG microstructures to the surface<sup>15</sup> and washed with a mixture of heptane/carbon tetrachloride (80 /20 v/v) and DiH<sub>2</sub>O.

*Scanning electron microscopy:* To perform scanning electron microscopy (JEOL 6320FV) samples were mounted onto aluminum stages and sputter coated with gold to a thickness of 200 Å and analyzed at a working distance of 20 mm.

*Protein adsorption:* TR-BSA was dissolved in PBS (pH = 7.4) at 100 µg/mL. To test for substrate exposure through protein adhesion, a few drops of the protein solution were evenly distributed onto the patterned substrates and incubated at room temperature for 45 minutes. All patterned surfaces were then washed and analyzed using an inverted fluorescent microscope (Axiovert 200, Zeiss).

*Fabrication of the microstructures within microfluidic channels:* The microstructures were made using a solution of 99.5 wt% PEGDM (MW 330, 550, or 50% 1000 dissolved in PBS) and 0.5 wt% of a water soluble photoinitiator 2-hydroxy-2-methyl propiophenone photoinitiator. Exposed and non-exposed microstructures were fabricated on the substrate using capillary force lithography<sup>21</sup>. Two different approaches were used to generate the substrates with varying features (**Figure 7.1**). To generate features with non-exposed substrates, a few drops of the PEG polymer were evenly distributed onto the substrate, whereas to generate features with the exposed substrate a few drops of the pre-polymer were evenly spread on the PDMS stamp. The PDMS mold was then placed directly on the polymer film and exposed to 365 nm, 300 mW/cm<sup>2</sup> UV light (EFOS Ultracure 100ss Plus, UV spot lamp) for 30 seconds.

Once the microstructures were fabricated, the devices were completed by plasma cleaning the slide (without disturbing the PDMS stamp) and the microfluidic mold for 2 minutes (60 W,



PDC-32G, Harrick Scientific, Ossining, NY). After plasma treatment, the PDMS stamp was peeled from the substrate and the microfluidic mold was aligned and brought in conformal contact with the substrate and firmly pressed to form an irreversible seal. In some experiments the devices were further supported by clamping the mold to the substrate.

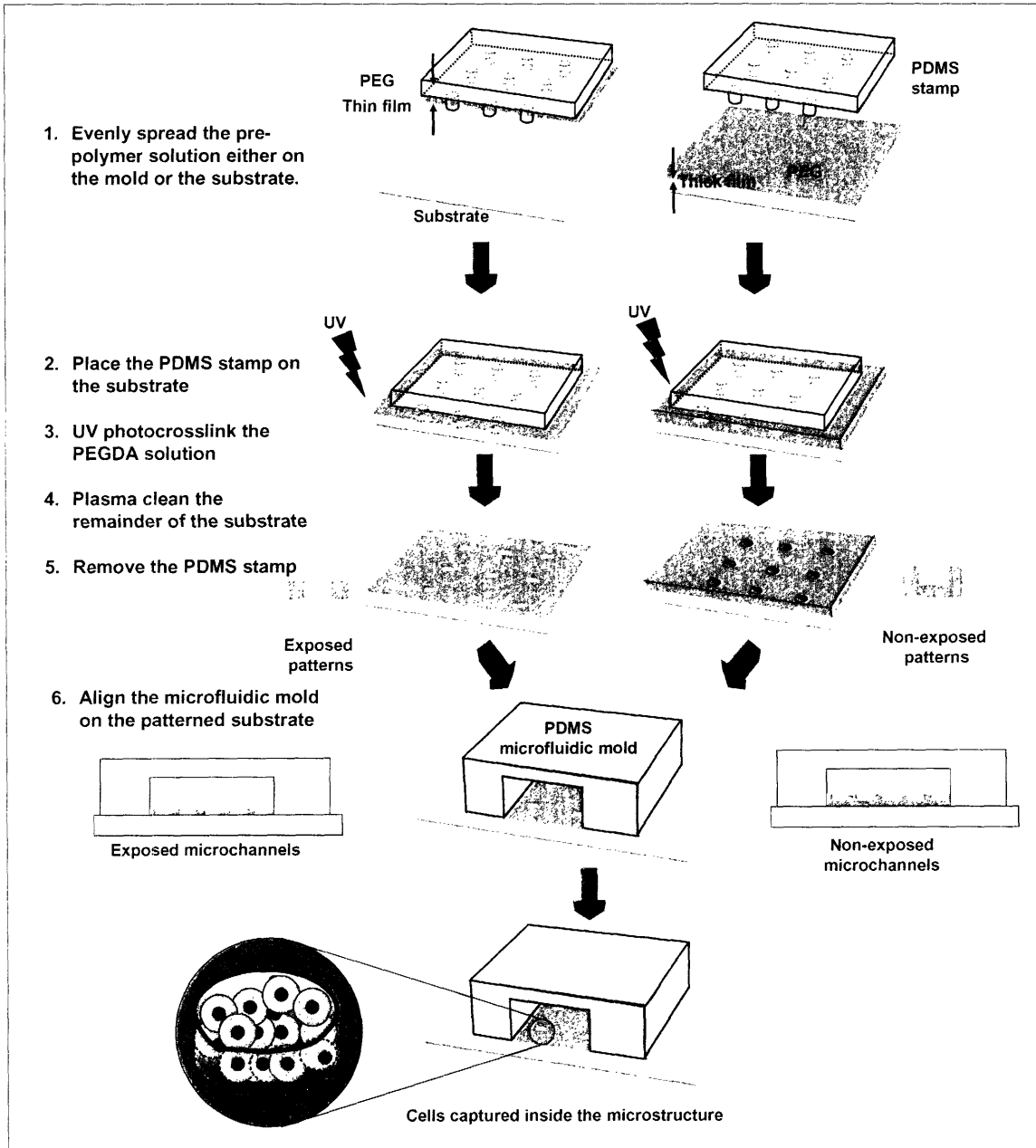


Figure 7.1: Schematic diagram for the fabrication of exposed and non-exposed microstructures inside microchannels.

Fluids were driven through the channels using a SP200i syringe pump (World Precision Instruments) that was connected to the device using polyethylene tubing. Transitions between different injections were facilitated with a Y connector that was used to redirect bubbles that were formed by changing the inlet solution.

*Docking and analysis of cells in microchannels:* All experiments involving cells inside the channels were carried out in a 37°C, 5% CO<sub>2</sub> environment chamber (Zeiss) and visualized under a fluorescent microscope. To immobilize cells within the microstructures, cells were trypsinized and resuspended in medium at a concentration of  $\sim 2 \times 10^7$  cells/mL and kept on ice. The channel was first treated with ethanol (95%) to clear potential air bubbles, followed by PBS for 10 minutes at a flow rate of 1  $\mu$ L/min. For cell adhesion studies, fibronectin (25  $\mu$ g/ml) was then flowed in the channel for 15 minutes. Cells were introduced into the channel and the flow was stopped to sediment the cells into microwells. After 10 minutes the flow was restarted and maintained at 1  $\mu$ L/min.

To analyze cellular viability, a live/dead assay was performed by flowing ethidium homodimer and calcein AM dissolved at 1  $\mu$ g/mL in DMEM containing 10% FBS through the channel for 20 minutes. Staining of ES cells was performed by flowing MC-480/SSEA-1 (diluted 1:10 in a PBS solution with 1% BSA) for 20 minutes and then phycoerythrin conjugated goat anti-mouse IgM (diluted at 2:1000 in 1% BSA) for 20 minutes, both at the flow rate of 1  $\mu$ L/min. PBS was then flowed through the channel to wash the channel and remove non-specific staining.

## **RESULTS AND DISCUSSION**

### **Fabrication of exposed and non-exposed microstructures**

Control over the features of microdevices including microfluidic channels is important for the development of analytical devices. We aimed to immobilize cells within microchannels by fabricating PEG microstructures that could facilitate the capture and analysis of cells with control over the adhesion of anchorage dependent cells. To fabricate PEG microstructures,

PEGDA was molded beneath a PDMS stamp and subsequently photopolymerized. PEGDA was used due to its ability to crosslink at short exposure times and its low viscosity which allow for its use at high concentrations to fabricate structures with a high aspect ratio<sup>21, 22</sup>.

To fabricate microstructures with a non-exposed substrate we molded the polymer onto the features of the PDMS stamp by placing a thick polymer film on the substrate and subsequently placing the stamp on the film (**Figure 7.1**). As shown in **Figure 7.2a**, the microstructures could be generated using this approach without the underlying substrate becoming exposed. Alternatively, to fabricate exposed substrates a layer of PEG was coated onto the PDMS stamp and subsequently molded onto the substrate. These thinner films resulted in the formation of microstructures with exposed substrates (**Figure 7.2b**). The PEG microstructures were ~25  $\mu\text{m}$  in height with good pattern fidelity (**Figure 7.2c-d**).

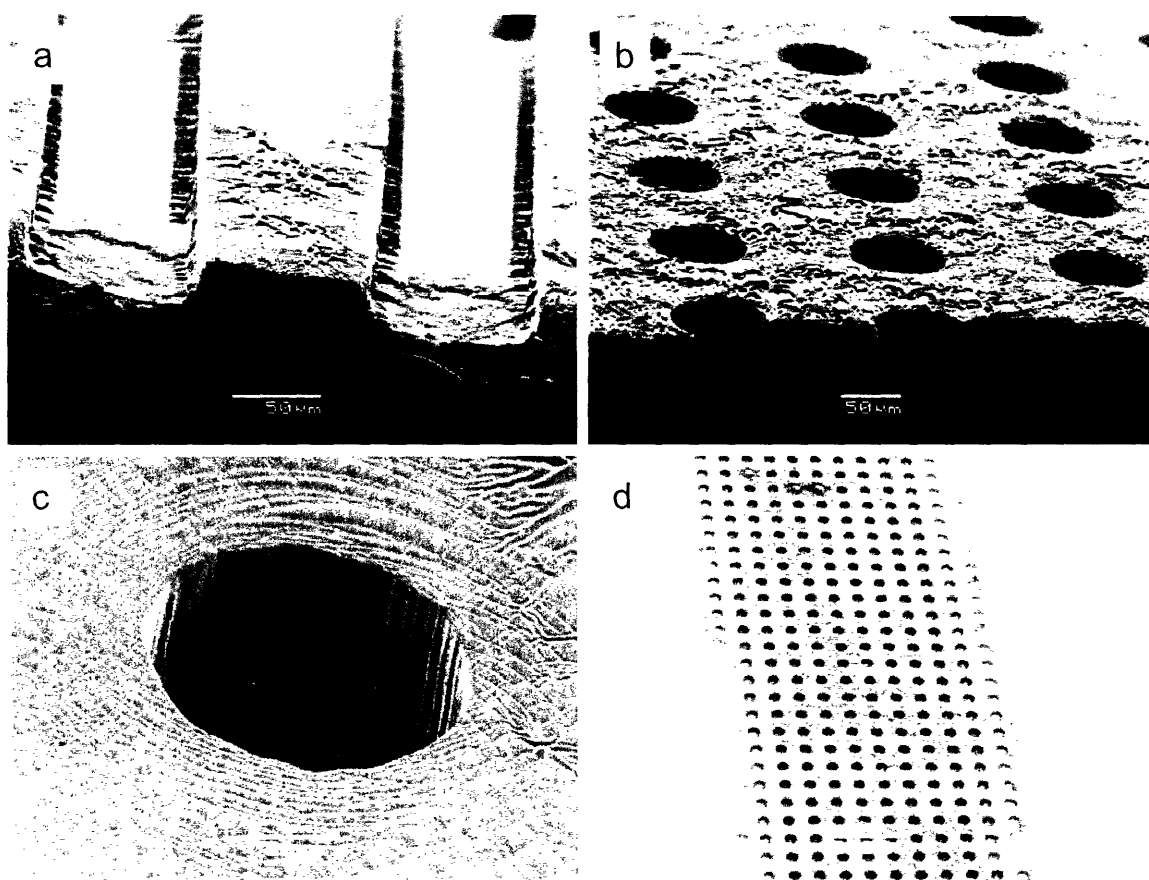


*Figure 7.2: Scanning electron micrographs of molded PEG lanes (a) or microwells (b-d). The underlying substrate could be either exposed (a) or non-exposed (b) based on the polymer film thickness. (c) Individual patterns of circular microwells demonstrate that the structures are  $\sim 25 \mu\text{m}$  in height.*

To demonstrate that the approach could be used to generate microstructures with exposed or non-exposed substrates, the ability of the PEG microstructures to resist protein adsorption was examined. Since PEG networks are protein resistant, it is anticipated that for the non-exposed patterns, the patterned regions will resist protein adhesion while for patterns with exposed substrates, proteins will adsorb onto the hydrophobic underlying substrate forming patterned regions. As shown in **Figure 7.3**, microstructure patterns that were treated with TR-BSA could be fabricated either with exposed substrates or without the substrates depending on the fabrication process. Further quantification of the degree of protein adsorption onto the PEG-based microstructures showed that ca. 98% of the protein adsorption was reduced as compared to that of exposed surface of the substrate. In addition, the ability of the exposed substrate to allow for adhesion of cells within the microstructures was examined by dipping the patterned

substrates in a solution of fibronectin. After adhesion of the protein onto the substrate the solution was washed and NIH-3T3 cells were seeded on the substrate. After 6 hours, the patterns were thoroughly washed to remove all non-adhered cells. As seen in **Figure 7.4**, cells adhered and spread inside microwells with exposed substrates while the cells on the non-exposed microwells were completely washed away even though they had been patterned within the wells.

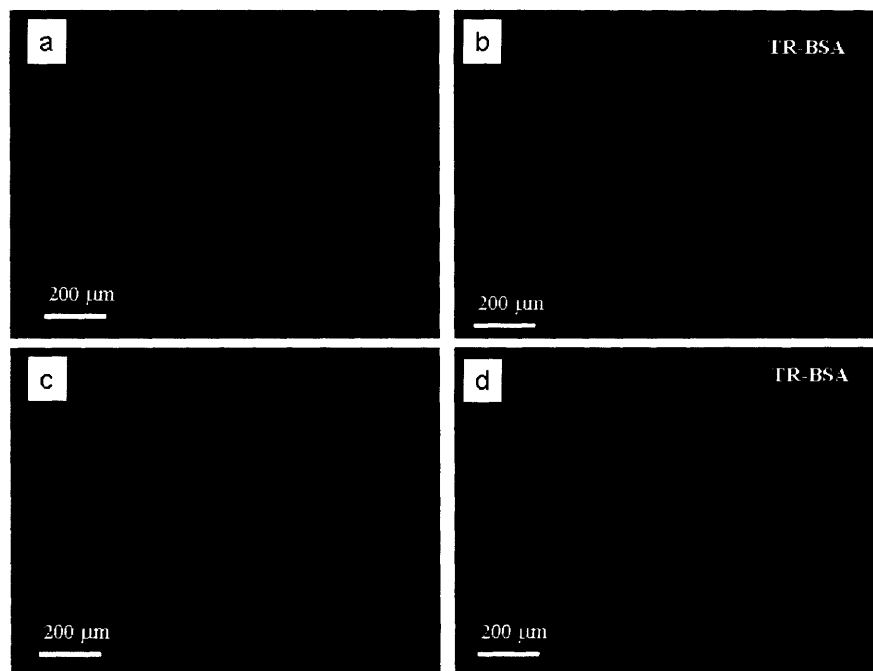


*Figure 7.3: Light (a, c) and fluorescent (b, d) images of microstructures with non-exposed (a-b) and exposed (c-d) underlying substrates. Substrate exposure was tested by testing the adsorption of TR-labeled BSA on the patterned surfaces.*

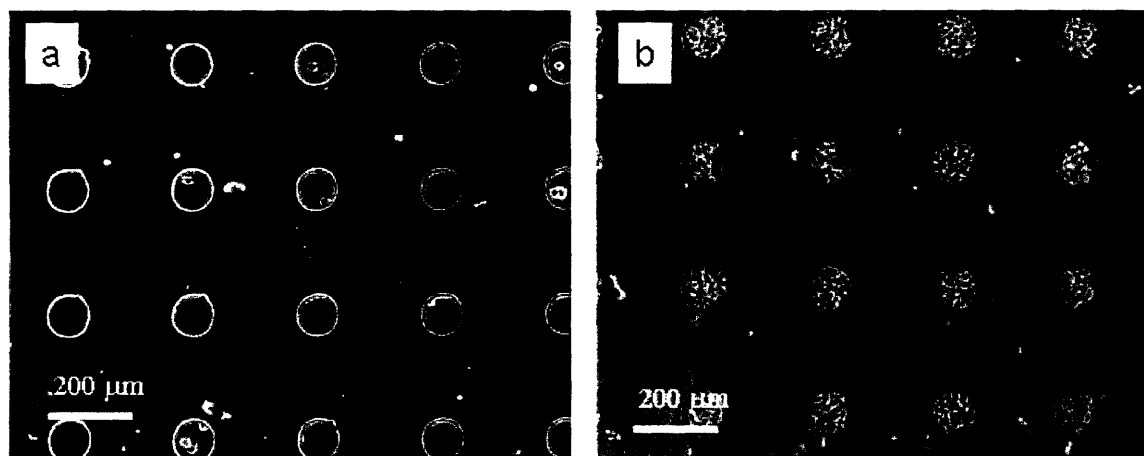


*Figure 7.4: NIH-3T3 cell adhesion of the non-exposed (a) and exposed (b) and PEG microwells. NIH-3T3 cells were seeded on substrates patterned with PEG polymer for 6 hours and subsequently washed and analyzed.*

PEGDA ranging in molecular weight from 330 to 1000 Da were successfully used to fabricate non-biofouling microstructures. However, for the experiments reported here PEGDA 330 and 550 Da were routinely used due to their improved mechanical strength, low swelling properties and ability to resist cells and proteins.

### **Fabrication of the device**

Although it is possible to UV crosslink PEG pre-polymer inside microchannels<sup>11, 17, 18</sup>, the direct crosslinking of the PEG polymer within microfluidic channels has not been shown to generate features with both exposed and non-exposed substrates. Therefore, we hypothesized that the molding of the PDMS stamp on a polymer film would allow for more control over the features of the microfluidic channel.

To fabricate PEG microstructures inside microwells, the microfluidic molds were aligned on substrates that had been pre-patterned with PEG microstructures. To ensure that the microfluidic mold could be irreversibly adhered to the substrate we patterned only a small region of the substrate to allow for plasma treatment of the remainder of the substrate. The PDMS stamp was left undisturbed after molding and the remainder of the substrate was plasma treated to allow for adhesion of the substrate to the PDMS mold (**Figure 7.1**).

One of the observations obtained using this approach was the ability of the elastomeric microfluidic mold to seal the channels despite the topographical differences between the patterned region and the surroundings (**Figure 7.1**). These microchannels were robust and could stand flow rates of  $> 5 \mu\text{L}/\text{min}$ . This could be attributed to the elastomeric properties of the mold.

### **Docking of cells within microstructures**

To evaluate the ability of the microstructures within the channels to capture cells, NIH-3T3 and ES cells were used as model cell lines. Both these cells are anchorage dependent thus they enable testing of the potential adhesion of these cells. In addition, trypsinized cells from both cell types can be used as a model for non-adherent cells. Initial experiments were performed

using various shaped features including lanes, grids and circles. Although numerous conditions were tested, two specific conditions facilitated cell docking. In the first approach, the flow rate was tightly regulated to enable flow of the cells inside the channel but was slow enough to allow for a fraction of the cells to be captured by the microstructures. Within standard microchannels (800  $\mu\text{m}$  in width and 80  $\mu\text{m}$  in height) using the parameters used in these experiments, a flow rate of  $\sim 0.3 \mu\text{l}/\text{min}$  was found to be optimized in that it allowed for docking of the cells, yet did not clog the tubes due to excessive clumping and aggregation of the cells. However, the optimized flow rate is a function of channel dimensions and geometry (determining shear stress), cell phenotype and concentration. The second approach was to stop the flow briefly to allow for the cells to settle into the microstructures. In general, it took less time with the latter technique to deposit cells within structures and was overall preferred for our subsequent experiments. As shown in **Figure 7.5**, cells successfully docked within features of various shapes. Furthermore, once the cells had settled within these regions, they remained in place and were not washed away even when the flow rate was increased to high values of  $> 5 \mu\text{l}/\text{min}$ .

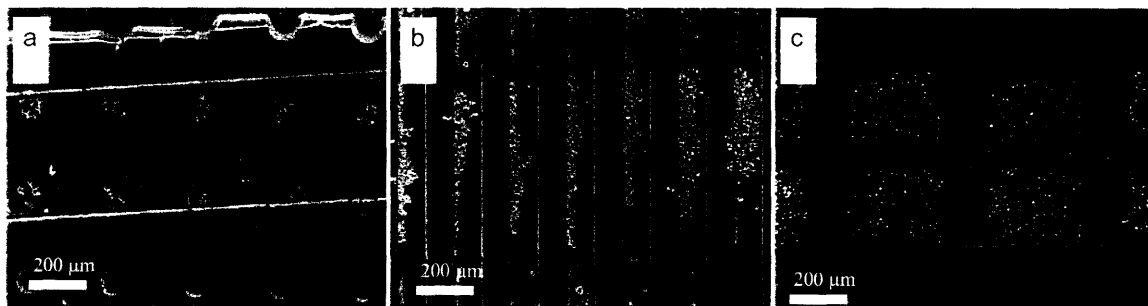


*Figure 7.5: Cells flowing through microchannels could be docked within microstructures of various sizes and shapes such as 100  $\mu\text{m}$  microwells (a), perpendicular lanes (b) and grids (c).*

### **Analysis of captured cells within microchannels**

To test for the ability of the microchannels to act as potential bioreactors and analytical tools, cells were analyzed using a variety of techniques. To analyze cell viability and the ability to perform enzymatic reactions, ethidium homodimer and calcein AM were allowed to flow through the channel. Ethidium homodimer is a DNA binding dye that stains the membrane

compromised cells. On the other hand, calcein AM is a membrane permeable substrate that is converted within the cells to a green fluorescent molecule that is membrane impermeable. Therefore 'live' cells can be visualized as green, while cells with compromised cell membranes show up as red. As expected, ~98% of NIH-3T3 cells that were immobilized within the channels remained viable based on the expression of the green fluorescent dye. In addition, the cells did not stain red indicating that the membrane integrity had not been compromised during the process (Figure 7.6 a-b).

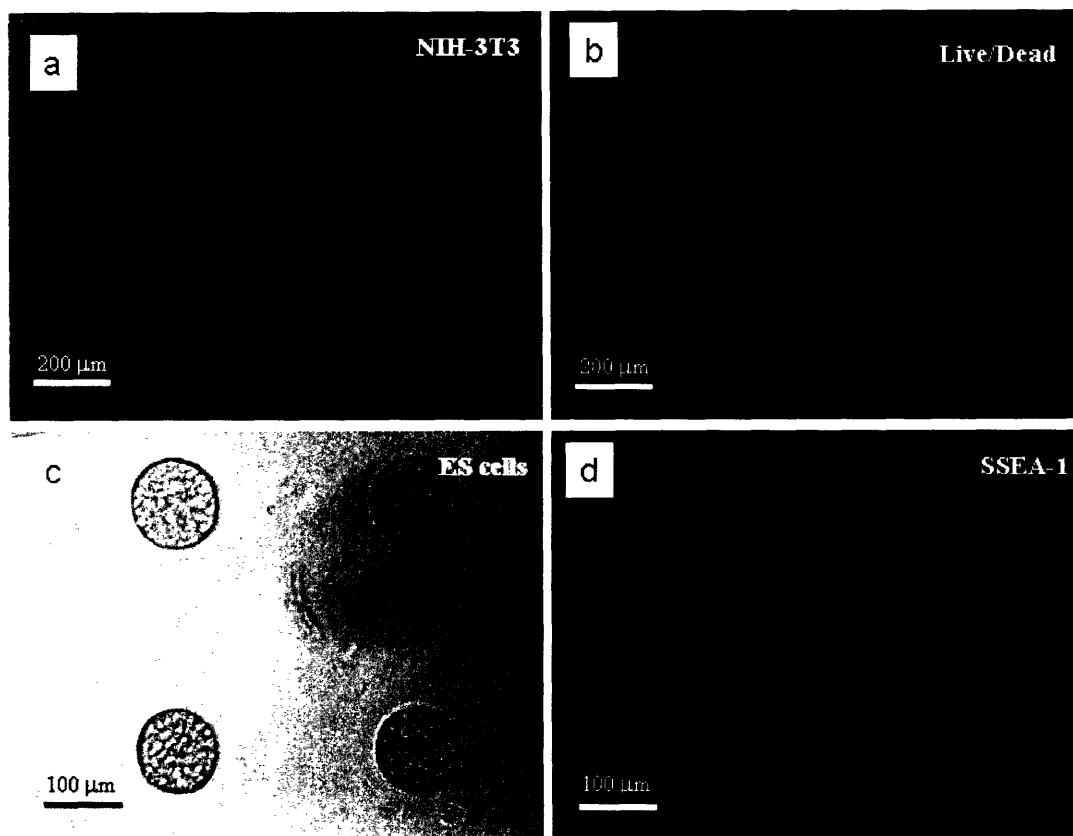


Figure 7.6: NIH-3T3 cells were immobilized within microwells generated from PEG microstructures (a). These cells remained viable as measured by live-dead staining. Live cells express the green color representing the formation of calcein while the nucleus of membrane compromised cells (dead cells) was stained with the red color. (c-d) Murine embryonic stem cell patterning (c) and SSEA staining (d) within non-exposed microfluidic channels.

A potential application for immobilizing non-adherent cells within microstructures is to analyze the cells for surface staining of various molecules. To examine the application of the microwells for cell surface staining, ES cells were docked within the channel and subsequently stained for



the expression of an undifferentiated stem cell marker, SSEA-1. This was obtained by performing a two-step staining process in which medium containing the SSEA-1 antibody was flowed in the channel followed by a solution containing the secondary antibody, followed by a non-fluorescent medium to wash non-specific binding. As shown in **Figure 7.6 (c-d)**, ES cells could be directly stained within the microstructures. Approximately 95% of the cells could be seen expressing SSEA-1, which is similar to the results obtained when the cells are stained and flown through a flow cytometer. These results demonstrate the potential application of this technique to capture cells for a wide range of subsequent applications such as bioreactors and analysis including antibody staining.

### **Cell adhesion onto exposed microwells within microfluidic channels**

As demonstrated earlier, microwells could be generated with exposed substrates that allow for protein adsorption and adhesion of cells. To test the application of this process within microchannels, we generated patterned channels (with exposed substrate) and analyzed the ability of cells to dock and adhere within these wells. FN was allowed to flow through the channels to coat exposed surfaces and promote cell adhesion and spreading. NIH-3T3 fibroblasts were then flowed through the channel and their ability to adhere within the channels was examined using morphological characteristics of the captured cells with time. As expected, cells adhered to the bottom surface of the microwells and elongated within 6 h (Figure 7).

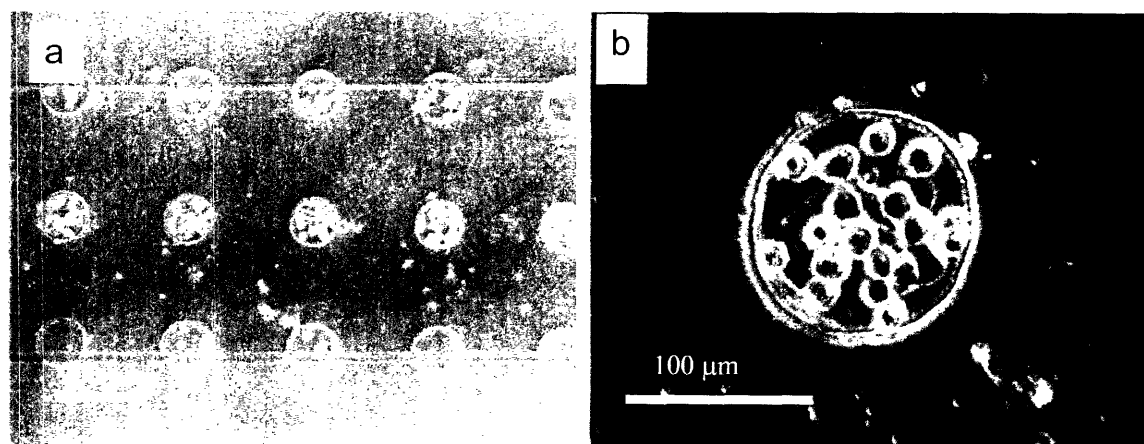


*Figure 7.7: NIH-3T3 cells were captured and adhered on channels with fibronectin coated substrates. Images were taken after 6 hours at low (a) and high (b) magnifications.*

There are a number of potential advantages associated with this technique for patterning cells within microchannels. For example, both non-adherent and adherent cells can be immobilized, with tight control over the substrate properties while minimizing the effects of shear, therefore widening the potential application of cell-based microdevices. Also, the fabrication process used here is simple and could be applied without the use of masks and special equipment required for photolithography. This fabrication process also has a number of limitations. For example, currently the alignment procedure of the channels on the patterned substrates is facilitated by aligning the PDMS mold on the microstructures. This approach may be cumbersome for complicated patterns that require precise positioning. It is anticipated that the use of micromanipulators could be of benefit in alignment and adhesion of the microfluidic mold with the patterned substrate. Also, there is a potential height barrier for the microstructures since the approach is limited to the elastomeric properties of the PDMS to conform to the height of the polymeric features at the interface of the glass surface and the pattern edge. Therefore, the development of specifically designed patterning stamps that can construct microstructures that can directly fit in the channel may help alleviate this problem.

## **CONCLUSIONS**

In conclusion, we have shown that PEG-based microstructures can be used to immobilize cells within microchannels, potentially an important tool for the development of cell-based biosensors and analytical devices. In addition, a method of generating microstructures inside robust microchannels was introduced capable of forming microwells with exposed or non-exposed substrates using simple modifications to the fabrication process. While both exposed and non-exposed microstructures allowed for stable docking and analysis of cells, only microwells with exposed substrates facilitated cell anchorage.

## REFERENCES

- (1) Andersson, H., van den Berg, A. Microfluidic devices for cellomics: a review. *Sensors and Actuators B-Chemical*, **92**, 3, 2003.
- (2) Li, P. C., Harrison, D. J. Transport, manipulation, and reaction of biological cells on-chip using electrokinetic effects. *Anal Chem*, **69**, 8, 1997.
- (3) Dittrich, P. S., Schuille, P. An integrated microfluidic system for reaction, high-sensitivity detection, and sorting of fluorescent cells and particles. *Anal Chem*, **75**, 21, 2003.
- (4) McClain, M. A., Culbertson, C. T., Jacobson, S. C., Allbritton, N. L., Sims, C. E., Ramsey, J. M. Microfluidic devices for the high-throughput chemical analysis of cells. *Anal Chem*, **75**, 21, 2003.
- (5) McClain, M. A., Culbertson, C. T., Jacobson, S. C., Ramsey, J. M. Flow cytometry of *Escherichia coli* on microfluidic devices. *Anal Chem*, **73**, 21, 2001.
- (6) Roper, M. G., Shackman, J. G., Dahlgren, G. M., Kennedy, R. T. Microfluidic chip for continuous monitoring of hormone secretion from live cells using an electrophoresis-based immunoassay. *Anal Chem*, **75**, 18, 2003.
- (7) Jeon, N. L., Baskaran, H., Dertinger, S. K. W., Whitesides, G. M., Van de Water, L., Toner, M. Neutrophil chemotaxis in linear and complex gradients of interleukin-8 formed in a microfabricated device. *Nature Biotechnology*, **20**, 8, 2002.
- (8) Borenstein, J. T., Terai, H., King, K. R., Weinberg, E. J., Kaazempur-Mofrad, M. R., Vacanti, J. P. Microfabrication technology for vascularized tissue engineering. *Biomedical Microdevices*, **4**, 3, 2002.
- (9) Takayama, S., McDonald, J. C., Ostuni, E., Liang, M. N., Kenis, P. J. A., Ismagilov, R. F., Whitesides, G. M. Patterning cells and their environments using multiple laminar fluid flows in capillary networks. *Proc Natl Acad Sci U S A*, **96**, 10, 1999.

- (10) Khademhosseini, A., Suh, K. Y., Jon, S., Chen, G., Eng, G., Yeh, J., Langer, R. A soft lithographic approach for fabricating patterned microfluidic channels. *Analytical Chemistry*, **76**, 13, 2004.
- (11) Heo, J., Thomas, K. J., Seong, G. H., Crooks, R. M. A microfluidic bioreactor based on hydrogel-entrapped *E. coli*: Cell viability, lysis, and intracellular enzyme reactions. *Analytical Chemistry*, **75**, 1, 2003.
- (12) Liu, V. A., Bhatia, S. N. Three-dimensional photopatterning of hydrogels containing living cells. *Biomedical Microdevices*, **4**, 4, 2002.
- (13) Fisher, A. B., Chien, S., Barakat, A. I., Nerem, R. M. Endothelial cellular response to altered shear stress. *Am J Physiol Lung Cell Mol Physiol*, **281**, 3, 2001.
- (14) Yang, M., Li, C. W., Yang, J. Cell docking and on-chip monitoring of cellular reactions with a controlled concentration gradient on a microfluidic device. *Anal Chem*, **74**, 16, 2002.
- (15) Revzin, A., Russell, R. J., Yadavalli, V. K., Koh, W. G., Deister, C., Hile, D. D., Mellott, M. B., Pishko, M. V. Fabrication of poly(ethylene glycol) hydrogel microstructures using photolithography. *Langmuir*, **17**, 18, 2001.
- (16) Koh, W. G., Revzin, A., Pishko, M. V. Poly(ethylene glycol) hydrogel microstructures encapsulating living cells. *Langmuir*, **18**, 7, 2002.
- (17) Koh, W. G., Itle, L. J., Pishko, M. V. Molding of hydrogel multiphenotype cell microstructures to create microarrays. *Analytical Chemistry*, **75**, 21, 2003.
- (18) Zhan, W., Seong, G. H., Crooks, R. M. Hydrogel-based microreactors as a functional component of microfluidic systems. *Analytical Chemistry*, **74**, 18, 2002.
- (19) Kim, Y. S., Suh, K. Y., Lee, H. H. Fabrication of three-dimensional microstructures by soft molding. *Appl Phys Lett*, **79**, 14, 2001.
- (20) Suh, K. Y., Kim, Y. S., Lee, H. H. Capillary force lithography. *Adv Mater*, **13**, 18, 2001.

- (21) Suh, K. Y., Seong, J., Khademhosseini, A., Laibinis, P. E., Langer, R. A simple soft lithographic route to fabrication of poly (ethylene glycol) microstructures for protein and cell patterning. *Biomaterials*, **15**, 3, 2004.
- (22) Khademhosseini, A., Jon, S., Suh, K. Y., Tran, T. N. T., Eng, G., Yeh, J., Seong, J., Langer, R. Direct Patterning of protein- and cell-resistant polymeric monolayers and microstructures. *Advanced Materials*, **15**, 23, 2003.

## 8. Cell docking inside microwells within reversibly sealed microfluidic channels for fabricating multiphenotype cell arrays

### INTRODUCTION

In previous chapters of this section we described methods of using surface patterning and topographical features inside microchannels to localize and capture cells. In this chapter, we build on this principle to develop new arrays of cells with enhanced functionalities over cell arrays that were presented in Sections 1 and 2. The need for such functional cell arrays comes from the demand for screening the effects of individual or combinations of biochemical signals on multiple cell types in a highly parallel manner. Current methods to perform such experiments are expensive and limited in the number of tests that can be performed. For example, commonly used methods for high-throughput analysis involve the use of multi-well plates (i.e., 384 or 96 well plates) that are operated using cumbersome manual or expensive robotics based operations<sup>1-3</sup>. Therefore, developing technologies that can perform such tasks cheaper, easier, and in a more high-throughput manner may be beneficial in many applications.

Microscale approaches such as cellular micropatterning<sup>4,5</sup> and microfluidics<sup>6,7</sup> hold great promise to perform high throughput experimentation. Recently, methods to simultaneously test different extracellular matrix proteins or synthetic materials on the behavior of embryonic stem (ES) cells have been elegantly demonstrated through the use of robotic based surface deposition<sup>8,9</sup>. In these approaches, an array of adhesive regions, each containing a unique extracellular material, was tested for their ability to direct the differentiation of ES cells. Aside from testing various stimuli on the same cell type, it is potentially important to test the effect on multiple cell types. Previous approaches to fabricate multiphenotype arrays involved a number of technique such as patterned co-cultures<sup>10-13</sup> and capturing cells within photocrosslinking<sup>14</sup> or natural<sup>15</sup> polymers. In patterned co-cultures, two cell types are positioned relative to each other, either by using selective adhesion of one cell type relative to the other to a patterned substrate<sup>10, 11, 13</sup> or by using the reversible adhesive properties of the substrate to position a cell type relative to the other cell type<sup>12</sup>. Patterned co-cultures are useful for controlling homotypic and heterotypic cell-cell interactions and enhancing the function of cell types that are hard to maintain *in vitro* (such as hepatocytes) through introduction of support cells that provide the signals to maintain these cells in culture.

However, most patterned co-cultures to date only employ two cell types patterned relative to each other. Although micropatterning and microfluidics are useful for controlling the microenvironment and probing cellular interactions in cell culture, techniques for co-culture based on those two platforms are needed. One such approach involves immobilization of cells within photocrosslinkable hydrogels using an injection molding technique<sup>14</sup>. Such systems have been used to pattern multiple cell types on a two dimensional substrate. Despite the significant capability of this approach, some potential challenges include the use of toxic photoinitiators and radiation to immobilize the cells inside the channels<sup>16</sup> and the need for expensive photolithographic patterning equipment. Also, by photocrosslinking the cells in a hydrogel, it is harder to retrieve the cells for subsequent analysis.

In Chapters 6 and Chapter 7 it was demonstrated that cells can be immobilized within microfluidic channels either on adhesive patterned regions<sup>17</sup> or within microstructures with regions of low shear stress<sup>18</sup>. In order to facilitate the fabrication of robust microdevices, PDMS molds were irreversibly sealed onto the substrates. However, the reversible sealing of PDMS on microfluidic molds on a substrate is a powerful approach to sequentially pattern surfaces or to deliver fluids sequentially to various spots on a two-dimensional substrate<sup>19</sup>.

Here, an approach to fabricate arrays of many different cell types is introduced that combines the ability to reversibly seal microfluidic channels on patterned substrates with the ability to capture cells in shear protected regions of microfluidic channels. The technique can be efficiently used to pattern multiphenotype cellular arrays on two-dimensional substrates or within individual microchannels. This was accomplished by a multi-step method. Initially, two PDMS molds containing either the microchannels or the microwells were fabricated and subsequently reversibly sealed to each other so that the microwells were positioned within the channels. Each cell type was flowed through a unique microchannel, and deposited onto the microwells within that channel. After the cells have filled the wells, the microfluidics mold was peeled from the substrate, while ensuring that the cells remained within the microwells, which generated a patterned array of multiple cell types. In order to facilitate high-throughput delivery of reagents to the various cell types, a secondary PDMS mold could be subsequently aligned orthogonal to the direction of the first array of channels. In this approach, each microwell on the substrate

could potentially be used to perform a separate experiment. Furthermore, microfluidic gradient generators upstream from the array of channels could be used to lower the number of independent inlets required and facilitate the delivery of a higher number of solutions to the various cell types.

## **MATERIALS AND METHODS:**

*Fabrication of PDMS microfluidic molds and stamps:* PDMS stamps and microfluidic molds were fabricated by casting PDMS (Sylgard 184 Silicon elastomer, Essex Chemical) against a complementary relief structure as previously described<sup>12, 18, 20</sup>. Two patterns were generated: a 5x5 array of circles of 75  $\mu\text{m}$  in diameter, and an array of 5 channels with an individual channel width of 150  $\mu\text{m}$ . These masks were subsequently used to generate a pattern of 80  $\mu\text{m}$  high SU-8 photoresist on silicon wafers using contact photolithography to generate a negative ‘master.’ Positive replicas were fabricated by molding PDMS by curing the prepolymer (a mixture of 10:1 silicon elastomer and the curing agent) on the silicon masters at 70°C for 2 hours. The PDMS mold was then peeled from the silicon wafer and cut prior to use. The stamps had protruding (positive) features that were used to fabricate replicate microfluidic molds or patterned microwells.

For each array of microchannels, holes were drilled through the inlets and the outlet. For the inlets, independent reservoirs measuring about 3mm in diameter were cut. Metal tubing was inserted into the outlet, sealed with epoxy, and connected to a piece of plastic tubing. This PDMS microchannel assembly was plasma cleaned for 30-45 seconds along with a 5x5 well patterned PDMS mold. The PDMS microchannels were manually aligned on the 5x5 PDMS substrates under a microscope, and were reversibly bound through bringing the two surfaces into contact and applying pressure. In some experiments, plasma treatment was limited to the regions of the PDMS molds immediately surrounding the microwell or microchannel arrays. This was done by covering the rest of the substrate with a reversibly sealed piece of PDMS. This process allowed the channels and the wells to be hydrophilic while allowing the rest of the substrate to remain hydrophobic.

*Cell cultures:* All cells were manipulated under sterile tissue culture hoods and maintained in a 5% CO<sub>2</sub> humidified incubator at 37°C. Cell lines were purchased from Advanced Type Culture



Collection (ATCC), and cell culture reagents were purchased from Gibco Invitrogen Corp. unless otherwise stated. Saos-2 and NIH-3T3 murine embryonic fibroblasts were maintained in Dulbecco's modified eagle medium (DMEM) supplemented with 10% fetal bovine serum (FBS). Once the cells were confluent, they were trypsinized (0.25% in EDTA, Sigma) and passaged at a 1:5 subculture ratio. AML12 murine hepatocytes were maintained in a medium comprised of 90% 1:1 (v/v) mixture of DMEM and Ham's F12 medium with 0.005 mg/mL insulin, 0.005 mg/mL transferrin, 5 ng/mL selenium, and 40 ng/mL dexamethasone, and 10% FBS. Confluent dishes of AML12 and NIH-3T3 cells were passaged and fed every 3-4 days. Murine embryonic stem (ES) cells (R1 strain) were maintained on gelatin treated dishes in 15% ES-qualified FBS in DMEM knockout medium. ES cells were fed daily and passaged every 3 days at a subculture ratio of 1:4. The prostate PC3 cell line was cultured in RPMI-1640 and Ham's F12K medium, respectively, supplemented with 100 U/ml aqueous Penicillin G, 100 µg/ml Streptomycin, and 10% fetal bovine serum. Confluent culture flasks were passaged every 4 days.

*Reversible sealing and cell docking:* To fabricate the device, the PDMS microfluidic mold was aligned under a microscope on the array of wells so that each row of wells was centered within the channels. Once the two PDMS pieces of PDMS were reversibly sealed, cells were deposited in the five inlet reservoirs and flown through the channels under negative pressure. The outlet was connected to a syringe pump (New Era Pump Systems Inc.) by polyethylene tubing, and the flow was regulated by operating the pump under either positive or negative pressures. To minimize the formation of bubbles within the microwells, ethanol was flowed through the channels at >10 µl/min, followed by a PBS wash. The channels were tested for leakage by flowing a visible dye such as Trypan blue in alternating lanes under negative pressure at 5-10 µl/min. To seed the cells, 25-50 µl of each cell suspension ( $3 \times 10^7$  cells/ml) was deposited in the inlet reservoir of a unique microchannel and flowed through the channel at a flowrate of 2-5 µl/min under negative pressure. In most experiments, negative pressures applied at the outlet were used in order to eliminate leakage and the need for multiple syringe pumps. To sediment the cells into the microwells, the flow was stopped for 10 min. Excess cells were removed by aspirating the cells from the inlet reservoir with a pipette, and flowing medium through the channel at flowrate of 5 µl/min. Once the cells were captured in the wells, the PDMS molds were put into a PBS bath, and the microfluidic mold was gently peeled from the substrate. This step

was required in most cases where the cells had not adhered within the channels to ensure that the cells remained in the wells, which resulted in the formation of multiphenotype cell arrays.

To allow the delivery of multiple fluids to the patterned cells, PDMS molds were subsequently placed on the aligned cells. In this process, the PDMS mold containing the multiphenotype cell arrays was dried in regions around the microwell array. Subsequently another PDMS microfluidic mold containing an array of channels was aligned and pressed onto the substrate, forming a secondary PDMS mold.

*Cell tracking and viability:* To stain with the cellular dye SYTO, cells were trypsinized and washed with DMEM medium without serum, and subsequently suspended at a concentration of  $1 \times 10^7$  cells/ml and incubated for 4 min at room temperature. To stain with carboxyfluorescein diacetate succinimidyl ester (CFSE) dye, cells were suspended in 10 mg/ml CFSE in PBS solution at a concentration of  $1 \times 10^7$  cells/ml and incubated for 10 min at room temperature. Both staining reactions were quenched with the addition of an equal volume of DMEM supplemented with 10% FBS and washed. To analyze cellular viability, a live/dead assay was performed by flowing ethidium homodimer and calcein AM dissolved at 1 mg/mL in DMEM containing 10% FBS through the channel for 20 min. PBS was then flowed through the channel to remove excess/non-specific staining.

*Contact angle measurements:* Static contact angles were measured with the system A Ramé-Hart goniometer (Mountain Lakes) equipped with a video camera was used to measure the static contact angles on drops of  $\sim 3 \mu\text{L}$  in volume. Reported values represent averages of at least 6 independent measurements.

## RESULTS AND DISCUSSION

### Approach

A novel technique to fabricate multiphenotype cell arrays is presented. This approach utilizes three distinct concepts (**Figure 8.1**): 1) capturing cells within microstructures that contain low shear stress regions; 2) reversibly sealing elastomeric molds onto patterned substrates; and 3)

orthogonally placing a series of microchannel arrays to deliver a unique set of fluids to particular ‘spots’ on a two-dimensional surface.

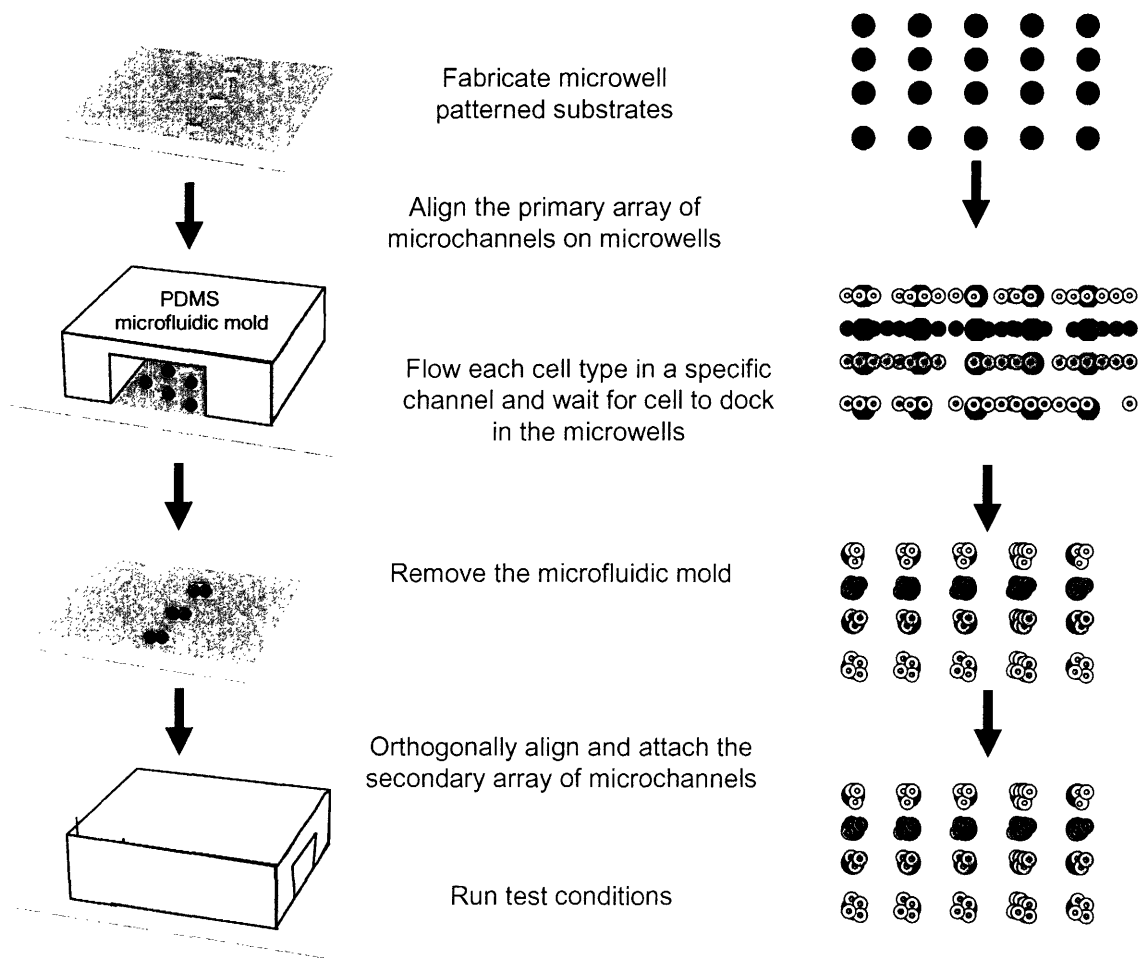


Figure 8.1. Schematic diagram of reversible sealing of microfluidic arrays onto microwell patterned substrates to fabricate multiphenotype cell arrays. Initially, a PDMS microfluidic array was aligned on an array of microwells. As each cell type flowed through an independent channel, they docked onto the microwells, which resulted in a patterned array of cells upon removal of the PDMS microfluidic mold. To deliver multiple solutions, a secondary array of channels could be orthogonally placed to create multiphenotype cell arrays inside each microchannel.

We have previously shown that cells can be captured within PEG microstructures and remain shear protected inside a variety of microstructures<sup>18</sup>. This approach provides a number of potential advantages for the fabrication of cell arrays, such as topographical height as a barrier to localize cells in particular spots on the arrays and the ability to pattern cells without the need for slow ‘cell adhesive’ processes. Also, the presence of microstructures allows for capturing multiple cells, in the form of aggregates which mimics the three-dimensional architecture of cell

structures *in vivo*. These low shear stress microwells could be formed with a protein coated or non-adhesive surfaces thus making them useful for both anchorage dependant or anchorage independent cell types.

### **Reversible sealing on patterned arrays of microwells**

Although the irreversible sealing is desired for devices comprised of static microchannels, reversibly sealed microchannels have been shown to be useful for a variety of applications such as surface patterning<sup>19, 21, 22</sup>. Furthermore, using the ability to multiple sets of channels it is possible to pattern complex patterns. Here, the cells were flowed through channels that had been reversibly sealed onto a substrate containing microwells.

To test the reversible sealing properties of PDMS molds both microwell patterned substrates and microfluidic molds were made from PDMS that was molded onto a master that was made from SU8 patterned onto silicon wafers. In most cases, unmodified PDMS substrates were used. Under these conditions PDMS-PDMS interactions were reversible. Here we used this property to immobilize multiple cell types onto microwell filled surfaces and then removed the mold. We found that reversibly sealed microchannels frequently leaked even under low positive pressures and flow rates of  $\sim 1$   $\mu\text{l}/\text{min}$  across the channel. To alleviate this problem, we used negative suction head by drawing the liquid from a common outlet on the microchannel arrays. As can be seen in **Figure 8.2**, this setup eliminated leaking from the channels for both primary channels (**Figure 8.2a-b**) and subsequently placed PDMS channels (**Figure 8.2c**). Furthermore, by having a common outlet, a single syringe and pump assembly was sufficient to regulate the fluid flow through many channels. To enhance sealing of the channels, clamps could also be used. However, with the use of negative suction head (i.e. syringe pump drawing fluid from a common outlet) the need for clamping was minimized.

In some instances, the surface of microchannels was modified using a variety of surface modification approaches. For example the surfaces were oxygen plasma treated to make the channels more hydrophilic or change the surface protein or cell adhesive properties. To make the PDMS surfaces cell and protein repellent, a silane-based anchoring PEG polymer (TMSMA-r-PEGMA) was flowed in the channels, which spontaneously formed a polymeric monolayer on

plasma treated PDMS surfaces<sup>20, 23</sup>. The PEG surface modification could be performed in these channels without modifying the leaking properties and could be used to reduce protein adhesion of up to 98 % and cell adhesion of up to 99 %<sup>24</sup>.

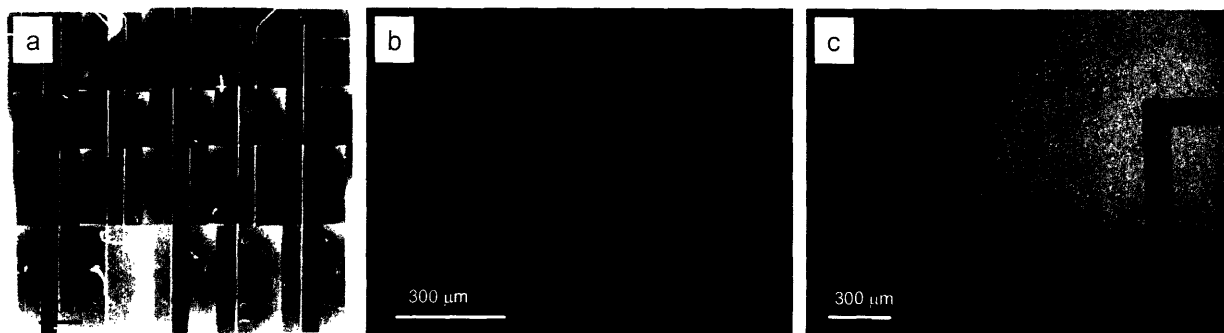


*Figure 8.2. Leak-proof reversibly sealed microfluidic channels. (a-b) represent the reversible sealing of a primary PDMS microfluidic mold on an array of wells while (c) represents the reversible sealing of a secondary array of channels on a substrate that was previously sealed. In figures (a) and (c) Trypan blue and PBS were flowed in alternating channels. In figure (b) red (rhodamine) and green (FITC) dyes in PBS (10  $\mu\text{g}/\text{mL}$ ) were flowed through the channels. The dye solutions do not leak, indicating that the primary and secondary sealing of PDMS / PDMS could be performed. Note: Figure (a) is a combined series of pictures to capture the entire microfluidic device.*

Alternatively, microwells were fabricated from photo-crosslinkable PEGMA and the microfluidic molds were directly immobilized onto PEG cured surfaces. When photocrosslinkable PEG fabricated devices were used to create a reversible seal, significant leaking was observed. This was caused by the permeability of PEG microstructures to water, which allowed the water to penetrate the substrates and move from one channel into the surrounding channels.

Another issue regarding the formation of PDMS based microchannels is the retention of bubbles within the channels. Since PDMS is typically hydrophobic and even under plasma oxidation does not become fully hydrophilic as measured by contact angles of  $73^\circ \pm 1^\circ$  and  $51^\circ \pm 2^\circ$  respectively, air bubbles can be captured within the microchannels. To solve this problem we devised a method of first flowing ethanol inside the channels to fill the microwells and then fill the channels with water. The ethanol has a lower surface contact angle either without ( $33^\circ \pm 2^\circ$ ) or with ( $15^\circ \pm 0.5^\circ$ ) oxygen plasma treatment, which allows it to wet the surface and fill the microwells. Once the initial surface wetting has occurred, the subsequent flow of medium and PBS will not cause bubble formation.

### **Delivery of reagents by serially placing microchannel arrays orthogonally on substrates**

Here, we demonstrated that the sequential alignment and removal of two arrays of microchannels orthogonally placed relative to each other on microwell patterned substrates could be used to fabricate a high throughput device. For example, if the first mold has M channels and the second mold has N channels the ability to expose each region at their intersection allows M x N unique testing conditions. Although more complicated channel designs using this sequential placement of microfluidic molds on patterned substrates could be envisioned, this linear microchannel array seems promising for its simplicity and ease of use in that the same microfluidic mold rotated 90° could be used as the secondary mold.

As a proof of concept, we designed a PDMS array of five parallel channels with independent inlets and a common outlet (**Figure 8.2a**). Complementary to this design, we built an array of 25 microwells which we placed directly underneath the microchannels when the two molds are aligned.

### **Fabrication of multiphenotype cell arrays**

To demonstrate that multiphenotype cell arrays could be generated, we used a variety of cell lines including murine embryonic stem (ES) cells, osteoblasts (Saos-2), hepatocytes (AML12), fibroblasts (NIH-3T3) and human prostate cells (PC3 cells) as model cells. Once the device was fabricated, the cells were stained with cell membrane dyes CFSE and SYTO which shows up as green and red respectively under fluorescence. After prefilling with medium and reversibly sealing, each cell type was loaded into the reservoir at the inlet of one of the channels. The stream of flowing fluid carried the cells in the channels where they could be deposited onto the low shear stress confinements within the microwells. As can be seen in **Figure 8.3**, the cells were captured within the microwells. All cell types, independent of source (human or mouse) or organ of origin, could be deposited within the microchannels. Although in most experiments cells remained in suspension, the ability to capture cells and allow for adhesion and spreading of cells at the bottom of the microwell will allow for the formation of multiphenotype arrays of adherent cell types. In order to seed the cells, the cells were either captured from the moving

fluid<sup>18</sup> or the fluid was stopped for <10 minutes to facilitate docking of the cells within the microchannels.

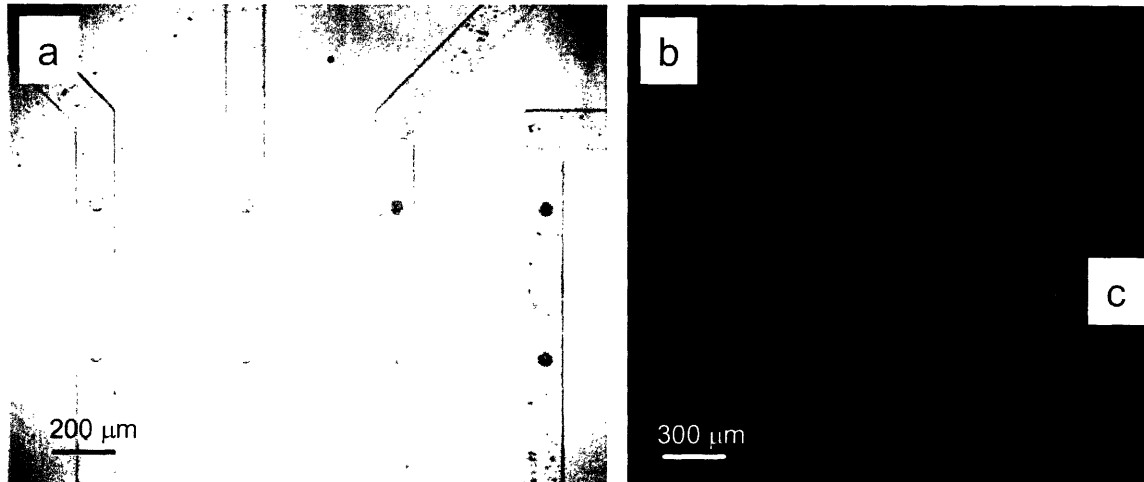


*Figure 8.3. Cell docking within microchannel arrays. Figure (a) represents the light microscopy image of ES cells flowing within an array of microchannels. Figure (b) is the fluorescent image of cells (right to left: ES / AML12 / Saos-2 / PC3 / NIH-3T3 cells) labeled with membrane dyes CFSE (green) and SYTO (red) as they flow through the channels. (c) Once the cells docked in the microwells, a cell-free solution was flowed through the channels to remove non-captured cells.*

Furthermore, the microfluidic channels could be used to fabricate multiphenotype cell arrays (**Figure 8.4**). The arrays could be fabricated either on two-dimensional surfaces (**Figure 8.4b**) or within microfluidic channels (**Figure 8.4c**). To fabricate the multiphenotype cell arrays on two dimensional substrates, cells were flowed in the channels and allowed to dock into the channels. Afterwards, the microfluidic PDMS mold could be removed. To ensure that the cells remained within the microstructures, the PDMS mold was carefully and slowly removed. The removal and the placement of subsequent molds is a delicate process that requires a balance between keeping the cells in a wet environment while allowing for the two PDMS pieces to adhere to each other under normal conditions.

Cells that were put throughout the docking process and the subsequent sealing of secondary microfluidic molds remained viable as measured based on their ability to exclude ethidium homodimer or metabolize ethidium homodimer. A live/dead stain was flown through channels of

unstained cells. The cells remained alive as marked by the green color. In addition the cells adhered to the wells as further indication that the cells remained alive during the process.

Through making use of the reversible adhesion between the PDMS microchannels and the underlying PDMS patterned microstructured substrate, multiple cell types were simultaneously probed with multiple probes. After the first channel was successfully removed, the cells remained immobilized within the wells. A secondary set of channels was aligned perpendicular to the first microfluidic channel set, and test solutions were flowed through each channel. As visualized in **Figure 8.3**, the new channels also did not leak, and maintained isolated channel environments.

### **Potential problems and future directions**

Our approach of docking cells within microstructures is an improved method of capturing cells inside microwells of variety reasons. Although it is possible to fabricate multiphenotype cell arrays on surfaces that are patterned by flowing the cells through an array of channels and waiting for them to adhere to the patterned regions, such approaches are cumbersome and could be difficult to employ practically. Another potential advantage of using the microwells to capture and immobilize cells is that the cells would be in a structure that is ‘sticking in’ the substrate. This allows the microfluidic mold to be realigned and moved without disturbing the cells, as would not be expected if the cells were adhered onto a flat surface or immobilized inside hydrogels.

One potential limitation of using microfluidic arrays for high throughput experimentation is the connection between the array of microchannels to macroscopic inputs. To reduce the number of independent inlets we integrated a variety of approaches such as the use of orthogonally placed array of channels. To further reduce such limitations we integrated microfluidic mixers that have been previously used to generate concentration gradients<sup>25, 26</sup> upstream from the array of channels. In these mixers a series of mixing and merging steps create various combinations of the inlet streams. As it can be seen in **Figure 8.5**, by using the upstream gradient generator, two independent inlets could give rise to a number of channels with a linear mixture of the two streams. For example, a decreasing concentration of a dye could be created on channels



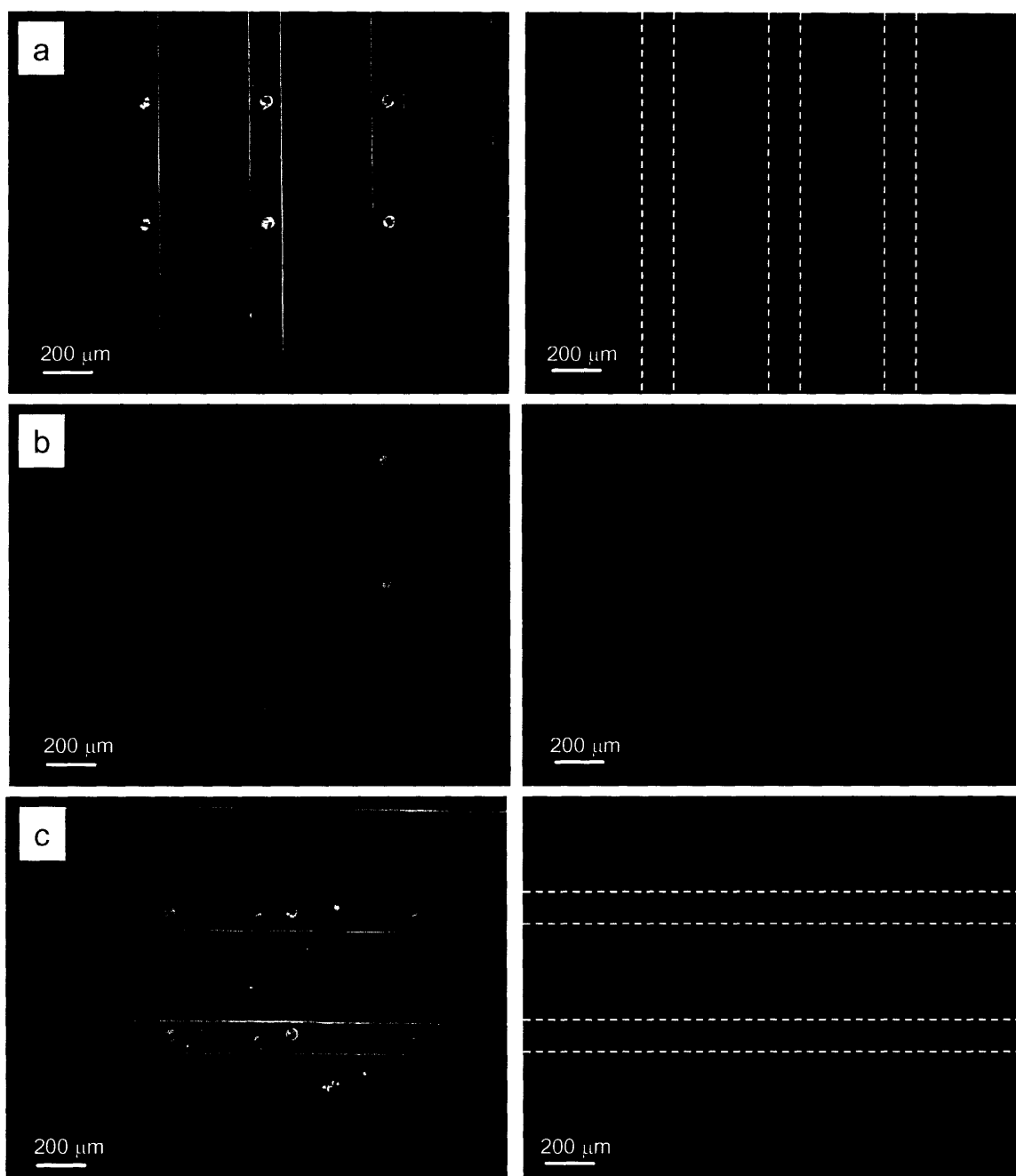
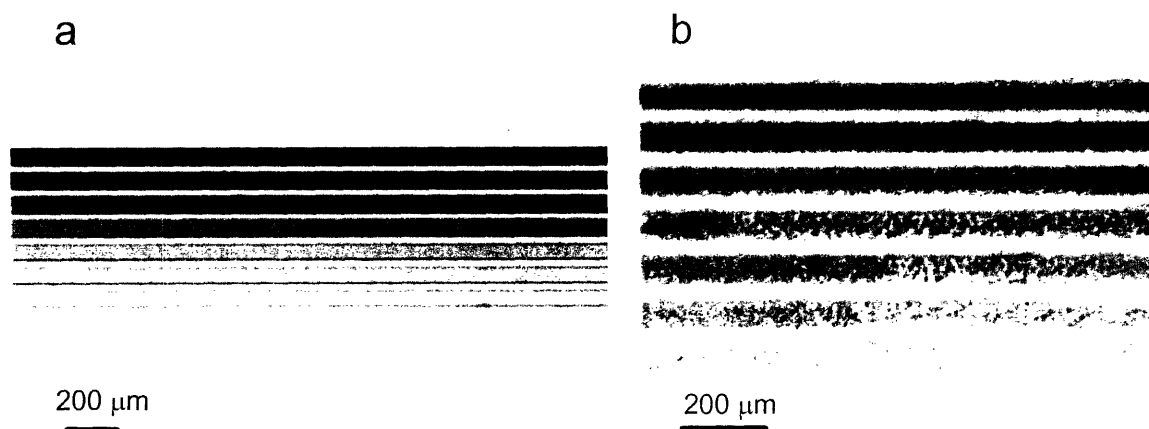


Figure 8.4. Formation of multi-phenotype cell arrays on two-dimensional substrates or within microfluidic channels. Figures (a-c) show the light and fluorescent microscope images of the steps required in fabricating multiphenotype arrays. The fluorescent images are those of various cell types stained with two membrane dyes, CFSE(green) and SYTO(red) (right to left: ES / AML12 / NIH-3T3 cells). (a) Each cell type is allowed to dock within microwells inside a microchannel. (b) The cells remain stable inside the microwells even after the PDMS mold is removed, giving rise to multiphenotype cell arrays. (c) Subsequently, microchannels were aligned orthogonally and reversibly sealed on patterned substrates, resulting in channels that contained a variety of cell types.

reversibly sealed on PDMS substrates with or without cells. These and other types of upstream modifications, such as the integration of fluidic valves, could further enhance the throughput of these devices by minimizing the number of independent inlets that are required to perform a large number of experiments.



*Figure 8.5. Microfluidic arrays with upstream microfluidic mixers. To lower the number of independent inlets into the device, micromixers could be incorporated upstream from the microchannel arrays. (a) Represents experiments in which a concentration gradient is generated on an array of channels and figure (b) an array of channels immobilized on a monolayer of NIH-3T3 cells.*

The reversible sealing properties of PDMS molds provide a powerful tool since it allows the integration of microchannels on patterned substrates. Although the seal is sufficient for low flowrates, research in making systems that can be operated under a variety of flow regimes may be beneficial. Future approaches for creating a robust reversibly sealed PDMS / substrate bonding may include making the surfaces surrounding the microfluidic channels hydrophobic. The hydrophobic surfaces can be used to minimize fluid retention during the conformal contact between the substrate and the PDMS mold. Alternatively, negative pressure (i.e. vacuum) systems could be used to hold the PDMS onto the substrate. It is anticipated that the use of these approaches could dramatically increase the bonding strength of the channels onto the substrate.

## **CONCLUSIONS**

In summary, a technique was developed based on reversible sealing of PDMS molds onto microwell patterned substrates to form multiphenotype cell arrays. Arrays of various mouse and human cell types were prepared by flowing a distinct cell type inside each microchannel. By allowing the cells to dock onto low shear stress regions and by subsequently removing the PDMS microfluidic mold, multiphenotype cell arrays were formed either on two-dimensional surface. The subsequent alignment and reversible attachment of orthogonally oriented array of channels facilitated the formation of multiphenotype cell arrays inside microchannels. This technique could enable a whole new class of investigations in which cell-cell interactions can be probed. In addition, this technique could have potential applications in high throughput screening or optimization of cell-soluble signal interactions for understanding biology or tissue engineering.

## REFERENCES

- (1) Chen, S. B.,Zhang, Q. S.,Wu, X.,Schultz, P. G.,Ding, S. Dedifferentiation of lineage-committed cells by a small molecule. *Journal of the American Chemical Society*, **126**, 2, 2004.
- (2) Wu, X.,Ding, S.,Ding, G.,Gray, N. S.,Schultz, P. G. Small molecules that induce cardiomyogenesis in embryonic stem cells. *Journal of the American Chemical Society*, **126**, 6, 2004.
- (3) Wu, X.,Ding, S.,Ding, Q.,Gray, N. S.,Schultz, P. G. A small molecule with osteogenesis-inducing activity in multipotent mesenchymal progenitor cells. *Journal of the American Chemical Society*, **124**, 49, 2002.
- (4) Cheng, J.,Fortina, P.,Surrey, S.,Kricka, L. J.,Wilding, P. Microchip-based Devices for Molecular Diagnosis of Genetic Diseases. *Mol Diagn*, **1**, 3, 1996.
- (5) Bhatia, S. N.,Toner, M.,Tompkins, R. G.,Yarmush, M. L. Selective Adhesion of Hepatocytes on Patterned Surfaces. *Biochemical Engineering VIII*, **745**, 1994.
- (6) McClain, M. A.,Culbertson, C. T.,Jacobson, S. C.,Allbritton, N. L.,Sims, C. E.,Ramsey, J. M. Microfluidic devices for the high-throughput chemical analysis of cells. *Anal Chem*, **75**, 21, 2003.
- (7) King, K. R.,Wang, C. C. J.,Kaazempur-Mofrad, M. R.,Vacanti, J. P.,Borenstein, J. T. Biodegradable microfluidics. *Advanced Materials*, **16**, 22, 2004.
- (8) Anderson, D. G.,Levenberg, S.,Langer, R. Nanoliter-scale synthesis of arrayed biomaterials and application to human embryonic stem cells. *Nat Biotechnol*, **22**, 7, 2004.
- (9) Flaim, C. J.,Chien, S.,Bhatia, S. An extracellular matrix microarray for probing cellular differentiation. *Nat Methods*, **2**, 2005.
- (10) Bhatia, S. N.,Balis, U. J.,Yarmush, M. L.,Toner, M. Probing heterotypic cell interactions: hepatocyte function in microfabricated co-cultures. *J Biomater Sci Polym Ed*, **9**, 11, 1998.
- (11) Bhatia, S. N.,Balis, U. J.,Yarmush, M. L.,Toner, M. Microfabrication of hepatocyte/fibroblast co-cultures: role of homotypic cell interactions. *Biotechnol Prog*, **14**, 3, 1998.

- (12) Khademhosseini, A., Suh, K. Y., Yang, J. M., Eng, G., Yeh, J., Levenberg, S., Langer, R. Layer-by-layer deposition of hyaluronic acid and poly-L-lysine for patterned cell co-cultures. *Biomaterials*, **25**, 17, 2004.
- (13) Bhatia, S. N., Yarmush, M. L., Toner, M. Controlling cell interactions by micropatterning in co-cultures: hepatocytes and 3T3 fibroblasts. *J Biomed Mater Res*, **34**, 2, 1997.
- (14) Koh, W. G., Itle, L. J., Pishko, M. V. Molding of hydrogel microstructures to create multiphenotype cell microarrays. *Anal Chem*, **75**, 21, 2003.
- (15) Tang, M. D., Golden, A. P., Tien, J. Molding of three-dimensional microstructures of gels. *Journal of the American Chemical Society*, **125**, 43, 2003.
- (16) Liu, V. A., Bhatia, S. N. Three-dimensional photopatterning of hydrogels containing living cells. *Biomedical Microdevices*, **4**, 4, 2002.
- (17) Khademhosseini, A., Suh, K. Y., Jon, S., Chen, G., Eng, G., Yeh, J., Langer, R. A soft lithographic approach for fabricating patterned microfluidic channels. *Analytical Chemistry*, **76**, 13, 2004.
- (18) Khademhosseini, A., Yeh, J., Jon, S., Eng, G., Suh, K. Y., Burdick, J. A., Langer, R. Molded polyethylene glycol microstructures for capturing cells within microfluidic channels. *Lab Chip*, **4**, 5, 2004.
- (19) Delamarche, E., Bernard, A., Schmid, H., Bietsch, A., Michel, B., Biebuyck, H. Microfluidic networks for chemical patterning of substrate: Design and application to bioassays. *Journal of the American Chemical Society*, **120**, 3, 1998.
- (20) Khademhosseini, A., Jon, S., Suh, K. Y., Tran, T. N. T., Eng, G., Yeh, J., Seong, J., Langer, R. Direct Patterning of protein- and cell-resistant polymeric monolayers and microstructures. *Advanced Materials*, **15**, 23, 2003.
- (21) Chiu, D. T., Jeon, N. L., Huang, S., Kane, R. S., Wargo, C. J., Choi, I. S., Ingber, D. E., Whitesides, G. M. Patterned deposition of cells and proteins onto surfaces by using three-dimensional microfluidic systems. *Proc Natl Acad Sci U S A*, **97**, 6, 2000.
- (22) Whitesides, G. M., Ostuni, E., Takayama, S., Jiang, X., Ingber, D. E. Soft lithography in biology and biochemistry. *Annu Rev Biomed Eng*, **3**, 2001.
- (23) Suh, K. Y., Khademhosseini, A., Eng, G., Langer, R. Single nanocrystal arrays on patterned poly(ethylene glycol) copolymer microstructures using selective wetting and drying. *Langmuir*, **20**, 15, 2004.

- (24) Jon, S. Y., Seong, J. H., Khademhosseini, A., Tran, T. N. T., Laibinis, P. E., Langer, R. Construction of nonbiofouling surfaces by polymeric self-assembled monolayers. *Langmuir*, **19**, 24, 2003.
- (25) Jeon, N. L., Baskaran, H., Dertinger, S. K. W., Whitesides, G. M., Van de Water, L., Toner, M. Neutrophil chemotaxis in linear and complex gradients of interleukin-8 formed in a microfabricated device. *Nature Biotechnology*, **20**, 8, 2002.
- (26) Burdick, J. A., Khademhosseini, A., Langer, R. Fabrication of gradient hydrogels using a microfluidics/photopolymerization process. *Langmuir*, **20**, 13, 2004.

## 9. Fabrication of Gradient Hydrogels Using a Microfluidics / Photopolymerization Process

### INTRODUCTION

Cell migration is controlled by gradients of soluble (chemotaxis) and immobilized (haptotaxis) molecules and substrate mechanics (durotaxis)<sup>1,2</sup>. For example, neuron growth cones are guided to various termination sites by gradients of guidance cues<sup>3</sup>. There have been numerous studies to investigate the influence of these gradients of molecules and cues on specific cellular behavior (e.g., migration or axon orientation), but these approaches have relied on complex and experimentally intensive techniques for gradient production<sup>4-6</sup>. Thus, it is of interest to develop techniques to fabricate model substrates that can be used to investigate these complex cell behaviors *in vitro* to provide information that can potentially be used for the development of therapies, such as scaffolding for tissue engineering.

Hydrogels are water swollen polymer networks that are being investigated for drug delivery and tissue engineering<sup>7, 8</sup> due to their biocompatibility and controllable properties (e.g., mechanics and degradation). For instance, poly(ethylene glycol) (PEG) hydrogels are inherently cell repellent (due to poor protein adsorption) and thus, cell interactions with PEG hydrogels are controlled by the incorporation of molecules without non-specific protein adsorption interfering<sup>9</sup>. Additionally, the physical properties of PEG hydrogels are controlled by monomer properties such as the molecular weight of the PEG or the macromer concentration<sup>10</sup> to provide a simple technique to alter the network crosslinking density.

In this chapter a new approach is described that we have utilizes microfluidic based systems incorporating a unique gradient maker channel that can be used to fabricate PEG-based hydrogels with gradients of tethered molecules and hydrogel crosslinking densities.

### METHODS AND MATERIALS

*Materials synthesis:* Poly(ethylene glycol)-4000 diacrylate (PEG-4000DA) and acryloyl-poly(ethylene glycol)-RGDS (Acr-PEG-RGDS) were synthesized as described previously<sup>9,10</sup> and the acrylation efficiency (95%) was confirmed with <sup>1</sup>H-NMR. Briefly, Acr-PEG-RGDS was

synthesized by the reaction of acryloyl-PEG-N-hydroxysuccinimide (3400 Da, Nektar Therapeutics) with GRGDS (Bachem) in 50 mM sodium bicarbonate buffer (pH 8.2) for 2 hours at room temperature. All chemicals were purchased from Aldrich and used as received unless noted otherwise. Macromers were dissolved in phosphate buffered saline (PBS) at desired concentrations and 0.5 wt% hydroxy-2-methyl propiophenone (a water soluble photoinitiator) was added. Glass slides were modified with methacrylate functional groups for immobilization of polymerized hydrogels by immersing slides in a solution of 30%  $\text{H}_2\text{O}_2$  and  $\text{H}_2\text{SO}_4$  (3:1 ratio) for 5 minutes, washing in  $\text{DiH}_2\text{O}$ , immersing in 10 mM 3-(trichlorosilyl)propyl methacrylate (TPM), and washing with heptane/carbon tetrachloride and  $\text{DiH}_2\text{O}$ <sup>11</sup>. Poly(dimethylsiloxane) (PDMS) molds were fabricated by curing prepolymer (Sylgard 184, Essex Chemical) on silicon masters patterned with SU-8 photoresist.

*Microfluidic channel fabrication:* Microfluidic devices were constructed by placing PDMS molds on the TPM slides and plasma cleaning (PDC-001, Harrick Scientific Co.) with the lower portion of the slides covered to aid in future detachment of the mold from the slide after hydrogel formation.

*Synthesis of gradient hydrogels:* The general procedure for gradient hydrogel formation involves the injection of two monomer solutions into a unique gradient maker that consists of a network of microchannels that repeatedly splits and mixes the injected solutions<sup>12</sup>. This channel system was previously used to investigate cell interactions with solution<sup>12</sup> and substrate bound<sup>13</sup> gradients. After passing through the gradient maker, the monomer solutions enter a larger viewing channel, where a stable gradient is formed (visualized with a fluorescent microscope where one monomer solution contained 1 wt% rhodamine) and the solutions are photopolymerized into a hydrogel with ultraviolet light exposure (200 mW / $\text{cm}^2$  for 60 seconds, EXFO Spot Curing System) through the PDMS mold. Although the rhodamine molecule is smaller than the injected PEG macromers, rhodamine fluorescence should give a good estimate of gradient production in the microchannel. The mold is then removed to leave a hydrogel structure (~80  $\mu\text{m}$  in height) immobilized on a glass slide. A similar procedure was used by Pishko and coworkers<sup>14-16</sup> to develop non-gradient hydrogel microstructures.



*Cell culture:* Human umbilical vein endothelial cells (HUVECs, Clonetics) were maintained in endothelial cell basal medium supplemented with the supplied Bulletkit (Clonetics). Upon trypsinization, cells were seeded on the hydrogel microstructures (washed several times in PBS and sterilized with ultraviolet light exposure in a laminar flow hood) at a density of 300 cells/mm<sup>2</sup>. After 3 hours, the hydrogels were rinsed with PBS, fixed in 2.5% glutaraldehyde (Polysciences) for 15 minutes, washed in PBS, and visualized (Zeiss Axiovert 200 inverted microscope). Cells were quantified by counting attached endothelial cells in a minimum of 5 images from 3 individual hydrogels.

*Synthesis and analysis of gels with varying crosslinking density:* Monomer solutions of various macromer concentrations (10 to 50 wt%) and macromer molecular weights (PEG1000 to PEG4000) were used to fabricate hydrogel microstructures with gradients in hydrogel mechanics. Samples were air dried, cut with a scalpel blade to obtain a cross-section, sputter coated with gold, and imaged using a JEOL 6320FV scanning electron microscope. Additionally, the change in crosslinking density across the gradients was visualized and quantified by the diffusion of rhodamine (1 wt%) entrapped in the hydrogel networks during polymerization and released into PBS.

## **RESULTS AND DISCUSSION**

### **Fabrication and characterization of microfluidic channels**

To form concentration gradients microfluidic channels were fabricated and characterized. These channels were capable of generating controllable and stable chemical gradients in channels ranging from 50-2200  $\mu\text{m}$  in width. The shape of these gradients could be directly controlled depending on the properties of the different inlet streams. Within these inlet streams, desired concentration gradients were obtained through sequential mixing and separating of channels within microfluidic networks as previously demonstrated<sup>13</sup>. The shape of the concentration gradient could be controlled from step-like drops to smooth concentration gradients (**Figure 9.1** and **Figure 9.2**).

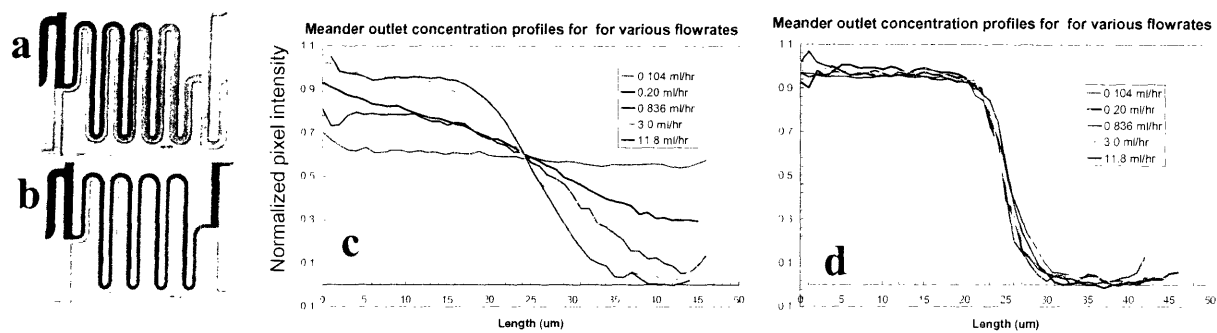


Figure 9.1 The effects of flow rates on the mixing properties of tracer dye within each channel. Figures (a-b) are micrographs of meanders in the gradient generator under flow rates of (a) 0.104, (b) 11.8 mL/hr respectively. As it can be seen at flow rates of 0.104 mL/hr, or lower, the solution leaving each meander is fully mixed. Figures c and d quantitatively show the inlet and outlet concentration profiles.

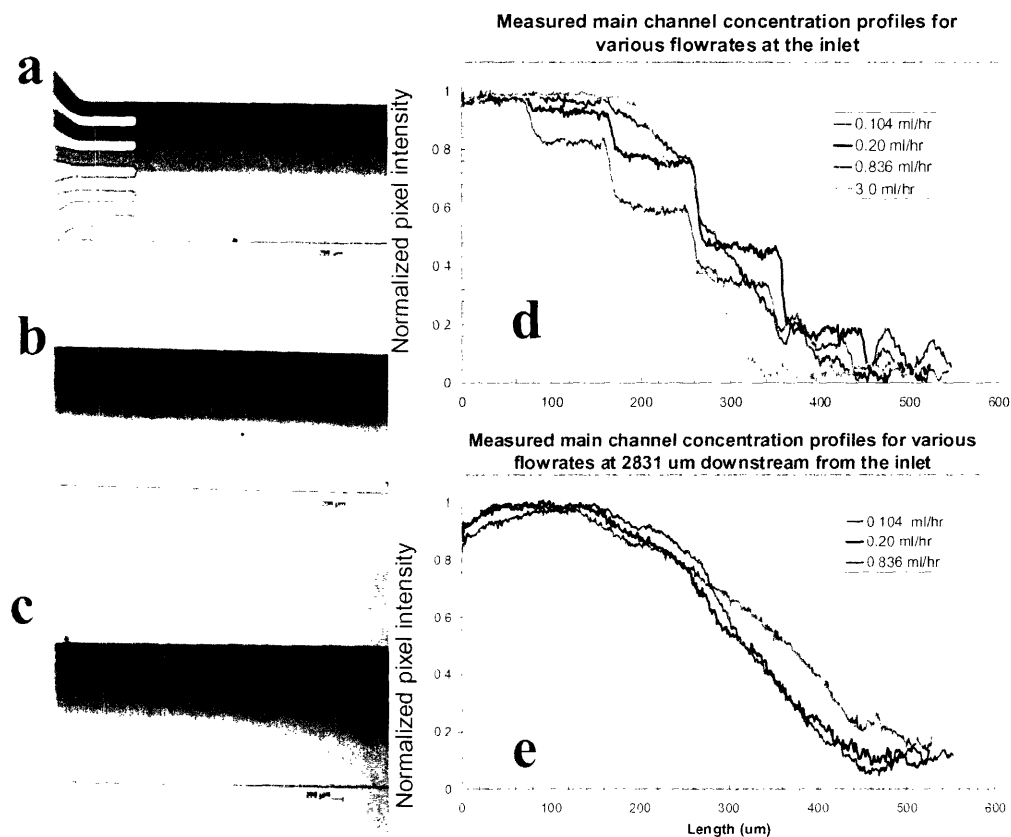
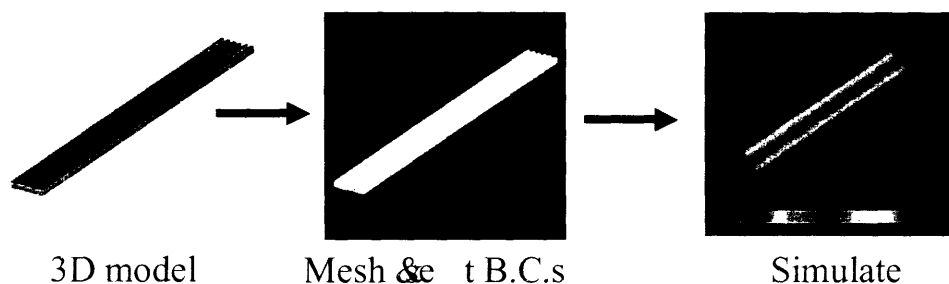


Figure 9.2 Effects of flow rate on the gradients in the main channel. Linear and complex concentration gradients were formed within the main channel. The shape of the gradients was dependant on the position downstream from the inlet as well as the liquid flow rate. Figures (a-c) represent the microscopic images of the concentration gradient at the inlet (a), and at 2.8 mm downstream from the inlet for flow rates of 11.8 mL/hr (b) and 0.104 mL/hr (c). Figures (d)-(e) represent the graph of concentration vs. position within the main channel at distinct points downstream from the inlet.

A representative figure from the microfluidic channels is illustrated in **Figure 9.1** and **Figure 9.2**. As illustrated, the concentration gradients were easily visible using a tracer dye. Furthermore, the concentration profiles were quantifiable by analyzing the pixel intensity of the images. It was observed that the shape of the concentration profile throughout the channel was a function of fluid velocity. As expected, the slower the velocity the longer the time for lateral diffusion and higher mixing. Furthermore, due to the use of syringe pumps (instead of reservoirs<sup>17</sup>) the concentration profiles generated within these channels remained stable for at least 24 hours.



*Figure 9.3. Schematic of the method used to model the microfluidic channel behavior.*

Experimentally obtained values were compared with computational fluid dynamics results. To model the mixing and diffusive behavior of fluids within the channels, finite element simulations were performed using Coventorware software. A 2 dimensional image of the region of interest was drawn, which was converted into a 3dimensional model of the channels. These models were then meshed and solved using numerical simulation techniques. **Figure 9.3** illustrates typical profiles for one set of fluid flow rates. Furthermore, the concentration profiles could be merged to obtain three dimensional rendering of the concentration within the channel. The simulations could be solved for various portions within the microfluidic network and simulated fluid mixing and gradient formation within the channels (**Figure 9.4**).

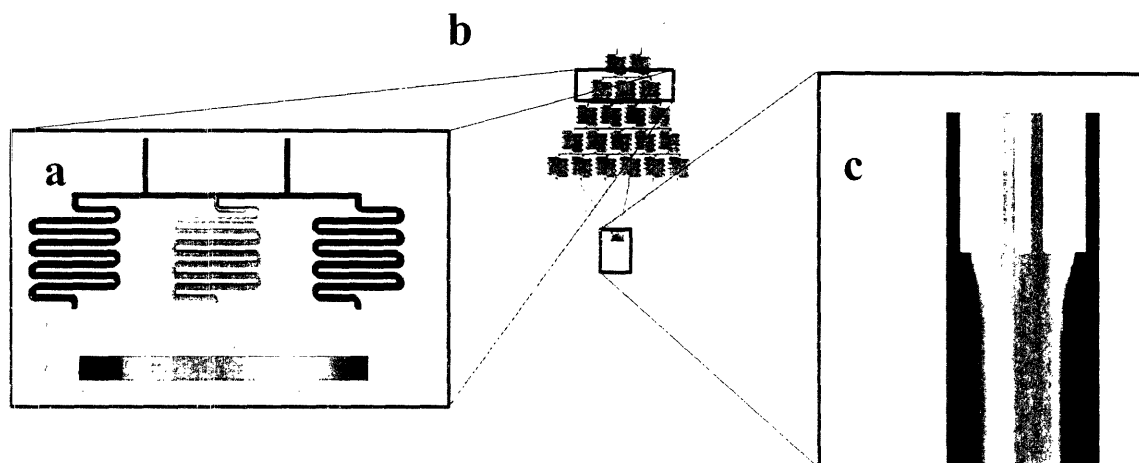


Figure 9.4. A microfluidic system was fabricated to generate stable concentration gradients of soluble molecules. Figure (a) shows a meander in which an input of high and low concentration is mixed to generate three outputs (high, intermediate and low). A network of meanders in series produces a set of parallel channels with decreasing concentrations which merge to form the main channel. Figure (b) illustrates the layout of the microfluidic channels in AutoCAD. The concentrated components are injected through the top two inlets circled in (b), the two side inlets are for introducing cells, the bottom circle is the outlet. Linear gradients in concentration spanning the  $550\ \mu\text{m}$  width of the main channel were created by passing the fluid through a network of mixers and meanders. The finest features of the devices are  $50\ \mu\text{m}$  wide. Figures (a) and (c) represent the *in silico* behavior of the system in response to an input of high and low concentrations.

To experimentally measure the mixing behavior within the networks of microfluidic trypan blue or rhodamine dye were used as tracer dyes. The gradients were visualized and digital pictures of the gradients were taken under Zeiss Axiovert 200 microscope. The images were then analyzed using Scion Image software for pixel intensity. It was found that the experimental results correlated closely to the model predictions at various positions in the channels for a particular set of input conditions (**Figure 9.5**).

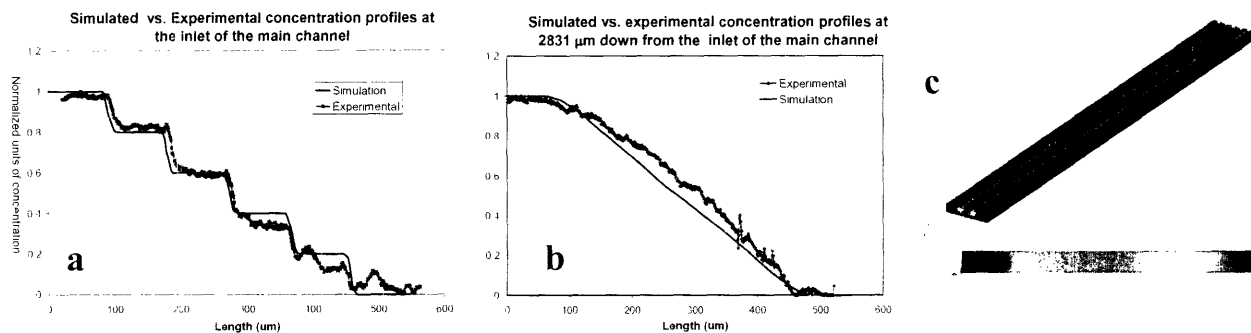


Figure 9.5. Comparison between the experimental and the simulation results. Figures (a) and (b) illustrate the direct comparison of the data for the flow rate of 0.104 mL/hr. The simulated values closely followed the results of the experimental values. Figure (c) illustrates the simulated concentration profile of the channel downstream from the inlet. As illustrated the concentration profile is stable over the length of the channel; for this flow rate, lateral diffusion is much slower than axial convective flow.

### Fabrication of gradient hydrogels

Gradient hydrogels were fabricated through a microfluidics/photopolymerization process which is detailed in **Figure 9.6A**. At the inlet to the viewing channel, the microchannel solutions merge and a step distribution of fluorescence is seen due to the incorporation of rhodamine in the inlet solutions. This distribution was quantified using NIH imaging software and is plotted in **Figure 9.6B** for initial injection rates of 0.05, 0.3, and 1.0  $\mu\text{l}/\text{min}$ . Although there are slight differences in the profiles, the step behavior is seen with all flow rates at the inlet. However, under proper flow rates the step gradient quickly formed a smooth gradient down the channel. At the outlet (20 mm downstream from the inlet) the solutions have mixed and a more linear gradient is seen (fluorescent image in **Figure 9.6A** and quantification in **Figure 9.6C**). For these systems, a flow rate of 0.3  $\mu\text{l}/\text{min}$  per inlet produced the best (most linear) gradient at the outlet. If the flow rate was too fast (i.e., 1.0  $\mu\text{l}/\text{min}$ ), there was not enough mixing and the gradient plateaus near the edges of the channel, whereas if the flow rate was too slow (i.e., 0.05  $\mu\text{l}/\text{min}$ ), there was too much mixing and the extremes of the gradient are minimized. These results indicate that the monomer solution flow rate is important on the solution mixing in the channels and that through the appropriate flow rate selection, a near linear gradient at the outlet is observed. Although our goal in this work was the formation of linear gradient profiles, complex profiles (e.g., step gradients, multiple peaks) could be obtained by variation in the number of inlets or solution flow rates<sup>12</sup>.

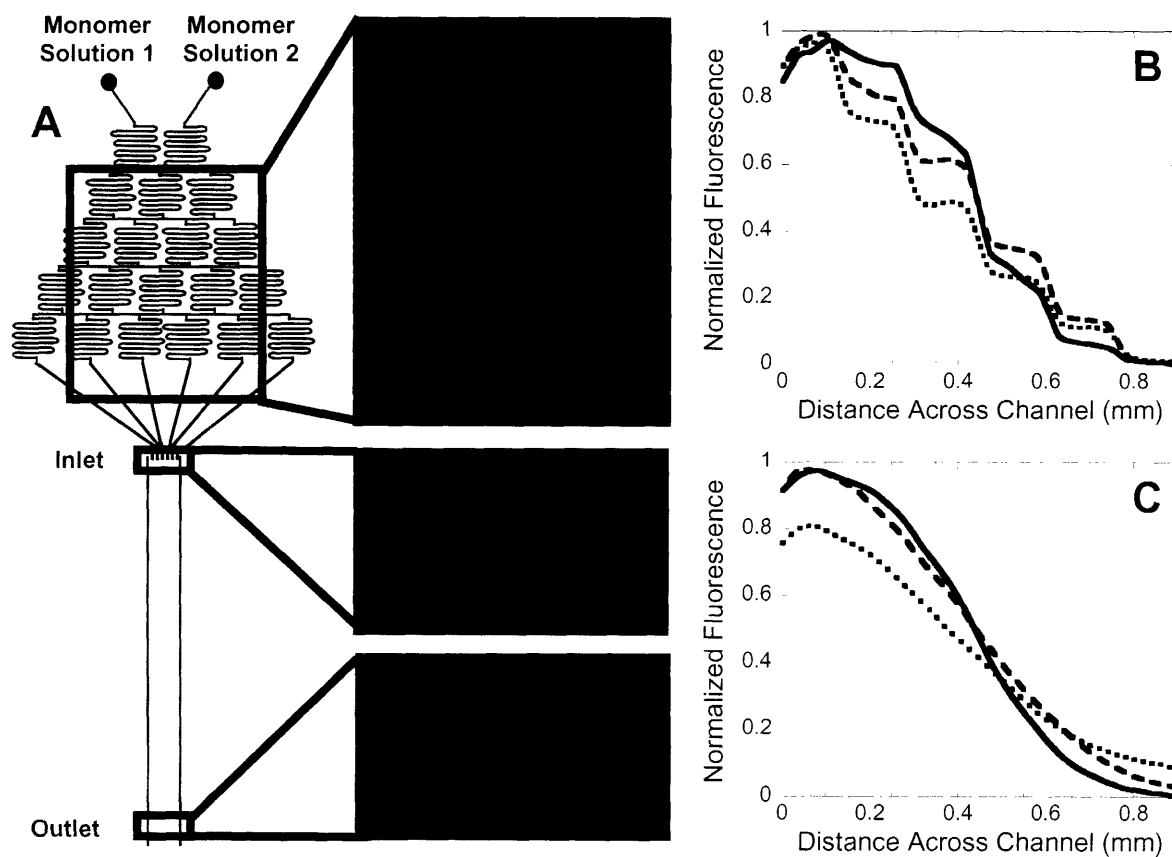


Figure 9.6. Schematic of the channel used in the microfluidics/photopolymerization process. (A) along with fluorescent images of the gradient maker and channel gradients at the inlet and outlet (~20 mm downstream of the inlet), where rhodamine is incorporated into monomer solution 1 and the monomer solutions are flowed at a rate of  $0.3 \mu\text{l}/\text{min}$ . Gradient quantification at the inlet (B) and outlet (C) for monomer solution flow rates of  $1.0 \mu\text{l}/\text{min}$  (solid),  $0.3 \mu\text{l}/\text{min}$  (dashed), and  $0.05 \mu\text{l}/\text{min}$  (dotted).

As an initial examination of this gradient process, adhesive ligands (e.g., RGDS) were tethered throughout the hydrogel networks via a poly(ethylene glycol) spacer. For gradient hydrogels, the Acr-PEG-RGDS was mixed in monomer solution 1, whereas monomer solution 2 only contained the PEG4000DA. HUVECs were seeded on the surface of hydrogel microstructures without RGDS (Figure 9.7A), with RGDS (Figure 9.7B), or with a gradient of tethered RGDS (Figure 9.7C) and visualized. A concentration of 5.0 mM Acr-PEG-RGDS was chosen due to preliminary results of HUVEC attachment on PEG hydrogels with a range of RGDS (results not

shown). On unmodified hydrogels, very few HUVECs attached and there was little spreading of the few attached cells due to the lack of protein adsorption on the hydrophilic surfaces. When RGDS was tethered to the hydrogels, HUVEC attachment and spreading was seen across the entire hydrogel microstructure. As expected, HUVEC attachment varied spatially across the hydrogels when the RGDS was tethered in a gradient. The HUVECs also appeared to spread better towards the high RGDS side of the hydrogel and were more rounded towards the unmodified RGDS side. As further evidence of cell adhesion on the surfaces of the hydrogel microstructures, the cells attached on the surrounding glass slides are out of focus and thus, on a different focal plane. Cell migration into the PEG hydrogels was not seen throughout the experiments, but future studies could also use this process to characterize cell migration through enzymatically degradable hydrogel networks with gradients of adhesive tethers or hydrogel crosslinking.

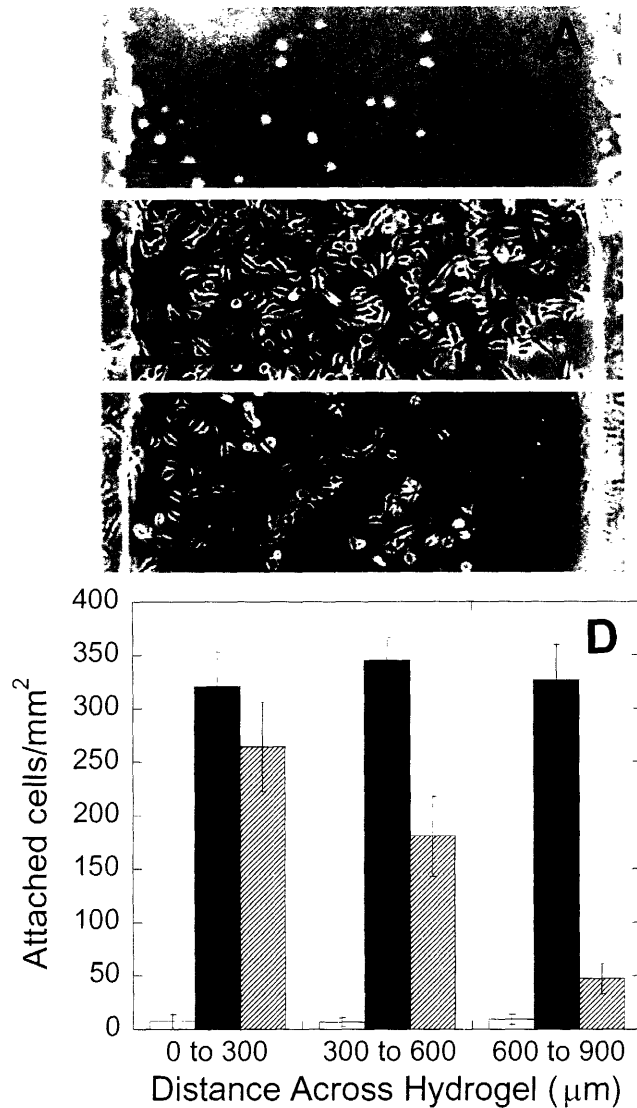


Figure 9.7. Light micrographs of endothelial cells attached (3 hours after seeding) to the surface of hydrogels fabricated without RGDS (A), with 5.0 mM Acr-PEG-RGDS (B), and with a gradient from 5.0 mM Acr-PEG-RGDS (left) to no RGDS (right) (C), bar = 200 μm. Quantification of spatial endothelial cell attachment (number of cells/mm<sup>2</sup> hydrogel surface) on 300 μm sections of hydrogels fabricated without RGDS (white), with 5.0 mM Acr-PEG-RGDS (black), and with a gradient from 5.0 mM Acr-PEG-RGDS to no RGDS (striped) (D).

When quantified (results in **Figure 9.7D**), the same trend was seen with higher cell attachment on the high RGDS side and less attachment on the lower to no RGDS side. For instance, the attachment on the left third of the gel was 224 cells/mm<sup>2</sup>, 481 cells/mm<sup>2</sup> for the middle third, and 47 cells/mm<sup>2</sup> for the right third. As expected, there was little difference in spatial cell adhesion on non-gradient hydrogels (either unmodified or completely modified with RGDS).



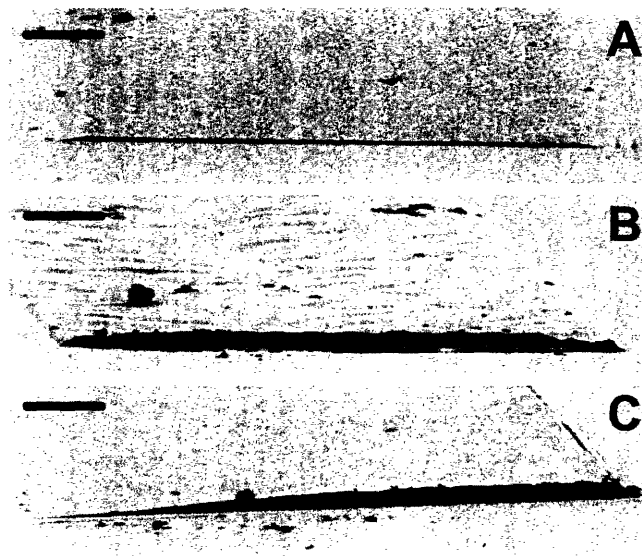
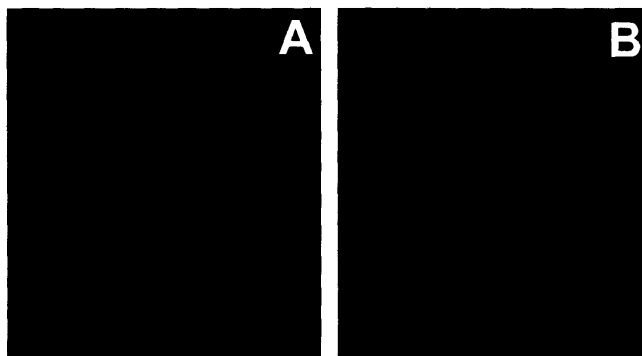


Figure 9.8. SEM micrographs of cross-sections of dried hydrogels fabricated from 10 wt% PEG4000DA (A), 50 wt% PEG1000DA (B), and a gradient of 10 wt% PEG4000DA (left) to 50 wt% PEG1000DA (right) (C), bar = 100  $\mu\text{m}$ .

Another potential benefit of this fabrication process is that hydrogels with gradients in crosslinking densities are easily produced by incorporating solutions of various molecular weights and macromer concentrations, which can influence the overall crosslinking density of the resulting hydrogel. This was investigated by injecting a solution of 10 wt% PEG4000DA (low macromer concentration, high macromer molecular weight) into one of the inlets and a solution of 50 wt% PEG1000DA (high macromer concentration, low macromer molecular weight) into the other inlet. After polymerization, these channels were dried and cut in order to visualize the channel cross-sections using SEM. The SEM images in **Figures 9.8A** and **9.8B** show that the control sample using only the 10 wt% solution produces a very thin network after drying (40  $\mu\text{m}$ ); whereas, the 50 wt% solution produces a network 50  $\mu\text{m}$  in thickness. The gradient hydrogel, shown in **Figure 9.8C**, produces a sloped network with the thickness varying from left (low crosslinking density) to right (high crosslinking density). It should be noted that large differences in the viscosities of the injected macromer solutions may influence the final hydrogel gradient and thus, is a limitation to this technique depending on the magnitude of differences in the macromer molecular weights and concentrations.



*Figure 9.9. Fluorescent micrographs of rhodamine encapsulated in a gradient hydrogel of 10 wt% PEG4000DA (left) to 50 wt% PEG1000DA (right) immediately after polymerization (A) and after 20 minutes of release in PBS (B), illustrating gradient-dependent diffusion with greater amounts of rhodamine released from the less crosslinked side of hydrogel structure and little release from the more crosslinked side (channel width = 900 $\mu$ m).*

As an additional measure of the gradients in crosslinking density, a fluorescent dye was photoencapsulated in the hydrogel. The hydrogel was then imaged immediately after polymerization (**Figure 9.9A**) and after 20 minutes of swelling in PBS (**Figure 9.9B**). A decrease in the fluorescence on the side of the hydrogel that is more loosely crosslinked (greater mesh size) indicates swelling and release of the fluorescent molecule from the network. On the more densely crosslinked side (smaller mesh size) a larger fraction of the fluorescent molecule remains entrapped. The fluorescent intensity was quantified for each image using NIH image software and showed a 77% decrease in intensity after swelling for the more loosely crosslinked side, whereas only a 22% decrease was seen on the more highly crosslinked side.

## CONCLUSIONS

In conclusion, we have introduced a simple technique for the fabrication of gradient hydrogels using a microfluidic system in combination with a photopolymerization reaction. Although not a focus of this study, future work could include the photoencapsulation of cells and molecules in these gradient hydrogel microstructures to produce unique tissue engineering scaffolds.

## REFERENCES

- (1) Parent, C. A., Devreotes, P. N. A cell's sense of direction. *Science*, **284**, 5415, 1999.
- (2) Wong, J. Y., Velasco, A., Rajagopalan, P., Pham, Q. Directed movement of vascular smooth muscle cells on gradient-compliant hydrogels. *Langmuir*, **19**, 5, 2003.
- (3) Tessier-Lavigne, M., Goodman, C. S. Neurobiology - Regeneration in the Nogo zone. *Science*, **287**, 5454, 2000.
- (4) Spijker, H. T., Bos, R., Busscher, H. J., van Kooten, T. G., van Oeveren, W. Platelet adhesion and activation on a shielded plasma gradient prepared on polyethylene. *Biomaterials*, **23**, 3, 2002.
- (5) Kapur, T. A., Shoichet, M. S. Immobilized concentration gradients of nerve growth factor guide neurite outgrowth. *Journal of Biomedical Materials Research Part A*, **68A**, 2, 2004.
- (6) Herbert, C. B., McLernon, T. L., Hypolite, C. L., Adams, D. N., Pikus, L., Huang, C. C., Fields, G. B., Letourneau, P. C., Distefano, M. D., Hu, W. S. Micropatterning gradients and controlling surface densities of photoactivatable biomolecules on self-assembled monolayers of oligo(ethylene glycol) alkanethiolates. *Chemistry & Biology*, **4**, 10, 1997.
- (7) Anseth, K. S., Burdick, J. A. New directions in photopolymerizable biomaterials. *Mrs Bulletin*, **27**, 2, 2002.
- (8) Lee, K. Y., Mooney, D. J. Hydrogels for tissue engineering. *Chemical Reviews*, **101**, 7, 2001.
- (9) Hern, D. L., Hubbell, J. A. Incorporation of adhesion peptides into nonadhesive hydrogels useful for tissue resurfacing. *Journal of Biomedical Materials Research*, **39**, 2, 1998.
- (10) Burdick, J. A., Anseth, K. S. Photoencapsulation of osteoblasts in injectable RGD-modified PEG hydrogels for bone tissue engineering. *Biomaterials*, **23**, 22, 2002.
- (11) Koh, W. G., Revzin, A., Pishko, M. V. Poly(ethylene glycol) hydrogel microstructures encapsulating living cells. *Langmuir*, **18**, 7, 2002.
- (12) Jeon, N. L., Dertinger, S. K. W., Chiu, D. T., Choi, I. S., Stroock, A. D., Whitesides, G. M. Generation of solution and surface gradients using microfluidic systems. *Langmuir*, **16**, 22, 2000.
- (13) Dertinger, S. K. W., Chiu, D. T., Jeon, N. L., Whitesides, G. M. Generation of gradients having complex shapes using microfluidic networks. *Analytical Chemistry*, **73**, 6, 2001.

- (14) Koh, W. G.,Itle, L. J.,Pishko, M. V. Molding of hydrogel multiphenotype cell microstructures to create microarrays. *Analytical Chemistry*, **75**, 21, 2003.
- (15) Koh, W. G.,Revzin, A.,Simonian, A.,Reeves, T.,Pishko, M. Control of mammalian cell and bacteria adhesion on substrates micropatterned with poly(ethylene glycol) hydrogels. *Biomedical Microdevices*, **5**, 1, 2003.
- (16) Koh, W. G.,Itle, L. J.,Pishko, M. V. Molding of hydrogel microstructures to create multiphenotype cell microarrays. *Anal Chem*, **75**, 21, 2003.
- (17) Takayama, S.,Ostuni, E.,LeDuc, P.,Naruse, K.,Ingber, D. E.,Whitesides, G. M. Laminar flows - Subcellular positioning of small molecules. *Nature*, **411**, 6841, 2001.

## 10. Summary and Outlook

### SUMMARY

In this thesis, techniques and tools were developed to engineer various aspects of the microenvironment of cells in culture using nano- and microfabrication technology. The ideological reasoning for using such approaches and length scales for biological experiments is to miniaturize assays, to increase the throughput of experimentation and to increase culture homogeneity and control. This thesis was divided into four main sections, each of which focused on a particular aspect of the cell's microenvironment.

The first section of the thesis aimed to control the interaction of cells with their substrate by patterning cells on adhesive islands. In order to facilitate easier use of such technologies, a soft lithographic method was developed to fabricate PEG microstructures. This lithographic method involves a molding process in which a uniform PEG film is molded with a patterned PDMS stamp by means of capillary forces. The patterned surfaces created by this method provide excellent resistance toward nonspecific protein and cell adsorption. The patterned substrates consist of two regions: the molded PEG surface that acts as a resistant layer and the exposed substrate surface that promotes protein or cell adsorption. It was found that the substrate surface can be exposed during the molding process due to the wetting properties of the polymer on the stamp, which is a key factor to patterning proteins and cells. Initially, photocrosslinkable PEG was used. However, to use the advantages associated with capillary force lithography in generating features of various length scales, a new polymer was developed. The synthesized polymer had the capability to crosslink as well as form polymeric monolayers. Through the merger of this polymer with patterning approaches, it was possible to fabricate nanostructures and microstructures with control over their shapes and sizes.

In the second portion of this thesis methods were developed to control the degree of homotypic and heterotypic cell-cell interaction in culture. In order to do this, polysaccharide patterns were generated, since they could be used to form layers which repelled cell adhesion. Particular attention was given to HA. It was demonstrated that HA can be directly immobilized onto hydrophilic substrates such as glass or silicon oxides without any chemical manipulation, allowing

for the formation of a stable adsorbed layer. The stable HA layer was successfully applied to soft lithographic techniques such as microcontact printing or capillary force molding, leading to well-defined patterns over large areas for a number of proteins (including bovine serum albumin, immunoglobulin G, fibronectin) and cells (fibroblasts, hepatocytes and embryonic stem cells). It was hypothesized that HA could be stabilized on these surfaces through hydrogen bonding between the hydrophilic moieties in HA (such as carboxylic acid (-COOH) or hydroxyl (-OH) groups) with silanol (-SiOH), carboxylic acid or hydroxyl groups on the hydrophilic substrates. Despite the water solubility, the adsorbed HA layer remained stable on glass or silicon oxide substrates for at least 7 days in phosphate buffered saline. These results demonstrate that HA can be used to coat surfaces through direct immobilization. Since HA is negatively charged layer-by-layer deposition of electrostatic molecules can be used for patterning co-cultures. After patterning the first cell type on HA patterned substrates, the subsequent ionic adsorption of poly-L-lysine (PLL) to HA patterns was used to switch the HA surfaces from cell-repulsive to cell-adherent thereby facilitating the adhesion of a second cell type. The utility of this approach to pattern co-cultures of hepatocytes or ES cells with fibroblasts was demonstrated. In addition, the versatility of this approach to generate patterned co-cultures irrespective of the primary cell seeding and relative adhesion of the seeded cells was demonstrated. Thus, controlled cellular co-cultures were fabricated with potential applications in studying cell-cell interactions and building tissue engineering constructs.

In the third portion of this thesis, methods were developed to interface cells and proteins within microchannels. Controlling the interaction of cells with microchannels could lead to improved analytical tools for the development of diagnostic assays and microreactors and for performing fundamental studies in cell biology by controlling cell-soluble signal interactions. Initially, a simple technique was developed to fabricate robust microchannels with precise control over the spatial properties of the substrate. In this approach, the patterned regions were protected from oxygen plasma by controlling the dimensions of the PDMS stamp and by leaving the stamp in place during the plasma treatment process. The PDMS stamp was then removed, and the microfluidic mold was irreversibly bonded to the substrate. The approach was used to pattern a PEG-based copolymer or HA within microfluidic channels. These non-biofouling patterns were then used to fabricate arrays of FN and BSA as well as mammalian cells. In addition, further

control over the deposition of multiple proteins onto multiple or individual patterns was achieved using laminar flow. Also, cells that were patterned within channels remained viable and capable of performing intracellular reactions and could be potentially lysed for analysis.

Despite the ease with which the previous approach could be used to pattern microchannels, patterning cells within these devices was cumbersome and difficult. To solve this problem, PEG microstructures were fabricated within microfluidic channels that could be used to capture cells by allowing the cells to dock within pre-defined locations that are shear protected. Microstructures of various shapes were used to capture and shear-protect cells despite medium flow in the channels. Using this approach, PEG microwells were fabricated either with exposed or non-exposed substrates. Proteins and cells adhered within microwells with exposed substrates, while non-exposed substrates prevented protein and cell adhesion (although cells were captured). Furthermore, immobilized cells remained viable and were stained for cell surface receptors by sequential flow of antibodies and secondary fluorescent probes. With its unique strengths in utility and control, this approach is potentially beneficial for the development of cell-based analytical devices and microreactors that enable the capture and real-time analysis of cells within microchannels, irrespective of cell anchorage properties.

The development of methods to capture cells within channels allows for the fabrication of more advanced techniques to fabricate multiphenotype cell arrays by capturing cells within an array of reversibly sealed microfluidic channels. The technique used reversible sealing of elastomeric PDMS molds on surfaces to sequentially deliver various fluids or cells onto specific locations on a substrate. Microwells on the substrate were used to capture and immobilize cells within individual channels. By using an array of channels, it was possible to deposit multiple cell types such as hepatocytes, fibroblasts, and ES cells on the substrates. Upon formation of the cell arrays on the substrate, the PDMS mold was removed, generating a multiphenotype array of cells. In addition, the orthogonal alignment and subsequent attachment of a secondary array of channels on the patterned substrates were shown to facilitate the formation of individual channels containing patterns of multiple cell types. The ability to position many cell types on particular regions within a two-dimensional substrate or to integrate multiphenotype arrays of channels inside microstructures could potentially lead to improved methods of high-throughput technology

applicable to drug screening and tissue engineering.

In the final section of this thesis, a method of fabricating photocrosslinked hydrogels with gradients of immobilized molecules and crosslinking densities was introduced. Such gradients will be important for controlling the interaction of cells with their surrounding. Two macromer/initiator solutions were injected into a unique PDMS channel system that produced a prepolymer gradient that was subsequently polymerized into a water swollen hydrogel with UV light exposure. The technique was investigated both through fabrication of adhesive ligand gradients that modulate spatial distribution of attached endothelial cells and gradients of crosslinking densities that led to unique hydrogel architectures and spatially dependent swelling.



## **OUTLOOK**

As it can be seen from this chapter, much progress has been made in controlling various aspects of cell microenvironment using BioMEMS. The integration of cells within microdevices may revolutionize the throughput and analytical capability of tomorrow's biology and medical labs. Potential applications range from analytical tools for high-throughput drug screening and chemical library analysis to enhanced bioreactors. However, despite significant progress, many challenges still remain in fully utilizing the power of such technologies.

Traditional approaches of performing 96 or 384 well plates are limited by the number of experiments that can be performed. Therefore, the development of techniques to generate functional or bioactive surfaces for immobilization of various molecules, patterning of cells and integration of these techniques into functional devices has significant clinical and basic biological implications. Although many tools have been developed, BioMEMS approaches have not been widely used in the biological and clinical communities. Therefore, a major thrust area regarding the direction of this research is the development of devices that incorporate cell patterning and microfluidics for high-throughput applications. One of the main challenges in making BioMEMS devices widely applicable is to overcome the challenge of replacing today's technologies. There are a number of barriers that must be addressed. The first such barrier is the lack of knowledge of the end users (i.e. biologists and the clinicians), regarding the capabilities and advantages of such devices in comparison to existing technology. The barrier in overcoming the existing technology is a challenge that must be addressed.

To widely use such devices, the fabrication process of microdevices must be addressed. Most BioMEMS devices (like most other microscale approaches) originate from expensive clean rooms and microfabrication facilities. These facilities are expensive and even today sparsely located in major research institutions. Therefore, the widespread use of these devices requires minimizing the use of expensive clean room technologies. Soft lithography is a potentially useful approach of limiting the amount of fabrication time by allowing the end user to fabricate devices directly in their lab.

Another area of development is to change BioMEMS from a two-dimensional to a three-dimensional system. It is clear that controlling the spatial distribution of cells on surfaces within three-dimensional matrices is beneficial for the study of cell biology, fabrication of cell-based devices, and tissue engineering constructs. Current approaches for cell patterning are typically limited to a single cell type immobilized onto a two-dimensional surface. These approaches would benefit from improvements in the patterning material, the number of cells and proteins that can be simultaneously patterned, and the ability to pattern and generate three-dimensional structures.

Another remaining challenge in integrating cells within microdevices for high-throughput experimentation is to miniaturize the accessories associated with these devices. Currently, expensive syringe pumps and microscopes are an integral part of these devices. However, novel methods of integrating components directly onto biochips could dramatically reduce the costs of these accessories. The linkage of the microscale to macroscale technologies has been a great challenge and is an area of active research.

Overall, as it can be seen from this thesis and other work referenced, great advances have been made in the development of nano- and microscale devices<sup>1-4</sup>. However, the continued lack of widespread use of these technologies by the biological and medical communities necessitates the development of ways in which these tools can be used without significant expertise. In addition, the power of these tools is starting to be demonstrated<sup>2, 5-9</sup>. While these examples have paved the way, additional applications of these techniques must be shown. The best way to do this is through answering important biological questions. This task is particularly suitable for biological engineers who are knowledgeable in both engineering and biology.

## REFERENCES

- (1) Bhatia, S. N., Balis, U. J., Yarmush, M. L., Toner, M. Effect of cell-cell interactions in preservation of cellular phenotype: cocultivation of hepatocytes and nonparenchymal cells. *Faseb J*, **13**, 14, 1999.
- (2) Bhatia, S. N., Balis, U. J., Yarmush, M. L., Toner, M. Microfabrication of hepatocyte/fibroblast co-cultures: role of homotypic cell interactions. *Biotechnol Prog*, **14**, 3, 1998.
- (3) Whitesides, G. M., Ostuni, E., Takayama, S., Jiang, X., Ingber, D. E. Soft lithography in biology and biochemistry. *Annu Rev Biomed Eng*, **3**, 2001.
- (4) Folch, A., Toner, M. Microengineering of cellular interactions. *Annu Rev Biomed Eng*, **2**, 2000.
- (5) Bhatia, S. N., Yarmush, M. L., Toner, M. Controlling cell interactions by micropatterning in co-cultures: hepatocytes and 3T3 fibroblasts. *J Biomed Mater Res*, **34**, 2, 1997.
- (6) Bhatia, S. N., Balis, U. J., Yarmush, M. L., Toner, M. Probing heterotypic cell interactions: hepatocyte function in microfabricated co-cultures. *J Biomater Sci Polym Ed*, **9**, 11, 1998.
- (7) Borenstein, J. T., Terai, H., King, K. R., Weinberg, E. J., Kaazempur-Mofrad, M. R., Vacanti, J. P. Microfabrication technology for vascularized tissue engineering. *Biomedical Microdevices*, **4**, 3, 2002.
- (8) Kaihara, S., Borenstein, J., Koka, R., Lalan, S., Ochoa, E. R., Ravens, M., Pien, H., Cunningham, B., Vacanti, J. P. Silicon micromachining to tissue engineer branched vascular channels for liver fabrication. *Tissue Engineering*, **6**, 2, 2000.
- (9) Vacanti, J., Cheung, W., Borenstein, J., Kaazempur-Mofrad, M., Shin, M., Sevy, A., Kulig, K. Hepatocyte and endothelial cell survival in a tissue engineered human liver device with its own vascular network. *Journal of the American College of Surgeons*, **197**, 3, 2003.



Room 14-0551  
77 Massachusetts Avenue  
Cambridge, MA 02139  
Ph: 617.253.5668 Fax: 617.253.1690  
Email: docs@mit.edu  
<http://libraries.mit.edu/docs>

## **DISCLAIMER OF QUALITY**

Due to the condition of the original material, there are unavoidable flaws in this reproduction. We have made every effort possible to provide you with the best copy available. If you are dissatisfied with this product and find it unusable, please contact Document Services as soon as possible.

Thank you.

**Some pages in the original document contain color pictures or graphics that will not scan or reproduce well.**